APPLICATION OF WATER MIST TO FUEL-RICH FIRES IN MODEL COAL MINE ENTRIES

by

Ian Morton Loomis

Thesis submitted to the Faculty of the
Virginia Polytechnic Institute and State University
in partial fulfillment of the requirements for the degree of

MASTER OF SCIENCE

in

Mining Engineering

APPROVED:

Malcolm J. McPherson, Chairman

Michael Karmis

Ertugrul Topuz

March 1995
Blacksburg, Virginia

APPLICATION OF WATER MIST TO FUEL-RICH FIRES IN MODEL COAL MINE ENTRIES

by
Ian Morton Loomis
Malcolm J. McPherson, Chairman
Department of Mining and Minerals Engineering

(ABSTRACT)

As the nature of coal mining changes, to higher production associated with higher mechanization, the way in which mine safety is approached must also change. This situation was clearly shown in a very devastating coal mine fire in late 1984. In the absence of effective fire-fighting procedures and equipment the affected mine was quickly rendered helpless. Of particular concern with coal mine fires is the possibility of entering a fuel-rich state. In this state current practices have proven to be of little use in gaining control over the conflagration. Recent experiences with the application of water mist to industrial fires has shown that use of fog can be an efficacious agent in controlling large scale fires. The postulations of this phenomenon concern the ability of the water, as a fog, to get deeply within the fire structure. In this manner it works to remove the three legs of the fire triangle; heat, oxygen, and fuel. The research contained in this thesis dwells in three associated areas. These are: the general theory of water mist application relative to current practices; the design and construction of a fire tunnel for experimental work; and the results obtained from experiments with fuel-rich fires in the simulated coal mine entry. The results of this research are most encouraging, not only for the more devastating fuel-rich fires, but also for application from the onset of fire fighting activities in the coal mine environment.

To the coal miners of the world, who fueled the industrial revolution.

ACKNOWLEDGMENTS

I wish to first recognize my parents, David and Evelyn.

I wish to thank Professor Malcolm McPherson, my academic advisor and committee chairman for his guidance and ear during the course of this work.

I wish to thank, also, the members of my committee, Professors Michael Karmis and Ertugrul Topuz.

I would like to recognize the effort of Mr. Wayne Slusser of the Department of Mining and Minerals Engineering, who assisted with the construction of the fire tunnel and with the set-up and conduct of the tests. He was also not afraid to show me the operation of the various machine tools, then allow me to make the bits and pieces that were needed.

Recognition for funding is extended to the Virginia Mining and Mineral Resources Research Institute, who funded much of this project. Funding was also received from the Graduate Student Assembly, at Virginia Tech, for tests 6 and 7.

Table of Contents

List of Tables

List of Figures

List of Plates

List of Symbols

Symbol	Description
a	linear acceleration ($\mathbf{L/T^2}$)
A	cross-sectional area ($\mathbf{L^2}$)
A_w	convective transfer contact air ($\mathbf{L^2}$)
c_p	specific seat ($\mathbf{E/Mt}$)
c_{ps}	specific seat at droplet surface ($\mathbf{E/Mt}$)
$c_{p\infty}$	specific heat of upstream air ($\mathbf{E/Mt}$)
D	diameter ($\mathbf{L}$)
D_0	Initial diameter ($\mathbf{L}$)
$\boldsymbol{D}$	Mass diffusivity ($\mathbf{L^2/T}$)
$\mathbf{E}$	Dimensional argument for Energy ($\mathbf{ML^2/T}$)
E	Modulus of Elasticity ($\mathbf{M/LT^2}$)
E	Dimensionless parameter for sustained fire propagation
Eu	Euler number (F_I/F_P)
F_E	Elastic Force ($\mathbf{ML/T^2}$)
F_G	Gravitational Force ($\mathbf{ML/T^2}$)
F_I	Inertial Force ($\mathbf{ML/T^2}$)
F_P	Pressure Force ($\mathbf{ML/T^2}$)
F_T	Tensional Force ($\mathbf{ML/T^2}$)
F_V	Viscous Force ($\mathbf{ML/T^2}$)
Fr	Froude number (F_I/F_G)
Gr	Grashof number
g_n	gravitational acceleration ($\mathbf{L/T^2}$)
H	heat of vaporization
h_c	convective transfer coefficient
$\mathbf{L}$	Dimensional argument for Length
L	Layering number
l	length ($\mathbf{L}$)
M	Mass ($\mathbf{M}$)
M_A	mass rate of air supplied to fire ($\mathbf{M/T}$)
$\mathbf{M}$	Dimensional argument for Mass
$\dot{m}_f$	mass flow rate of fuel ($\mathbf{M/t}$)
$\dot{m}_{fog}$	mass flow rate of fog ($\mathbf{M/T}$)
$\dot{m}_\infty$	mass flow rate upstream of fire ($\mathbf{M/t}$)
$\dot{m}''$	mass transfer flux ($\mathbf{M/L^2T}$)
p	Differential pressure ($\mathbf{M/LT^2}$)
P	Fuel Loading in Duct ($\mathbf{M/L}$)
P	Pressure ($\mathbf{M/LT^2}$)

Symbol	Description
Q	Heat of Combustion
$\dot{Q}$	heat flow (**E/T**)
$\dot{Q}_l$	heat flow away from fire (**E/T**)
$\dot{Q}_f$	Source fire strength
$\dot{q}''$	heat transfer flux (**E/L^{2}T**)
$\dot{q}_w$	convective heat transfer (**E/L^{2}T**)
R	Turbulent Resistance
r	fuel to air stoichiometric ratio
Re	Reynolds number (F_I/F_V)
Ri	Richardson number
Ri_{cr}	Critical Richardson number
RR	Reaction Rate
S_L	Laminar flame speed (**L/T**
t	Dimensional argument for temperature
T_i	initial temperature (**T**)
T_{ig}	Temperature of ignition (**T**)
T_f	Flame temperature (**T**)
T_0	Ambient temperature (**T**)
T_∞	Temperature upstream (**T**)
T	Dimensional argument for Time
u	velocity (**L/T**)
u	u_b/V_∞
V	Velocity (**L/T**)
W	airway width (**L**)
x,x_i	Distance parallel to flow (**L**)
$Y_0^{(0)}$	oxygen concentration upstream of fire (%)
y	Distance normal to flow (**L**)
α	Thermal diffusivity (**L^2/T**)
β	temperature coefficient of thermal expansion (**L/T**)
Δ	Difference (of argument, ie difference in pressure = Δp)
δ	Flame reaction zone thickness (**L**)
δ_{fog}	density of fog (**M**/L^3)
ϕ	Equivalence Ratio
λ	thermal conductivity (**E/tMT**)
λ_{air}	thermal conductivity of air (**E/tMT**)
μ	absolute viscosity
ν	kinematic viscosity (**L^2/T**) (Momentum diffusivity)
ρ	Density (**M/L^3**)
σ	Surface tension (**M/T^2**)

Symbol	Description
subscript	
$_{wb}$	wet bulb
$_{db}$	dry bulb
$_{s}$	surface condition
$_{\infty}$	far field condition
$_{BP}$	boiling point
$_{o}$	initial condition
$_{i}$	initial condition
$_{w}$	water fraction
$_{p}$	products of combustion
$_{air}$	air fraction

1. *INTRODUCTION*

The public address system blares out: "There is a fire in the underground, this is not a drill." Whether one is on the surface or in the underground at the time this message is reported the first response is likely the same, "Where is it?"

Fortunately most fires that occur in the underground are small and brought under control and extinguished quickly. Unfortunately, without quick and decisive action a small fire can become a large fire, and some fires just start that way. Of the 298 fires reported to the Mine Safety and Health Administration (MSHA) in the 20 year period of 1970 through 1989, 5 are reported to have resulted in the total loss of life of 40 miners (Timko and Kissel 1993).

Under current regulations, in the United States, the Mine Safety and Health Administration must be notified of a fire if any of the following occur (Timko and Kissel 1993, anon. 1994a):

(a) A fatality of an individual at the mine (30 CFR 50.2 h (1)),

(b) An injury to an individual at the mine which has a reasonable potential to cause death (30 CFR 50.2 h (2)),

(c) An unplanned fire not extinguished within thirty minutes of its discovery (30 CFR 50.2 h (6)).

An, admittedly, few of these fires progress to the point of inflicting such major damage to the mine. This thesis reviews the nature of those fires that grow to extend beyond the locale of their origin and effect the entire mine or a significant portion of it. The intent of the work is to evaluate the efficacy of water mist as an extinguishing agent for those fires that have grown to immense proportion relative to the scale of the mine entry. To accomplish this task a scale model wind-tunnel was designed and constructed at the Virginia Polytechnic Institute and State University. The work documented here covers three general areas:

(1) A basic review of the nature of the fires that are being considered in this thesis is provided in this chapter. Included in this section are the definition and nature of oxygen-rich and fuel-rich fires, and the manifestation of fuel-rich fires as experienced at three coal mines in the United States. Literature regarding previous research in the field of fuel-rich mine fires and the application of water mist as an extinguishing agent is reviewed in chapter 2. The underlying theory of the fires and of the water mist system is covered in chapter 3.

(2) The design and construction of a wind tunnel in which the environment of a coal mine undergoing a fuel-rich fire could be simulated is covered in chapter 4. The testing of the tunnel systems is covered in the early part of chapter 5.

(3) The actual fire tests are covered in the later part of chapter 5, with a discussion of the results in chapter 6 and conclusions drawn in chapter 7.

As an introduction to the subject of oxygen-rich and fuel-rich fires in coal mine entries this chapter discusses the relative differences of these fire types, the mechanism by which a fire can spread when it is contained in a mine entry, the effect of fuel-rich fires in three mine environments, and the purpose for conducting the research covered. This should provide the reader with a starting base for the more detailed analysis that is to follow.

1.1. Oxygen-Rich and Fuel-Rich Fires

Three very basic elements are required for a fire to ignite or propagate: fuel, oxygen, and heat. Without any of the three a fire is not possible. One can envision this simply with a common match. To begin with, the match (fuel) is held in the air (oxygen) and no combustion is taking place. When the match is struck, friction (heat) ignites the match head which burns vigorously. The burning of the head provides heat to the match stick causing the wood to vaporize (or produce gaseous fuel) which reacts with the oxygen in the air producing the observable flame of fire. Eventually, despite the heat and oxygen the match goes out, what is left is a stick of incombustible ash. The fire went out when it ran out of fuel. This is the basic idea of fire that one is likely to receive from grammar school onward, and is a relatively sufficient starting point.

Expanding the scale of the above fire, consider an open fireplace. Under this condition a larger quantity of fuel is available, as is a relatively unlimited supply of fresh air. As one can observe, the fire spreads from the kindling to the logs, by direct contact of the flame to the next element of fuel that will be burnt. The exhaust from the fire mixes readily with the available fresh air diluting and cooling the gases produced by the burning. The resulting products downstream of the fire are relatively cool; with a significant quantity of

oxygen, an elevated level of carbon dioxide, and little carbon monoxide. The exhaust may not, however, be capable of supporting life. This is the type of fire referred to as oxygen-rich.

Consider, now, a fire burning with a distributed and unlimited fuel supply that has a limited supply of fresh air. This fire may begin slowly in an oxygen-rich state, however, as it grows and begins to consume all the available oxygen its nature changes drastically, on the larger scale. When the oxygen concentration in the exhausts falls to a level of about 15 percent there is sufficient heat being carried away from the fire to cause spreading without direct contact with the flame structure. A fire burning in this state can quickly accelerate to produce exhausts that contain virtually no oxygen, and very high levels of both carbon dioxide and carbon monoxide, and that leave the location of the fire very near the flame temperature.

It has been assumed that the flame structure is that of a turbulent diffusion flame, in which the vaporous fuel and the oxygen react in stoichiometric proportion at the flame front, coupled with turbulent flow conditions. Furthermore, neither fuel nor oxygen is transported through the reaction interface, but are carried in the bulk flow away from the reaction zone. For a more detailed discussion of this phenomenon refer to chapter 3 of this thesis.

1.2. Duct Fire Mechanism

Once a fire has been ignited in a coal mine entry it can quickly begin to consume the entry where it began, and spread with the airflow downstream. Once the fire begins to spread

with the airflow, what began as a limited open fire takes on characteristics that make the fire both difficult and dangerous to fight directly. Fires in fuel lined ducts, such as coal mine entries, have three distinct characteristics separating them from normal open combustion. First the physical limits of the entry contain the fuel for the fire. Second the supply of air is limited to that being delivered through the duct or airway. Third, only a relatively small percentage of the overall heat generated by the fire is lost from the duct in the immediate vicinity of the fire. The dangers and problems associated with a mine fire can be contemplated by investigating the development and transformation of a hypothetical mine fire.

Consider a typical coal mine entry, as shown in figure 1-1a, in which roof coal has been left. Let a small fire begin as shown in figure 1-1b. As the fire develops, the air is locally warmed around the fire, but the down stream air remains relatively unaffected. As the fire begins to consume more of the available fuel the local temperature continues to rise, the hot gases from the smoke plume run along the ribs beginning to warm the coal. The rib coal then begins to contribute fuel to the fire. Ever hotter fumes begin to lap across the roof volatizing the coal there. During this time more and more of the available oxygen is being consumed in the fire.

When the volatizing fuel from the roof coal ignites, the fire has begun to completely engulf the entire drift and consequently the whole air supply, figure 1-1c. During this process the temperature of the exhaust continues to rise. It can easily be shown that the highest reaction temperature from the fire occurs when there is a stoichiometric balance between the available oxygen and fuel, see figure 1-2.

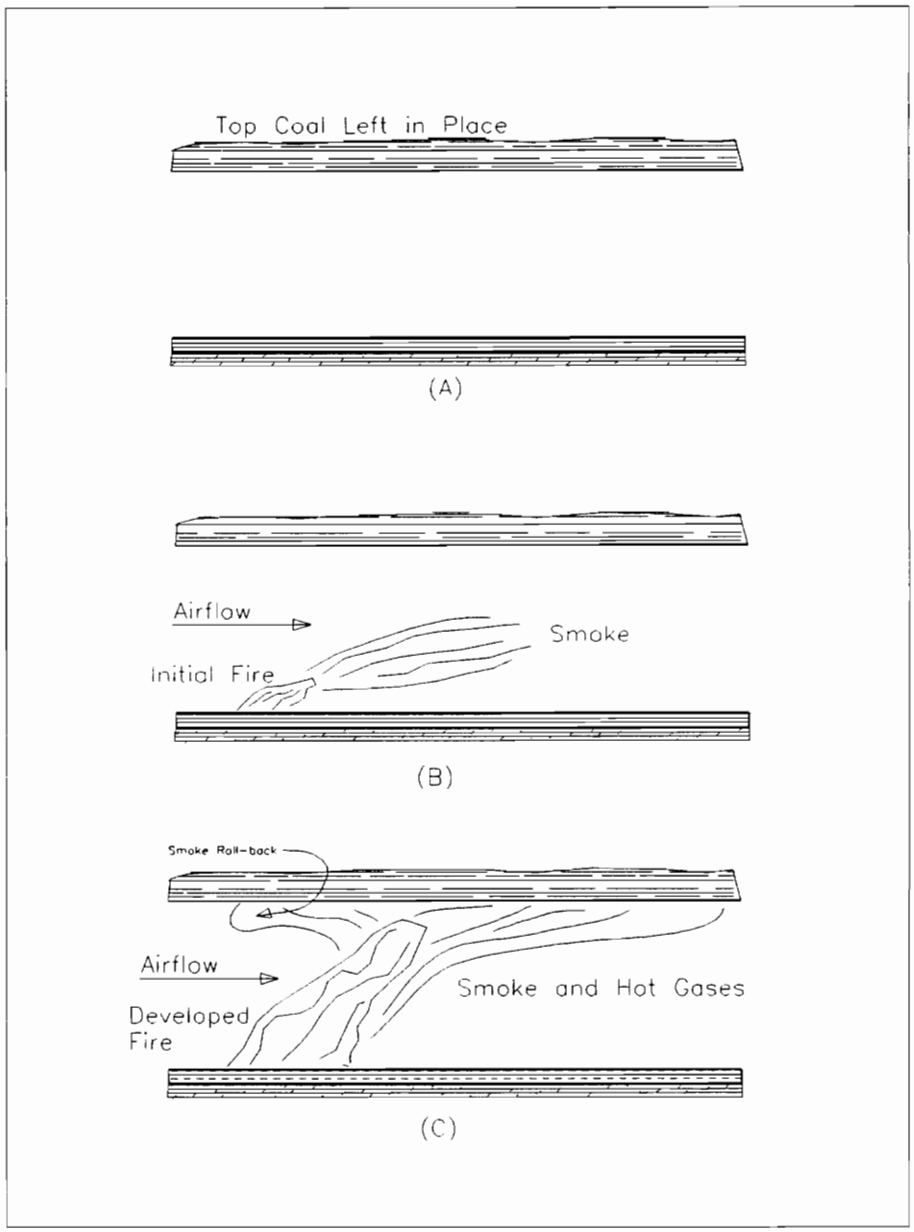

Figure 1-1: Stages in Fire Development.

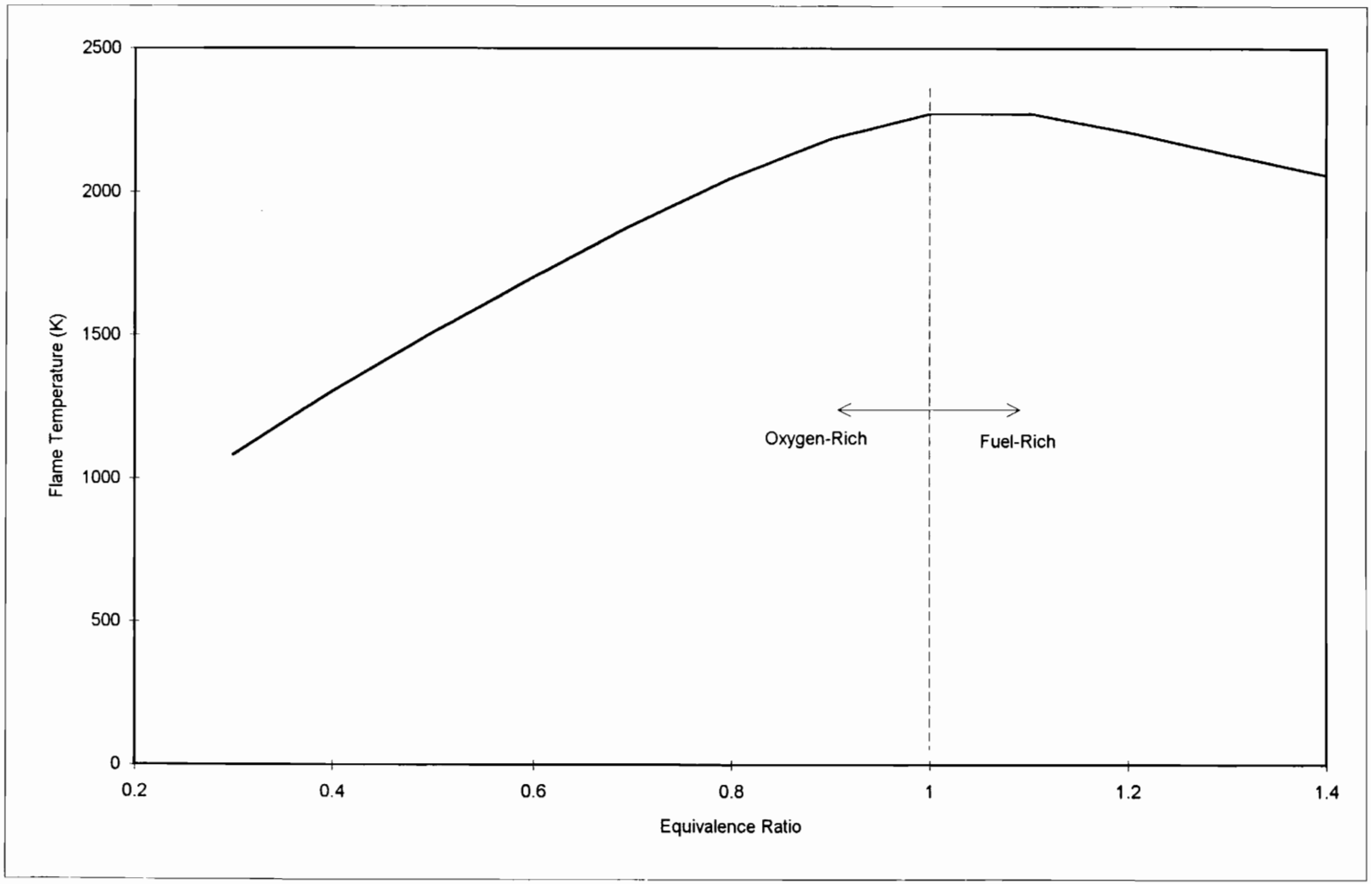

Figure 1-2: Typical Relationship Between Fuel/Air Mixture and Flame Temperature for Hydrocarbon Fuel

Some of the heat generated during combustion is used to volatilize fuel downstream. The combustion reactions can continue until, theoretically, all the oxygen has been consumed. The exhaust from the fire is now near its adiabatic reaction temperature. As the exhaust leaves the fire and begins to cool, the only direction for heat transfer is to the drift surfaces. This heat transfer is capable of volatizing the coal, since there is not sufficient oxygen available the excess fuel is carried along with the exhausts. The condition that now exists is a fully developed fuel-rich fire in a coal mine entry. The general differences between the oxygen-rich and fuel-rich regimes are illustrated in figure 1-3.

The hazard of this fire is compounded when a cross-cut is added to the visual model, figure 1-4. At this point consider that exhaust gases are leaking out of the fire drift to the fresh air drift. If the exhaust temperature is still above that required for ignition, the fire will re-erupt at the cross-cut. At this point a fully volatized fuel mixture is being mixed with fresh air, the flames that erupt start the entire process again, except that the fire is likely starting along the roof. It is in this manner that a fuel-rich fire can spread at rates up to ten times that of an oxygen-rich fire.

With a little more imagination one can perceive that the fire cannot be returned to an oxygen-rich state by increasing the airflow. Such an action would result in unreacted fuel to be combusted, increasing the total heat liberated allowing even more fuel to be volatized thus consuming the additional oxygen added to the system.

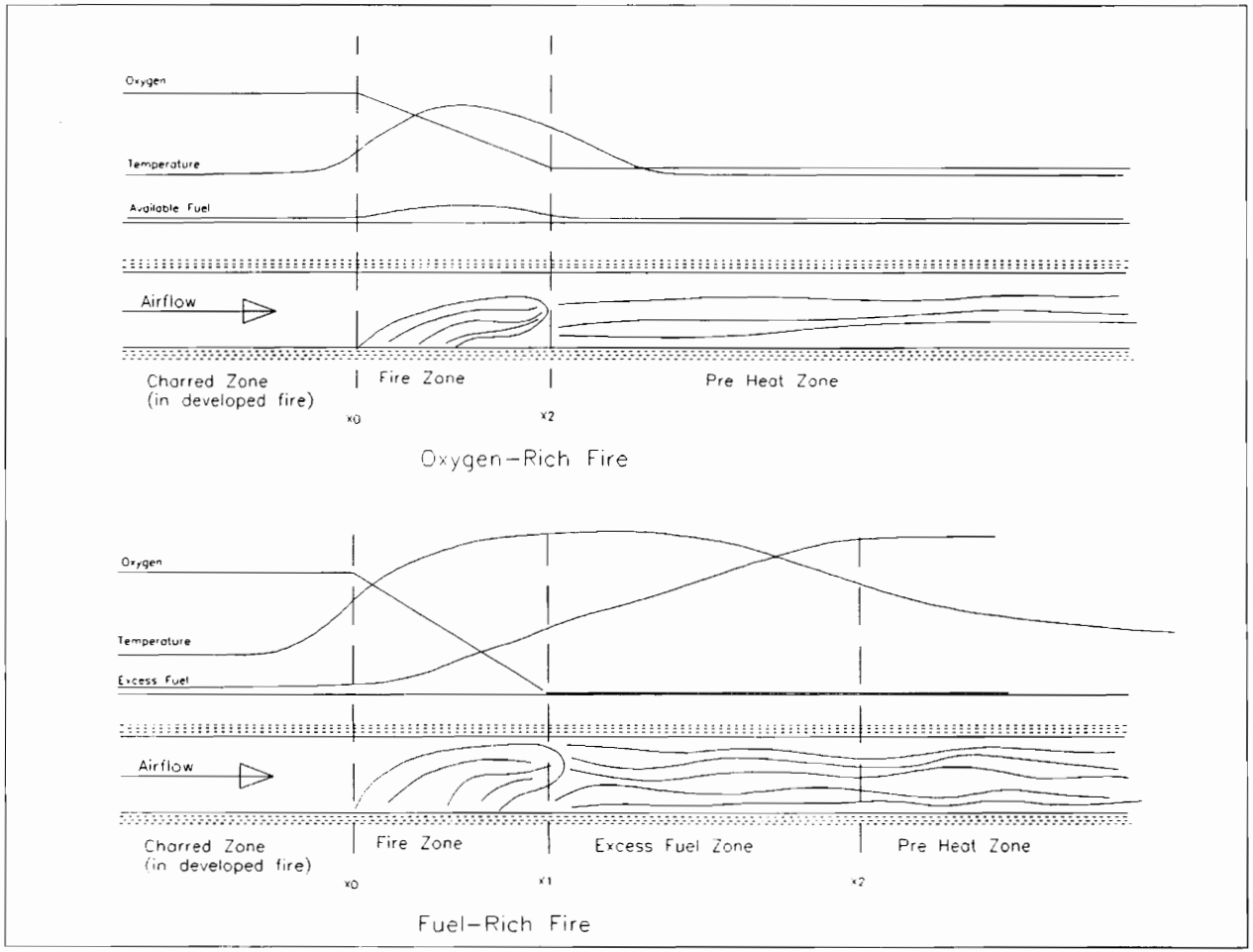

Figure 1-3: Comparison of Oxygen-Rich and Fuel-Rich Fires (after: de Ris 1970).

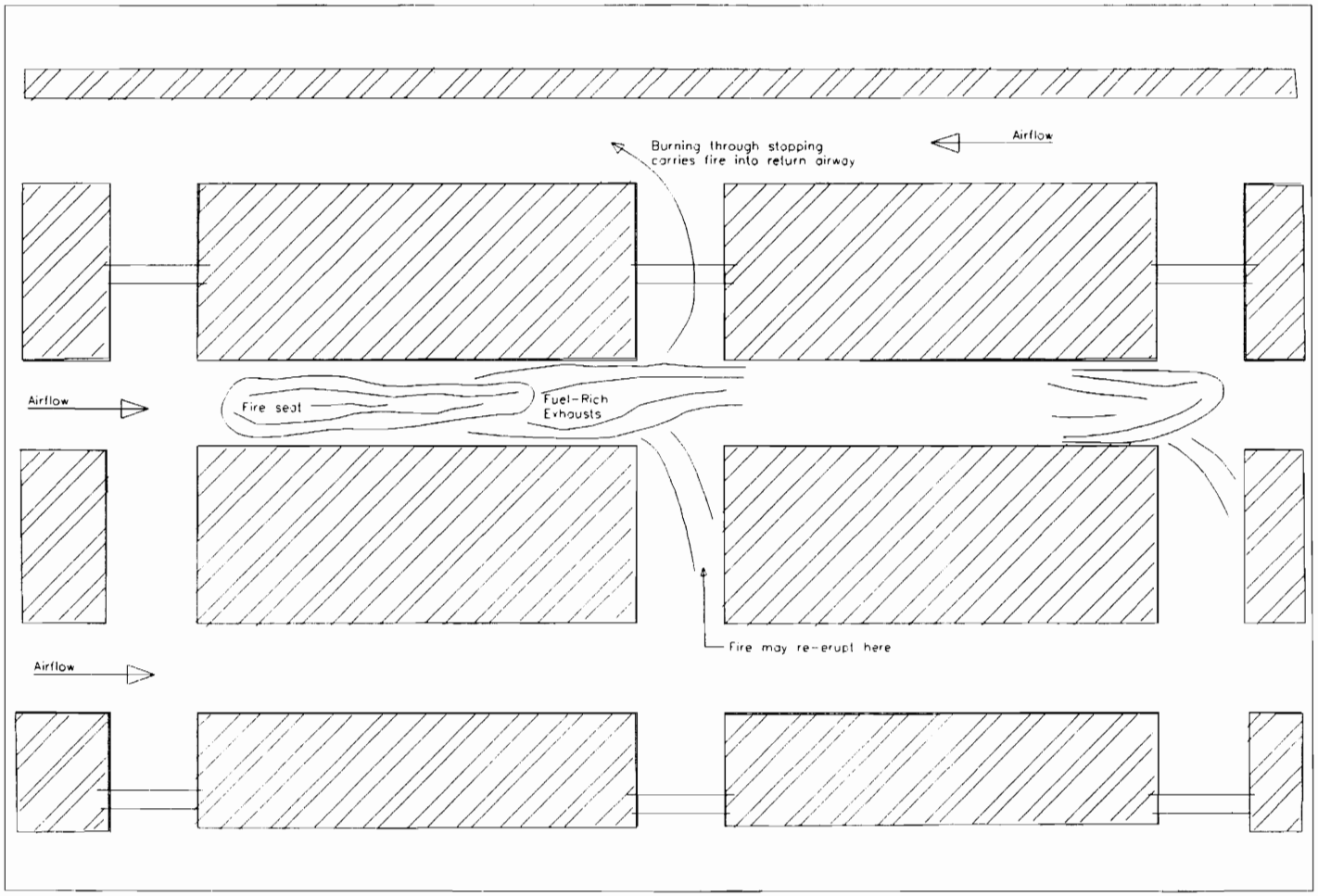

Figure 1-4: Spread Pattern of a Fuel-Rich Fire

1.3. Actual Fuel-Rich Mine Fires

The realization that a fuel-rich fire could develop spontaneously in a coal mine entry was made as the result of a mine fire in West Virginia in 1965. Considering the report of this incident one can hypothesis that the fire became fuel-rich as the result of the misguided action being taken by the mine operator. In this case, addressed in detail below, one can ascertain that the action taken was the result of a lack of knowledge, both of the actual situation and the likely outcome of actions to be taken. (No attempt to lay blame or imply negligence is intended.)

The three case studies reviewed below show several things of significance to this research: (1) understanding the conditions in and around the fire is very difficult, even for those who are intimately familiar with the mine configuration, (2) that the fire can become fuel-rich, as the result of the wrong action, or of insufficient action, and (3) once the fire has become fuel-rich, sealing of the affected area or entire mine is soon to follow. In the examples below, the development of the fuel-rich state does not follow the neat hypothetical model described above. From these examples, however, an understanding can be gained into what the mine fire-fighters are up against and what tools they may need in their attempts to save the lives of others, their own lives, and if possible the mine.

1.3.1. Mars Number 2 Mine, October 1965

Late in the evening of 16 October 1965 a fire was ignited in the Mars Number 2 Mine operated by Clinchfield Coal Company, in Wilsonberg, West Virginia. The events that

followed the initial ignition indicate that this fire may have become fuel-rich as a result of the attempts made to control the fire (Roberts and Blackwell 1969).

As a piece of mining equipment was being moved, workers used belting to insulate the equipment from live trolley wires. Apparently the belting wore through allowing the trolley wire to arc to the machine. The intense arcing, caused by a failure of the circuit breaker, ignited the belting, coal and, eventually, the machine's hydraulic oil. Approximately forty-five minutes after the fire was lit the main fan was stopped in an effort to slow the spread of the fire. The resulting "roll-back" of smoke and fumes drove the fire-fighters away from the fire. About 20 minutes after the fans were turned off they were restarted to clear the smoke and fumes from the fire. This action resulted in an explosion spreading debris and igniting new fires for long distances in the affected entry (Anonymous 1966).

Evidently, after the fans were stopped, the fire continued to burn liberating excess oil vapors so that a fuel-rich condition was achieved. When the fans were restarted, the supply of fresh air allowed the fire to flare-up engulfing the highly volatile mixture of oil vapors near the fire (Roberts and Blackwell 1969, Mitchell 1990).

Seven miners downstream of the fire died of carbon monoxide poisoning (Anonymous 1966). These deaths were reported as asphyxiation by Mitchell (1990), which is not an uncommon practice in carbon monoxide related incidents, since death occurs due to oxygen starvation. Although not indicative of a fuel-rich fire on its own, it is quite obvious that such a fire would produce quantities of carbon monoxide that would tax the

capacity of a conventional self-rescuer, not to mention the effects of the total depletion of oxygen. At this time the Self-Contained Self Rescuer (SCSR) did not exist.

1.3.2. Wilberg Mine, December 1984

On the evening of 19 December 1984 a fire erupted in an intake airway of the Wilberg Mine in Emery County, Utah. This fire exhibited characteristics that provide irrefutable evidence that a fuel-rich fire can occur in a mine, as suggested by Dr. A. F. Roberts, of the United Kingdom's Safety in Mines Research Establishment, in 1969.

The official Mine Safety and Health Administration (MSHA) report identifies an air compressor located in an intake airway to be the most likely source of ignition for this fire (Huntly, et al. 1984). Assuming that this was the case, it is likely that most of the nearly 30 gallons of oil in the compressor were discharged into the cross-cut where the compressor was located. It is believed that the oil, as a fine mist, came in contact with a highly heated component of the compressor and erupted into flames, much like a flame-thrower. In a supplemental report to the MSHA, Nagy (1987) states "The rapidity at which the fire developed and spread is consistent with fire from the heated oil fuel."

Reports of the fire fighting activities indicate that the fire had progressed nearly six hundred feet in the first four hours and between the fourth and fifth hours the fire had progressed to nearly eleven hundred feet (Mitchell 1990). Mine Rescue and Fire Fighting teams reported flare-ups when doors where opened. This was probably due to allowing fresh air to the hot fuel-rich gas mixture (Huntley, et al. 1984; Mitchell 1990).

The reports supplied by eye-witnesses indicate that "roll-back" of smoke and heat was not occurring in the airway of the fire during the initial stages (Huntley, et al. 1984). Later reports from the fire fighting teams indicated significant smoke "roll-back" (Mitchell 1990).

After over four days of fire fighting and rescue efforts, sealing of the area began. Recovery work began in February 1985 with the origin of the fire not being reached until July 1986.

1.3.3. Orchard Valley Mine, June 1986

On 1 June 1986 a fire occurred at the Orchard Valley Mine near Paonia, Colorado. This fire resulted in the sealing of the mine at its portals and shafts. This fire was determined to be, most likely, the result of spontaneous combustion (Derick 1993).

Based on the paper "Mine Emergency Response" by Mr. R. L. Derick a brief synopsis of this fire (Derick 1993) is:

1) Operation of one of the two main fans was terminated. The mine was idle and therefore no personnel were underground. Smoke and hot air were observed to be flowing upstream, against the airflow.

2) Use of foam generating equipment began using two foam generators. During this time the fire was starved of fuel due to the foam.

3) Once the available foaming agent had been depleted the mine was evacuated, the second main fan turned off, and the intake fire doors sealed.

4) With the reduction in airflow and the increase in available fuel the fire quickly transformed from and oxygen-rich to a fuel-rich fire, evidenced by a nearly six fold increase in the fuel consumption rate.

5) Eventually the entire mine was sealed. Production from the mine resumed in December 1986.

1.4. Purpose of this Research

Going back to the fire triangle one should be able to extinguish any fire by removing any of the individual legs (fuel, oxygen, or heat). The method chosen to effect the appropriate leg may be based upon the material that is burning, the location of the fire relative to combative personnel, or the availability of extinguishing agents. In a typical open fire in a coal mine entry the methods available to the fire-fighters are control of the airflow to the fire, application of water, or inertization techniques. These common practices are covered in some detail in chapter 2 of this thesis.

Attempting to control an open fire by limiting the ventilating airflow to the fire may slow its spread, at least temporarily. Even during conservative airflow restriction it is possible that the velocity of the airstream may be reduced to the point that the buoyant forces generated by the fire overcome the inertial forces of the airstream. When this occurs, smoke and exhausts from the fire will begin to "roll-back" against the in coming fresh air.

This situation may lead to restricted visibility and these gases could be explosive and/or toxic, increasing the hazard to the fire-fighters. Over-restriction of the air into an established fire, that is one that has begun to extend beyond its point of origin, may lead to the increased likelihood of an explosion as the fire accelerates from oxygen to fuel-rich combustion.

The direct application of water can be hindered in the mine by the great distances over which the underground workings may cover and the relative dearth of areas covered by sprinkler systems. This leaves a direct attack with hoses and nozzles as the initial means to apply water. Under current regulations and existing nozzle technology the effective range of a conventional water attack may be less than thirty feet (Mitchell 1990). This condition is further compounded by the inability of conventional systems to produce water droplets that can be carried a significant distance in the air stream, thus restricting the capability to get water deep into the established fire.

Water may also be carried to the fire region in the form of a high expansion foam. This foam is carried along the drift by the airflowing across its surface, as the plug develops. Once the foam plug has been developed the airflow pressure drives it forward, hopefully towards the fire. Foam plugs are restricted by several associated phenomenon; since they restrict airflow to the fire the problems associated with ventilation changes need to be considered, the amount of water carried by the foam plug is small compared to the amount of air within the plug, and radiant heat from the fire can cause the plug to break down before it gets close enough to affect the established fire.

Inerting methods control the fire by removing most or all of the oxygen from the fire location in such a manner as to cease the combustion process. The inerting agents commonly employed include nitrogen, carbon dioxide, and the products of combustion from jet engines. Inerting requires rather extensive action to implement, ranging from the staged construction and closing of seals to changing the mine infra-structure to accommodate the transmission of the inerting agent; not the mention the provisions to generate large quantities of the inerting agent.

With the recent philosophy whereby the Halon fire extinguishing agents have fallen out of favor, much research has centered on an effective replacement for this fire-fighting agent. One means that has shown promise in industrial applications, including oil storage fires, is water mist, or fog. The general theory behind the use of water fog lies in the ability for it to affect all three sides of the fire triangle and its ability to be carried for extensive distances in the air stream. As applied here the scale of the fog is that which is found in nature with particle sizes ranging from 5 to 50 microns in diameter. As the fog enters the fire the liquid water is converted to water vapor consuming heat, the water expands some 1700 times between the liquid and vapor states displacing oxygen, beyond the fire the condensing water coats the available fuel. In this manner the fog works against all three sides of the fire triangle at once.

It is postulated that the application of water mist to a mine fire, particularly one that is fuel-rich, can make the fire more manageable for the engineers and fire-fighters, reducing the chance of loss of life and decreasing the likelihood that the capital investment of the mine will be lost. This research is intended to investigate the hypothesis that a large scale, fog generation system could effectively be used to combat fuel-rich fires in coal mine

entries. This investigation will be limited to work in a scale model with the general results extrapolated back to the defined prototype, coal mine entry.

2. *LITERATURE REVIEW*

Research into the field of fires appears to be divided chiefly into two distinct studies of its mechanism. The first dealing with the application of fire for the benefit of human society, the second dealing with the means to minimize the damage caused by fires that are unwanted.

With the technology available for use in the subsurface environment today there is little need for open fires in support of mining activities. Further, with the distinct differences between building and compartment fires versus duct and mine fires the scope of this review will therefore be limited, with a few exceptions, to that literature of interest; that is the mechanisms that affect the development and spread of fires in ducts and mines, the tactics of fighting such fires, and the current research surrounding them.

In late 1969, Dr. A. F. Roberts and J. R. Blackwell published a paper entitled "The Possibility of the Occurrence of Fuel-Rich Mine Fires" (Roberts and Blackwell 1969). Through the publication of this paper the mining community was introduced to the general concept of a fuel-rich fire, and its causes and implications. In the introduction to this paper the authors cite a previous work by D. G. Wilde, in which Mr. Wilde makes the

statement "...in the very largest [mine] fires wood has nearly always been a major, if not the principal fuel..."(Wilde 1967, Roberts and Blackwell 1969).

Another paper is that of Dr. M. J. McPherson entitled "The Development and Control of Open Fires in Coal Mine Entries" published in 1993 (McPherson 1993a). One of the important factors of this paper is the brevity by which Dr. McPherson describes the causes and impacts of open fires in coal mines. Dr. McPherson observes that despite, and perhaps because of, the evolving technology applied to mining and mine ventilation systems "...the past decade has seen a renewed concern with respect to mine fires and explosions." He bases this as being due to the plethora of hydrocarbon materials being used in the modern mining environment. Dr. McPherson reiterates the concern that once a mine fire has progressed to a fuel-rich condition there is little chance of extinguishing without sealing the fire off. He does, however, suggest that a means may be available to gain control of the fire by the application of water as a natural scale fog. It is this theory that forms the basis of this research project.

2.1. Mechanics of Coal Mine and Duct Fires

By reviewing the previously mentioned paper by Roberts and Blackwell, and a later publication "Duct Fires," by John de Ris (1970), one can quickly gain a feel for the mechanics surrounding a fire burning in a fuel lined duct and the corollary in a coal mine airway. In an address of comments to de Ris's (1970) paper Roberts (1971a) identifies three regimes of duct fire behavior. These surround the likelihood that the ignition source results in an oxygen-rich fire or a fuel-rich fire regardless of the size; or a condition whereby the fire may be oxygen-rich or fuel-rich depending on the size of the ignition

source. He seems to leave the question as to the characteristics that will cause the result of one of these outcomes.

An investigation into the critical conditions of duct fire development is presented by Hwang and Litton (1984). They define a dimensionless parameter (E) to evaluate the likelihood that ignition can take place or that sustained propagation will occur. This parameter is defined as:

$$E = \frac{\dot{Q}_f}{\left(\dot{m}_\infty c_{p\infty} T_\infty\right)}.$$

With the necessary condition for ignition being:

$$E \geq \frac{\left(T_{ig} - T_\infty\right)}{T_\infty}.$$

Where $\dot{Q}_f$ is the source fire strength, $\dot{m}_\infty$ is the mass flow rate of air upstream, $c_{p\infty}$ is the specific heat of the upstream air, T_∞ and T_{ig} are the upstream and ignition temperatures, respectively. Based on their research a value of $E > 1.5$ is required of the ignition of untreated timber. Sustained combustion requires $E > 3$ for untreated timber and $E > 5$ for treated timber. The researchers note that the relevant value for E is dependent on the configuration of the available fuel and that critical E is inversely proportional to the fuel loading density.

The general means for the propagation of a steady-state fire in a duct or mine entry can be expressed in the following manner. Fresh air enters the combustion zone of the fire where

consumption of oxygen begins by rapid chemical reaction. In this region fuel is being vaporized from the solid phase and reacting with available oxygen. Once all of the oxygen has been consumed the products are still at a temperature above that required to vaporize the solid fuel. These heated products transfer heat to the solid fuel on the surrounding surfaces, vaporizing fuel that continues in the products stream unreacted. Once the products have cooled below the temperature required to vaporize the fuel they continue to pre-heat the fuel until the initial ambient temperature is re-established. For this type of fire numerical models of the phenomenon ordinarily assume that the vaporized fuel does not recondense and that the velocity of the fire is small compared to the velocity of the air stream (Comitis, Glasser, and Young 1994).

2.2. Fuel-Rich Fires

Once a fire has been ignited in a duct or mine entry there exists the possibility of the fire making the transition from an oxygen-rich state to a fuel-rich state. Dr. Roberts defines three situations in which a fuel-rich fire may develop (1) by the unrestricted growth of an oxygen-rich fire, (2) by the action of a very large ignition source, or (3) by the action of reducing the ventilation quantity to an oxygen-rich fire (Roberts 1970a).

While an oxygen-rich fire may represent a fairly limited phenomenon, as described above, a fuel-rich fire can quickly become overwhelming and encompassing. In a response to "Duct Fires," by de Ris (1970), Roberts states that, in its fully developed condition, a fuel-rich duct fire may encompass some 370 times the duct characteristic dimension (Roberts 1971a). He breaks this down, beginning at the first significant temperature rise, as:

120 Diameters	Burnt-out zone
100 Diameters	Charcoal zone
30 Diameters	Pyrolysis zone
120 Diameters	Pre-heating zone
370 Diameters	Total involved length

The configuration of this is somewhat different than that presented by later authors, Comitis and others (1994). When one considers a fire that has been burning for some period of time, the principle omission is the lack of the specific excess fuel zone. Although he is not explicit, it is probably safe to assume that Roberts included this in the definition of the pre-heating zone.

Roberts further goes on to state, in the same paragraph, that the charcoal zone may have an important part in the overall picture as it may lower the level of oxygen reaching the pyrolysis zone. Presumably the charcoal zone could reduce the oxygen content to a point that an existing fire would become fuel-rich as the oxygen is remove from the incoming air. It is unclear what Dr. Roberts expects of this type of a fire, since flaming combustion ceases when the oxygen concentration drops to between 16 and 17% (Burrell and Seibert 1912). The total or near total consumption of oxygen in the charcoal zone appears unlikely due to the relatively slow burning in the charcoal compared to that of the flaming combustion. This is because the vast majority of the volatile materials have been burned off leaving only the slow burning elemental carbon (Haessler 1989).

2.3. Transition from Oxygen-Rich to Fuel-Rich

As we begin to look at the transition from the oxygen-rich to fuel-rich states the concept of the fuel/air and equivalence ratios should be introduced. The fuel/air ratio represents

the relationship between the available fuel and oxygen at a molar level. The stoichiometric fuel/air ratio represents relative concentrations whereby all of the fuel and oxygen will be consumed in the completed combustion reaction. The equivalence ratio expresses the existing fuel/air ratio to the stoichiometric fuel/air ratio (Kuo 1986).

$$\phi = \frac{\left(fuel/air\right)}{\left(fuel/air\right)_{stoich}}$$

While the fire is in the oxygen-rich regime ($\phi < 1$) it is spreading by radiation and convection from the flames to the local wood. The heating of the bulk air stream is insignificant beyond the local region, thus does not affect the spread of the fire. As the fire grows in size the temperature of the airstream rises to a point where it can play a role in the spread of the fire. Heat transfer from the exhausts can cause pyrolysis of the fuel downstream of the fire without direct contact of the flames. In this manner, a fire burning in a fuel lined duct can accelerate to a stage such that all of the available oxygen is reacted in the fire (Roberts and Clough 1967a). This is the fuel-rich condition where $\phi > 1$. Additional volatile fuel is carried away from the fire in the exhausts. This volatized fuel may ignite should the exhausts come in contact with oxygen while still at elevated temperatures. A cooled exhaust and fresh air mixture may be explosive, depending on the ratio of the mixture.

In evaluating the likelihood that a fire will make the transition from the oxygen to fuel-rich regimes, Roberts and Clough (1967a) observed that the tendency to make this transition is inversely proportional to the size of the airway. That is, the smaller the passage the more likely the fire is to spontaneously transition from an oxygen-rich to a fuel-rich state.

Chaiken, Singer and Lee (1979) observed that, in their tunnel with coal fuel, when the fuel was limited to the floor surface the fire propagation was limited to the oxygen-rich state. In further tests with coal on all four of the interior surfaces the fires began oxygen-rich, transitioned to fuel-rich, and returned to oxygen-rich as the fire died out.

The presence of top coal is indicated in the Mars No. 2 mine fire, discussed in chapter 1, above, the USBM report indicated ignition of the "coal roof and ribs" (Anonymous 1966). No indication of top coal is given concerning the Orchard Valley mine fire (Derick 1993, Timko, Derick, and Thimons 1987) , it is known, however, that this fire began spontaneously as a concealed fire, and was made fuel-rich by the fire fighting efforts.

Once the fire has made the transition from oxygen-rich to fuel-rich it is likely that its rate of advance will accelerate to nearly ten times that of the oxygen-rich state (Roberts and Blackwell 1969).

2.4. Transition from Fuel-Rich to Oxygen-Rich

So long as there is fuel for the fire to burn there is no direct mechanism that will cause a fuel-rich fire to return to an oxygen-rich state. Experimental evidence reported by Roberts (1970a) showed that, "A fourfold increase in ventilation rate to a fuel-rich fire only had the effect of making it burn more vigorously."

One can imagine that if the fuel-rich fire can be brought back to an oxygen-rich state it will be easier to combat. The oxygen-rich state can be approached more readily from upstream, and does not present the same degree of hazard when attempting make an

approach from downstream. The ability to reduce the fire back to oxygen-rich has been proposed by McPherson (1993a). The mechanism by which this regression is postulated is based on attacking the fire on all three sides of the fire triangle. The net effect being to cause the fire to regress by removing the elements of the fire itself; fuel, heat, and oxidizer.

2.5. Current Coal Mine Fire Fighting Tactics

Without a doubt water is by far the most versatile fire extinguishant in use today. The use of water in fighting fire is so fundamental that even when preparations are underway for more drastic methods, direct attack with water should continue for as long as possible (Ramlu 1991).

2.5.1. Water

A major part of fighting any mine fire begins with the application of water. During fire fighting activities with water it is best to stay upstream of the fire. In this manner the personnel remain in relatively fresh air and should have a clear means of escape. The general philosophy behind the use of water is very much the same as its application in fires on the surface. Where there is a large supply of oxygen available to the fire, water works against two of the sides of the fire triangle, heat and fuel. The increase in sensible heat and the latent heat of evaporation accounts for some 2600 kJ/kg to convert water from a liquid at 20°C to vapor at 100°C. Furthermore, the water that is not vaporized begins to coat the fuel reducing the production of volatile fuel gases. Under some conditions, such as limited fresh air sources the generation of water vapor will serve to displace oxygen, reducing its role in the combustion process.

The overall utility of water as a fire fighting agent lends it self well when coupled with the relative ease at which water distribution systems can be installed and maintained. During fire fighting activities the water available will not only be required for direct attack against flames but may be required for other roles, including, cooling stoppings and spraying in the entries down stream of the fire. The total water requirements during a fire may exceed 38 liters per second at a minimum delivery pressure of 345 kiloPascals (600 gal/min at 50 psi) (Gallick 1991).

In order to assist the utilization of water during a fire scenario several considerations should be made. These include, concurrent flow between the air in the drift and the water in the pipe, locations of valves and fittings in strategic locations. Underground water pumps and their power supplies should also be carefully laid out to minimize the likelihood of disruption during a fire (McPherson 1993b). It is also important that the team fire fighting gear be inspected on a routine basis and replaced as necessary, even if never used.

Fire drills and exercises are an important part of a mines basic fire control strategy. On a small scale these can be used to train the miners in the operation of the basic fire fighting equipment that is available to them. On a large scale these exercises can be used to train the line and staff management, engineering, and labor personnel in the complexities and possible outcomes of various fire scenarios (Eschenburg 1982).

The direct application of water to the fire requires that personnel get fairly close to the fire. As the fire grows hot gases and smoke are likely to begin to "roll-back" against the incoming fresh air; hampering the visibility towards the fire, providing a source of toxic

gases to the fire-fighters, and further increasing the ambient temperatures upstream of the fire. To combat the role-back, fire-fighters may have to expend some of the water as a spray directed against the roof. This action can counter act the inertia of the flowing stream and cool the gases. Once in the vicinity of the fire, the attacking personnel must try to spray as much water as possible into the fire. Of particular importance here, since the fire is being fought from only one direction, is getting the water as deep into the fire as possible. The ability to spray deeply into the fire can be hampered by a number of phenomena, in particular the size of the particles generated by the nozzle, and the delivery pressure of the water.

Typical mine conditions limit the effectiveness of water sprays to about 10 meters. This is due to the design of, and available pressure at the nozzles. Current legislation in the United States limits waterline pressure to 690 kPa (100 psi). It has been projected that line pressures on the order of 800 to 1400 kPa would be required to increase the effective range of the typical water spray to 30 meters (McPherson 1993b, Mitchell 1990).

Two particularly interesting observations are made by Scheffey and Williams (1991a and 1991b) regarding the application of water to fires. They observed that in open, outdoor fires a water flow rate per surface area of 27.5 g/m^2s was required to extinguish the larger, test scale, fires. Their best overall results were obtained with a total water supply of 2.6 l/m^2 of burning surface. During tests concerning ship board, compartments fires they found that 10 to 20 times as much water may be required compared to the outdoor test fires. They attribute most of the increase to the inefficiencies of fighting the larger fires in a compartment, versus fighting the fires in the open and under laboratory conditions.

Fire fighting by the application of water from the upstream side should be the first consideration when developing the mode of attack. This procedure does have its limitations and if the fire cannot be brought under control by a few hours effort plans should be made to begin more rigorous efforts (Ramlu 1991).

2.5.2. Foam

In *Mine Fires and Mine Rescue*, Ramlu (1991) reports that the use of foam plugs has been successful in fighting mine fires in roadways where direct attack with water is not possible. With sufficient ventilating forces and a properly generated foam, research by the USBM has shown that a foam plug may be transported over 300 meters (1000 ft) (Nagy, Murphy, and Mitchell 1960).

The experiments conducted by Nagy, Murphy, and Mitchell (1960) showed that the foam plugs could be efficacious against coal, oil and wood fires in a full scale coal mine entry. The tests involved fires covering floor, rib, and roof fuels in varying configurations. Where the water content of the foam was less than 0.20 kg/m^3 (0.0125 lb/ft^3) the foam was not capable of controlling the fire. Above this water content, the foam appeared to be capable of controlling the experimental fires.

The application of foam plugs must be closely monitored, as the reduction in airflow across the fire may cause an originally oxygen-rich fire to become fuel-rich (McPherson 1993b).

Several factors work against the application of foam for fighting mine entry fires. Foam does not appear to be effective against deep seated, rapidly advancing, buried or dead end fires (Ramlu 1991). An insufficient amount of foaming agent that leads to running out of foam prior to controlling the fire may be as bad as no foam at all, a condition that was experienced at the Orchard Valley Mine (Derick 1993; Timko, Derick, and Thimons 1987).

2.5.3. Inertization

The use of the practice of inerting the atmosphere within the mine fire area has been employed in most of the mining world. The techniques used and the levels of success vary from continent to continent. In North America and Europe the gas of choice tends to be nitrogen, with some minor application of Carbon Dioxide, while the Eastern Europeans and the Russians prefer the use of the products of combustion. Each of these methods have, as can be expected, their strengths and weaknesses. A very good comparison of these three inerting media is presented by Bacharach, Craven, and Stewart (1986). A synopsis of their comparison is given in Table 2-1.

The generation of large quantities of inert gas is a relatively straight forward process. Nitrogen or Carbon Dioxide are delivered to the site in a liquid form. The liquid is pumped into an evaporator to generate the gas. The gas can then be piped into the mine through existing, or specially laid, pipes. Major controlling factors to consider are the rate at which the liquid (or solid) phase can be delivered to the site and the availability and size of evaporation systems. Either of these can limit the quantity of the inerting agent that may be applied to the fire. The type of the evaporator may also affect the quantity of gas

Table 2-1: Comparison of Inerting Media, (after Bacharach, Craven, and Stewart 1986)

Products of Combustion		Nitrogen		Carbon Dioxide	
Advantages	Disadvantages	Advantages	Disadvantages	Advantages	Disadvantages
Can be generated on site Relatively inexpensive Can produce high rates of inert gas Can be brought on line quickly Exhaust contains large quantities of water to aid cooling Can maintain normal ventilation flow to the fire area due to the inert gasses	Large quantities of fuel, water and fresh air are required Products vary on concentration and may contain undesirable gasses Products may contain over 1% O_2 Products delivered at a relatively high temperature (80-90°C) Difficulties exist in transporting the gasses over long distances High water content may cause water gassing May have adverse effects on mine ventilation system Not a permissible system Cannot use gas analysis to monitor the state of the fire	Inert Readily available in large quantities Does not interfere with gas analysis downstream of the fire Density near that of air Mobile evaporation plants are readily available May be delivered as a liquid to the fire site	Storage results in large evaporative losses More expensive than Products of Combustion Gaseous delivery to the fire will be limited by the size of the evaporator	Commercially available as a liquid or solid Extinctive Commercial evaporation plants are available Can be delivered to the fire at reduced temperatures High density may be used to fight fires in depressed areas and down dip.	Expensive Corrosive in presence of water Affects ability to use gas analysis to monitor the state of the fire Affects prediction of explosibility Gaseous delivery limited by the capacity of the evaporator High density may cause separation in the airflow, reducing overall effectiveness

that can be produced. An ambient temperature evaporator will not produce significant quantities of gas compared to an externally heated unit. The externally heated evaporator presents further strains on the infra-structure by requiring provisions for the fuel system (natural gas, propane, diesel oil, electricity, etc.) and for the heat transfer systems, whether direct fired or by hot water (Bacharach, Craven, and Stewart 1986).

The use of Products of Combustion (POC) as an inerting agent has usually been achieved with the application of a turbojet engine equipped with an after-burner. Such systems developed by Russian and Polish agencies have proven capable of producing up to 30 m^3/s of inerted gases. The hot exhausts are cooled through a water filled radiator. The hot water is then rejected as waste or piped through an evaporative cooler. Due to the low delivery pressure of the exhaust gases the system must be placed relatively close the fire, or be assisted with the application of ducts and blowers. An obvious problem with this type of system is that the jet engine is not, by nature, permissible in the coal mine environment. It is possible, though, to argue that this fact is of little consequence in a mine that is already engaged in fighting an existing fire (Bacharach, Craven, and Stewart 1986).

Some of the first field applications of inerting fires appear to come from the United States, where in the late 1940's carbon dioxide was used to control two fires in the Illinois coal fields. The first of these fires (Valier Mine) resulted from an electrical failure, the fire was burning in a caved area and it was believed that the burning coal was buried beneath the roof fall. Rather than attempt to fight the fire directly the mine management decided to try to seal the affected area. This technique failed to control the fire and resulted in two explosions inside the sealed area. Experiencing these failures the management then

attempted to flood the area with water, behind dams. Officials from the USBM found that the dams would not be sufficient to contain the expected hydrostatic head and suggested that they attempt to flood the area with gaseous carbon dioxide. The theory was that the CO_2 would render the atmosphere behind the seals incapable of becoming explosive while the seals were reconstructed to isolate the fire. Forty-five hundred kilograms (10000 lbs) of CO_2 were piped through an existing sprinkler system pipe to the affected area of the mine. It is believed that the introduction of the CO_2 extinguished the fire following its introduction. A feel for the size of the fire can be gained from the reported 1900 tonnes (2060 st) of rock, coke and coal that was later removed from the fire area (Westfield, Brumbaugh, and Whittaker 1950).

The second of the fires (Peabody No. 59) in Illinois proved that there were some problems with the use of Carbon Dioxide. This fire was also of electrical origin, resulting from a train collision in a main haulage road. Initial attempts to control this fire consisted of a direct attack with rock dust and excavation of burning material. Some three days following the eruption of the fire mine management decided to attempt to seal the fire. Based on the success of CO_2 flooding experienced at the Valier Mine, and with the assistance of USBM personnel, inertization of the atmosphere in the affected area was to be attempted. Over a period of some 31 hours, 19 tonnes (21 st) of gaseous CO_2 was piped into the area, believed to be sealed, surrounding the fire. The volume of the CO_2 gas is reported to be "well in excess" of the volume of the affected area. In the aftermath it was found that the CO_2 had not been completely successful in extinguishing the fire, a large quantity appeared to have leaked into previously abandoned workings. The CO_2 did, however, cool the fire area sufficiently to allow the sealed area to be reopened without the risk of the fire rapidly regaining strength (O'Connor, Malesky, and Higgins 1950).

An early application of Nitrogen as an inerting agent is reported from a British colliery (Fernhill Colliery). The reported fire occurred as an ignition related to blasting. Early attempts to control the fire were made with water, which appeared to be successful. A follow up team later found the fire to be spreading. About 12 hours after the ignition the mine management decided to seal the affected area. They expected that this action would cause the atmosphere around the fire to become extinctive, however, the desired effect did not occur and further attempts were made to plug all the leaks in the seals. Experiencing continued failure to control the fire in this manner the decision to use Nitrogen as an inerting agent was made by the mine management. By applying N_2 as an inertant the managers wanted to: dilute the combustible gases (which were increasing in concentration), reduce the oxygen content to below 12 percent to further eliminate the possibility of an explosion and make the atmosphere extinctive, and allow normal mining activities to continue in the remainder of the mine. Engineers at the mine determined that an nitrogen plant capable of producing 0.4 cubic meters per second (840 ft^3/min) at 99.5% pure would be required. Injection of the nitrogen was attempted no less that four times, each for periods extending for several days, with actual nitrogen flow rates between 0.2 and 0.4 m^3/s (420 and 840 ft^3/min). Each time, after the nitrogen injection was suspended the fire appeared to rekindle and grow. While this fire was eventually brought under control it points out several factors and weaknesses relevant to inertization. The application of nitrogen allowed exploration to be conducted without an explosion hazard, and allowed work to continue in the remainder of the mine. However, the effectiveness of the nitrogen was limited by the leakage occurring around the affected area. The ability of the nitrogen injection to be efficacious may have been limited by the time that was required to secure and set-up the nitrogen gassification plant (Vaughn-Thomas 1964).

Later application of Nitrogen to fighting mine fires is discussed concerning the French mining industry by Froger (1986). The application of nitrogen in France is used to control spontaneous fires in gobs, and to hinder the eruption of fires by preventative injection of nitrogen. Typical injection systems use liquid nitrogen transported to the site in tanks and a truck mounted evaporator. The advantages to using nitrogen in the French mines arises from reducing the likelihood of spontaneous combustion in mines subject to this hazard. This does not come without a relatively high cost. To reduce the cost of the injected nitrogen some French mines have connected into commercial nitrogen pipeline systems.

Experience with inertization techniques has proven to give marginal to limited success in the coal mines of India. Applications in India have been made using gaseous carbon dioxide and nitrogen, direct use of liquid nitrogen, and flue gases from fuel oil combustion. Where applied, the fuel oil was burned on the surface, with the exhaust gases being piped to the underground (Banerjee 1987).

2.5.4. Sealing

The most drastic measure to be taken as a result of a mine fire is the complete sealing of the affected section or sections or even the entire mine. Despite the severity of this measure, it is frequently taken as a normal course of action when efforts to fight the fire begin to seem futile. Once the affected areas have been sealed, several months to several years may be required before the areas can be reopened.

The construction of seals can be a complicated and drawn-out process that often places the emergency personnel in significant danger. During the sealing process the atmosphere may pass through the explosive range, which can result in an explosion that destroys the seals being constructed. Such conditions were experienced at the Valier Mine fire discussed above (Westfield, Brumbaugh, and Whittaker 1950). In addition, sealing of the fire area may be dependent on closing off all sources of access to the fire area. Unknown break-throughs to abandoned workings, or other mines can have an affect on attempts to seal a fire, as will break-throughs to the surface.

Many of the advantages and problems associated with sealing a fire can be seen in the aftermath of the Wilberg mine, Emery County, Utah fire of December 1984, as reported by Moon (1993). The source and severity of this fire has been discussed previously (section 1.3.2), so only the sealing efforts will be discussed here. Construction of temporary seals at the Wilberg mine began about 4 days after the fire erupted. The same day that the temporary seals were started, the mine was evacuated as gas analysis showed a trend towards an explosive environment. Two days following the evacuation, fire reached the intake portals to the mine. At this point the plans were started to seal the 15 active mine openings, and over the next 12 days these entries were sealed. Construction of the seals was performed from locations outside of the mine. Bore holes were drilled into the entries near the mine portals, through which concrete was pumped to cap the rubblized material near the adits; working inby to outby until the entire portal area was sealed. Completion of three inby remote seals, one in each entry, allowed the rubblized caps to be removed so that the areas surrounding the remote seals to be grouted. Following the grouting the seals and exposed coal seam were shotcreted to prevent air from leaking into the mine. About 6 months following the construction of these original

remote seals the fire showed signs of regaining strength. To further seal the entries boreholes were drilled inby the original remote seals, and more flyash and concrete mix was pumped into the mine drifts. About one and a half times as much material was pumped during the second seal construction as was applied in the initial sealing efforts.

Following the construction of the second seal the fire showed a continued downwards trend. Prior to attempting to reopen the affected areas a mixture of rock dust and water was pumped into the workings around the seals to cool the area and quench any place that may have still been burning. This entire effort proved effective in gaining control over the fire, however, over two years elapsed between the initial construction and the removal of the seals. Further compounding the construction of these seals was the very rugged, mountain terrain surrounding the mine (Moon 1993).

In a 1989 incident in France, a seal was constructed remotely to isolate a fire burning in a caved waste area (Naquet 1990). The mine management desired two factors in attempting to fight the fire. First, they did not want to reverse the mine ventilation. Second, they wanted to minimize the need for any personnel to work downstream of the fire. The first course of action selected was to barricade the region and flood it with nitrogen through a pipeline from an upper level. This action did not appear to have an effect on the fire. With this observation the management decided to isolate the fire and try to fully inert it with nitrogen. Three holes were drilled into the return airway so that a concrete dam could be constructed, followed by injection of a resin foam to complete the seal. This technique proved to be satisfactory in gaining control over the fire.

2.6. Current Research

On going research into fires and the application of extinguishing agents can be found from two sources of noteworthy interest. The United States Bureau of Mines (USBM) has conducted research into the nature of mine fires at its Pittsburgh, Pennsylvania office and at the Lake Lynn laboratory in the Allegheny mountains of Pennsylvania. This research has dealt with the origination and development of fires in mine entries, both in scaled and full sized models. Furthermore, the USBM has performed research dealing with the products of combustion in mine fires and the nature of explosions in mine entries. The research of interest from the general industrial sector is that which deals with the application of water mist to industrial and marine fires. The use of water mist in industrial is related to the forthcoming limitations on the application of Halon agents. Marine fire utilization is concerned with gaining the best use of limited water on board ocean going vessels.

2.6.1. United States Bureau of Mines

A great deal of research into the characteristics of duct and mine fires has been performed by the United States Bureau of Mines. This research covers both physical experiments and numerical analysis.

Hwang and Chaiken (1978) performed analyses pertaining to the interaction of a fire in a duct, or mine entry, with the ventilation airflow. This paper analytically relates observed phenomenon with theoretical work performed earlier by Hwang, Chaiken, Singer, and Chi (1976). The earlier (1976) paper presents a two-dimensional model by which one can

investigate plume behavior in a duct or mine entry. Their flow model allows for the consideration of buoyancy effects and the fire intensity. In this manner it is possible, using their model, to determine when and under what conditions reversal of flow in the mine entry will occur.

Experiments conducted by the USBM concerning the behavior of coal fires in model entries is reported by Chaiken, Singer, and Lee (1979). This paper documents 6 experimental fires conducted in a 28 cm square by 9.1 meters long coal fire tunnel at the USBM Pittsburgh center. One of these tests was configured with a 1 meter long slab of coal on the floor only, the remainder had 1 to 3 meter long slabs of coal placed on all four internal surfaces. The authors report that the floor fire spread and remained in an oxygen-rich burning mode. Whereas, all of the four-surface fires began oxygen-rich, transformed to fuel-rich, and dropped back to the oxygen-rich state as the fuel was consumed. They further report that these fires were accompanied by stratification and reversal of flow due to the throttling effects of the fires.

Experiments conducted by the USBM concerning the behavior of wood fires in model tunnels is reported by Lee, Chaiken, Singer, and Harris (1980). The intent of these studies, as stated by the authors, was to complement the work performed earlier by Roberts (1950) and Roberts and Blackwell (1969). They wanted to investigate the growth of the fires and the transient interaction between the fire and the ventilation airflow. This research was conducted in a 30 cm square by 10 meter long fire tunnel at the USBM Pittsburgh center. The transition from an oxygen-rich to fuel-rich state of burning was observed during the tests that they reported. Additionally, reports are made of airflow reversals occurring in the duct air flows. The fan settings were adjusted during

most of these tests to maintain a continuous flow rate of fresh air into the fire. These authors also make the note of the difficulty in sizing the ignition source to produce a self sustaining fire without overpowering the tunnel fire that is being observed.

Investigations into the relationship between a small fire's development and its detection is reported by Egan (1993). These tests were conducted to determine the relationship between the ventilation rate, the fire spread, and the response of the fire detection equipment. An intermediate scale, 80 cm square by 10 m long, wind tunnel was used.

2.6.2. Industrial Fire Protection

In March of 1993 the United States Department of Commerce, National Institute of Standards and Technology (NIST) conducted a workshop dealing with the application of water mist for fire suppression. This workshop dealt with the potential for water mist systems to replace halons and other industrial fire suppressants, and the potential to apply water mist technology in residential and aviation applications (Notarianni and Jason 1993).

The application of water mist appears to have a significant potential for industrial fire protection systems. In particular, water mist has been shown to be efficacious against fires involving flammable liquid pools, high pressure jets, room fires, and special risk areas including submarines and aircraft (Mawhinney 1993). Experiments cited have demonstrated the effectiveness of water mist in extinguishing 200 MW methane jet fires (Mawhinney 1993, Evans and Pfenning 1985), and against diesel fuel, crude oil, and hydraulic fluid pool fires (Mawhinney 1993, Olsson and Ryderman 1990; Wighus 1991).

The research documented by Evans and Pfenning (1985) indicated that for a gas well head fire, exceeding 185 megawatts the mass flow rate of the water needed to at least 1.6 times the mass flow rate of the gas. This ratio was based on four spray nozzles radial around the well head. If the number of nozzles was decreased to two the ratio could more than double, based on small scale tests. They also found that the application of water sprays decreased the radiation emissions by about 30%, even when the fire was not extinguished. The authors report that this decrease could be attributed to a number of phenomena, including the changes to the shape of the plume and absorption of energy by the water spray.

In this industrial type of application there appear to be several factors that will affect the ability of the mist to have a positive impact on the state of the fire. Two that are very important are the spray density and the particle kinetic energy. The spray density provides an indication of how much water will be available for fighting the fire, the particle kinetic energy will affect the ability of the mist to interact turbulently with the flame (Mawhinney 1993). Turbulent interaction with the flame is an important consideration when attempting to quench diffusion type flames. It is this factor that "tears" the flame apart, interrupting the spread of the combustion reaction.

The effect of water mist may be controlled by several of the factors surrounding the fire itself, including; the size and type of the fire, and the degree of enclosure. For instance, in a large enclosed fire the displacement of oxygen by water vapor may be more prevalent than the cooling effect of the intact mist. Whereas in a smaller or unenclosed fire the greater effect may be the cooling nature of the mist rather than the presence of water vapor that plays a greater role (Mawhinney 1993).

The presence of the water mist was investigated by Reischl (1979) to determine its ability to attenuate radiant heat emitted from the subject fire. The purpose of this research was to quantify the shielding effect that water sprays have on the fire-fighters tackling the blaze. The results of this research indicate that the presence of the water mist significantly reduces the amount of radiant heat present behind the nozzle. The degree of attenuation appears to be related to the spray angle and to the flow rate. The greatest attenuating factor behind the mist appears to be the mist itself, which affects the radiant heat by reflecting heat back towards the fire, refracting the radiation away, and absorption of the radiated energy into the water droplet. The ability of the water to attenuate the radiated heat decreases as the mist is converted to vapor (Reischl 1979). Attenuation of radiation occurs as an exponential process in air as a function of the vapor content and the distance from the source (McPherson 1993b). Since the attenuative capacity increases as the water vapor content increases it is reasonable to assume that the presence of free water, in the form of a mist, will greatly enhance this capacity over the existing water vapor.

Due to the complex and interactive nature of water mist and vapor on the fire in question Mawhinney (1993) states: "It is not yet possible to set design criteria that are applicable to the full range of fuels, fuel configurations and compartment conditions for which water mist systems are being considered." The key then appears to be adequate definition of the conditions under which the specified water mist system will be efficacious.

3. *BASIC THEORY*

The phenomena associated with mine fires is a mixture of combustion and heat transfer in what can amount to a relatively adiabatic system. Based on de Ris (1970) as much as 66% of the heat released from the combustion is available for the vaporization of coal in the fuel lined entry. The remainder of the heat is used to warm the rock mass around the mine workings. This is apparent if one considers that the temperature of the air leaving the mine will remain basically constant during the duration of the fire.

In order to develop a basic theory into the effects of the water mist extinguishing system it will be important to review some basic fundamentals of the combustion and thermal processes. In particular, a review will be made of flame structure, heat transfer processes in the mine, and interactions of extinguishing agents and the fire.

3.1. Flame Structure

The structure of flames is of a very complex nature that is well beyond the scope of this thesis. However, in order to provide a better understanding of the role that the fire plays in this research the basic processes involved in four types of flames will be covered. These

include: the pre-mixed flame, diffusion flames, turbulent diffusion flames, and glowing combustion. The pre-mixed and the laminar diffusion flame structures do not appear to play a direct role in the fuel-rich fire scenarios; however, they provide a basis of familiarity as a reference. It should be mentioned that methane and coal dust explosions, as they are prone to occur, represent the realm of pre-mixed combustion in the turbulent regime.

Since combustion is a chemical reaction phenomenon it is controlled by a reaction rate (*RR*) that will limit the speed at which the chemical reactions are capable of occurring. The reactions that compose the combustion process require a relatively high activation energy, and thus, are highly temperature dependent. In order to begin the chemical reactions the reactants must be raised to a significantly high temperature. The reaction can be curtailed by cooling the reaction zone below the temperature necessary to sustain the reaction, although this means cooling an overall exothermic reaction.

3.1.1. Pre-mixed Flame

The pre-mixed flame, as its name implies, undergoes the combustion process after the fuel and oxidizer have been thoroughly mixed together. A very basic example of this process, in the laminar regime, is the Bunsen burner or the burner of a gas range.

Based on research by Mallard and Le Châtelier, the laminar flame is divided into two regions, the pre-heat zone and the reaction zone. In the reaction zone chemical energy in the fuel is converted to thermal energy, through oxidation. Some of the heat generated by this reaction is conducted to the incoming fuel and oxidizer to raise the mixture temperature to the ignition point (Kuo 1986). The theories of Mallard and Le Châtelier

are based on thermal considerations that rely on three assumptions. First, that there is a flame speed that is unique to the mixture. Second, that heat is not transferred to the walls or downstream, although heat is conducted upstream. Third, that the reaction zone is a thin layer compared to the rest of the flame structure and is distinct from the pre-heating zone (Strehlow 1984). This theory leads to the conclusion regarding the flame speed (S_L):

$$S_L = \frac{\lambda}{\rho c_P} \frac{\left(T_f - T_0\right)}{\left(T_i - T_0\right)} \frac{1}{\delta}.$$

Where λ is the thermal conductivity, ρ the density, c_p the specific heat at constant pressure, and δ the reaction zone thickness. The temperatures, T_f, T_i, and T_0 are those of the flame, ignition point, and ambient mixture, respectively. By rearranging they were able to show that the flame speed was related to the thermal diffusivity (α) and the Reaction Rate (RR) by the proportionality (Glassman 1977):

$$S_L \propto \sqrt{\alpha RR}.$$

A more comprehensive theory regarding the laminar flame speed has been presented by Zeldovich, Frank-Kameneskii, and Semenov who added to the above theory by including the effects of the diffusion of the molecular species present. Their theory is simplified by making the initial assumption that the thermal, mass and momentum diffusivities are all equal. Thus the Prandtl (Pr), Schmidt (Sc), and Lewis (Le) numbers are all equal to one, where:

$$\mathrm{Pr} = \nu / \alpha$$
$$\mathrm{Sc} = \nu / \boldsymbol{D}$$
$$\mathrm{Le} = \alpha / \boldsymbol{D}$$

with ν as the momentum diffusivity (kinematic viscosity), and D the mass diffusivity. This research further confirmed the observations of Mallard and Le Châtelier, the propagation of the laminar flame is a diffusional process related to the square root of the diffusivity and the reaction rate (Glassman 1977).

3.1.2. Diffusion Flame

The basic diffusion flame theory considers that the oxidizer and the fuel diffuse together with the combustion reaction occurring at the interface where the fuel/oxidizer concentrations are in stoichiometric proportions. A general example of the laminar diffusion flame is the candle or gas light. These flames exhibit their illuminating characteristics due to the luminescent soot produced as a result of the diffusive nature of the combustion.

Diffusion flames do find their way into daily application beyond the occasional use in candles. The basic combustion structure of diesel engines, liquid fueled turbine combustors, and some types of coal fire boilers exhibit diffusion flames. Unlike the pre-mixed flames that can be characterized in several manners, fuel/air ratio, flame speed, etc., the diffusion flame has no distinctive characteristic. A general assumption that is made, concerning the process rate, is that it is not controlled by the reaction rate, rather by the much slower diffusion rates. (Gaydon and Wolfhard 1970).

Some work has shown that the flame height may be a defining characteristic, since in both over and under ventilated conditions it represents the location where the fuel and oxidizer

are reacting in stoichiometric proportions. The physical significance of this state is small, however, since the mixture will react anywhere within its flammability limits (Gaydon and Wolfhard 1970). One way to imagine a diffusion flame is illustrated in figure 3-1. Notice that the fuel and air are flowing at the same velocity from the different tubes, thus no shear is immediately present at the fuel/air interface. The fuel is flowing in the inner tube and the oxidizer in the annulus around the fuel tube. Shown above the tubes is a diagram representing the relative proportions of fuel, oxidizer, products, and inerts in the cross-section. This diagram can represent any location along the length of the existing flame. The flame front represents a sink for the oxygen and the fuel, thus the concentrations of both are assumed to drop to zero at this point. One would assume that the concentrations of the products and the inerts would be zero in the center of the fuel plume. This, however, is not the case, some of each diffuse towards the center even though the bulk flow is outward, away from the flame (Glassman 1977).

In a system as described above the over-ventilated, or oxygen-rich, condition results in a flame that is closed at the top, similar to a candle flame. When the system is under-ventilated, or fuel-rich, the flame spreads out to contact the walls of the outer tube extension. The remaining fuel-rich mixture is vented out of the tube.

This type of profile was observed in the tunnel tests where fuel-rich (under-ventilated) fires fully engulfed the duct cross-section. In this configuration, the fuel was diffusing outwards from the duct surfaces towards the oxidizer in the center. The net result, however, was the same, with the fuel fully consuming the available oxygen and the excess fuel and products being exhausted. The fires in the duct were compounded by the turbulent airflow and the effect on the flame structure.

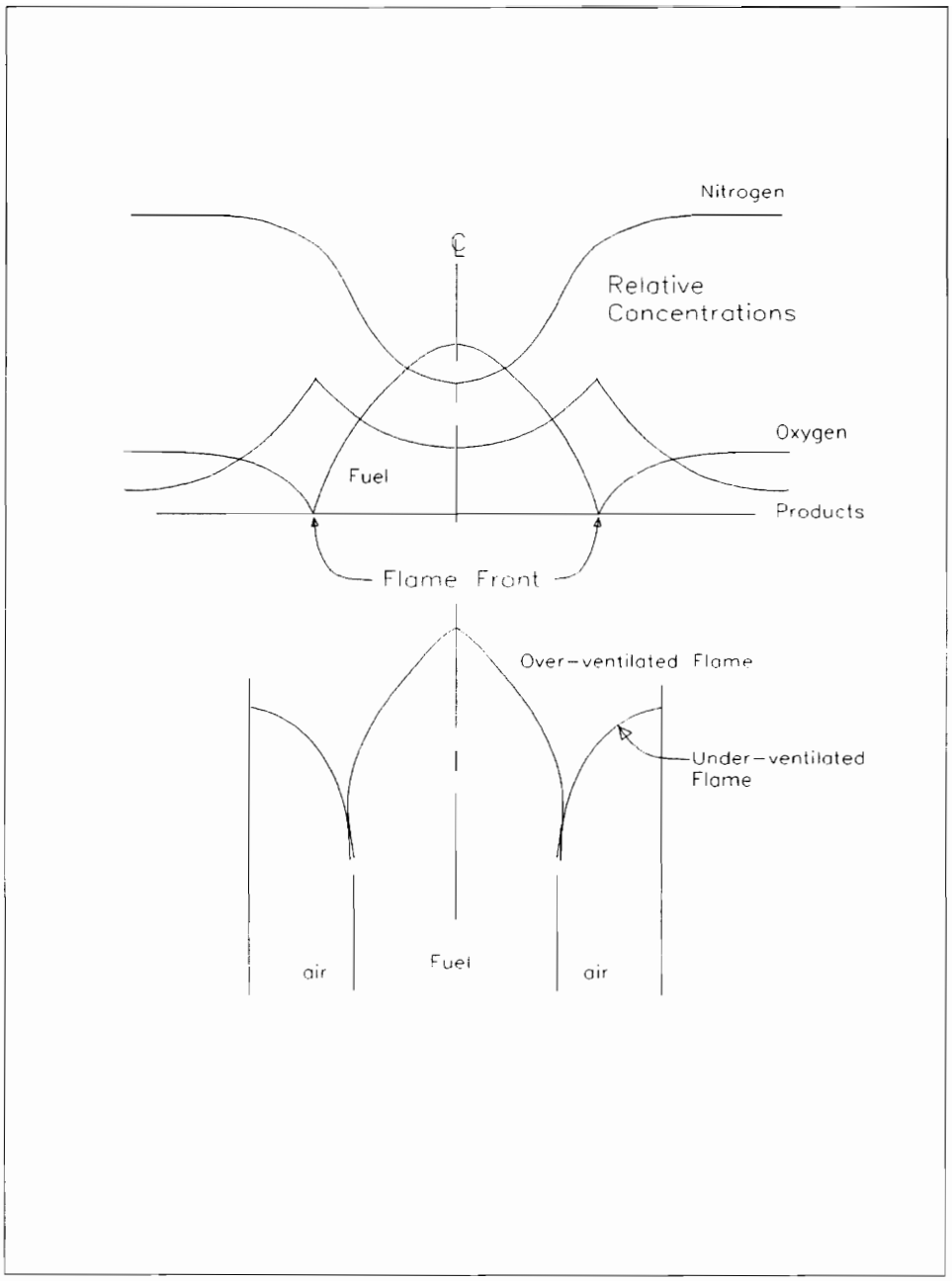

Figure 3-1: Diffusion Flame Profile (after; Glassman 1977)

3.1.3. Turbulent Diffusion Flame

The turbulent diffusion flame is the rolling, licking flame that occurs in the common fireplace. This is the common flame for open fires, the flame structure is carried upwards in the buoyant column of air rising from the fire seat.

Much of the theory concerning the study of turbulent diffusion flames centers on a laminar diffusion flame analogy. The basic theory seems to be that the turbulent flame can be thought of as occurring as a wrinkled, laminar diffusion flame within the turbulent flow structure. With this in mind, it is possible to imagine that with sufficient energy the flame structure can be affected by increasing the turbulence. Increasing the turbulence has the possible effect of stretching the flame to the point of extinction (Graydon and Wolfhard 1970).

Flames of this type, as others, require a means of stabilization to hold and maintain the chemical reaction process. When applied to jet type combustors the "flame holder" can take on several shapes, such as bluff bodies, sudden expansions or opposed jets (Strehlow 1984). The desired effect is to create a recirculation zone where some of the products of combustion are being carried back towards the flame holder to ignite the incoming fuel and air. In the case of the combination extinguisher, see section 3.4.2 of this thesis, the turbulent diffusion flame was stabilized in the air swirl created by the fan driving air into the combustion chamber.

Another theoretical approach involves the longitudinally burning surfaces where flame structure is held within the boundary layer of the flow field. In this case the vaporized fuel diffuses outwards through the boundary layer, while the oxidizer diffuses inwards. The flame is then held within the boundary layer (Glassman 1977).

An acceptable analogy for the flame stabilization technique in the open fires may the sudden expansion technique, where the flame is held in position in the recirculation zone in the step region. Such an approach seems somewhat more intuitive for visualizing the form of the combustion field. The flame structure is being held by the interaction of the airflow, buoyancy, and diffusion process.

3.1.4. Glowing Combustion

Glowing combustion can occur to a significant degree at two phases of a mine fire. The first being the result of self-heating of the coal, resulting in spontaneous combustion. This phenomenon results from the interaction of physical and chemical processes at the coal surface. Within the possible ranges of airflow there can exist a critical range whereby there is sufficient oxygen to result in the generation of heat, but insufficient airflow to effectively remove the heat. The excess heat is retained in the coal, ultimately leading to increased oxidation and incandescent conditions (McPherson 1993b). That self-heating may lead to a fuel-rich fire is evident in the case involving the Orchard Valley Mine, section 1.3.3. Mitchell (1990) reports that coal can burn in the glowing phase nearly indefinitely, even in the absence of oxygen in the air. Under these conditions the combustion process is utilizing the oxygen available in the coal itself.

The second phase at which glowing combustion is significant is in the so-called charcoal zone. During the flaming combustion process of solid hydrocarbon fuels, wood or coal, the pyrolitic decomposition cause the gaseous release of fuel vapors. These vapors burn in the flames that are readily visible. As the bulk of the fuel is pyrolized, with the associated loss of mass, the initial fuel is reduced to elemental carbon and ash, akin to charcoal or coke. When the fire has reached this stage the original orange flames have been reduced to light bluish surrounding the burning embers. The light blue flames arising from the conversion of carbon monoxide to carbon dioxide (Heassler 1989).

It is the glowing combustion phase that presents the concern regarding the generation of water gas. When water comes into contact with the incandescent coal the reaction of the water with the coal can produce as products hydrogen and carbon monoxide gases. This is an endothermic reaction requiring about 31.4 kilocalories per mole (Chaiken and Martin 1992), see section 3.4 of this thesis.

3.2. Heat Transfer to the Duct Walls

The transfer of heat generated by the fire to the surrounding rock mass occurs by an interaction of the three basic heat transfer processes; conduction away from the entry surface, convection within the airflow, and radiation from the fire to the surrounding surfaces. One significant situation regarding duct and mine entry fires is the fact that relatively little of the heat generated is lost from the system. About 66% of the heat generated by the fire is used in the vaporization of additional fuels and pre-heating of the mine airway, the remainder is lost permanently from the system (Roberts and Clough 1967b, de Ris 1970).

3.2.1. Conduction

Conduction of heat away from the entry accounts for a limited amount of heat loss. Ordinary approaches to the modeling of the heat transfer process in the mine entries assumes that the heat transfer in this manner is small compared to that carried by convection.

Considering that the conduction of heat will be much greater radially away from the entry than axially, a one-dimensional analysis, normal to the entry axis, of the heat equation provides an acceptable solution. A second dimension may be employed to account for the cooling of the gases as they progress downstream. The conduction of heat to the entry surfaces results in both the warming of the surrounding strata and the liberation of additional fuel. De Ris (1970) expresses the conductive effect by the second order, steady state, partial differential equation:

$$\rho_s C_{ps} V \frac{\partial T}{\partial x} + \dot{m}'' C_{ps} \frac{\partial T}{\partial y} + \lambda_s \frac{\partial^2 T}{\partial y^2} = 0$$

$$\text{for} \quad 0 \le x \le x_2; \quad 0 \le y \le \infty$$

Where the first term, with ρ_s as the wall density, C_{ps} as the specific heat of the wall, and V as the fire spread rate, represents the change in temperature along the length between the beginning of the fire and the end of the excess fuel zone. The second term, with $\dot{m}''$ as the mass transfer flux, represents the energy that is conducted to the surface to vaporize the fuel. The third term, with λ_s as the thermal conductivity of the strata (presumed constant), represents the heat that is conducted away from the fire as lost heat. Due to the

volatilization process the surface temperature in this region can be assumed to be at the vaporization temperature of the fuel.

Within the expressed ranges, x_2 is the end of the excess fuel zone. It is intuitively obvious that, at distances exceeding x_2, although vaporization of fuel may not be possible heat transfer to the surfaces will continue. At least, so long as the gases are above the temperature of the entry surfaces. Under these conditions then the second term of the differential equation is equal to zero. A similar condition occurs upstream of the fire where the air is preheated as it passes through the burnt-out zone (de Ris 1970).

3.2.2. Convection

The process of forced convection accounts for most of the heat transfer. It is by this process of hot products from the fire flowing along the entry walls that additional fuel is vaporized, the second term in the above partial differential equation. Once the fire has reached a stable fuel-rich state it can be treated as a constant temperature heat source (Kennedy and Taylor 1967).

Convective heat transfer is estimated by Charters, Gray, and McIntosh (1994) using Newton's law of cooling:

$$\dot{q}_w = h_c A_w \Delta T .$$

Where $\dot{q}_w$ is the convective heat transfer from the plume to the entry surfaces, A_w is the contact area of the plume on the surface, ΔT is the temperature difference between the

plume and the surface, and h_c is the convective heat transfer coefficient. The convective heat transfer coefficient is a function of the flow profile, and can be expressed for turbulent flow as:

$$h_c = \frac{0.296(\mathrm{Re})^{0.8}(\mathrm{Pr})^{0.33}\lambda_{air}}{x}.$$

Where Re is the Reynolds number, Pr is the Prandtl number, λ_{air} is the thermal conductivity of the air, and x is the distance from the fire to the point of interest.

In the model presented by Bolstad, Foster and Gregory (1983) the value of x above is replaced with the duct equivalent diameter. These researchers also point out that for large temperature differences the heat transfer coefficient is a function of the duct geometry, mass rate of flow, properties of the fluids and temperature differences.

The above models for convective heat transfer are based on the conditions whereby none of the heat is being used for the liberation of fuel. The first model was applied to lined road and railway tunnels and the second case for ventilating ducts, such as those in buildings. The application of the convection effects would be the same as those for the conduction, where volatilization of fuel would only be occurring where the bulk temperature of the gases is above the vaporization temperature.

3.2.3. Radiation

The effect of radiation is only a particular concern in the near vicinity of the fire. Once the gases have past away from the seat of the fire the emissivities of the symmetric molecules

(nitrogen and oxygen) are sufficiently low so that they do not play an important factor. Some significance may arise in the presence of heterpolar gases such as carbon dioxide and water, or in the thick smoke (Bolstad, Foster, and Gregory 1983, Hottel 1954). It is conceivable that the presence of high quantities of water vapor associated with the use of a water mist system could absorb a significant quantity of thermal radiation on both the upstream and downstream side of the fire. This could affect the radiative feed back of thermal energy to the fire seat.

Radiative feedback of heat does play an important role at the seat of the fire.

3.2.4. Heat Balance in Duct Fire

The heat balance of the fire is important to be able to predict the severity and speed of the fire. In terms of the fire velocity V, the heat balance is shown to be (de Ris 1970):

$$V = \frac{M_A Y_0^{(0)} Q / r - \dot{Q}_L}{\mathrm{P} H_{vap}}.$$

Where M_A is the mass rate of air supplied to the fire, $Y_0^{(0)}$ is the oxygen concentration upstream of the fire, Q is the heat of combustion, r is the fuel to air stoichiometric ratio, $\dot{Q}_L$ is the heat flow away from the fire, P is the fuel loading per unit length of the entry, and H_{vap} is the heat of vaporization of the fuel at the ambient temperature. From this information one can deduce that the spread of the fire will be related to the fuel properties. This was in fact seen in the field tests where the fires developed much more rapidly for the plywood fuel than for the coal fuel.

The term $\dot{Q}_L$ is represented by the third term ($\lambda_s \partial^2 T/\partial y^2$) in the differential equation in section 3.2.1 of this thesis. Tests conducted by Roberts and Clough (1967b) indicate that the magnitude of $\dot{Q}_L$ is approximately 34% of the total heat liberated.

3.2.5. Buoyancy Effects

As the fire begins to develop the heated air and gases will begin to affect the ventilation system of the mine. The result of the local heating can be to cause stratification of the airflow with hot and cold air masses moving concurrently and counter-currently. Wide ranging impacts to the mine ventilation system can be to throttle the airflow in the local vicinity or the entire mine and to affect the natural ventilation conditions of the mine.

3.2.5.1. Stratification

As the air and gases from the fire are heated, at a constant pressure, their density falls and they become buoyant in the local airstream. A detailed model of this effect is given by Hwang, Chaiken, Singer, and Chi (1976), in which they describe, by two-dimensional analysis, the reversal of flow in duct fires. They describe the development of the buoyant plume above the fire and the resulting trajectories of the gases in relationship to the normal ventilation flow within the mine entry.

Where top coal has been left in the entry there is the possibility that the hot gases rising from a floor fire can cause the fire to spread to the roof. This may be due to the fire spreading up the ribs or by direct contact of the plume with the roof.

Vanpée and Wolfhard (1960) describe experiments whereby explosive mixtures of gases where ignited by the introduction of hot gases into the mixture. One of the observations of their research is the transfer of heat between the hot jet and the explosive mixture. Such an observation is easily extrapolated to the heat transfer from the rising plume to the top coal. Provided that the plume is of sufficient temperature and duration there appears no reason that pyrolysis of the available fuel should not begin.

Such a condition is of concern in the mine entries, but has also been extensively studied in its relationship to building and room fires. Research by Cooper (1982) and Vafai and Lacalle (1989) indicate the heat transfer is of differing magnitudes in side of the stagnation zone and outside of the stagnation zone above the plume. Furthermore, the heat transfer will be affected by the walls as a smoke layer begins to form in the room.

As the buoyant effects of the plume begin to overcome the inertial effects of the incoming fresh air "roll-back" of the plume can occur. Under these conditions smoke and hot gases are flowing counter-current to the main airflow in the affected drift. Stratification of the smoke and gases can occur downstream of the fire as well. Conditions can exist where the macro scale of the fire may be oxygen-rich, but producing a fuel-rich stratified region at the top of the drift. The stratified flow can move along the drift with both regions (hot and cold) in the turbulent regimes but separated by a laminar layer (de Ris 1970). Another concern with the degree of stratification is the relative location of the fire with respect to the effective end of the entry. It is conceivable that with sufficient heating of the air in the fire that the airflow along the floor of the fire could be reversed to draw fresh air from a source downstream of the fire.

Another important factor in the development of stratified flow is the inclination of the airway. When the airflow is ascensional the development of a stratified layer will be will be enhanced, requiring a greater mixing length for the stratification to be overcome. In conditions of decensional airflow, the tendency for the heated gases to flow uphill, counter current, will assist in the development of stratified flow as the angle of inclination increases. With regards to methane (ρ = 0.554), McPherson (1993b) shows that in an entry ascentionally ventilated that the velocity required to minimize layering at a 45 degree inclination is nearly 1.56 times that of a level entry. While, under the same conditions the required airflow for a descentional airway is slightly below that of the level entry. Furthermore, for slightly declined airways the required velocity drops below that required in level entries.

The role of the airway slope is covered by the inclusion of a cosine function of the angle of inclination in the Richardson number, see section 4.1.3. Under these conditions an inclined airway is shown to reduce the value of the Richardson number, effectively reducing the velocity at which the backing layer is likely to develop.

By dimensionless analysis, stratification and counter flow of the gases, is likely to occur when the inertial forces are overcome by the buoyant forces. This ratio is referred to as the Froude number and is discussed in some detail in section 4.1.3 of this thesis. The scaling of the fire section, of the experimental tunnel, was based on matching Froude numbers for similitude in the experiments conducted.

3.2.5.2. Throttling of Airflow

As the air entering the fire begins to expand its performs work against the surrounding air. This effect is in both directions, relative to the incoming airflow. This effect is known as throttling or choking (McPherson 1993a, 1993b). The treatment of this condition is based on the development of an effective resistance of the airways caused by changes in the density of air. In covering the subject McPherson shows that this effective resistance is proportional to the square of the absolute temperature. He cautions that this condition is an approximation to allow for the continuation of analysis by incompressible flow assumptions.

A somewhat different analysis is given by Sengupta (1988), where he develops the relationship that the new pressure drop along the affected airway is related to the original pressure drop by the temperature ratio.

A minor effect on both of the above analyses is the increase in mass flow associated with the products of combustion. Throttling could be affected as well by the increase of mass due to the evaporation of water from the liquid to gas phase associated with the water mist system. Of a much greater effect, however, will be the increase in volume due to the nearly 1700 times volume increase due to the vaporization of water.

3.2.5.3. Affects to Natural Ventilation

Beyond the local effects of buoyancy described in section 3.2.5.1, the buoyant forces induced by the fire may result in more widespread changes to the mine ventilation system. The wide spread impacts may be more pronounced when the fire is in a shaft or inclined airway. Under these conditions the fire may develop a heated air mass with sufficient buoyancy to restrict or reverse decensional airflow. The effect could be to increase the airflow to the fire if the airway carried ascensional airflow. In either case the fire may result in the spread of gases to parts of the mine that would be inaccessible to the normal airflow pattern. It is possible, under these conditions, that the fire establishes zones of uncontrolled recirculation of the toxic gases (McPherson 1993b).

3.3. Extinction of Combustion

This thesis is principally concerned with the attempts to gain control over a fuel-rich mine fire by returning it to an oxygen-rich state. However, many of the aspects of fire extinction play a role in this desired result. It is theorized that if one can gain control of the fuel-rich fire by returning it to an oxygen-rich state, the fire will be much easier to extinguish by conventional methods.

Extinction of combustion is accomplished by the removal of any of the three sides of the fire triangle. One additional means that is available is the interruption of the chemical chain reactions within the combustion process.

3.3.1. Removal of Fuel

Clearly the removal of the fuel will result in the cessation of the combustion process. The difficulty with this practice is getting the removal agent to the fuel source. Typical application of this method is the use of modified water based agents, which include detergent Aqueous Film-Forming Foams (AFFF), diammonium phosphate solutions, brines, and bentonite or borax slurries. Dry agents that are employed to remove the fuel source include monoammonium phosphate, graphitized coke, and dry salts (Haessler 1989).

Isolation of the fuel in this manner is most appropriate for solid fuel fires, although there is some application for the use of foam agents in fires involving fuel not miscible with water (Haessler 1989). For gaseous fuels the concept of fuel removal may be extended to the introduction of inert gases to the reaction zone. In this manner the partial pressure of the fuel (and oxidizer) is reduced, which in turn reduces the frequency of collisions between the reactants. This is a somewhat artificial view point since it does not actually remove the gas phase fuel, rather it merely reduces the potential for reaction between the fuel and the oxidizer.

3.3.2. Removal of Heat

One of the most familiar means of fighting a fire is the direct application of water. This action serves to remove heat from the reacting materials and is most appropriate for surface fires of solid materials. The heat energy removed by water is approximately 2600 kJ/kg when the water temperature is raised from 20°C to a vapor at 100°C. In open

conditions it is not practical to assume that further heating will occur since the vapor is likely to rise away from the fire area.

Other means of cooling the fire are the application of water as a spray fog, or in a modified form such as foams or slurries. In some instances the introduction of carbon dioxide as a liquid or solid directly to the fire serves to remove some heat as well as to displace the oxygen.

3.3.3. Removal of Oxygen

The dilution of the oxygen concentration is usually accomplished by flooding the fire with an inert gas, such as nitrogen, argon, or carbon dioxide. This means of attack is most appropriate for flammable liquid and electrical fires.

The concept of the application of water mist can also fall within the realm of oxygen removal. This mode of extinguishment may be the affective agent for those fires burning within enclosures or other locations with a limited supply of fresh air. Under these conditions the heat within the environment may vaporize the water droplet before it has physical impact on the seat of the fire. The vaporizing water displaces the oxygen, reducing the effective concentration and partial pressure of the oxidizer.

The role that the partial pressure of the oxygen can be explained using a gas kinetics model for the gas phase chemical reactions. This theory is based on the collision frequency of the gaseous molecules. It can be shown (Kuo, 1986) that the collision frequency between two different molecules is proportional to the concentrations of the

species. In this manner, the introduction of inert species reduces the rate of interaction of the active species.

3.3.4. Interruption of the Free-Radicals

The consideration of radicals in the combustion process opens depth to the basic fire triangle, producing a tetrahedron. This concept is put forth by Haessler (1989) to explain the additional mode of depth to the fire condition, in which he expresses the principle features of chemical and physical attacks on a fire. Interruption of the exchange of radicals and resulting chain branching reactions is the basic theory behind the application of the halogenated hydrocarbons (Halons) as an extinguishing agent.

The presence of free radicals, in particular H and OH, play a critical role in the combustion of hydrocarbons. These radicals induce the chain branching reactions that cause the self-sustained combustion process to continue. A typical reaction of this type is:

$$H + O_2 \rightarrow OH + O$$

where two radicals are formed by the interaction between a single radical and a molecule (Kuo 1986). One typical application of radical interruption can be illustrated with Bromotrifluromethane (CF_3Br), also known as Halon 1301. The series of reactions can be shown, in general, as:

$$CF_3Br + H \rightarrow HBr$$
$$HBr + OH \rightarrow Br + H_2O$$

The production of the CF_3, Br, and H_2O go on to terminate the chain reactions. This chain breaking action is also the principal factor in the use of dry-chemical extinguishing agents such as sodium bicarbonate, potassium bicarbonate, potassium chloride, potassium carbonate, and monoammonium phosphates (Haessler 1989).

3.4. Extinguishing Systems Tested

Both of the extinguishing systems tested, water mist alone and water mist in association with a propane combustor, are at least partially dependent on the size of the water particles generated. Water mist systems for use against fires in enclosures and liquid pools have effectively used particle sizes up to 400 microns in diameter. In quiescent air a water droplet of 400 micron diameter behaves as a large particle exhibiting a terminal settling velocity of about 160 cm/s. This implies that the particle is likely to settle out of the air stream before it can effectively reach a fire in a mine entry. Below a 50 micron diameter the water droplets begin to behave as a Stoke's particle with a terminal settling velocity of less 1.8 cm/s in quiescent air. The smaller droplets are also more likely to remain entrained in the turbulent airflow.

These smaller particles are also effective for increasing the degree and rate of evaporation as the particles approach and enter the fire. Based on the single particle evaporation equation, it can be shown that (Kuo 1986, Vandsburger 1994):

$$t_{evap} = \frac{D_0^2}{\lambda_{evap}}.$$

Where t_{evap} is the time required for the evaporation of the droplet (seconds), D_0 is the initial diameter of the droplet (meters), and λ_{evap} is the evaporation rate coefficient given as:

$$-\lambda_{evap} \equiv -\frac{8\rho_s \alpha_s}{\rho_l} \ln(1+B) = \frac{dD^2}{dt}$$

$$B = \frac{C_p(T_\infty - T_{BP})}{L + C_L(T_{BP} - T_0)}$$

Where C_p and C_L are the specific heats of the vapor and the liquid phases, ρ_l and ρ_s are the densities of the liquid and at the droplet boundary, α_s is the thermal diffusivity of the water vapor, and T_∞, T_{BP} and T_0 are the far field temperature, liquid boiling temperature and liquid initial temperature respectively. The evaporation model above can also be expressed with the $\rho_s \alpha_s$ replaced with λ/C_p; where λ is the thermal conductivity of the evaporating gas (Lefebvre 1989). In the analysis presented by Lefebvre, k is used to represent the thermal conductivity, for consistency this has been change to λ for this thesis.

This analysis has assumed that the droplet is of infinite conductivity and that the Lewis number is equal to 1. Using this analysis it is possible to make the following conclusions regarding the life of the droplet as it approaches the fire. The very small droplets will likely evaporated before reaching the seat of combustion, whereas the larger droplets may pass through the fire with no significant loss in mass. A basic evaluation of the evaporation times for various size droplets versus the field temperature is show in table 3-1. This table illustrates the estimated time to evaporate a single droplet into effectively dry

air. The effect of a spray would be to increase the time required to evaporate the droplet since the driving force of evaporation diffusion would be reduced due to the higher water vapor content of the surrounding air.

Table 3-1: Lifetime in Seconds of Single Water Droplets for Various Conditions.

T_{BP} =	100 deg C	C_p =	1.842 kJ/(kg K)	ρ_s =	0.77 kg/m^3
T_0 =	20 deg C	C_L =	4.183 kJ/(kg K)	ρ_l =	1000 kg/m^3
L=	2256.7 kJ/kg	a =	2.58E-05 m^2/s	k =	1.60E-05 kJ/(s m K)

Dia.\ T_∞	200 °C	300	400	500	600	700	800	900
625μ	81.86	42.29	29.08	22.46	18.48	15.82	13.92	12.49
500	52.39	27.07	18.61	14.38	11.83	10.13	8.91	7.99
400	33.53	17.32	11.91	9.20	7.57	6.48	5.70	5.11
300	18.86	9.74	6.70	5.18	4.26	3.65	3.21	2.88
250	13.10	6.77	4.65	3.59	2.96	2.53	2.23	2.00
200	8.38	4.33	2.98	2.30	1.89	1.62	1.43	1.28
150	4.72	2.44	1.68	1.29	1.06	0.91	0.80	0.72
100	2.10	1.08	0.74	0.58	0.47	0.41	0.36	0.32
75	1.18	0.61	0.42	0.32	0.27	0.23	0.20	0.18
50	0.52	0.27	0.19	0.14	0.12	0.10	0.09	0.08
25	0.13	0.07	0.05	0.04	0.03	0.03	0.02	0.02
5	0.01	0.00	0.00	0.00	0.00	0.00	0.00	0.00

Based upon the $\rho\ C_p$ model.

One likely concern related to the use of water mist on a coal fire is the generation of a mixture of carbon monoxide and hydrogen, referred to as water gas. Both of the product gases are capable of forming an explosive mixture in air (CO 12.5 to 74.2% in air, H_2 4 to 74.2% in air). The chemical reaction involved:

$$H_2O + C_s \rightarrow CO + H_2 - 31.4\,\text{kcal / mol}$$

is endothermic (Chaiken and Martin 1992). This condition is likely to cool the reaction quickly. Haessler (1989) reports that this reaction becomes significant near 650°C and complete near 1370 °C. Furthermore, he illustrates that the rate of this reaction is between .1 and 0.01 percent of that for the carbon/oxygen reaction. Since, one mole of gas reacts with one mole of solid carbon to produce 2 moles of gas a doubling of the volume will be associated with this reaction. This will result in a change in both the volumetric and mass flow rates.

3.4.1. Water Mist

The application of a fog or water mist to a fire, particularly in a mine environment, presents several possible advantages to the fire fighting crew. The use of small to very small droplets would allow the water to remain suspended in the airflow so that it could be carried deep into the fire seat. The small droplets, about the same size as a natural fog, can be expected to be relatively unaffected by obstructions to the airflow. The application of low pressure fog generation system can make the fire fighting effort less dependent on having a high line pressure in the underground water reticulation system (McPherson 1991).

The application of water mist to fighting fires has received a good deal of attention recently for commercial and industrial application. Although it is not yet considered a valid alternative for wide spread use, water mist is seen by some as an alternative to the utilization of halogenated hydrocarbons (Mawhinney 1994). The interest that has been generated has led the National Fire Protection Association to begin developing a standard on water mist systems (Solomon 1994).

The action of the water mist is described by McPherson (1993a) as having a distinct effect on each side of the fire triangle. The evaporation of the water displaces oxygen reducing the effective concentration of the oxidizer, and removes heat; the later recondensing of the water could effectively isolate the available fuel downstream of the fire.

Water exhibits an increase in volume of about 1721 times as it evaporates from a liquid to a vapor at its normal boiling point. Given a sample case of 5 m^3/s airflow and 2 l/s of water converted to fog, McPherson (1993a) shows that the evaporation of the water will decrease the oxygen concentration from 21% to about 13.5%. This analysis neglects any effect that the fire may have to choke the incoming airflow.

The heat removal effect of the evaporating water can easily be ascertained from a thermodynamic steam table. To raise the water from an initial temperature of 20°C to a superheated vapor of 750°C (at a constant pressure) requires some 4000 kJ/kg. Continuing with his example, McPherson (1993a), shows computationally that nearly 7.8 MW of heat are required to raise the 2 l/s of water from 20°C to 800°C. The heat required to raise the air temperature over this range is about 870kJ/kg or about 5.1 MW.

It is expected that the gases and water vapor will quickly cool as they pass from the active fire zone. As the gases cool the water vapor will recondense, with the net effect to "rain" water on all surfaces of the mine entries. This liquid on the entry surfaces will inhibit the spread of the fire since it must be re-evaporated for the fire to spread. In this way the water mist should inhibit the spreading fire by functionally isolating the fuel source. This effect can be considered to be minimal in its impact compared to the other two effects

since the recondensation is likely to occur some distance downstream of the last point of combustion.

3.4.2. Combination Extinguisher

As a result of the work performed early in this research, a new design of extinguisher was proposed for study (Loomis 1994). The device, which has been referred to as the Combination Extinguisher, utilizes the controlled combustion of propane and the injection of water into the hot gases to reduce the overall oxygen concentration to below 13%. This section details the general design of the extinguisher.

The reduction of the oxygen content is accomplished in a two step process. First a propane burner is used to consume about 25% of the available oxygen. The basic combustion reaction is expressed as:

$$C_3H_8 + 5O_2 \rightarrow 3CO_2 + 4H_2O$$

Overall, this reaction alone would reduce the total oxygen content to about 15.75%. This reaction will also liberate a large quantity of heat (46.3 MJ/kg of propane) which will allow the application of the second step. Most of the heat is used to vaporize water to a superheated steam, further reducing the oxygen content. It is estimated that this process could reduce the oxygen in the intake air to between 10 and 13%. At this level of oxygen content flaming combustion in the fire zone will be extinguished (Loomis 1994).

The design of the combination extinguisher is shown in block form in figure 3-2. The design process is given below. The basic assumption for the combustor is that complete combustion occurs. This is a gross simplification; however, it provides sufficient accuracy for the basic design and function. The stoichiometric reaction of propane in air can be expressed as:

$$C_3H_8 + 5O_2 + 18.8N_2 \rightarrow 3CO_2 + 4H_2O + 18.8N_2.$$

The produces a theoretical Fuel/Air ratio of 0.0643 kg fuel per kg air. The combustor was designed as a steady-state, steady-flow reactor with an over supply of air 150% of the theoretical requirements. A further assumption was made that the combustor would be adiabatic, the implications of this assumption are discussed below. From the general design parameters the work done in the combustor control volume is zero, the heat added to the control volume is zero, as is the change in potential energy. The change in kinetic energy of the gases is also assumed to be zero. Based on the first law of thermodynamics, the enthalpy of the reactants will be equal to that of the products. In the chemical energy form this is expressed as:

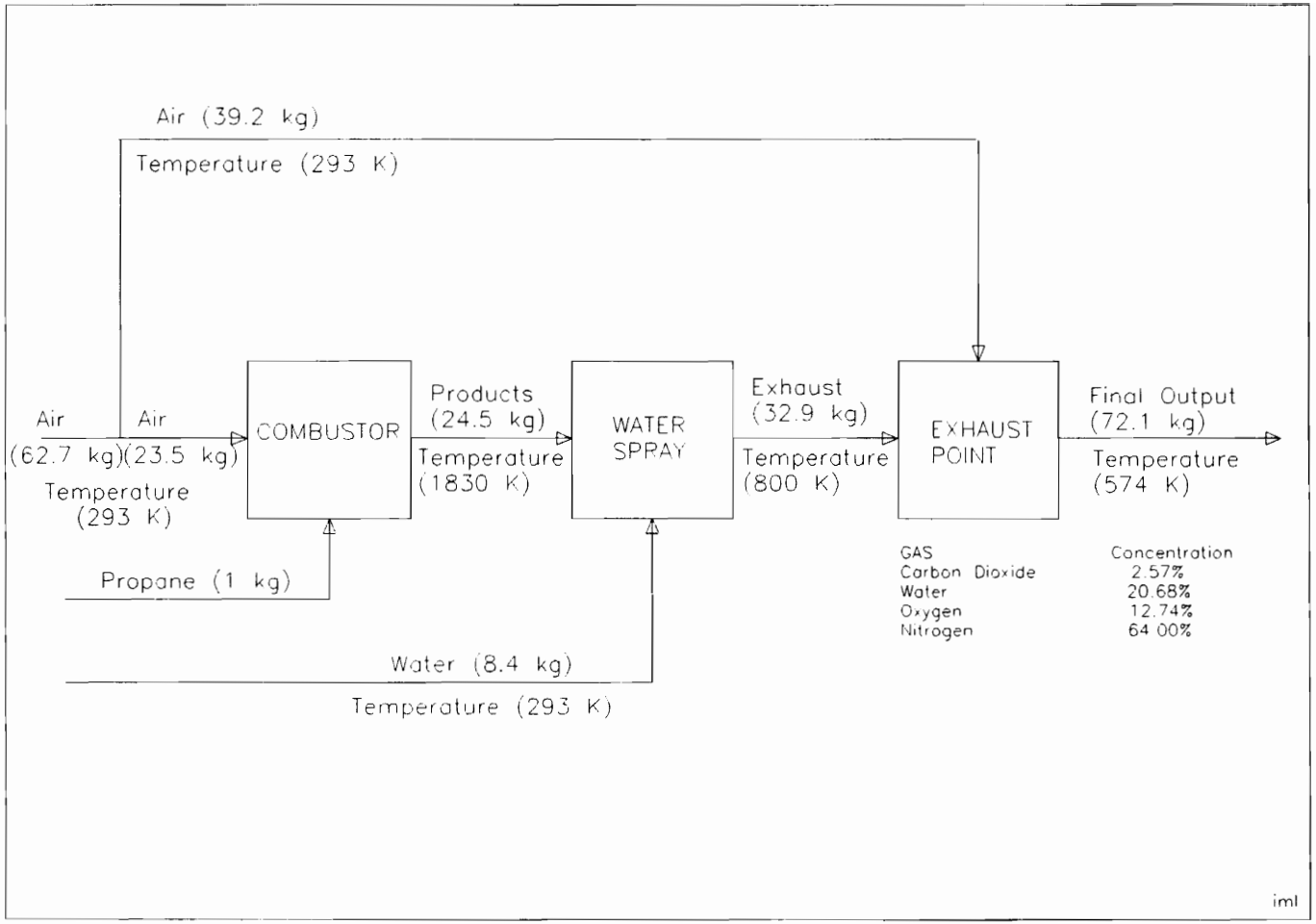

Figure 3-2: Block Diagram of Combination Extinguisher

$$\sum_R n_i\left(\bar{h}_f^\circ + \Delta\bar{h}\right)_i = \sum_P n_e\left(\bar{h}_f^\circ + \Delta\bar{h}\right)_e$$

where n_i and n_e are the reaction coefficients for the respective species, $\bar{h}_f^\circ$ is the heat of formation of the species, defined as zero for elemental species, and $\Delta\bar{h}$ is the change in the enthalpy of the species with respect to a reference condition. By setting the reference base at the ambient conditions the reactants term is simply the heat of formation for the fuel, $\bar{h}_f^\circ(C_3H_8)$ = -103847 kJ/kmol. The second term is expanded to the form:

$$\sum n_e\left(\bar{h}_f^\circ + \Delta\bar{h}\right)_e = 3\left(\bar{h}_f^\circ + \Delta\bar{h}\right)_{CO_2} + 4\left(\bar{h}_f^\circ + \Delta\bar{h}\right)_{H_2O} + 2.5\left(\Delta\bar{h}\right)_{O_2} + 18.8\left(\Delta\bar{h}\right)_{N_2}.$$

The solution to the adiabatic flame temperature must be arrived at by iteration based on the properties of the products. The heat of formation for the CO_2 and H_2O are fixed at: $\bar{h}_f^\circ(CO_2)$ = -393522 kJ/kmol and $\bar{h}_f^\circ(H_2O)$ = -241827 kJ/kmol. It can be determined that the temperature lies between 1800 and 1900K, at which temperatures the gas properties are given in Table 3-2.

Table 3-2: Energy of Products at Bounding Temperatures

Temperature (K)	$(\Delta\bar{h})CO_2$ (kJ/kmol)	$(\Delta\bar{h})H_2O$ (kJ/kmol)	$(\Delta\bar{h})O_2$ (kJ/kmol)	$(\Delta\bar{h})N_2$ (kJ/kmol)	H_P (kJ/kmol)
1800	79442	62609	51689	48982	-148597
1900	85429	67613	55434	52551	-611

Data From: Van Wylen and Sonntag, 1986

The adiabatic flame temperature can be interpolated between the two temperatures to be approximated at 1830K or 1557°C. The composition of the products of combustion are estimated as those listed in table 3-3.

Table 3-3: Estimated Products of Combustion from Propane Burner

Species	Mole	Mole %	Density kg/kmol	Mass kg	Mass %
CO_2	3	7.96	44.01	132.03	12.30
H_2O	4	10.61	18.06	72.06	6.72
O_2	2.5	6.63	32.00	80.00	7.46
N_2	28.2	74.8	28.01	789.97	73.62
Total	37.7	100.0		1073.09	100.00

Knowing the temperature of the products of combustion it is now possible to determine the quantity of water that must be added to reduce the temperature to a point that the total products can be introduced to the main airstream. The final temperature in the main airstream must be high enough to keep the water vaporized (>100°C) but below the volatilization temperature of coal (say 400°C). Consider then, that the products of combustion are to be cooled to 527°C (800K), by the injection of water. To simplify the problem, assume that the products of combustion behave as an ideal gas.

Again, making the assumption that work, heat exchange, and changes in kinetic and potential energy are zero in the control volume the energy balance can be expressed as:

$$\dot{m}_p h_{pi} + \dot{m}_w h_{wi} = \dot{m}_p h_{pe} + \dot{m}_w h_{we}$$

Where $\dot{m}$ is the mass flow rate of the products of combustion and water as indicated by subscript, and h_i and h_e are the enthalpies at the initial and exit temperatures of the products and water. The properties of interest for the products and the water are listed in table 3-4.

Table 3-4: Thermodynamic Properties of Products and Water

Temperature (°C)	Enthalpy (kJ/kg)
Air	
1527	2003
527	822
Water	
25	105
527	3542

Data From: Van Wylen and Sonntag, 1986

Basing the mass flow of the products on 1 kg of propane the mass flow rate of water can be determined from the energy balance as:

$$\dot{m}_w = \frac{\dot{m}_p\left(h_{pi} - h_{pe}\right)}{\left(h_{we} - h_{wi}\right)}.$$

By evaluating this expression for $\dot{m}_p$ = 24.5 kg, (23.5 kg air + 1 kg propane), the mass rate of water is determined to be 8.4 kg per kg propane. Following the evaporation of the water introduced to the products the gaseous mixture has the composition listed in table 3-5.

Table 3-5: Ratios of Species Following Injection of Water

Species	Mole	Mole %	Density kg/kmol	Mass kg	Mass %
CO_2	3	5.2	44.01	132.03	9.2
H_2O	4	6.9	18.06	72.06	5.0
O_2	2.5	4.3	32.00	80.00	5.5
N_2	28.2	48.2	28.01	789.97	54.8
H_2O (injected)	20.4	35.1	18.06	368.4	25.5
Total	58.1	100.0		1442.5	100.00

Considering that 62 percent of the available air from upstream by passes the combustor the final temperature and mixture can be determined by again using the thermodynamic mixing of the two streams. The first consideration is to determine the final mixture downstream of the combustor. Reducing to a balance based on 1 kilogram of propane fuel the by pass air mixture, and the products of combustion and the injected water can be assumed as shown in table 3-6. The final mixture is listed in table 3-7.

Table 3-6: Concentrations of By Pass Air Mixture

Species	Mole	Mole %	Density kg/kmol	Mass kg	Mass %
By Pass Air Fraction					
O_2	0.285	21.0	32.00	9.13	23.3
N_2	1.074	79.0	28.01	30.07	76.7
Total (air)	1.359	100.0		39.2	100.0
Combustor Products Fraction					
CO_2	0.069	5.2	44.01	3.03	9.2
H_2O	0.555	41.9	18.06	10.03	30.5
O_2	0.057	4.3	32.00	1.81	5.5
N_2	0.644	48.6	28.01	18.03	54.8
Total (prod.)	1.325	100.0		32.9	100.0

Table 3-7: Final Mixture Downstream of Combustor

Species	Mole	Mole %	Density kg/kmol	Mass kg	Mass %
CO_2	0.069	2.57	44.01	3.03	4.2
H_2O	0.555	20.68	18.06	10.03	13.91
O_2	0.342	12.74	32.00	10.94	15.17
N_2	1.718	64.00	28.01	18.03	66.72
Total	2.684	100.0		72.1	100.0

The final mixture has an oxygen concentration less than 13 percent by volume and can be expected to exhibit extinctive characteristics. The final step in evaluating the design is to

estimate the final temperature of the system downstream of the combustor. This is made by again considering the thermodynamics of the mixture based on a constant enthalpy. To simplify the problem the oxygen, nitrogen and carbon dioxide fractions will be assumed to exhibit ideal gas characteristics. The water vapor fraction will be treated as a superheated vapor.

By using the same analysis as used to determine the combustor outlet temperature, it is possible to estimate the final temperature downstream of the combination extinguisher. The relevant heat balance for this case becomes:

$$\dot{m}_{air}h_{air,i} + \dot{m}_p h_{p,i} + \dot{m}_w h_{w,i} = \dot{m}_{air}h_{air,e} + \dot{m}_p h_{p,e} + \dot{m}_w h_{w,e}\,.$$

In this equation the enthalpy of the water vapor in the products has been separated out for convenience in estimating values from tables. The by-pass air and the air fraction of the products has been assumed to exhibit ideal gas behavior. The enthalpy values for relevant conditions are listed in table 3-8.

Table 3-8: Enthalpy (kJ/kg) of Air, Products, and Water

	25 °C	127 °C	327 °C	527 °C
Air	293.17	400.98	607.2	
Products		400.98	607.02	821.94
Water		3278.2	3704.7	4158.6

Data from: Van Wylen and Sonntag, 1986

The estimated final temperature can be interpolated between the values of 127 and 327 °C to be 300 °C, as shown in figure 3-2. Thus the final estimated temperature is below the value of 400 °C that was specified above as the upper limit temperature. This value is

assumed to be independent of the partial pressures of the vapors since enthalpy is a function of temperature only, in the ideal gas case (Van Wylen and Sonntag 1986).

4. *TEST PARAMETERS*

4.1. Scaling Factor

In order to obtain experimental results that can be scaled to real life conditions a degree of similitude must be maintained. The similitude between the model and the prototype can be based on geometry, kinematics, or dynamics. Complete similarity between the model and the prototype is obtained when there is satisfaction of the geometric, kinematic, and dynamic requirements.

For geometric similarity the proportions of the model and the prototype must be identical, that is width, length, and depth ratios are equal. It follows then, that the surface areas will vary as a square function and the volumes as a cubic function between the model and the prototype.

Kinematic similarity arises when the forces acting on the model are exactly proportional to those acting on the prototype. If this condition can be met then exact kinematic similitude can be achieved.

Dynamic similarity arises when the forces affecting the flow field are held in similitude. The forces are associated with pressure, inertia, gravity, elasticity, and surface tension. They are generalized by the following equations (Vennard and Street 1976).

$$F_P = (\Delta p)A = (\Delta p)l^2 \qquad \text{(Pressure)}$$

$$F_I = Ma = \rho l^3\left(\frac{V^2}{l}\right) = \rho V^2 l^2 \qquad \text{(Inertial)}$$

$$F_G = Mg_n = \rho l^3 g_n \qquad \text{(Gravitational)}$$

$$F_V = \mu\left(\frac{dV}{dy}\right)A = \mu\left(\frac{V}{l}\right)l^2 = \mu V l \qquad \text{(Visocous)}$$

$$F_E = \mathrm{E}A = \mathrm{E}l^2 \qquad \text{(Elastic)}$$

$$F_T = \sigma l \qquad \text{(Tensile)}$$

Where: p is pressure, A is area, l is length, M is mass, a is linear acceleration, ρ is density, V is velocity, g_n is gravitational acceleration, μ is the absolute viscosity, y is the distance from a boundary, and σ is the surface tension. The symbol E is used here to indicate the modulus of elasticity. These forces can be combined as ratios of the inertial force to describe the flow field conditions. When the flow fields are similar all of the following simultaneous equations will be satisfied (Vennard and Street 1976).

Euler Number: Ratio of Inertial to Pressure Forces

$$\left(\frac{F_I}{F_P}\right)_p = \left(\frac{F_I}{F_P}\right)_m \Rightarrow \left(\frac{\rho V^2}{\Delta P}\right)_p = \left(\frac{\rho V^2}{\Delta P}\right)_m$$

Reynolds Number: Ratio of Inertial to Viscous Forces

$$\left(\frac{F_I}{F_V}\right)_p = \left(\frac{F_I}{F_V}\right)_m \Rightarrow \left(\frac{Vl\rho}{\mu}\right)_p = \left(\frac{Vl\rho}{\mu}\right)_m$$

Froude Number: Ratio of Inertial to Gravitational Forces

$$\left(\frac{F_I}{F_G}\right)_p = \left(\frac{F_I}{F_G}\right)_m \Rightarrow \left(\frac{V^2}{lg_n}\right)_p = \left(\frac{V^2}{lg_n}\right)_m$$

Mach Number: Ratio of Inertial to Elastic Forces

$$\left(\frac{F_I}{F_E}\right)_p = \left(\frac{F_I}{F_E}\right)_m \Rightarrow \left(\frac{\rho V^2}{\mathrm{E}}\right)_p = \left(\frac{\rho V^2}{\mathrm{E}}\right)_m$$

Weber Number: Ratio of Inertial to Surface Tensile Forces

$$\left(\frac{F_I}{F_T}\right)_p = \left(\frac{F_I}{F_T}\right)_m \Rightarrow \left(\frac{\rho l V^2}{\sigma}\right)_p = \left(\frac{\rho l V^2}{\sigma}\right)_m$$

In order to gain similitude between the model and the prototype all five of the above simultaneous equations must be met. However, due the nature of the models being tested and the dynamic range of the process some of the equations can be neglected. In particular the Mach and Weber numbers. This case will reduce the number of variables that must be met when seeking similarity. For the base of the fire tunnel design each of the remaining ratios (Euler, Reynolds, and Froude numbers) will be quantitatively analyzed

and discussed below. Similitude of the fire tunnel model to a prototype mine opening will be sought based upon the relevant relationships.

For the sake of this design, consideration shall also be made of the ratio of Momentum to Thermal Diffusivities and the ratio of Momentum to Mass Diffusivities. These ratios are referred to as the Prandtl and Schmidt numbers respectively. For the cases of simple model gas the ratios are both equal to one and for simple real gases both are nearly equal to one. These ratios become important when multiple transport phenomenon are occurring simultaneously (Foust, et al. 1980).

Drysdale (1985) presents two forms of fire modeling, one based the Froude number and the other based on pressure. Froude modeling can be employed where viscous forces are negligible. Use of Froude modeling preserves the Froude Number group when scaling is performed. Scaling in this manner requires that the velocities are scaled to the square root of the principle dimension, i.e. $(u/\sqrt{l})$ remains constant (Drysdale 1985). Furthermore, it has been shown (Drysdale 1985, de Ris 1970) that

$$u \propto \dot{Q}^{\frac{1}{5}}.$$

Pressure modeling can cope with both laminar and turbulent flow. By use of the Grashof Number:

$$Gr = \frac{\rho^2 g l^3 \beta \Delta T}{\mu^2}.$$

Where ρ is the density, g is the gravitational acceleration, l is length, β is temperature coefficient of volumetric expansion, ΔT is the temperature difference, and μ is the absolute viscosity. The system can be scaled where $\rho^2 l^3$ is maintained constant. However, without the ability to perform highly pressurized tests this scaling method is impractical (Drysdale, 1985).

To this end only the Froude modeling method will be considered in the design of the Fire Tunnel.

4.1.1. Euler Number

This number represents the ratio of inertial to pressure forces. It has been defined as:

$$\mathrm{Eu} = V\sqrt{\frac{\rho}{2\Delta P}} \Rightarrow \left(\frac{\rho}{2RA^2}\right)^{\frac{1}{2}}$$

where R is the turbulent resistance. It can be observed, therefore, that the Euler number seeks to find a state of similitude between the resistances to flow for a given duct size for the model and prototype. Based on the second form a constant Euler number exists for a given duct and a given fluid density. Seeking similitude between a model and prototype can therefore be achieved by altering the model cross-section. This may affect the geometrical relationship of the model to prototype and the model resistance.

The Euler number is important in matching the characteristics between the model and the prototype based on differences in surface effects (resistance to flow). The Euler number is independent of the flow.

An attempt, in the design, will be made to characterize the Euler number based on the change in air density and the apparent change in the airway resistance as a result of the duct fire.

4.1.2. Reynolds Number

The Reynolds number is the expression for the ratio of inertial to viscous forces. Although the forms of the Reynolds number expression may vary from text to text it can be reduced to:

$$\mathrm{Re} = \frac{Vl}{\nu} = \frac{D\bar{v}\rho}{\mu}$$

Regardless of the form used to determine the Reynolds number two ducts that are operating at the same Reynolds number are dynamically similar regardless of size.

Let us consider two lengths of geometrically similar pipe, that are scaled by a factor of n. Now consider that the centerline velocity and all geometrically corresponding velocities are related by a constant ratio then both of the flow fields are kinematically similar. Furthermore, if the inertial forces (kinetic energy per volume) and the viscous forces (fluid stress) bear a constant ratio, in the absence of other significant forces, then the flow fields are dynamically similar (Foust, et al. 1980).

Obtaining similitude for most model testing is normally related to a similar Reynolds number between the model and the prototype. This is true, for example, when testing conventional airfoils in low-speed conditions (Pope and Harper 1966). Under these conditions the surface tension, compressibility and gravity effects are negligible. Thus if the Reynolds numbers are matched then the condition of similitude is established.

In the case of Fire Tunnel testing the buoyancy created by differential densities within the flow field leads to gravity being an effective agent. For the case of scaled fire testing it is important to obtain similar gravity/buoyancy situations. The effects of the flow condition (laminar or turbulent) expressed by the Reynolds number are also important to ensure that representative mixing is occurring upstream, within, and downstream of the fire zone.

4.1.3. Froude Number

The Froude number represents the ratio of Inertial forces with respect to the gravitational forces. It can be expressed as:

$$\mathrm{Fr} = \frac{V}{\sqrt{lg_n}} = \frac{\left(\frac{\Delta\rho}{\rho}\right)D}{\frac{V_0^2}{g_n}}$$

The Froude number is used as a key factor in the modeling of fire situations (Drysdale 1985) using the Froude Modeling method. This holds also true for mine and duct fires. One can apply the Froude number to determine if smoke and other products of

combustion will flow upstream on a horizontal airway. This phenomenon is commonly referred to as "roll-back." As the buoyancy induced in the air by the fire overcomes the inertia of the airflow, Froude Number ≥ 1, the smoke and gases may move upstream along the top of the duct.

Based upon arguments presented by Drysdale (1985) and de Ris (1970), modeling the effects and scale of the fire based on a similitude of the Froude number is more important than the use of any of the other scaling ratios. It is assumed that when analyzing fire for turbulent conditions the magnitude of the Reynolds number is insignificant.

It is conceivable that even under turbulent flow conditions a separation can occur, by gravity, whereby hot air flows downstream along the roof and cold air downstream along the floor. The cold air is intake air passing through the fire zone without involvement in the combustion process. The hot air may be fuel-rich in its products of combustion profile. The two layers are separated by a thin laminar layer. Gravity is acting in such a manner as to prevent mixing of these two otherwise turbulent fluids (de Ris 1970).

Turbulent mixing of the layers can be predicted with the Prandtl mixing length hypothesis. Mixing can be expected when the cold eddy characteristic vertical kinetic energy is greater than the increase in potential energy across the mixing length. In the form of the Froude number, downstream turbulent mixing will be completely suppressed when the Froude number is greater than 0.8 (de Ris 1970).

This leads to a brief comparison between the Froude number and the Layering number. The Layering number (L) is routinely used to determine the distance downstream that will

be required for initially stratified fluids to become mixed. The Layering number is expressed in terms of the dimensionless relationship (McPherson 1993b):

$$\mathrm{L} = \frac{u}{\left(g \frac{\Delta\rho}{\rho} \frac{Q_g}{W} \right)^{\frac{1}{3}}}$$

where u is the airflow velocity, Q_g is the rate of gas emission, W is the airway width, and $\Delta\rho/\rho$ is the difference in the densities of the two gases. The Layering number can be used to estimate the distance over which the stratification will exist, whereas the Froude number is useful in determining the existence of stratification and counter current flow based on the differential densities of the fluids.

Another approach to the problem of determining the extent or probability of gas stratification is by application of the Richardson number (Ri). Hwang, et al. (1976) express the local Richardson number as:

$$\mathrm{Ri} = \frac{g(\rho_\infty - \rho_b)\delta_b}{\rho_\infty (V_\infty + u_b)^2}$$

where ρ_∞ and ρ_b are the densities of the ventilation stream and the backing gas layer, respectively, δ_b is the thickness of the backing gas layer, V_∞ is the ventilation air velocity, and u_b is the velocity of the backing layer. The equation as presented by Hwang, et al., contains a cosine(ϕ) factor in the numerator that accounts for the angle of inclination of the airway. Through massaging of the differential equations Hwang, et al., show that a critical Richardson number exists where:

$$Ri_{cr} = \rho\left(\frac{u}{1+u}\right)^2$$

where u = u_b/V_∞. In this manner the critical Richardson number provides the value at which the backing ceiling layer ceases to exist. The Froude number, as presented in this thesis, predicts the presence of stratified flow when its value is greater than 1, whereas the Richardson number can be used to predict the conditions at which the ceiling layer will cease to exist. The Froude number expressed by Hwang, et al., omits the $\Delta\rho/\rho$ term that is shown in the expression above the result being a dimensionless relationship for the duct that does not account for the buoyant gradients within the fluid. They do, however, employ a relationship, attributed to Thomas (1958, 1968) in which he replaces the $\Delta\rho/\rho$ term with $\Delta T/T$. That the density and temperature terms are interchangeable can be shown when one considers an ideal gas situation. Assuming that there is very little change in the pressure between the two states the temperature is inversely proportional to the density, therefore the ratios between the change in the property and the original state are equal.

4.2. Tunnel Layout

The layout of the fire tunnel was configured to facilitate two goals. The first being to allow simulation of the conditions that could be expected in a fuel-rich fire in a typical coal mine entry. The second goal was to support the operational requirements of the experiments. It is helpful, here, to describe the tunnel in two basic sections, the fire section where the actual experimental fires were constructed, and the pre-fire sections where the airflow was metered and "conditioned" prior to entering the fire section. The

upstream pre-fire section was designed as a matter of course to support the experimental section.

Before designing the experimental section, the basic prototype coal mine entry was identified. The prototype entry provided a point of comparison to which the expected reactions in the tunnel could be evaluated. The next step was to determine the size requirements for the model entry. The model section had to be large enough to conduct the experiments at a scale that supported the desired similarities with relative ease. This section was restricted in size to keep the amount of coal fuel that was being burned fairly small, and by the physical size and cost of constructing the facility.

4.2.1. Prototype

The prototype for the Fire Tunnel is a typical coal mine entry 6.1 meters wide by 1.52 meters high (20 by 5 feet), for the sake of consistency it is assumed that this is a single entry without cross-cuts. The k factor used and applied to this airway is 0.012 kg/m^3 (65 $lb_f \cdot min^2 \cdot ft^{-4}(10^{10})$). Evaluation of similitude will be based on the average airway velocities shown in table 4-1. For the purpose of design all airflow calculations will based on an air density of 1.21 kg per cubic meter (0.0698 lb_m per cubic foot).

Table 4-1: Case Number and Airflow Velocity for Study (prototype scale)

Case	v(m/s)	v(ft/min)
1	0.46	90
2	0.51	100
3	0.76	150
4	1.02	200
5	1.27	250
6	1.52	300
7	1.78	350
8	2.03	400
9	2.29	450
10	2.54	500

The model (wind tunnel) was designed, as closely as reasonable possible, to represent the relevant conditions that exist in an actual fire in the prototype drift. In order to accomplish this the model was to seek to represent the fire situation as closely as possible by scaling those factors most important to the fire dynamics. Hence, the first area of concern was the dynamic condition involving the Euler, Reynolds, and Froude numbers as discussed previously.

The parameter table for the prototype case is given in table 4-2, this outlines the values determined for Quantity, Pressure Drop, Euler number, Reynolds number, and two values of the Froude number (based on differing $(\Delta\rho/\rho)$ values).

Table 4-2: Parameters for Prototype Case

Case	V_0(m/s)	Q(m³/s)	Δp(Pa)	Eu	$Re(10^{-3})$	Fr(1/2)	Fr(2/3)
1	0.46	4.24	0.17	0.82	72.57	35.70	47.60
2	0.51	4.71	0.21	0.82	80.67	28.89	38.52
3	0.76	7.07	0.48	0.82	121.00	12.84	17.12
4	1.02	9.42	0.85	0.82	161.33	7.22	9.63
5	1.27	11.78	1.33	0.82	201.67	4.62	6.16
6	1.52	14.13	1.92	0.82	242.00	3.21	4.28
7	1.78	16.49	2.61	0.82	282.33	2.36	3.14
8	2.03	18.84	3.41	0.82	322.67	1.81	2.41
9	2.29	21.20	4.31	0.82	363.00	1.43	1.90
10	2.54	23.55	5.32	0.82	403.33	1.16	1.54

4.2.2. Model

With the prototype established it was possible to determine the characteristics desired in the model. For the sake of size limitations a tunnel with a square opening of thirty by thirty centimeters (1 foot by 1 foot) was selected. It appeared that this configuration provided a good trade-off between the area within the tunnel and the overall size of the facility. The resulting parameters for the model case are listed in tables 4-3 and 4-4.

Table 4-3: Case Number and Airflow Velocity for Study (model scale)

Case	v(m/s)	v(ft/min)
1	0.21	41.3
2	0.23	45.3
3	0.36	71.0
4	0.47	92.5
5	0.59	116.1
6	0.70	137.8
7	0.82	161.4
8	0.93	183.1
9	1.06	208.7
10	1.18	232.3

Table 4-4: Parameters for Model Case

Case	V_0(m/s)	Q(m³/s)	Δp(Pa)	Eu	$Re(10^{-3})$	Fr(1/2)	Fr(2/3)
1	0.21	0.02	0.02	1.17	4.13	33.05	44.07
2	0.23	0.02	0.02	1.17	4.56	27.10	36.14
3	0.36	0.03	0.05	1.17	6.97	11.61	15.48
4	0.47	0.04	0.09	1.17	9.14	6.75	9.00
5	0.59	0.05	0.14	1.17	11.53	4.24	5.66
6	0.70	0.06	0.20	1.17	13.70	3.00	4.00
7	0.82	0.07	0.27	1.17	16.09	2.18	2.90
8	0.93	0.08	0.35	1.17	18.26	1.69	2.25
9	1.06	0.10	0.45	1.17	20.67	1.32	1.76
10	1.18	0.11	0.56	1.17	23.06	1.06	1.41

The wind tunnel was divided into three general sections, each having its own set of parameters, capacities and effects. Each of these three, the fan, the flow control and fogging, and fire test sections, are reviewed and discussed separately. The discussion begins at the fire test section and work towards the fan.

Due to the expectation that a highly fuel-rich gas mixture would be coming out of the fire section, and to preclude the leakage of fresh air into the tunnel a forced ventilation arrangement was selected.

4.2.2.1. Fire Test Section

The fire test section included three sub-sections, the entrance, fire chamber, and post fire sections. These are illustrated in figure 4-1. This section was supported above the ground on stacked cinder block and shims. Supports were provided at the beginning and end of each of the sub-sections.

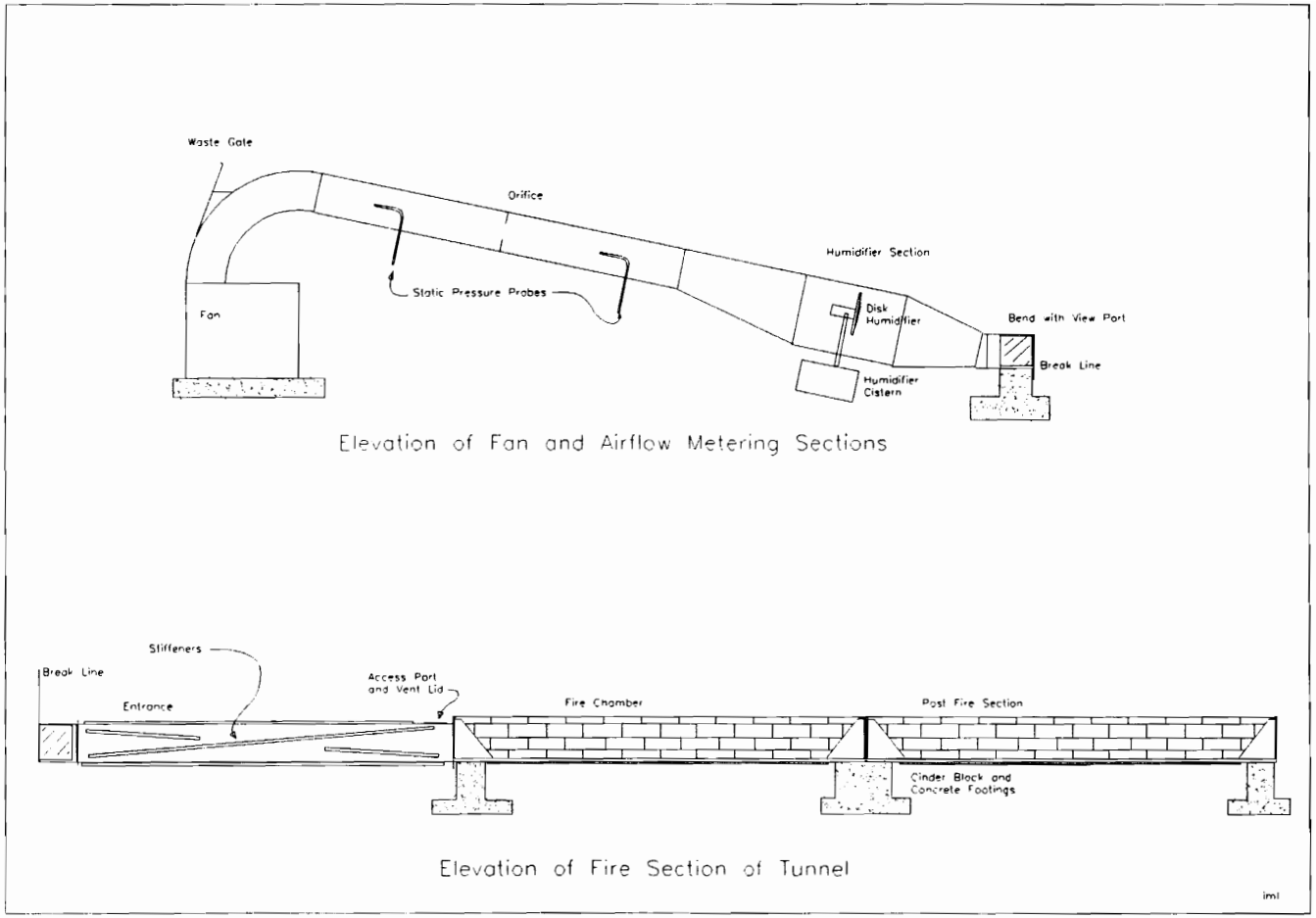

Figure 4-1: Elevation of Wind Tunnel for Fire Tests

4.2.2.1.1. Fire Entrance

The fire entrance section provided a length of tunnel 10 diameters long to separate the fire itself from the closest upstream disturbance. This allowed for the establishment of a "flat" velocity profile in the air stream prior to entering the fire. The degree to which this condition was successfully accomplished is covered in chapters 5.1.1 and 6.1.2 of this thesis.

Construction of this section is of stiffened 1/8" A36 steel plate.

4.2.2.1.2. Fire Chamber

The fire chamber section provided the capability of supporting a fire 6 to 10 diameters in length. This was based on experience shown by the United States Bureau of Mines (Chaiken, Singer, and Lee 1979) in which, for a 0.3 by 0.3m tunnel roll back of smoke was not experienced until the available fire section was some 2 meters in length.

Construction of this section was full thickness fire brick mortared together on the thin faces. The bricks were supported on the bottom by a stiffened tray constructed of 1/4" A36 Steel plate. For this section, and the following, the bricks were set in the form of a trough with completely separate lids. The lids were formed of four fire bricks adhered to a plate. During the course of a test the lids were placed over the trough with fiberglass insulating tape on the lid/trough and lid/lid interfaces. Plate 4-1 shows the last of the lids being set in place prior to a test fire.

Plate 4-1: Setting Last Lid on Tunnel for First Test.

4.2.2.1.3. Post Fire Section

The post fire section was to be approximately 10 diameters in length. This length was intended to provide thorough mixing of all exhausts under turbulent conditions, provided such mixing will take place. The length ensured that "duct-fire" conditions were maintained, that is that the fire was not able to induce counter-current draft flow in the post fire section.

Construction of this section is identical to that of the fire section.

4.2.2.2. Ventilation System

The fire tunnel was ventilated with a centrifugal fan in a forced airflow configuration. The airflow was metered to the desired level by the combined application of an orifice and waste gate. A set of ten orifices was prepared to provide the desired level of airflow at each of the cases conceived with a constant pressure drop through the orifice in place. That is, the pressure drop through orifice 10 for case ten is designed to be the same as through orifice 6 for case six. Any excess air from the fan was disposed of through the waste-gate.

The waste-gate position can be adjusted to provide a range of airflows through any of the given orifices. The possible ranges for the tunnel are between 0.13 m^3/s and 0.014 m^3/s, with orifice 10 and the waste gate closed, and orifice 1 and the waste gate open, respectively.

4.2.2.3. Fogging System

The initial fogging system employed a spinning disk humidifier. This style of system is typically used in controlling the humidity in greenhouses or other locations where large volumes of water need to be added to the air. A typical unit of this type is illustrated in figure 4-2. The object of this type of system to produce a fog in which the droplet size is representative of that found in a meteorological fog (5 - 50 μm diameter). The unit used in the wind tunnel was a model 30-C (30 Series) from Industrial Ventilation, Inc.

The operating scheme is such that while the disk is spinning water is pumped to the center of the disk. As the water accelerates to the outside of the disk the film of water thins. When the film of water reaches the edge of the disk it separates from the disk. The film strikes the stator attached to the shroud of the disk. The stator is configured with tiny vanes protruding into the water film separation area. When the separated film strikes the vanes it is dispersed into natural fog size droplets.

The spinning disk system was employed for two of the tests (1 and 3), involving plywood. However, it was felt that this system was not producing a sufficient quantity of fog to affect the coal fire tests. Based on observations much of the fog that was being generated by the system was being lost in the elbow, upstream of the fire. Therefore, a new fogging system was constructed that employed a number of air atomizing pressure spray jets. These jets use a small quantity of compressed air to assist the breakup of the water jet as it exits the nozzle. An array of twelve of these jets was constructed and configured in the

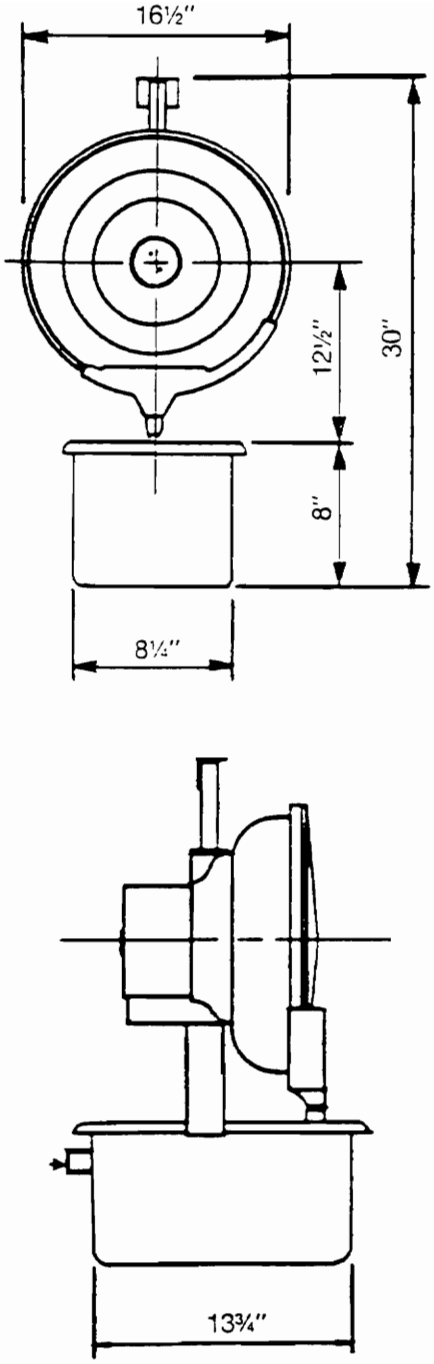

Figure 4-2: Illustration of Typical Spinning Disk Humidifier (from: Anon. 1992).

fire entrance section of the fire tunnel, approximately 4 diameters upstream of the fire ignition point.

The water and compressed air were metered to the system using rotameter flow meters. The schematic of this system is illustrated in figure 4-3. The nozzles used were model 1/8JJ-SUJ11 air atomizing spray nozzles manufactured by Industrial Spray Systems.

Furthermore, two additional experiments were conducted using the products of combustion and water vapor to gain control of the fuel-rich fire. For these experiments a custom combustor/evaporator system was constructed. The schematic of the system is shown in figure 4-4. This system used the combined effects of two processes to lower the concentration of oxygen in the intake air to a level that would not support flaming combustion. The combustor burned propane gas to consume a portion of the available oxygen, the heat generated was used to evaporate the water mist that was injected into the combustor near its exhaust point.

The combustor was configured such that a small fan forced air into the burner section, propane was added using a "rosebud" type heater head. In this situation the rosebud supplied straight propane (for routine usage in this device, propane and oxygen would be premixed before entering the rosebud). Mixing of the air and propane occurred in the combustor body to provide swirl stabilized diffusion flames.

The injection of water mist was accomplished through the application of four air atomizing pressure spray jets, one jet placed on each of the sides of the combustor. The nozzles were model 1/8JJ-SUJ11 air atomizing spray nozzles from Industrial Spray Systems. The

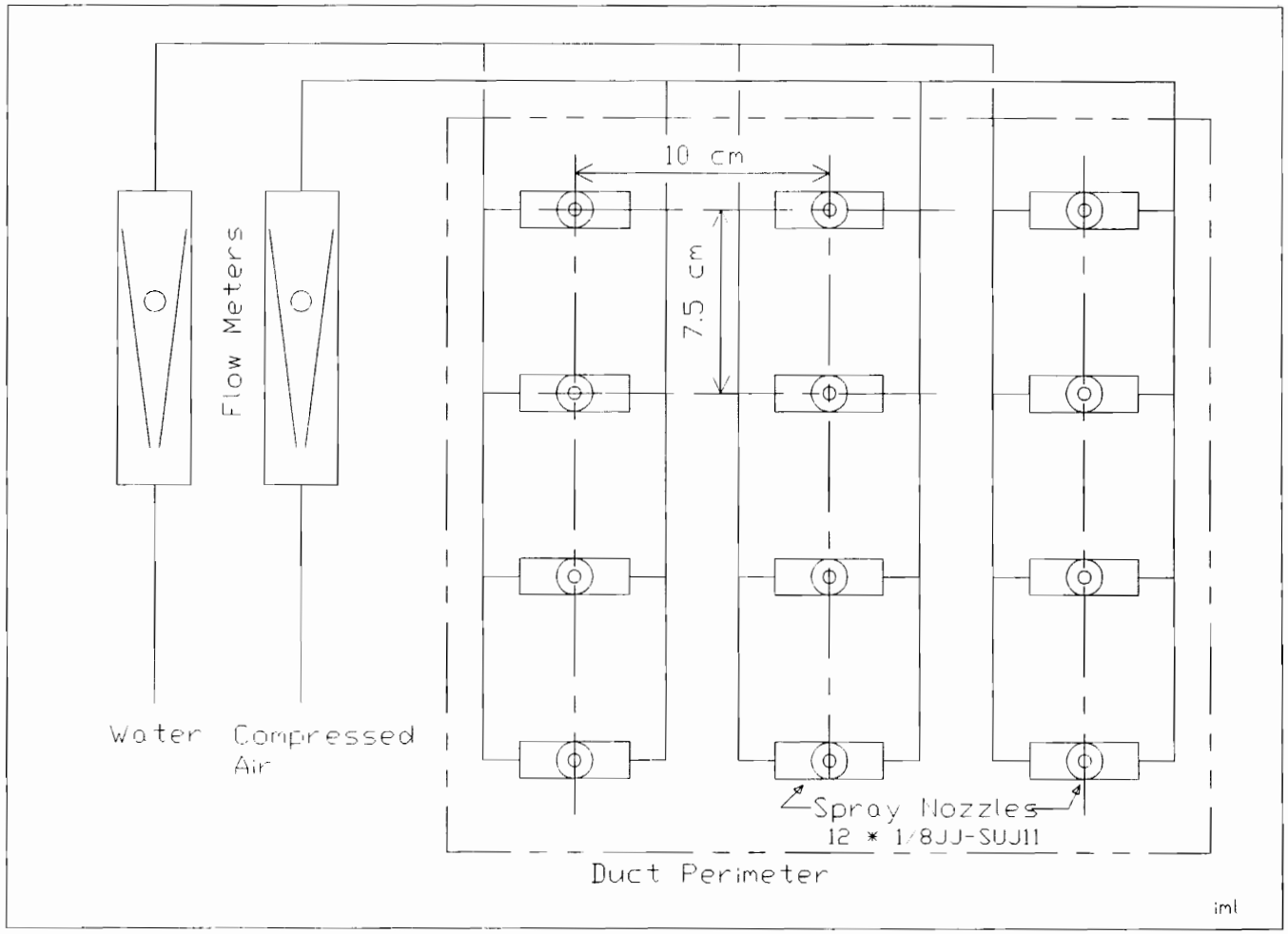

Figure 4-3: Schematic of Air Assisted Spray Nozzle Arrangement

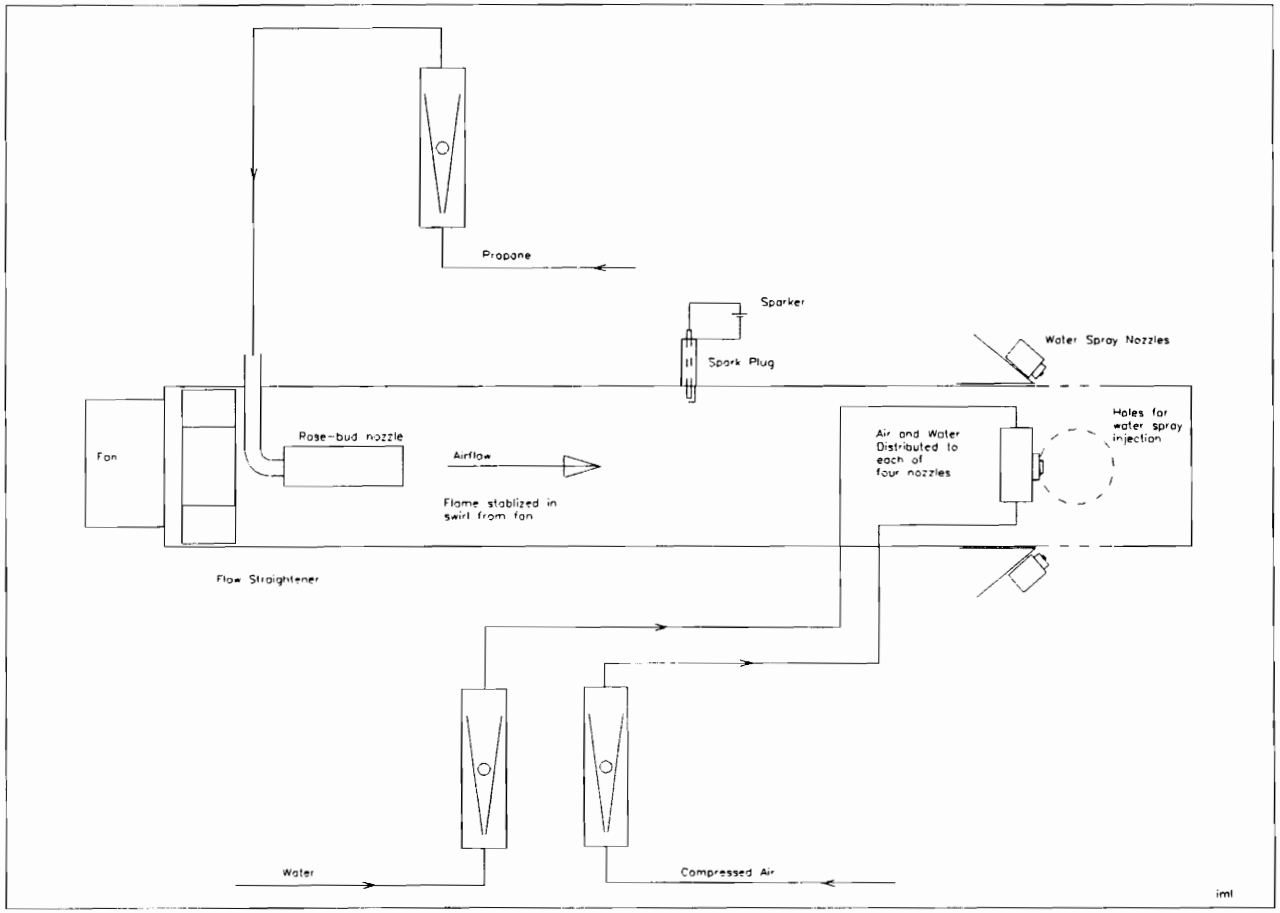

Figure 4-4: Schematic of Combination Extinguisher

jets were directed acutely to the flow of the products of combustion from the burner. In this manner the water mist was mixed with the hot gases exiting the burner and converted to vapor. Photographs of the extinguisher bench tests are shown on plate 4-2.

4.2.3. Monitoring System

A data logging system was used to collect data during the course of the tests. A general schematic is shown in figures 4-5 and 4-6. The instrument panel is shown in position next to the fire tunnel in plate 4-3.

The data logging system employed was an existing 16 channel Omega data logger operating in an IBM PC/XT. The system hardware and control software allows the channels to be configured for various data input types, in particular voltage, current, thermocouples, etc. As applied to the fire tests, voltage signals were used for gas concentrations, current for pressure measurements, and the thermocouples where directly wired for voltage measurement, using the logging system thermocouple function.

The control program (Omega Software) is written in the BASIC language and operates under BASICA as provided with MS-DOS 3.3. The Omega software allows the user to specify the signal type and range (0-10 Volts, 4-20 mA, etc.), as well as set the output units (Pa, ppm, %, °C). The user can also specify the logging parameters such as frequency, resolution, and time per channel. During the course of logging the data can be displayed in columnar format on the screen or as a running graph on the screen (anon. 1989).

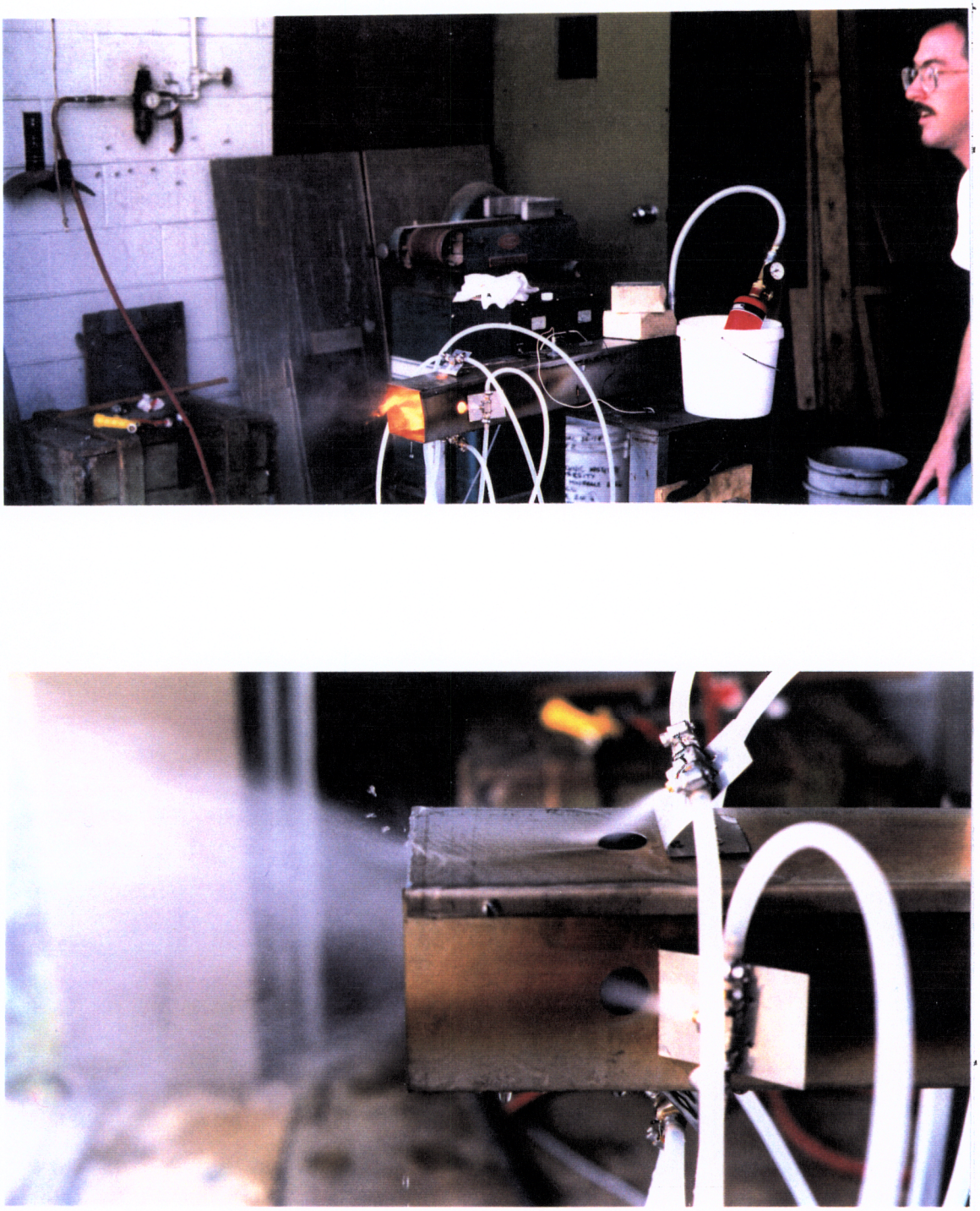

Plate 4-2: Views of Combination Extinguisher During Bench Test.

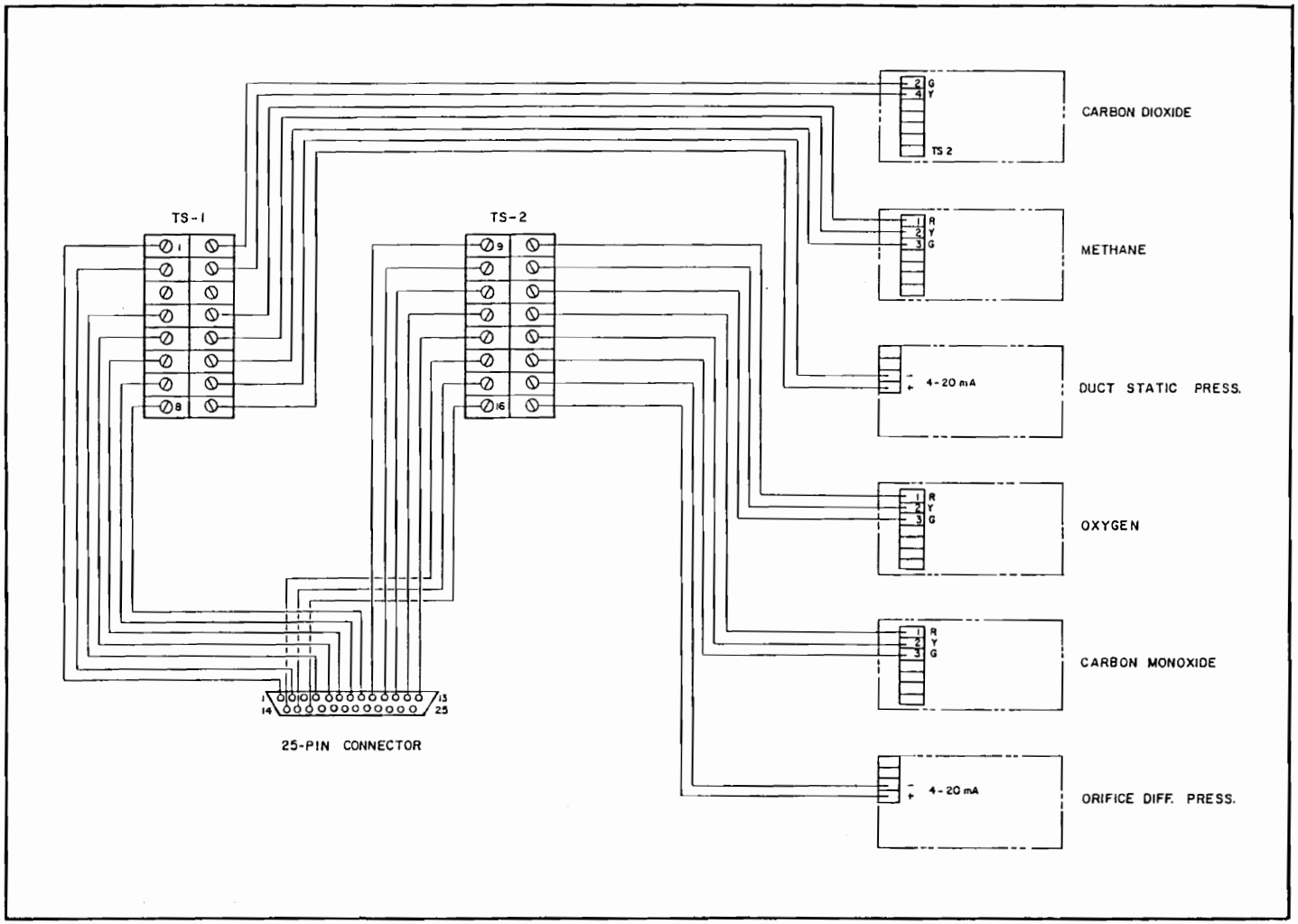

Figure 4-5: Schematic of Wiring Layout for Monitoring Transmitters

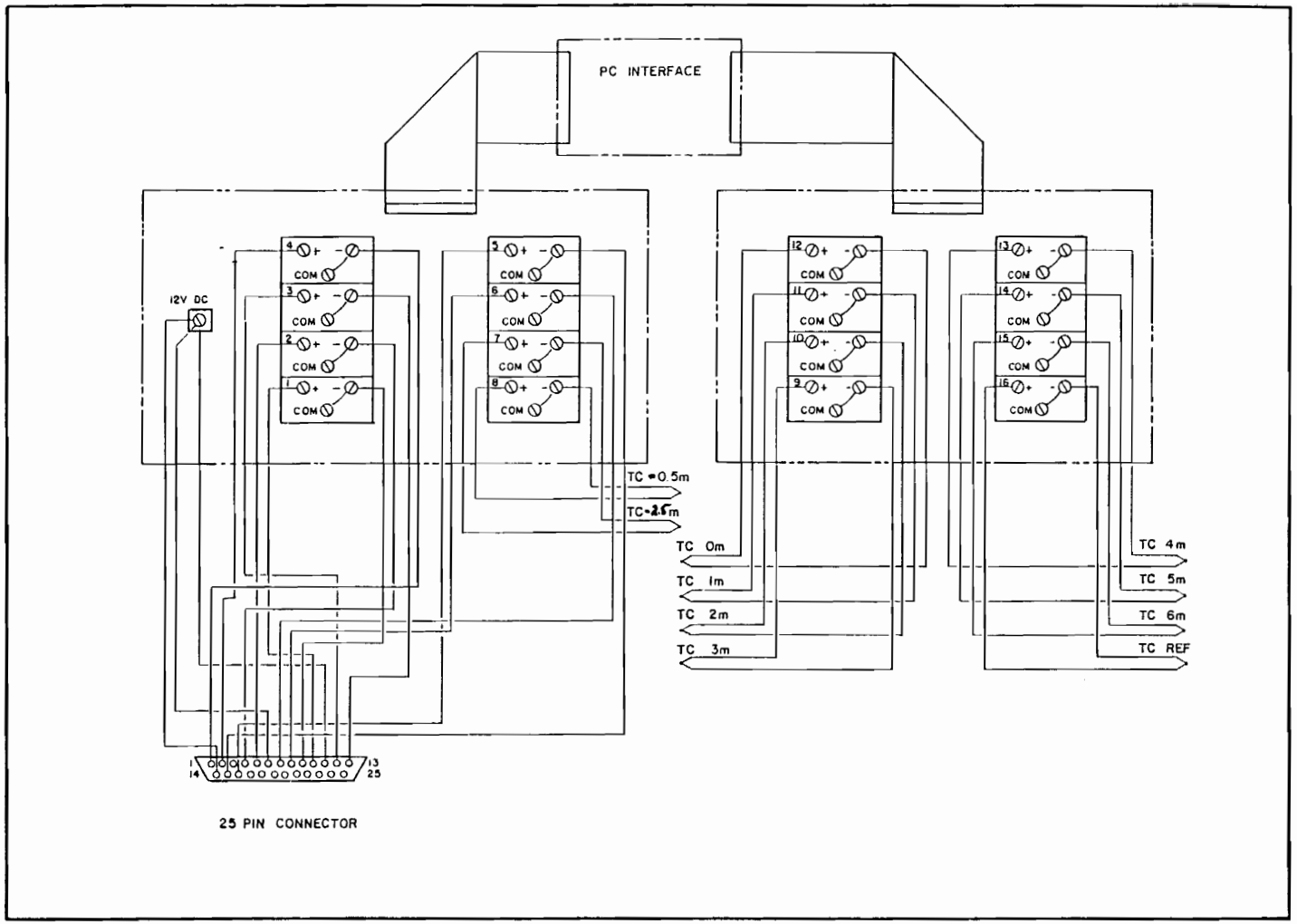

Figure 4-6: Schematic of Wiring to Data Aquisition Board

Plate 4-3: Instrument Panel with Tunnel in Background.

The configuration used for the testing is listed in table 4-5. Variations to this scheme are annotated.

The logger hardware card connects to the computer via an XT slot. The card can support two external terminal boards, with eight channels each, sixteen channels total. The monitoring equipment is connected to the terminals as shown in the schematic in figures 4-5 and 4-6.

4.2.3.1. Gases

Monitoring was conducted for 4 different gases: carbon dioxide, carbon monoxide, oxygen, and methane. The gas sample was drawn from the wind tunnel through a manifold located approximately 10 cm above the floor and 50 cm from the end of the tunnel. The sample was drawn through a steel pipe configured as a counterflow gas to water heat exchanger. See the illustration in figure 4-7. The cooled sample then flowed through a tube from the heat exchanger to an instrumentation board.

At the instrumentation board the sample was filtered and metered. The first filter used was a conventional inline compressed air filter, this proved to be unsatisfactory (see test descriptions for tests 1 and 2, in sections 5.2.2 and 5.2.3) so a disk type filter with disposable elements was built. Metering of the air was accomplished with a Dwyer Ratemaster Flowmeter.

Table 4-5: Test Configurations

Test	Fuel	Control	Pressure		Gases				Temperatures								
			Orf	Diff	O2	CO_2	CO	CH_4	-2.5	-0.5	0	1	2	3	4	5	6
1	Wood	?[1]	x		x	x	x	x	x								
2	Wood	N/A	x	x	x	x	x	x	x	x	x	x	x	x	x	x	x
3	Wood	Yes[1]	x	x	x	x	x	x	x	x	x	x	x	x	x	x	x
4	Coal	N/A	x	x	x	x	x	x	x	x	x	x	x	x	x	x	x
5	Coal	Yes[2]	x	x	x	x	x		x	x	x	x	x	x	x	x	x
6	Wood	Yes[3]	x	x	x	x	x		x	x	x	x	x	x	x	x	x
7	Coal	Yes[3]	x	x	x	x	x		x	x	x	x	x	x	x	x	x

[1] Extinguishing System - Spinning Disk Humidifer
[2] Extinguishing System - Spray Nozzle Array
[3] Extinguishing System - Combination Extinguisher

The Ratemaster is a small rotameter type of flowmeter. The rate of flow is control with a needle valve on the inlet side with the flow rate indicated by a ball "floating" in the calibrated columnar face. In this application the inlet flowmeter was used to indicate the total flow through the vacuum pump collecting the sample.

The carbon dioxide meter is equipped with a vacuum pump, as shown in figure 4-7. This pump was used to collect the entire sample used for analysis, as shown. The sample drawn through the flowmeter then enters the vacuum pump and is passed through the carbon dioxide cell. When the air leaves the carbon dioxide cell it splits. The majority of the sample was passed to the diffusion manifold for the Oxygen and Methane monitors. A small amount was metered to the Carbon Monoxide meter.

As discussed below, the carbon monoxide meter has a range of 0-50 ppm, much less than the >10000 ppm that are possible from a fuel-rich fire. To compensate for this weakness the sample was diluted with an inert gas mixture, in particular welding Argon (75% Ar, 25% CO_2).

4.2.3.1.1. Carbon Dioxide

The carbon dioxide monitoring system employs an infra-red sensor that provides a 0 to 1 volt output signal on a two wire system from the monitor op-amp. The two wires connected to the OMEGA terminal board are the ground and signal voltage. The input voltage for the CO_2 monitor is supplied from the 110 volt AC input supplied to the

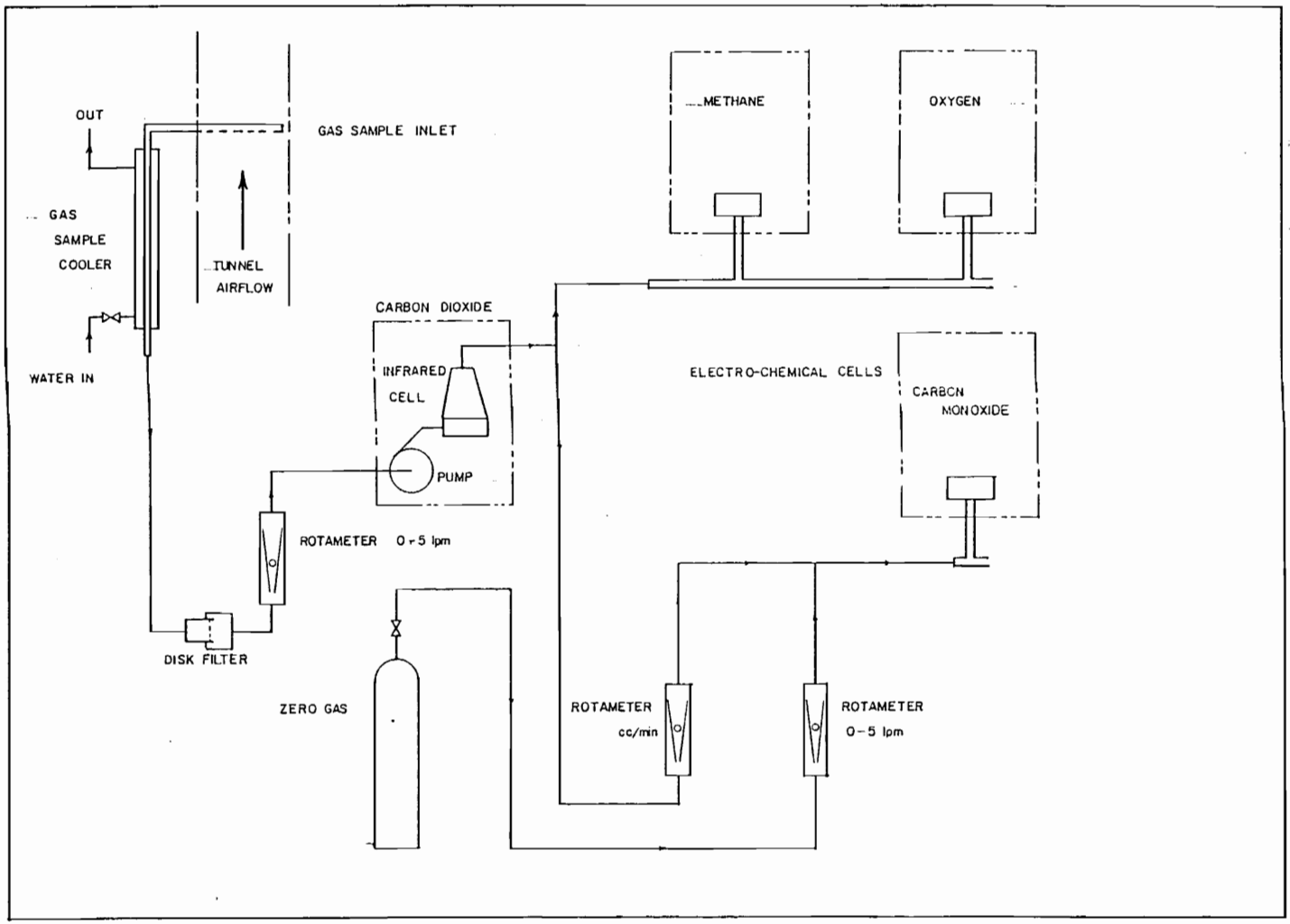

Figure 4-7: Schematic of Gas Sampling System

monitor. The input voltage supplies the power required to operate both the measurement system and the sample pump.

Calibration of this monitor was accomplished by measuring the voltage output for three CO_2 concentrations (0.3, 2.5, and 25%). The use of the 25% CO2 sample represented a 250 percent over-range of the instrument. For this reason the three points were used to generate the calibration line. The slope of which represents the scale, and y-intercept the offset to the OMEGA software. A typical calibration chart is shown in figure 4-8, the correlation coefficient is given for the line based on the three point regression.

Based upon a conversation with technical personnel at REL-TEK, the CO_2 monitoring system supplier, the above approximation is appropriate. The Infra-red sensor element is capable of handling a range up to about 45% carbon dioxide. The output range of the amplifier is nominally 0-1V dc, with 1 volt corresponding to 10% CO_2, at output ranges above 1 volt the supplier does not ensure linearity. Based on the close correlation of the three data points to a straight line, the linear approximation appears appropriate over the broad range of the data (0-23% CO_2).

4.2.3.1.2. Oxygen

The sensor system used to monitor the Oxygen concentration was a model MC-4110 diffusion type supplied by American Mine Research, Inc. This instrument is scaled to indicate 0-25% O_2. The unit was configured to supply a 0.1 to 4.0 volt signal on a three wire system. The three wire system provides ground, input voltage and signal voltage. The arrangement of the wiring is illustrated in figures 4-5 and 4-6.

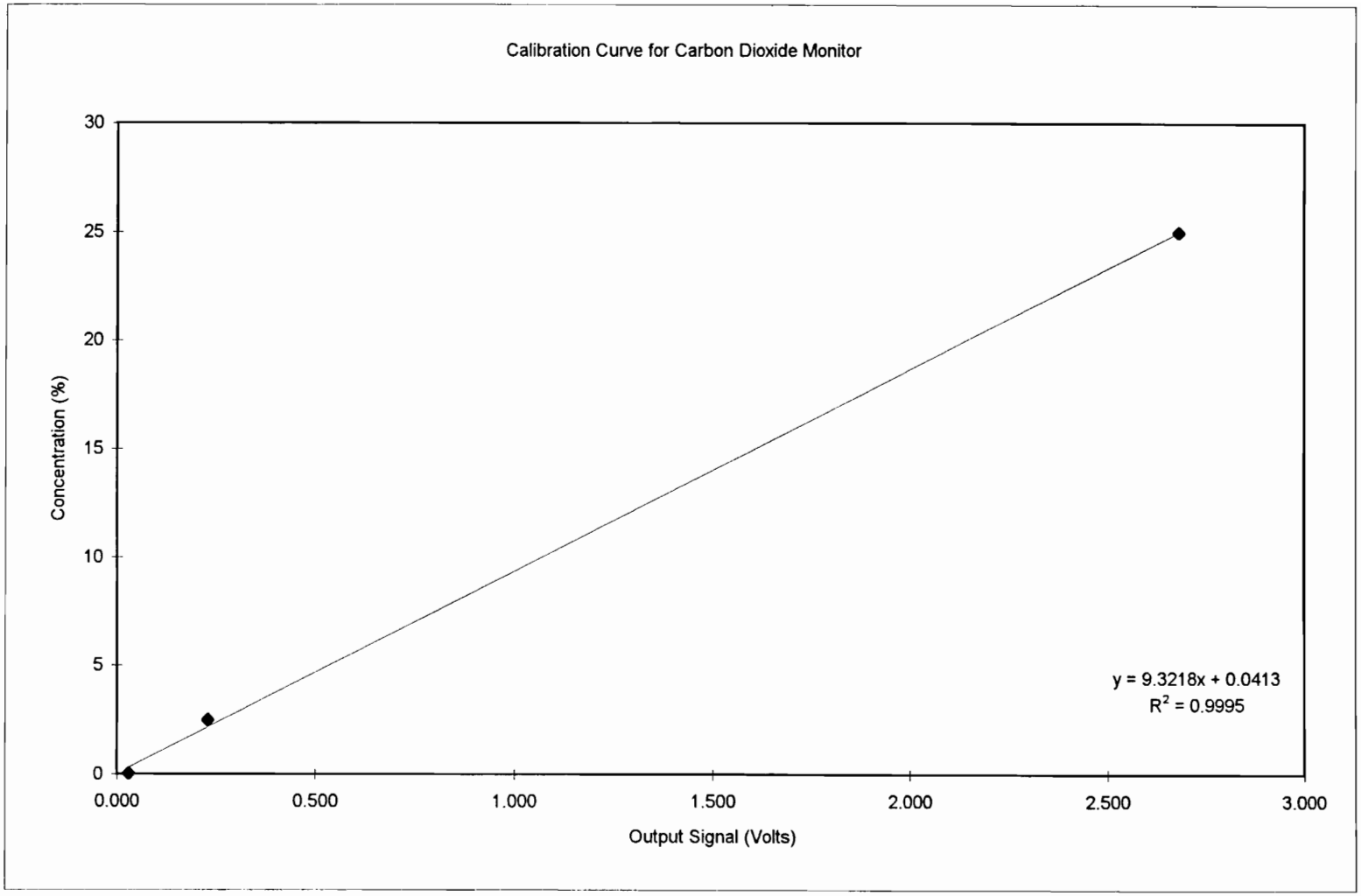

Figure 4-8: Typical Calibration Chart for Carbon Dioxide Sensor.

Calibration of the Oxygen sensor was accomplished in a two stage process. First, the normal atmospheric oxygen level (taken as 21% O_2) was set using the magnetic switch on the monitoring unit. Second, the output voltages where measured for the normal oxygen level and for 0% oxygen. From these measurements a two point calibration provided a line, the slope of which represents the scale and the y-intercept the offset to the OMEGA software. A typical calibration chart for the oxygen monitor is shown in figure 4-9. The output of the sensing element was reported by the supplier as sufficiently linear for the two point calibration over the nominal range. The sensor cell manufacturer's bulletin reports the nominal range to be 0-25%, the resolution to be 0.1%, and the maximum overload to be 30% (Anon. 1992b).

The "zero-gas" employed in the calibration was either welding argon (75% Ar, 25% CO_2) or nitrogen evaporated from a liquid, depending on availability.

4.2.3.1.3. Methane

The methane (CH_4) monitor employed during the testing (tests 1, 2, 3 and 4) was a model MC-4110-CH4 supplied by American Mine Research, Inc. This monitor uses a pellistor sensor.

This system was calibrated using a two step process. First, the zero point was set using the magnetic switch located on the monitor. Second, the output voltage was measured for 0 and 2.5% methane. The voltages provided for a two point calibration line, the slope of which represents the scale, and y-intercept the offset to the OMEGA software. A typical

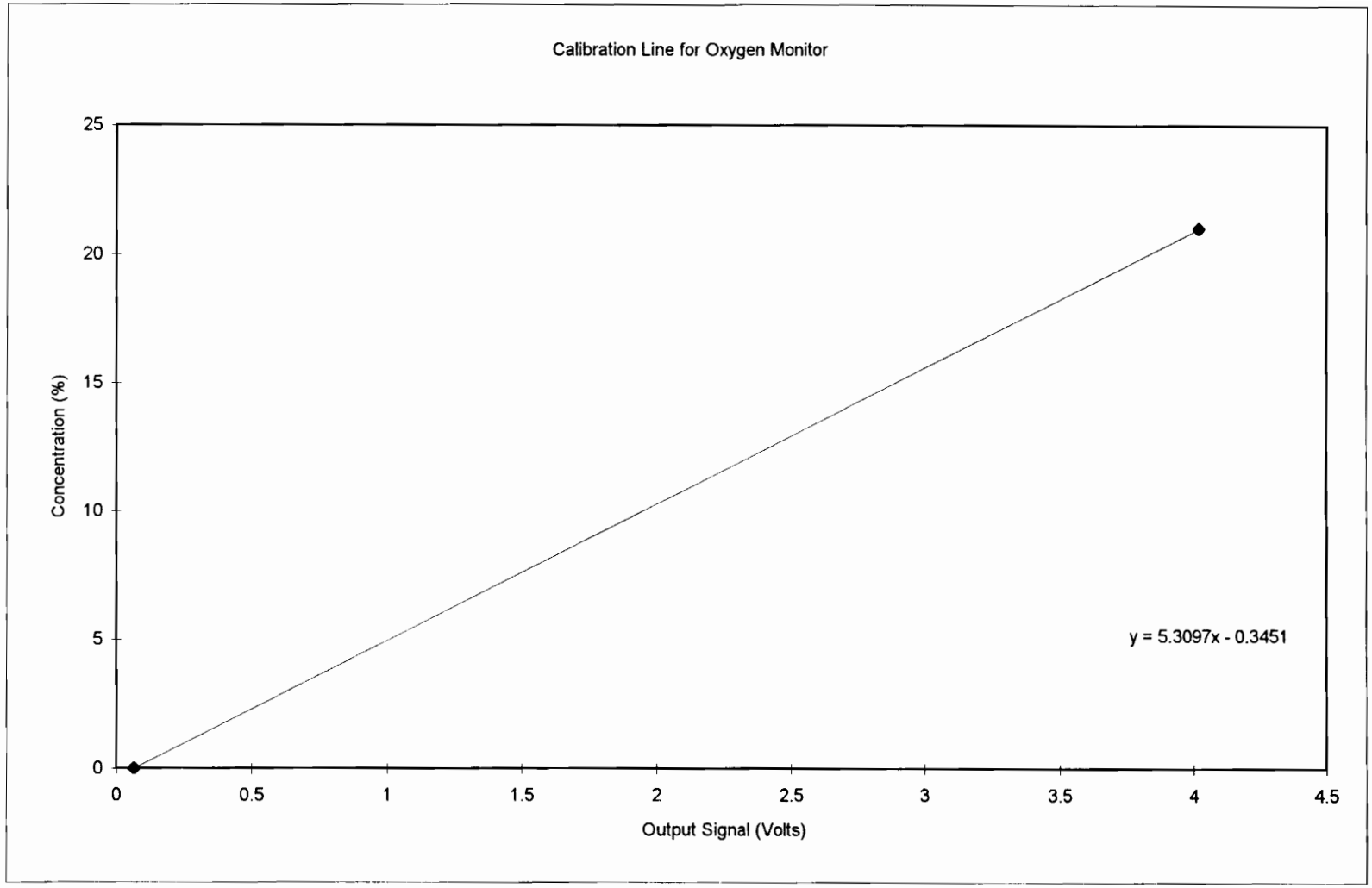

Figure 4-9: Typical Calibration Chart for Oxygen Sensor.

calibration chart for the methane monitor is illustrated in figure 4-10. This is the calibration procedure applied by the manufacturer.

Although this instrument was used in the first 4 tests several problems with its application are worth noting. First, the sensor requires "normal" levels of oxygen to properly determine the quantity of methane (and other combustible) gas in the sample. Second, this gauge experiences a great deal of drift due to poisoning of the cell. The methane monitor eventually died as a result of this treatment during the fourth test (the first test with coal as the fuel).

4.2.3.1.4. Carbon Monoxide

The measurements of Carbon Monoxide were made using a model CO-2112 diffusion type monitor supplied by American Mine Research. This monitor uses a three wire system, configured as ground, input voltage, and signal output. The output signal is nominally 0.1 to 4.0 volts, linearly proportional to the CO concentration. The nominal range of this instrument, as configured using internal dip switches, is 0 to 50 ppm CO. Calibration of this instrument using a 60 ppm CO check gas allowed for an over-range of 20%.

Calibration of this instrument was accomplished in a two step process. First, the zero was set using the magnetic switch provided. Second, the output signals were measured for both 0 and 60 ppm CO. A two point calibration yielded a line of which the slope represents the scale and the y-intercept the offset to the OMEGA software. A typical calibration chart for the Carbon Monoxide monitor is shown in figure 4-11. The range of the CO cell was given as 0-1000 ppm by the manufacturer (City Technology LTD) with a

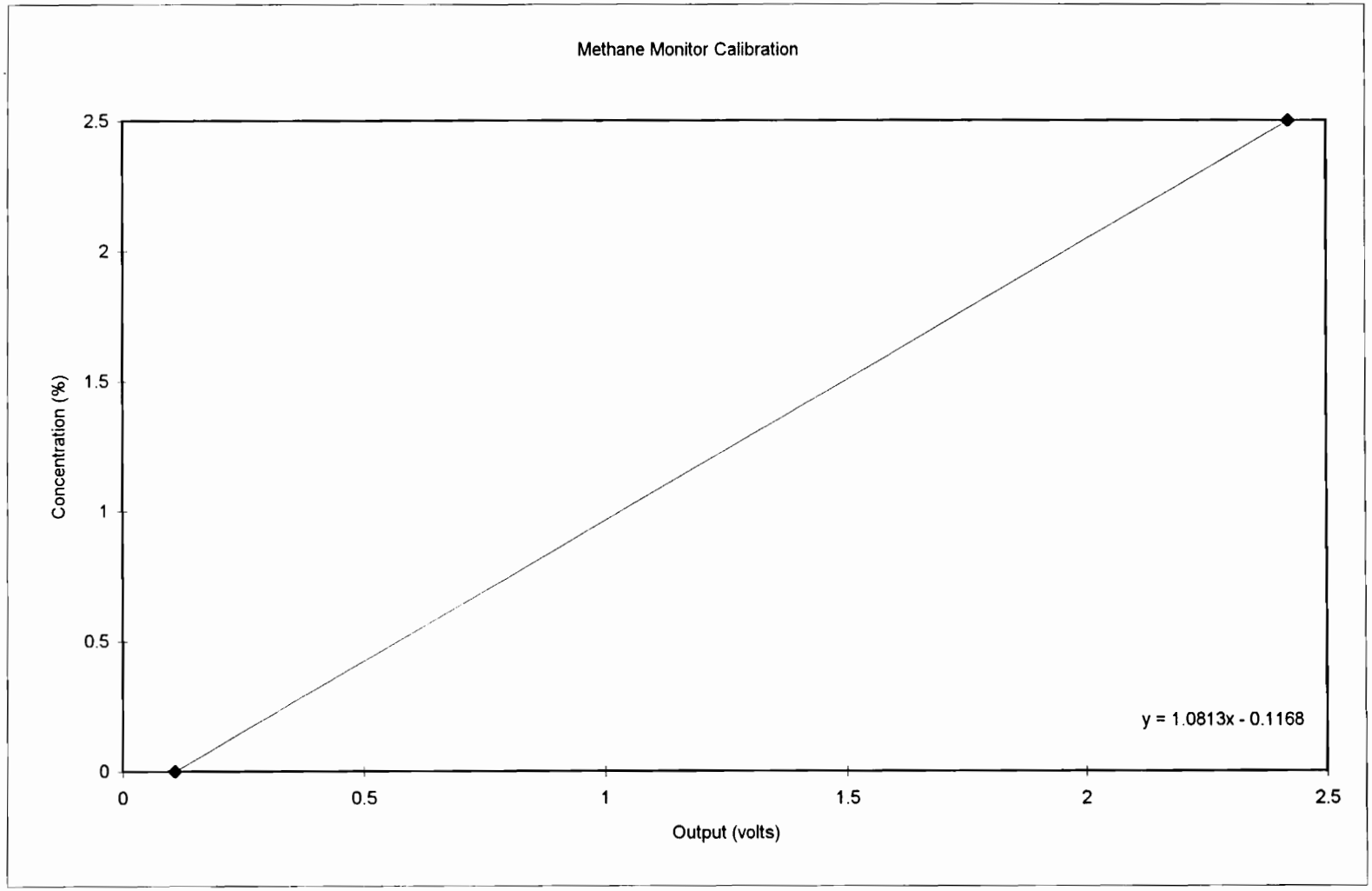

Figure 4-10: Typical Calibration Chart for Methane Sensor.

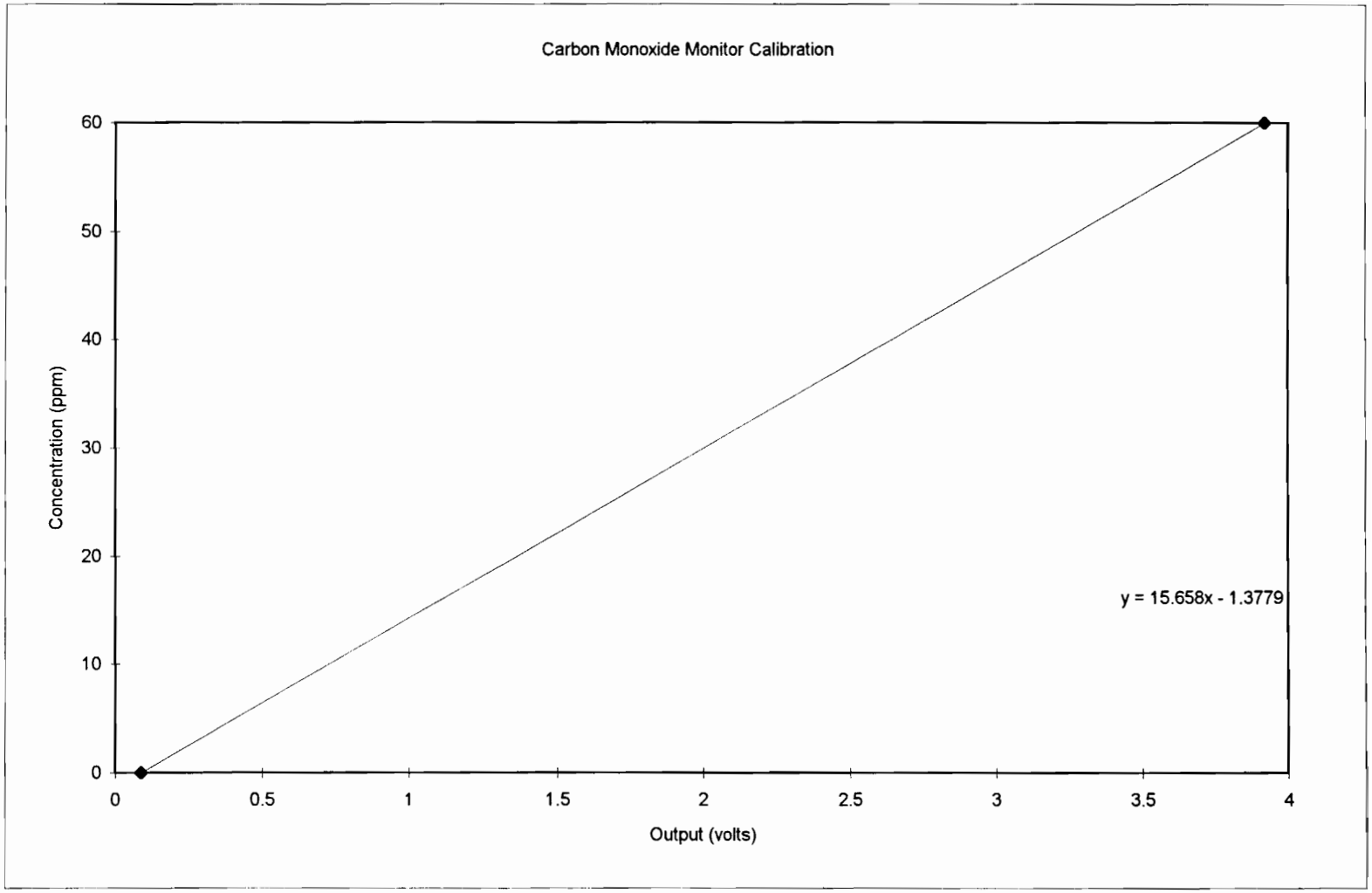

Figure 4-11: Typical Calibration Chart for Carbon Monoxide Sensor.

maximum overload of 2000 ppm. The linearity of the output was based on a maximum output of 4 volts from the monitor op-amp, corresponding to a reading of 50 ppm.

As mentioned above, the range capability of the Carbon Monoxide monitor is significantly less than levels that can be expected from a fire. For this reason the CO monitoring system was configured to provide a diluted sample to the monitor. This was accomplished by mixing a metered gas sample with a metered quantity of welding argon (75% Ar, 25% CO_2). Typically, these were mixed at the rates of 10 cc/min sample with 5000 cc/min diluent. The arrangement of this system is illustrated in figure 4-7. The dilution system introduced a delay of about 4 minutes between the other gas measurements and the Carbon Monoxide readings.

4.2.3.2. Pressure Measurements

Measurements of pressure were taken across the orifice plates for all tests. A measure of the static pressure in the duct, down stream of the orifice was taken for all tests except for the first. These measurements were taken using MODUS Instruments type T40 differential pressure transmitters. The operational element of this instruments is a capacitance cell in which the capacitance is varied by a diaphragm that deflects with an applied pressure. These transmitters supply a nominal 4-20 mA signal linearly scaled from 0-3 inches water gauge that has a rated accuracy of ±1% of the range. Application in the OMEGA software allowed the 4-20 mA signal to be expressed in Pascals rather than inches water gauge.

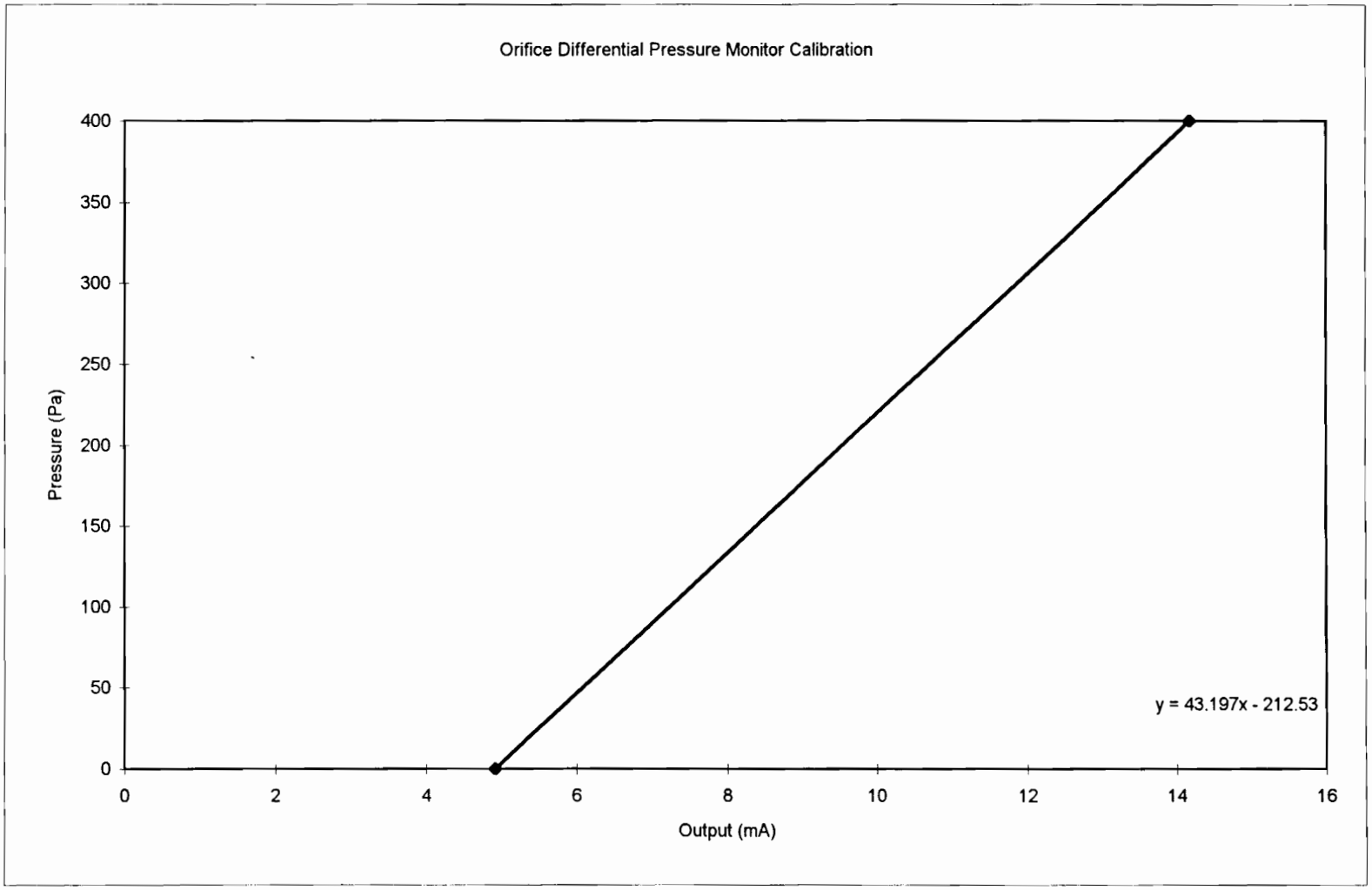

Figure 4-12: Typical Calibration Chart for Differential Pressure Transmitter.

Calibration of these gauges was accomplished using a stable pressure source to generate a differential pressure. The output signal, in milli-Amps, was monitored using the OMEGA software. A two point calibration results in a line the slope of which yield the scale and the y-intercept yielding the offset required by the OMEGA software to produce the desired output units. A typical calibration chart for these instruments is shown in figure 4-12.

4.2.3.3. Temperature Measurements

Measurements of temperature where taken using J-type thermocouples consisting of a twisted pair of iron and constantan wires. During the first test a single thermocouple was used to measure the temperature of the air in the tunnel upstream of the fire. This thermocouple was connected to a transmitter that produced a 4-20 mA output signal, linearly proportional to the temperature indicated by the thermocouple. This system was calibrated in a similar fashion to the pressure transmitters.

From the second test onwards 10 J-type thermocouples were used, rather than the single one used in the first test. To support these, the thermocouple feature was used in the OMEGA software to determine the temperature, rather than the transmitter above. In this manner each thermocouple was terminated at the OMEGA terminal board. The software, instructed that the appropriate terminals are J-type thermocouples, converts the induced voltage to a temperature indication on the desired scale (°C).

For the tests using multiple temperature measurements the thermocouples were placed near the top of the tunnel, on the inside, at locations of -2.5, -0.5, 0.0, 1, 2, 3, 4, 5, and 6 meters; the zero point being the interface between the pre-fire and burner sections of the tunnel. Placements at the positive positions were affected by the lid sections and therefore did not fall precisely on the distance desired.

5. *RESULTS*

This section will review the procedures employed and the results obtained for the experiments. Since the wind tunnel used for these experiments was specifically constructed for them it is appropriate to cover the start-up testing prior to a discussion on the results from the intended studies.

Such an approach is relevant for two reasons: (1) it validates the original design, (2) it will be useful in determining the actual conditions employed during the fire tests to follow. Furthermore, the fire tests are divided into two groups, those for which the fuel was wood and those for which coal was the fuel.

5.1. Start-up Testing

Start-up testing was conducted on the elements of the wind tunnel to determine the level to which it met with the original design. Two key areas of the tunnel to be verified were the airflow control system and the fog system efficiency.

5.1.1. Orifice Flow Tests

As described earlier, an orifice, in conjunction with a waste gate, is used in the tunnel to control the airflow into the fire section. The procedure employed for this testing provided observations of the flow for each orifice considered under each of three settings of the waste gate.

5.1.1.1. Procedures

The following procedure was used to determine the airflow rate through the wind tunnel for the designed and available configurations.

1) With waste gate open and no orifice installed start the wind tunnel fan.

2) Zero micromanometer, then connect to static pressure taps across flow control section.

3) Fix guide plate, for pitot tube/hot wire anemometer, over the vent opening at the pre-fire to fire section interface.

4) Insert desired orifice plate and adjust waste gate to desired depth and lock in place with small clamp.

5) With fan running and appropriate orifice installed, record the Barometric Pressure (P), and Wet and Dry Bulb Temperatures (t_{wb} and t_{db}) on the test log sheets

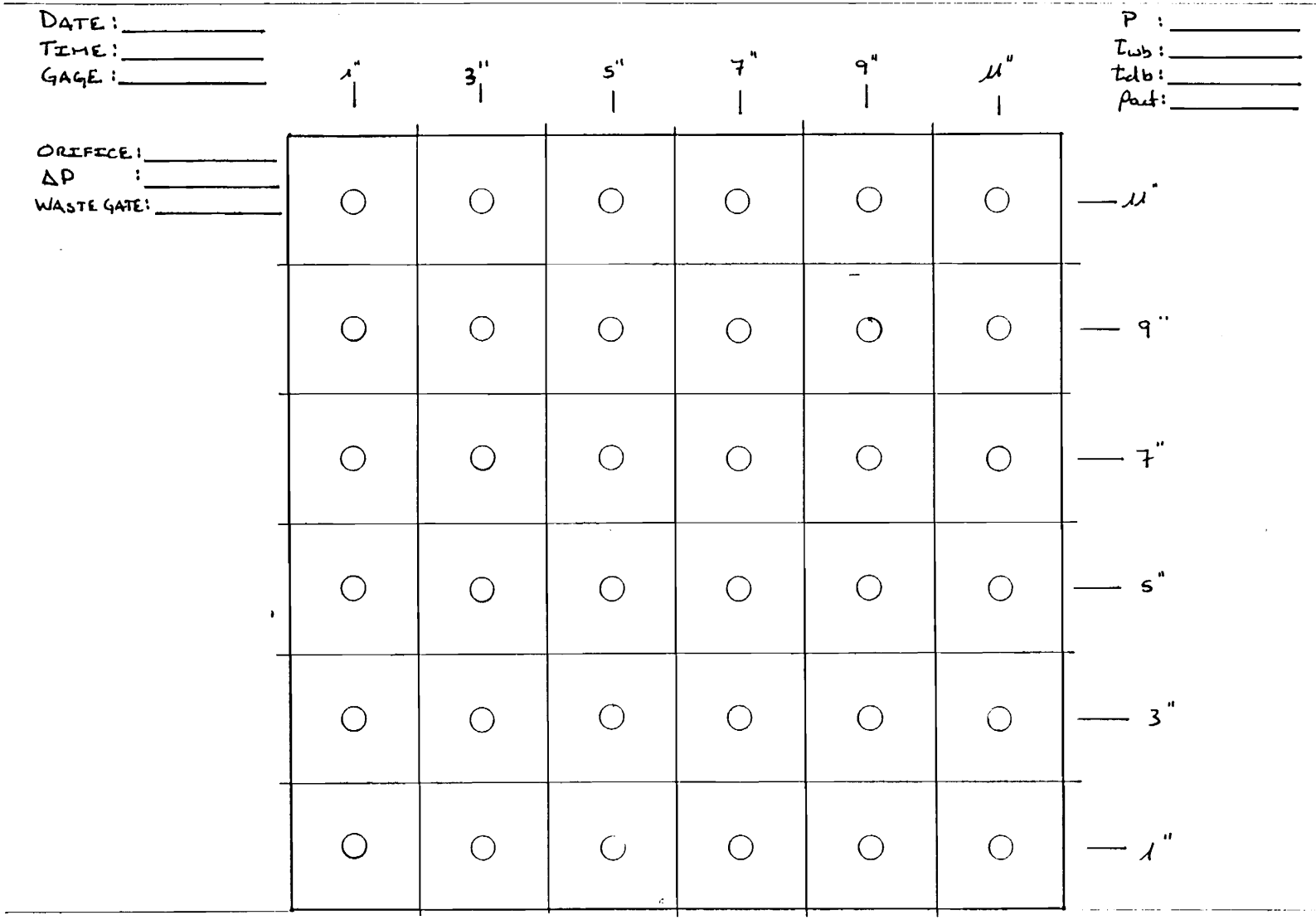

Figure 5-1: Air Velocity Data Collection Sheet

(figure 5-1). Record the remaining data, Orifice Number, Waste Gate Position, Pressure Drop across orifice, time, gauge number, and date on the test log sheet.

6) When using pitot-tube continue at step 7, when using hot-wire anemometer continue at step 9.

7) Disconnect micromanometer from the flow control section static pressure taps, check zero, and configure to the pitot tube.

8) Use pitot tube to measure the velocity pressure in the pre-fire section at the points indicated on the log sheet. With this complete return to step 4 and continue for the next desired configuration.

9) Use the hot-wire anemometer to obtain velocity readings in the pre-fire section at the points indicated on the log sheet. With this complete return to step 4 and continue for the next desired configuration.

5.1.1.2. Results

The pressure - quantity diagrams for the open tunnel and for orifice 6 are shown in figures 5-2 and 5-3, respectively. The results of the orifice tests indicate that for the conditions recorded a flat velocity profile existed across the tunnel cross-section leading into the fire section. See figure 5-4. This figure was produced using the SURFER package available from Golden Software, Inc.

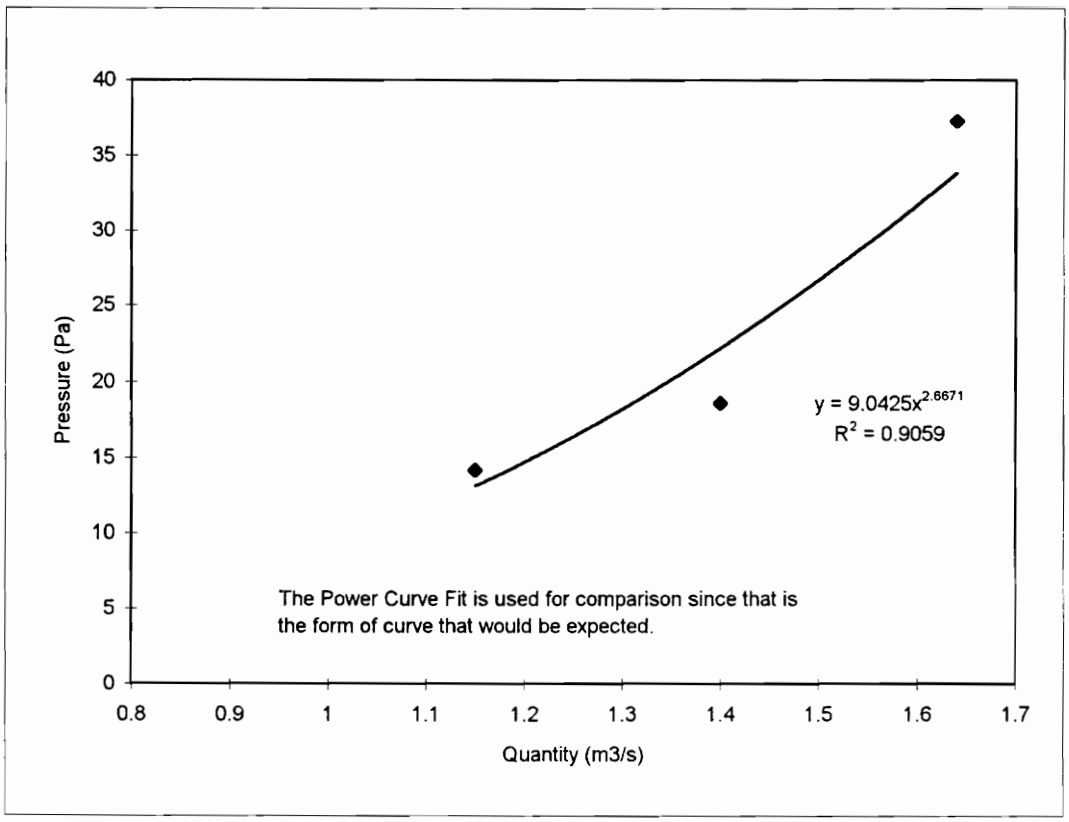

Figure 5-2: Pressure - Quantity Diagram for Un-restricted Tunnel.

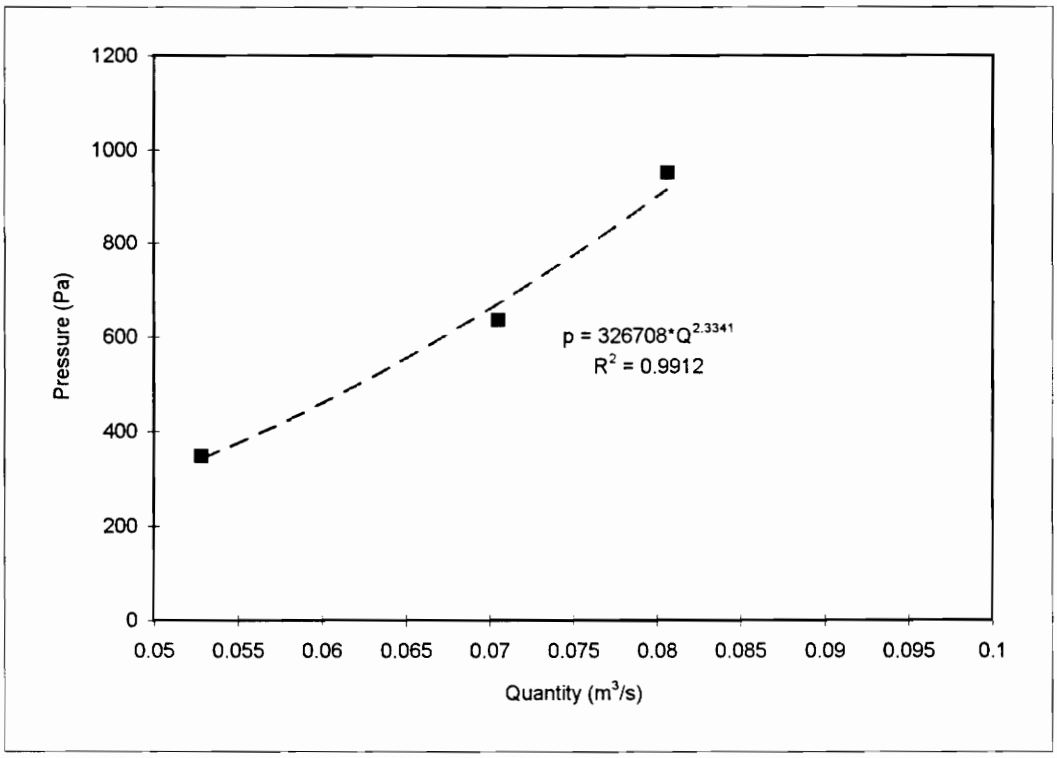

Figure 5-3: Pressure - Quantity Diagram for Tunnel with Orifice Number 6.

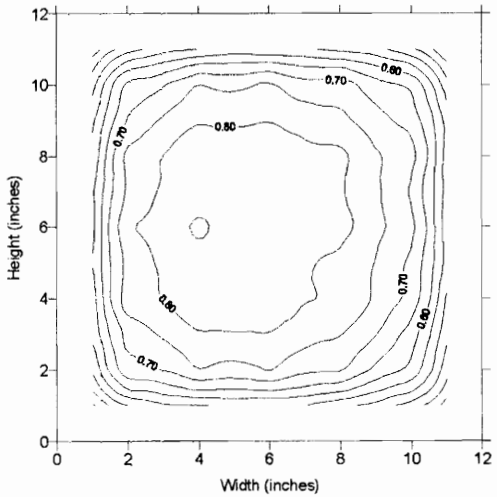

Waste Gate Closed

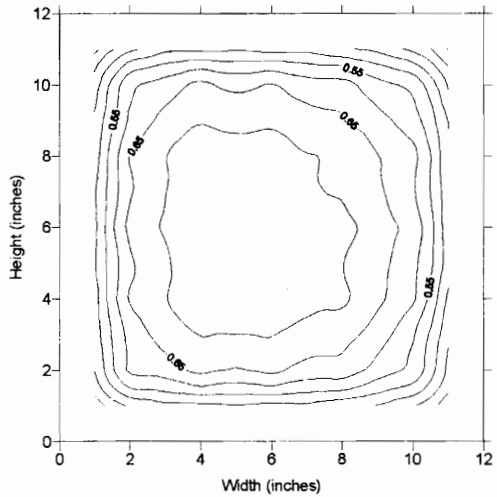

Waste Gate Half Open

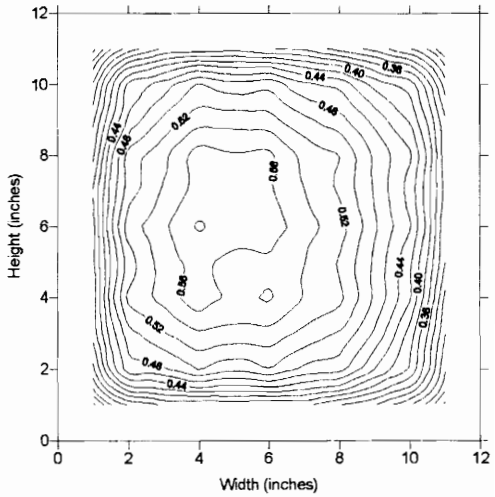

Waste Gate Open

Figure 5-4: Air Velocity Profiles (m/s) at Entrance to Fire Section for Orifice 6

Since the orifices are being used to meter the flow through the tunnel it is necessary to know the resistance of each orifice so that the appropriate pressure drop can be determined. Under normal airflow conditions the following relationship is known to exist:

$$p = RQ^n$$

Given that both pressure drop (p) and airflow quantity (Q) are known, the resistance (R) and the index (n) can be computed by linear regression if the equation is rewritten in the form of a line:

$$\ln(p) = n\ln(Q) + \ln(R)$$

When this is done the slope of the line is the index and the y-intercept is the natural log of the resistance. Based on the actual field tests, corrected to a density of 1.21 kg/m^3, the resistance and index of each orifice is listed in table 5-1.

The values for the index were expected to be around 2.0, to be in accordance with the square law normally used to associate the pressure drop with the quantity, satisfying the proportionality:

$$p \propto Q^2$$

Table 5-1: Orifice Resistances and Indices

Orifice	Resistance	Index
None	9.1516	2.6308
10	113185	2.3669
9	159035	2.3800
8	353122	2.5979
7	392806	2.5500
6	326621	2.3300
5	2000000	2.5737
4	382793	1.9874
3	996626	2.2355
2	2000000	2.1281
1	451428	1.7118

With the exception of orifice 4 the indices appear to vary significantly from 2.0, most of them are higher than 2. One possible explanation for this deviation may be the relatively short distances used in obtaining the pressure drop readings. That is the static pressure taps, placed in the center of the air flow may have been too close to the orifice and elbow at the fan. Such proximity to disturbances could account for incorrect, actual, pressure readings. Subsequent use of the developed curves did prove, however, that they would reliably predict the airflow in the wind tunnel based on the relative pressure differential measured across the orifice in place.

5.1.2. Fog System Efficiency Tests

The fog system efficiency tests were conducted to determine two basic factors. First was the rate at which the fog system actually consumed water and second to determine the density of the fog being created.

5.1.2.1. Procedures

The fogging system efficiency tests were conducted by the procedure outlined below.

1) With the waste gate open and no orifice installed start the tunnel fan. When fan has started insert desired orifice and set waste gate to the desired depth.

2) Zero the micromanometer then attach to the static pressure taps across the flow control section.

3) Record the Barometric Pressure (P), wet and dry bulb temperatures of ambient air (t_{wb} and t_{db}), pressure drop across flow control section (Δp), and the orifice and waste gate settings on the test log sheet.

4) From a measured bucket fill the cistern below the fogger. Record the total quantity of water in the cistern (Q_1). (This worked out to be 9.5 liters (10 quarts)).

5) Place buckets at probable leak points to collect dripping water (figure 5-5).

6) Start fogger by plugging it into the extension cord (no distinct switch is provided). Start stopwatch when fog is visible exiting the wind tunnel.

7) While the fog is operating record the temperature of the saturated fog at the exit of the wind tunnel (t_{fog}) and record on the test log.

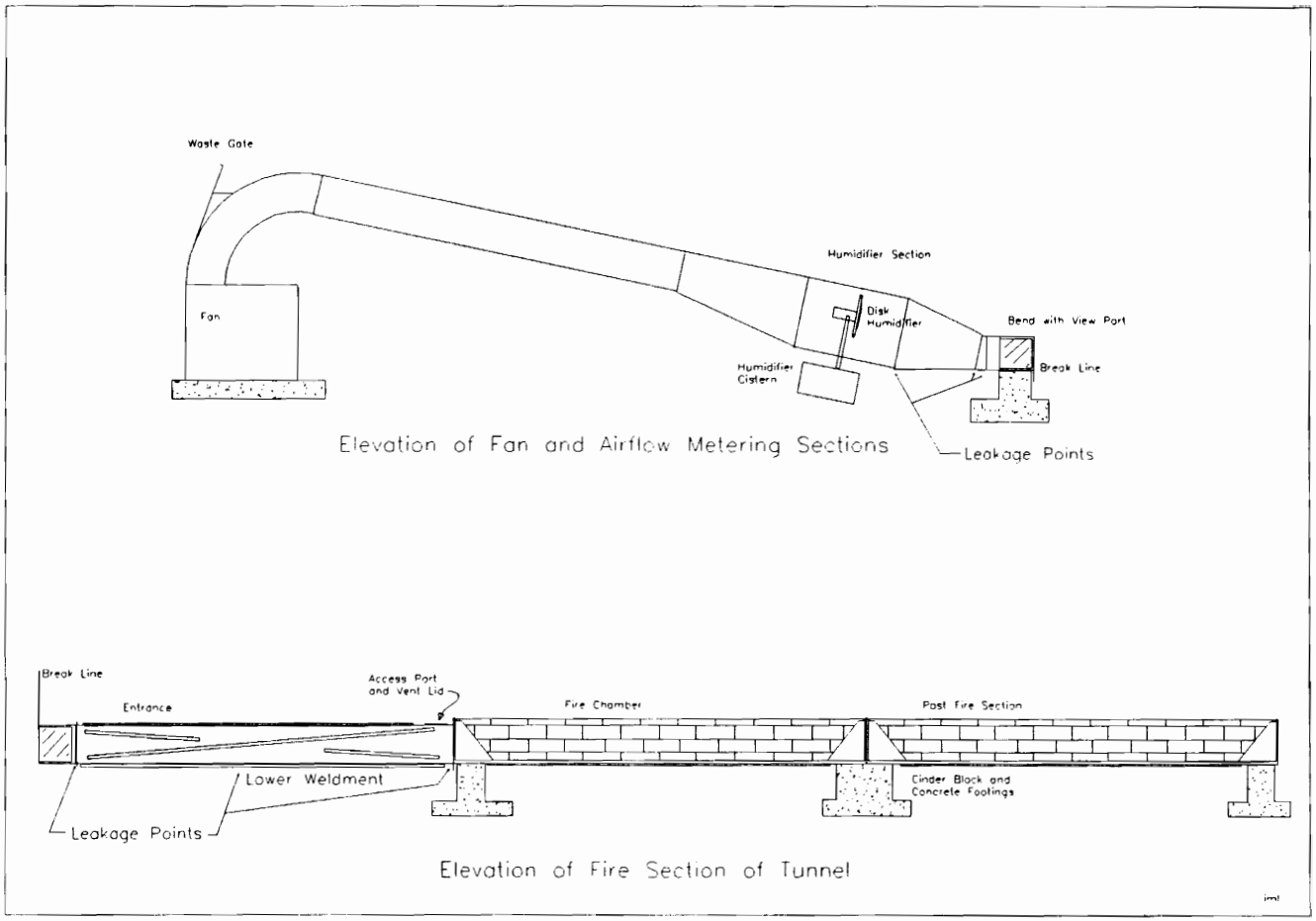

Figure 5-5: Illustration of Water Leakage Points

8) Stop the stopwatch when fog is no longer visible exiting the tunnel, then stop the fogger by unplugging. Remove the cistern from the fogger and collected any remaining water in it, record this on the test log (Q_3). This will be about 1 quart.

9) Collect all the water that has leaked out of the tunnel and record on the test log (Q_2). Dispose of all the water collected.

10) Continue at step 3 to obtain a total of three sets of data for the current configuration.

11) Set new wind tunnel configuration and repeat test beginning at step 3. At least three configurations should be observed, including the full fan capacity and conditions expected during fire testing.

5.1.2.2. Results

The results showed two very distinct characteristics of the fogging system both of which become intuitively apparent when one steps back to review the results. The first is the density of the fog is inversely proportional to the rate of airflow. The second is that the efficiency at which the water is carried away as fog is proportional to the rate of airflow.

Table 5-2 shows a reduced data table for the tests conducted to determine the characteristics of the fogging system. The configurations are identified numerically and

individual tests with an alpha designator. Efficiency is defined as the proportion of the water that exited the system in the form of a fog.

Table 5-2: Results from Fog System Tests

Test	Time (min)	Airflow (m^3/s)	Airflow (kg/s)	Fog Rate (kg/s)	Efficiency (%)
1a	7.97	1.16	1.28	0.0124	72.25
1b	8.00	1.16	1.28	0.0104	58.33
1c	7.50	1.16	1.29	0.0122	65.17
1 (ave)	7.82	1.16	1.28	0.0117	
2a	7.62	1.68	1.84	0.0122	65.56
2b	7.75	1.71	1.88	0.0122	66.67
2c	7.50	1.71	1.87	0.0126	67.42
2 (ave)	7.62	1.70	1.86	0.0123	
3a	8.95	0.11	0.11	0.0085	54.55
3b	8.20	0.11	0.11	0.0081	46.67
3c	9.50	0.11	0.11	0.0074	33.33
3 (ave)	8.88	0.11	0.11	0.0080	

In the above table, the test 1 group was conducted with a clean tunnel with the waste gate open, the test 2 group was conducted with a clean tunnel with the waste gate closed, and the test 3 group with orifice 10 in place and the waste gate at about 1/2 open.

The relationship of the fog density and the fog rate against the airflow rate is shown in figure 5-6. As mentioned above, the fog rate varies proportional to the airflow, and the fog density varies inversely proportional to the airflow. It is interesting to note that the relationships extend over an entire order of magnitude. This condition allows the application of the trend down to the airflow rate of about 0.070 m^3/s that are associated with the fire tests, conducted with orifice 6. Regression analysis shows that the fog density versus airflow rate has a correlation coefficient of 0.992 to a logarithmic fit. An

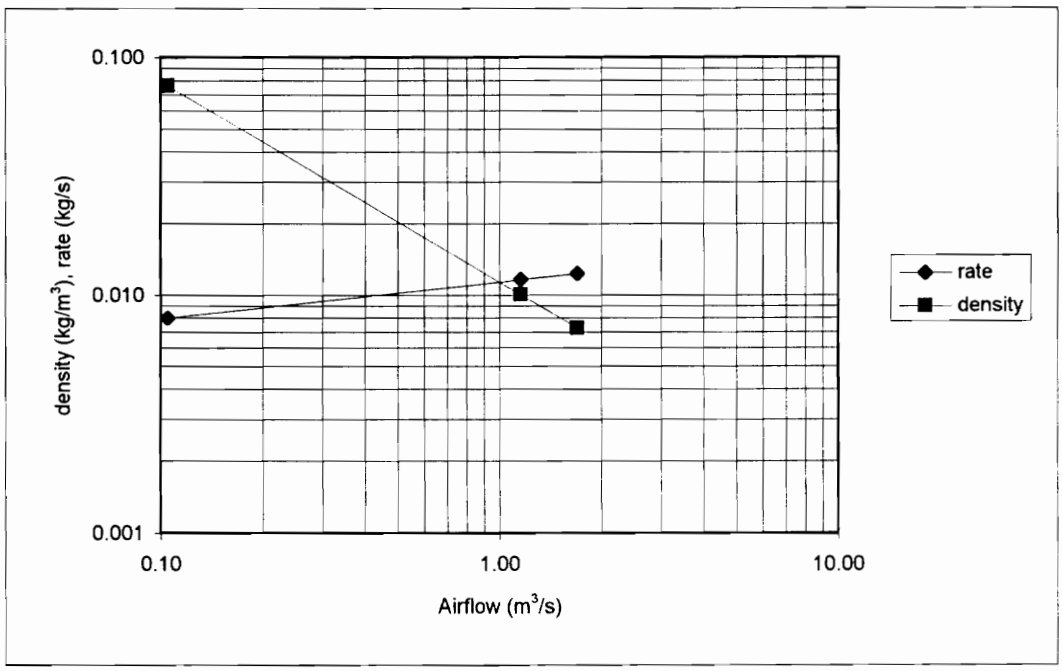

Figure 5-6: Log-Log Plot of Fog Rate and Density as a Function of Airflow Rate.

analysis of the fog rate versus airflow rate shows a correlation coefficient 1.0 to a logarithmic fit.

$$\delta_{fog} = -0.0257 \ln\left(\dot{Q}_{air}\right) + 0.0176$$

$$\dot{m}_{fog} = 0.0015 \ln\left(\dot{Q}_{air}\right) + 0.0115$$

The relationships between the rate and the density to the airflow rate appear to make good physical sense. When one considers the fog generator to be producing the water mist at a constant rate, independent of airflow, the amount of water being carried per unit volume of air should decrease as the airflow increases. The first response to the other relationship is that the fog rate should remain constant if the production rate is constant. However, one can imagine that as the fog density increases, the interaction of the mist particles will increase. The increased interaction leads to the initially small particles combining into larger particles. The large droplets of water that form cannot be held in suspension and drop out, leading to a decreasing fog carrying rate as the airflow decreases.

5.1.2.3. Pneumatic Assisted Spray System

Bench tests of the pneumatic assisted spray nozzle system seemed to indicate that it would provide good dispersion of fine droplets into the air stream. When the system was installed into the wind tunnel, it appeared that a relatively large quantity of the water was being lost due to impingement and coalescing of the water particles. A set of quantitative measurements were made at an airflow rate of 0.071 m^3/s (150 cfm), and pneumatic assist airflow of 0.001 m^3/s (2.3 cfm). Water flow rates of 0.037 kg/s (35 gph) and 0.042 kg/s (40 gph) were used revealing a fog generation efficiency of about 55%. Of the remaining

45 percent about half of this water flowed into the fire section of the tunnel and the other half leaked from the tunnel without getting to the fire section.

5.2. Wood Fire Tests

In order to obtain a general feel for the response of the tunnel to the fire and to observe the response of the fire to the various extinguishing attempts four tests were conducted using plywood as a fuel. These tests (number 1, 2, 3, and 6) made use of the lower energy fuel source to demonstrate the basic procedures for the operation of the tunnel and the extinguishing equipment. A typical wood fueled fire is illustrated in the photographs of plate 5-1.

5.2.1. Procedures

Prior to setting the tests up in the field, the gas monitoring instruments were individually calibrated. The results of the calibration were applied to the logging data for each specific test. The gas monitors were calibrated prior to and following each test since they were coming in direct contact with the gases produced in the fire. The pressure monitors were not calibrated prior to each test since they were isolated from the fire, and would not be sensitive to "poisoning" by the fire gases.

The wood fueled tests were conducted using conventional plywood as the fuel source. The wood was formed into an open ended box to fit within the fire section of the tunnel. A wrap of fiberglass insulation was made around the wood to seal the interface between the fuel and the incoming air at the point of ignition.

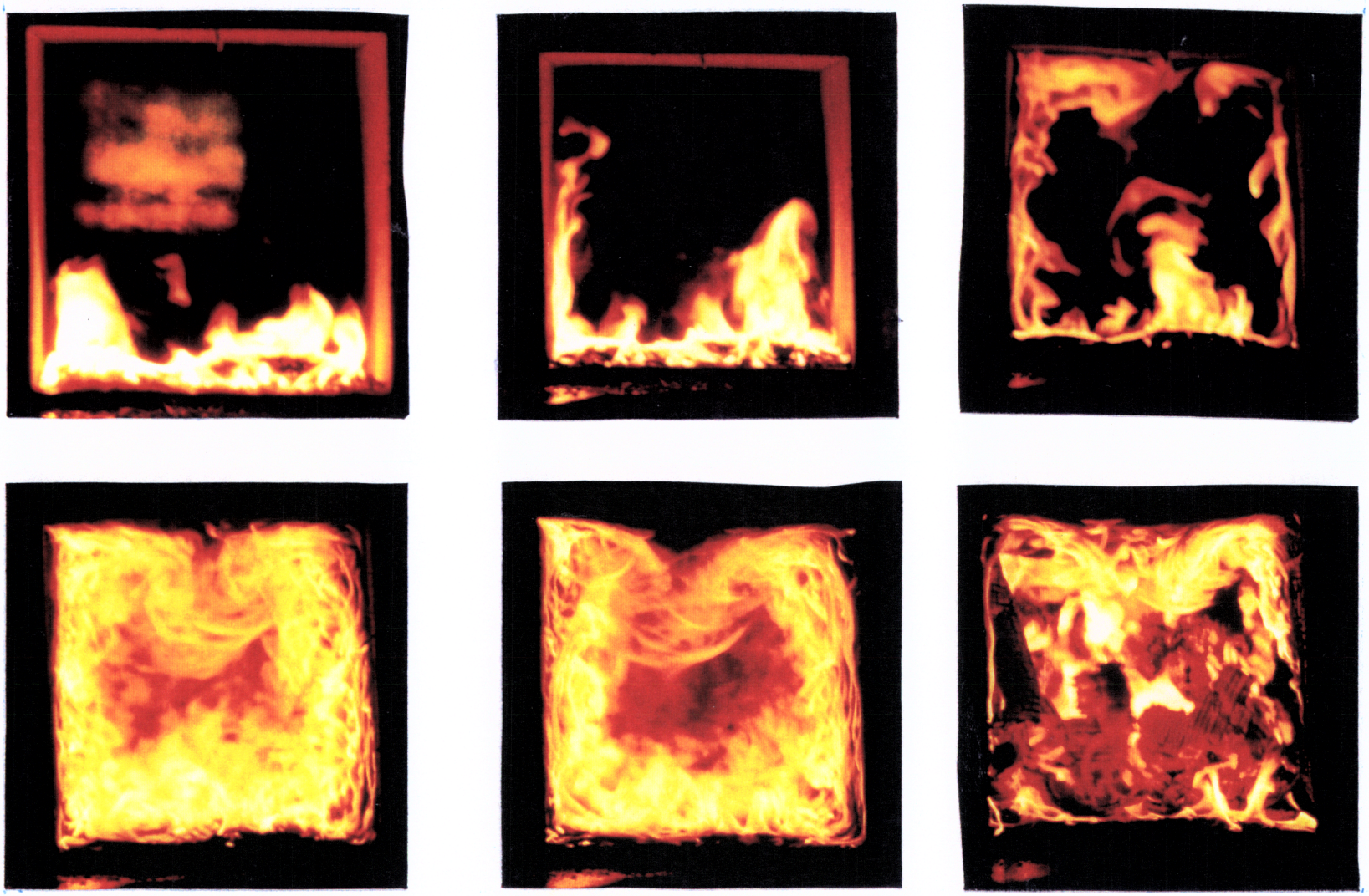

Plate 5-1: Views of Wood Fire

Once the fuel was in place in the tunnel, the lids were put in place. At appropriate intervals the thermocouples were inserted between the lids, as they were put in place. The thermocouple wires were supported above the tunnel lids to prevent the insulation from being melted as the tunnel was heated. Once all of the lids were in place the fan was started at the desired flow level.

Water hoses were connected to the disk humidifier cistern and to the gas intercooler. The cistern was filled automatically by a float valve within the tank. The intercooler was filled by opening the ball valve at the inlet end. After the cooler was filled with water the valve was closed to preserve water, and reduce the quantity of mud generated by free flowing water.

The instrument panel was prepared by placing a clean filter in the filter house (or cleaning the fixed element for tests 1 and 2). A hose connected the intercooler to the filter inlet for gas samples. The pressure connections were made between the manometers and the static tubes in the tunnel. The thermocouples were connected to the appropriate contacts on the data logger. The instrument panel was connected to the data logger by means of the 25 pin connector.

Prior to igniting the fire the vacuum pump in the CO_2 monitor was turned on to begin the gas sampling, and the balance was set between the CO sample and the diluent gas. When the fire was ready to be set the data logger was activated. The valve to the intercooler was again opened.

The ignition of the wood was made using diesel fuel. In the first test the diesel oil was held in a pan. In subsequent tests the diesel oil was spilt on the wood, and over a pile of saw chips. The pan method proved to inadequate, as some of the fuel needed to be splashed out in order to accelerated the fire growth. Even the oil spilt directly on the fuel proved to be marginal, as one of the tests required additional fuel to be added to accelerate the fire to a fuel-rich state.

An active test is illustrated in the photographs of plate 5-2.

Following the tests the gas monitors were again calibrated to evaluate any significant drift that may have occurred during the course of the test.

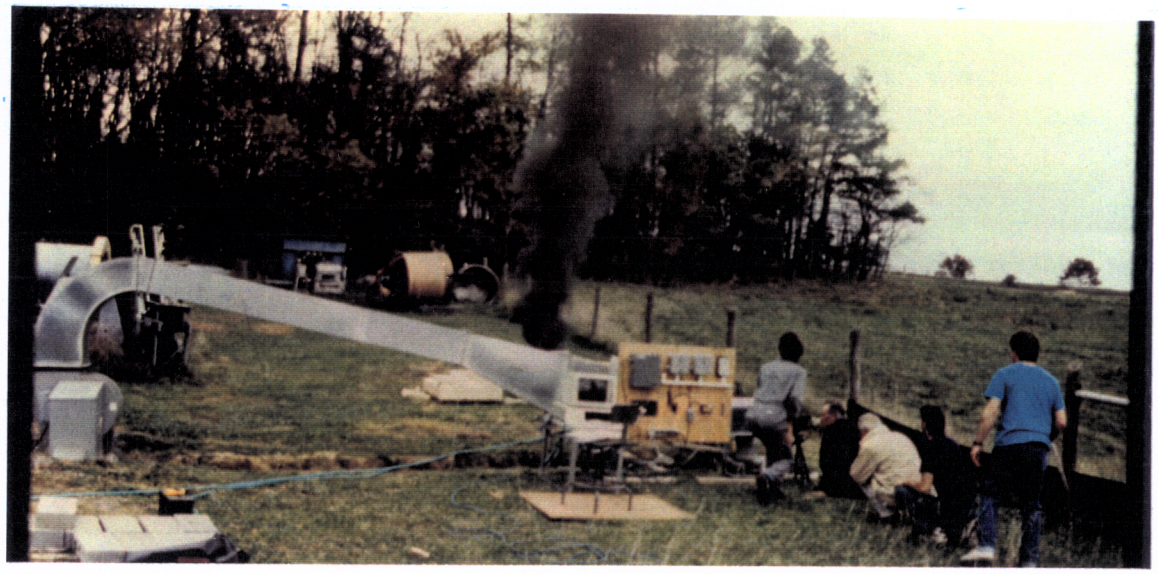

Plate 5-2: Photographs of Active Test.

5.2.2. Test 1

Test number 1 was the initial run of the fire tunnel with all of the systems in place. This test used a small fuel charge of plywood, about one-half of that used is subsequent tests.

5.2.2.1. Gas Trace Profile

The gas traces from this test are shown in figure 5-7. For clarity each gas is shown on a separate set of axes. With no other analysis, one can quickly identify the mirror image relationship between the oxygen and carbon dioxide traces. This is a condition that was found throughout the following tests and is indicative of the completed combustion reaction whereby the carbon in the fuel and oxygen in the air are converted to carbon dioxide. With two oxygen atoms present in the oxidizer and in the product it makes sense that as long as the reaction is carried to completion the increase in carbon dioxide will equal the loss of oxygen.

The oxygen trace exhibits the following characteristics. After the fire was lit the concentration slowly decreases as the fire accelerates. Once the fire has "caught" the oxygen concentration rapidly decreases. It is this transition that was selected to represent the time zero point for all of the tests, in this manner the relative times could easily be compared from test to test. The oxygen concentration drops below 15% about 30 seconds after the fire begins to accelerate. The water mist is begun, from the spinning disk humidifier, three minutes after the fire acceleration point. The oxygen concentration had been making a slight increase (5.7 to 6.7 percent) in this time frame. Once the water mist

is initiated the oxygen concentration drops from 6.7 to just over zero percent in 2 minutes. Following this brief drop the oxygen concentration rapidly rises back to the 15% level over in about 2 minutes. From this point the oxygen concentration slowly rises back to the 21% level over the next 20 minutes. No change in the slope of the oxygen concentration is apparent when the water mist is ceased at the reference time 17 minutes after the fire began to accelerate.

The carbon dioxide trace shows a very similar pattern, in mirror image. An increase in the carbon dioxide concentration follows the initiation of the misting system, followed by a rapid decrease in CO_2 levels. As in the oxygen case, the rate of change of the carbon dioxide decreases as the fire decays.

The carbon monoxide trace, figure 5-7c, indicates a very rapid growth in concentration at about -1.5 minutes that peaks and falls rapidly as the fire begins its full acceleration at time 0 minutes. During this test the CO monitor was sampling an undiluted sample of the fire exhaust gas. It is most likely that that the pattern exhibited by this trace is due to an overload of the monitor and therefore the trace shows no significant data.

The methane trace, figure 5-7d, shows a growth in concentration from time 0 minutes through time 3 minutes, to a concentration of about 0.65 percent. Two spikes in the concentration occur at 4 and 5 minutes. The first of these spikes can be correlated to the initiation of the fogging system. It is unclear as to what may have induced the second spike, which shows a near doubling of the methane concentration.

It is unclear from the data whether or not the fogging proved efficacious in this case. The burn time for the fuel load was very short, and much of the fuel had most likely been consumed near the time of the fogging system initiation. A video tape was made of this fire for analysis, a synopsis of the tape is provided in table 5-3.

5.2.2.2. Pressure Profile

The monitored pressure across the orifice reveals a constant airflow of about 0.0723 m^3/s. This is shown in figure 5-8. The histogram of the airflow data appears to be normally distributed about the mean. This data shows no obvious signs of a throttling effect during the course of the fire. The data that is shown here extends to reference time 22 minutes. At this time the fire was essentially burnt-out and the airflow was increased by closing the waste gate. This change resulted in a step in the data that shows a similar pattern of consistency. To show this data in figure 5-8 would result in the data being skewed due to a known outside influence. Therefore, the additional data has been omitted from this presentation. A small bump can be seen in the oxygen and carbon dioxide traces in figure 5-7, that correlate to this point in time, 22 minutes.

Table 5-3: Test 1 Video Tape Synopsis

Ref. Time	Description
-0:03:00	Diesel Fuel Lit
-0:01:40	Fuel splashed from pan, flames from fuel reaching top
-0:01:05	Flaming evident on left rib
-0:00:10	Flames on left rib reaching top
0:00:03	Charring (smoke) on right rib
0:00:13	Flame left to right on top licks right rib
0:00:20	Heavy smoke (charring) on right rib floor to top
0:00:48	Flame circling clockwise full around, very heavy white smoke from right rib
0:00:53	Right rib begins to flame - flow clockwise
0:00:55	Counter-clockwise flow begins at right rib and top
0:01:06	Twin vortex flow along top centered
0:04:30	Fogging begins
0:14:33	Fire no longer visible
0:06:30	Camera moved to exhaust end
0:06:42	Flaming on top, embers with some flame on ribs and floor
0:07:27	Yellow flaming on floor ceases
0:08:18	Piece falls from top-right (previous left), yellow flaming on floor
0:08:22	Jet of flame from top to floor, extinguishes piece that fell at 0:14:48
0:08:50	Yellow flames on top now top quarter
0:09:14	End of wood fuel on left side peels back, red flames reaching to top
0:09:15	Top of fuel begins to fall - yellow flames from inside only
0:09:17	Fire not visible on tape (camera moved)
0:09:40	Fire again visible
0:09:45	White and yellow flame visible on left and right ribs, end of fuel charge peeling towards center
0:09:48	Opposing twin vortex yellow flames along top
0:10:01	Camera moved off fire
0:10:20	Camera returns to fire
0:10:34	Piece of roof collapses, yellow flame on floor

Table 5-3: Test 1 Video Tape Synopsis - Continued

Ref. Time	Description
0:10:39	Yellow/white flames for piece hanging half way down from back
0:11:05	Large piece begins to separate from top
0:11:26	Piece swings over to right rib, yellow flaming limited to right top and rib
0:11:41	White flaming begins right floor, ceases right top
0:13:13	white flames from right floor cease
0:14:00	Flames on top cease
0:14:05	Flames on right top re-appear
0:14:08	Piece falls from right rib
0:14:11	flames on top cease - smoke visible from this
0:14:17	Right rib collapses
0:14:22	Light visible from vent port, upstream of fire
0:14:32	Vent port closed
0:15:01	Light visible from vent port
0:15:29	Vent port cover removed
0:15:46	Vent port cover replaced
0:15:47	Yellow flames right floor extinguish
0:16:13	Yellow flames return
0:16:43	Viewport (window at elbow) visible
0:16:56	"Shimmer" at viewport appears to become more vigorous
0:24:00	Video of fire stops, embers burning on floor

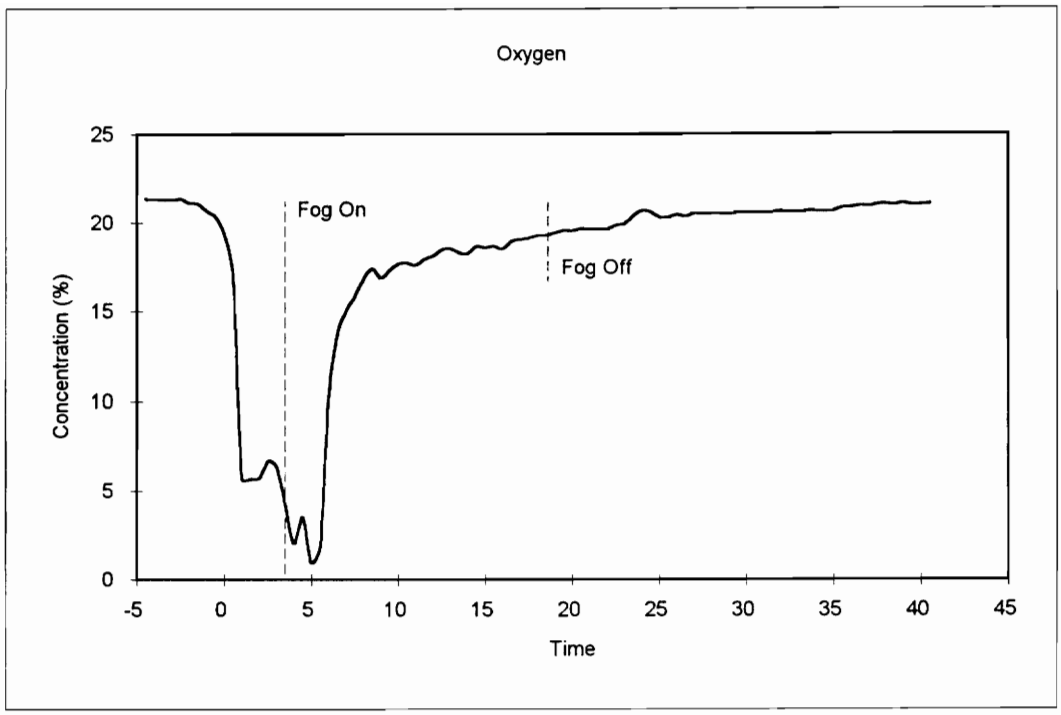

(a)

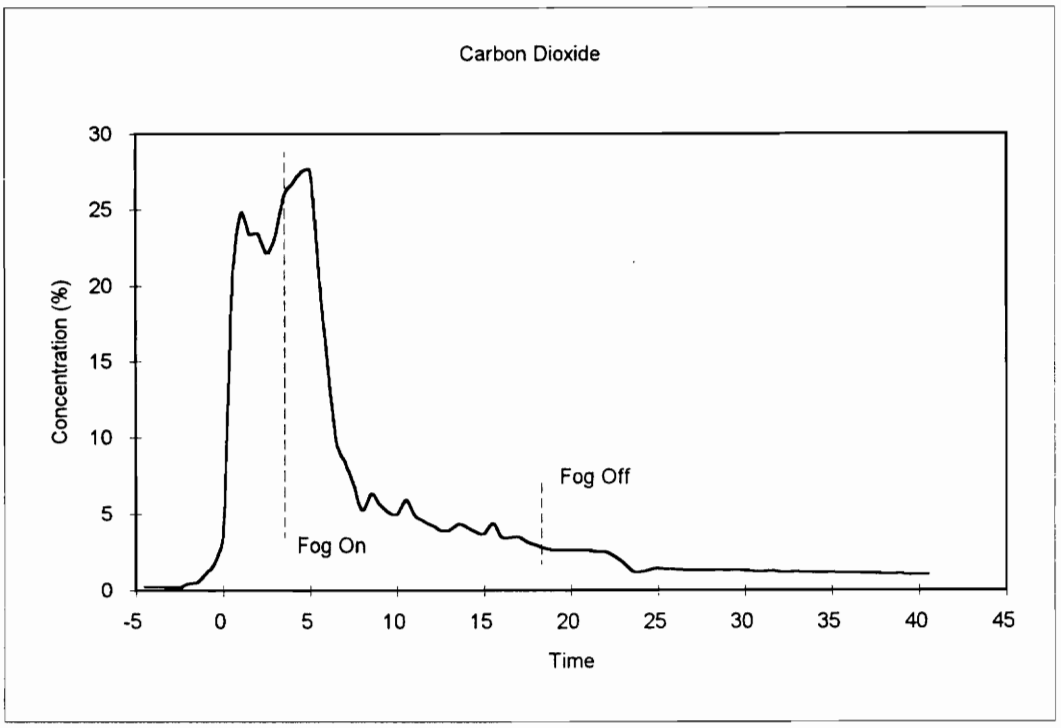

(b)

Figure 5-7 (a, b) Oxygen and Carbon Dioxide Gas Traces for Test 1.

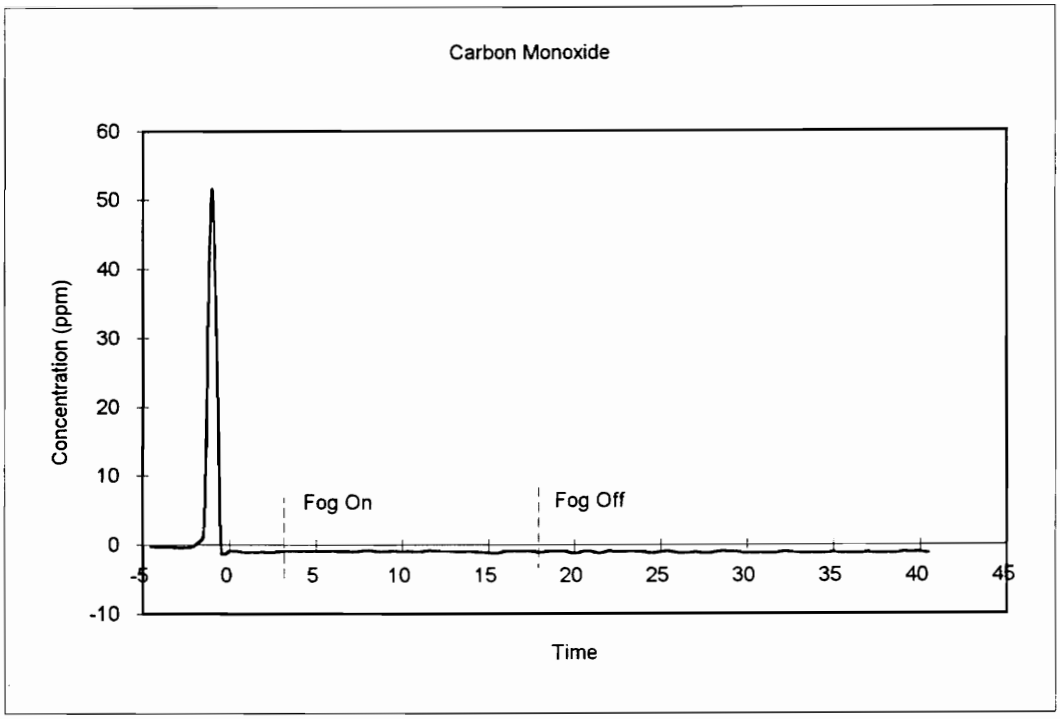

(c)

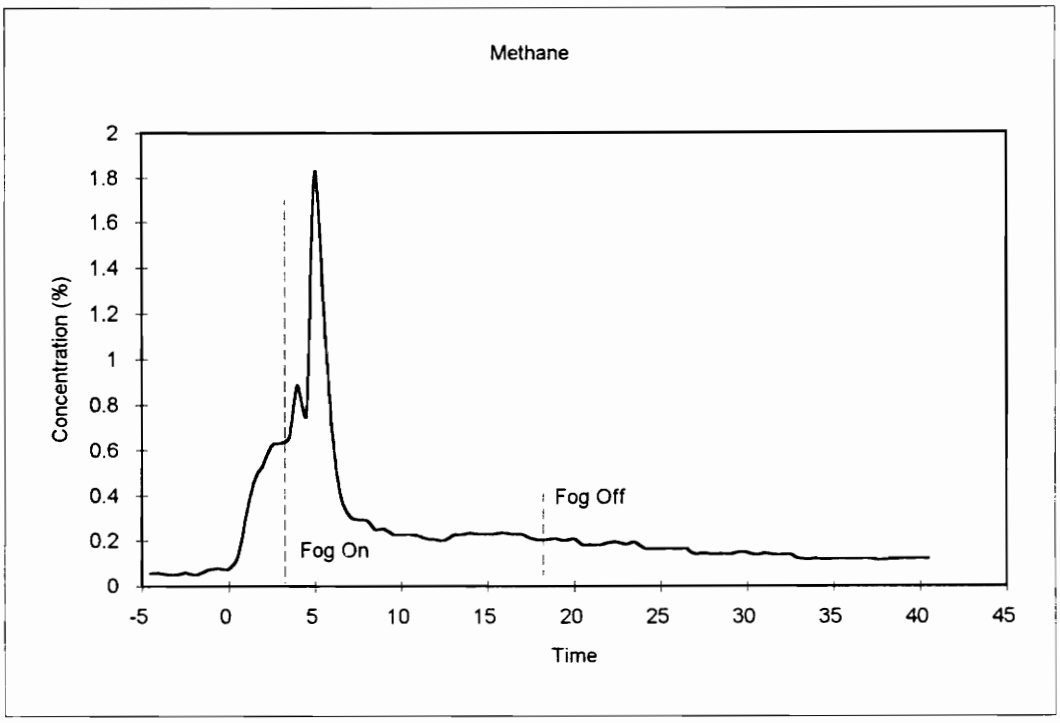

(d)

Figure 5-7 (c, d) Carbon Monoxide and Methane Gas Traces for Test 1.

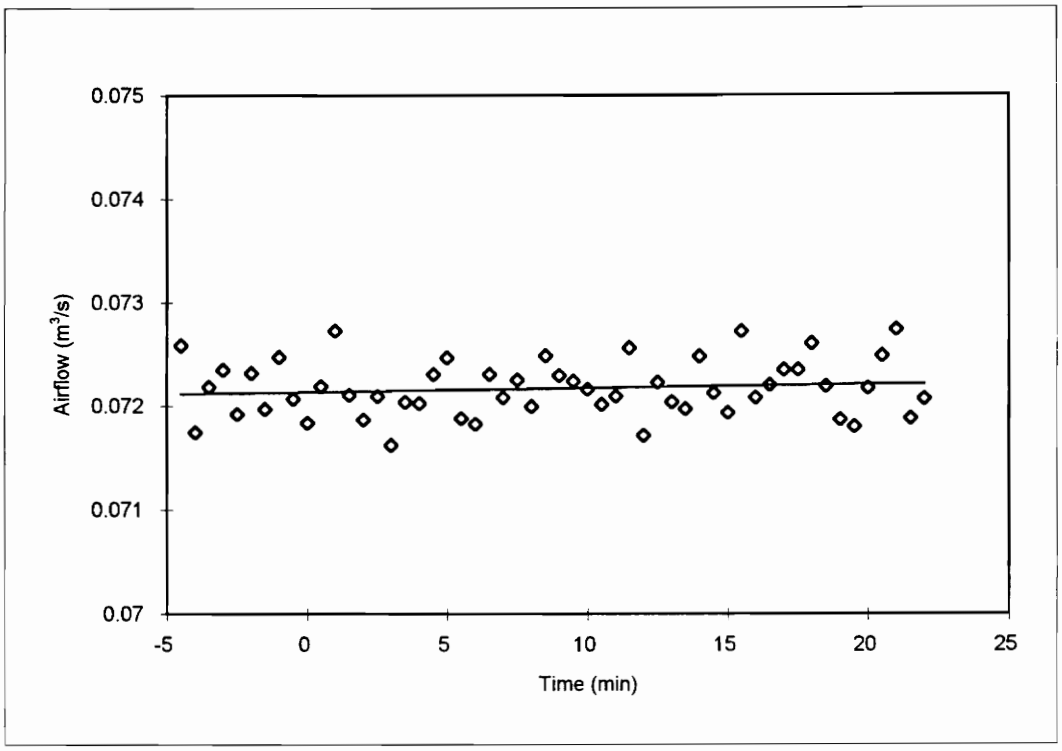

Airflow	Frequency
0.071	0
0.07125	0
0.0715	0
0.07175	3
0.072	12
0.07225	21
0.0725	12
0.07275	6
0.073	0
More	0

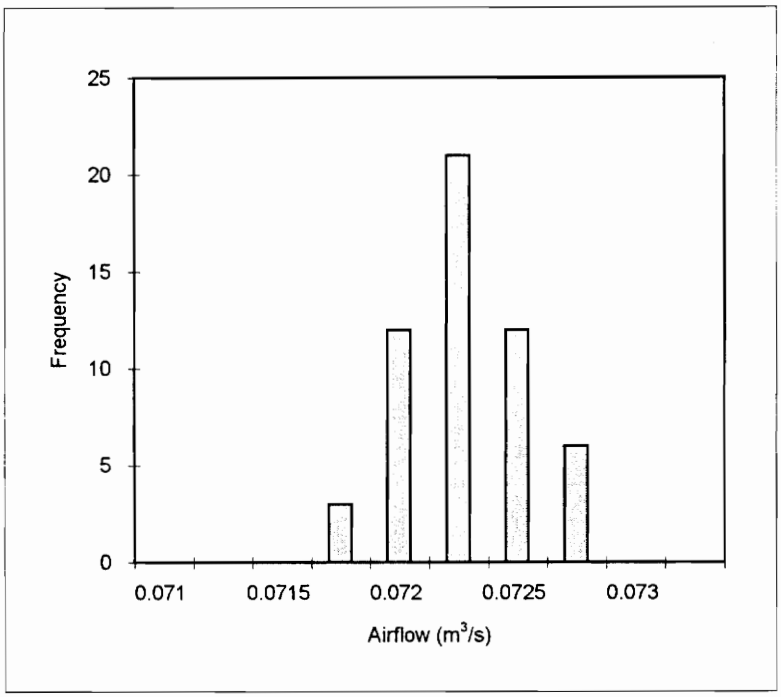

Figure 5-8: Airflow Profile and Histogram for Test 1.

5.2.3. Test 2

This test was the first using a full sized fuel charge of plywood. The purpose of this test was to obtain a baseline data set for the plywood fire. This test allowed the fire to burn to completion without attempts to bring it under control.

5.2.3.1. Gas Trace Profile

The gas traces from this test are shown in figure 5-9. For clarity each gas is shown on a separate set of axes. A video tape was made of this fire, a synopsis of the tape is provided in table 5-4. The gas traces show much less data than the time on the video tape indicates. This is due to the fact that the gas sample filter became clogged with soot approximately 10 minutes after the fire began to accelerate, reference time 0 minutes.

The section of the gas data that is known to be valid indicates that the growth of the fire was similar to that of test 1 and of the following tests.

5.2.3.2. Pressure Profile

The pressure profile, figure 5-10, across the orifice indicates an airflow for this test varying between 0.072 and 0.074 m^3/s with an average of about 0.073 m^3/s. The airflow trend shows a decrease in the airflow as the fire accelerates, with an increase in the airflow as the fire begins to die away. The initial drop in airflow represents a decrease of about

1.5 percent. The histogram shows a distribution that appears to be normally distributed, although slightly skewed to the lower end.

The relative pressure in the tunnel, figure 5-11, shows the same pattern as the airflow, a slight decrease in the pressure as the fire accelerates, returning the initial level as the fire intensity drops. The histogram of this data shows a distribution that appears skewed to the lower end.

5.2.3.3. Temperature Profile

The in-duct temperature data collected is illustrated in figure 5-12. This figure illustrates the strong temperature front of the fire, compared to the upstream portions of the duct. This conditions indicates that little or no reverse stratified flow was occurring. The existence of reverse stratified flow is also not supported by the video tape recording.

Figure 5-12a illustrates the rate at which the fire reached its highest temperature and remained there for a period of about 10 minutes. The reverse view, figure 5-12b, illustrates the rather slow rate of decay of the fire temperatures, relative to the rate of growth. The jagged top of these surfaces may be due to the rejection of data that was evidently related to over-ranging the thermocouples, causing obviously erroneous data.

Table 5-4: Test 2 Video Tape Synopsis

Ref. Time	Description
	Diesel fuel lit
-0:03:10	Time mark appears
-0:03:05	Vent closed
-0:02:58	Frame fitted to show full fire area
-0:02:13	Flame licking up left side
-0:02:06	Downstream virtually opaque, flame licking about half way up left side
-0:01:45	Downstream totally opaque
-0:01:02	Flames momentary contact with top on left side
-0:00:52	White vapor begins to be visible on left side
-0:00:34	Flames licking with top on left side
-0:00:23	Flames licking about half way up right side
0:00:05	Gas sample rake (+5.5m) visible
0:00:15	Flames licking over half way across top from left, nearly reaching top on right side
0:00:20	Bottom of tunnel at exhaust visible and distinguishable
0:00:25	Flame licking top from right side
0:00:35	Light from lower half of tunnel exhaust visible, Flames nearly contact from right and left across top
0:00:58	Most of exhaust of tunnel clearly visible
0:01:23	Flames beginning to intermingle on top from right and left, white smoke beginning to appear along centerline on top, strong "tongue" beginning to form on centerline at bottom, flaming about half way up
0:01:54	Strong vortex beginning to form on top with flames from right and left at centerline
0:02:27	Apparent contact of flames form vortex and tongue
0:02:37	Tongue weakens; vortex flames reaching about half way down
0:02:41	Daylight not visible from tunnel exhaust
0:03:15	Tunnel has flames nearly 100%
0:03:30	Flames on floor and sides appear crenulated while vortex appears smooth
0:04:20	Upstream fuel on left engulfed

Table 5-4: Test 2 Video Tape Synopsis - Continued

Ref. Time	Description
0:06:43	Wood appears to be separating on left side
0:06:53	Piece falls from left side
0:06:58	Piece falls from left side
0:07:08	Piece from left side protruding about a quarter of the way across opening
0:07:12	Protruding piece collapses, right side appears to be separating
0:07:22	Piece from top collapses
0:07:30	Right and left sides curling inwards
0:07:34	Piece falls from top
0:07:36	Pieces from top and left fall
0:07:40	Collapse of right and left sides
0:07:44	Opening about 50% blocked by charred wood, large droop from top
0:07:56	Upper right corner collapses and opens
0:08:44	Piece in left center falls away
0:08:56	Wood Collapsing from left upper center to block tunnel, embers fill lower half of tunnel
0:09:23	Sample rake visible center right
0:10:50	Jet of flame down near left edge
0:11:01	Piece from center top begins to fall
0:11:04	Piece falls, daylight visible from extent of exhaust
0:11:26	Jet of flame down near right limit
0:11:43	Flame on near left limit out
0:12:15	Flame on near right limit out
0:12:40	Top appears to begin to swell
0:12:52	Piece falls out of top
0:13:01	Swell from top collapses covering opening of tunnel
0:13:05	Swell falls - opening tunnel
0:13:26	Piece falls from upper left corner
0:14:30	Daylight visible through right side wood/tunnel interface
0:15:30	Left side slips slightly, right side leaning inwards noticeably, mostly burning embers, flame on left side only
0:15:57	Left side collapses leaving a little flaming in lower left

Table 5-4: Test 2 Video Tape Synopsis - Continued

Ref. Time	Description
0:17:16	Flames in lower left disappear
0:17:30	Embers (black) visible on right, brick visible in left and top
0:18:35	Remaining wood on right side begins to collapse
0:19:10	Piece falls out of lower right
0:21:59	Piece falls out of middle right
0:27:10	Video of fire ends, piece (embers) still on right side

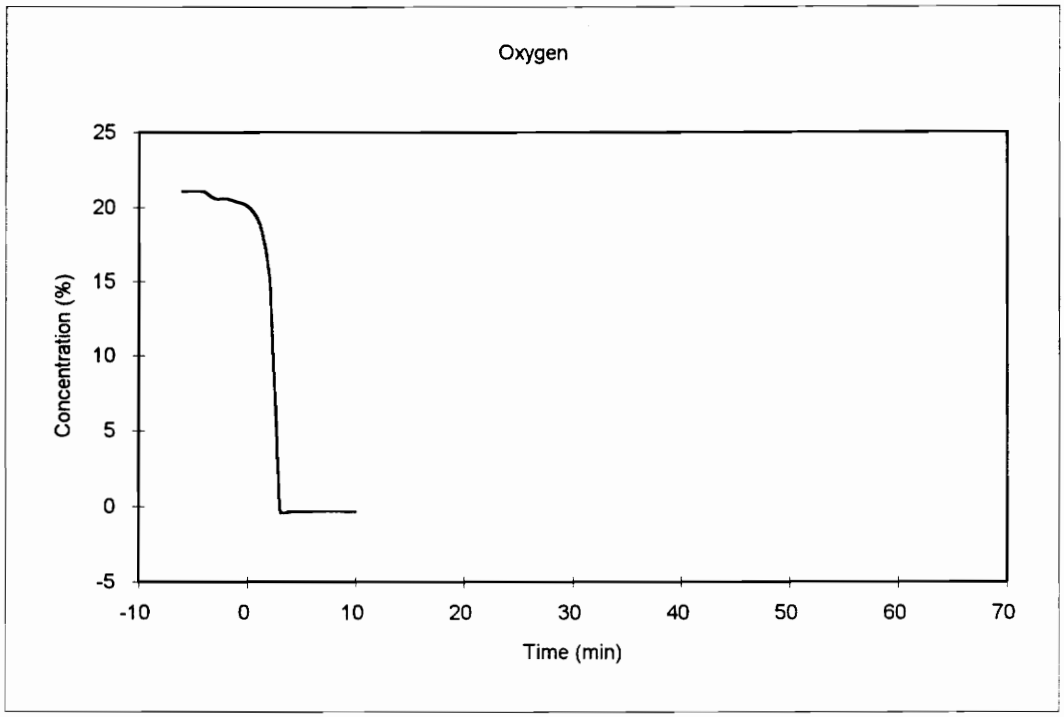

(a)

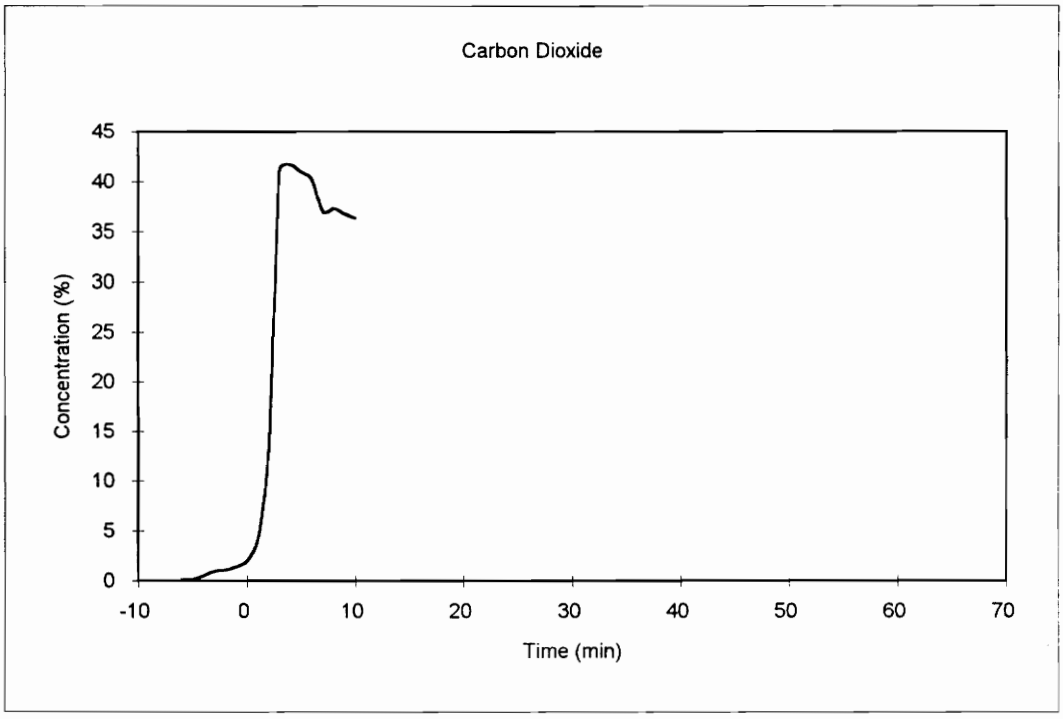

(b)

Figure 5-9 (a, b) Oxygen and Carbon Dioxide Gas Traces for Test 2.

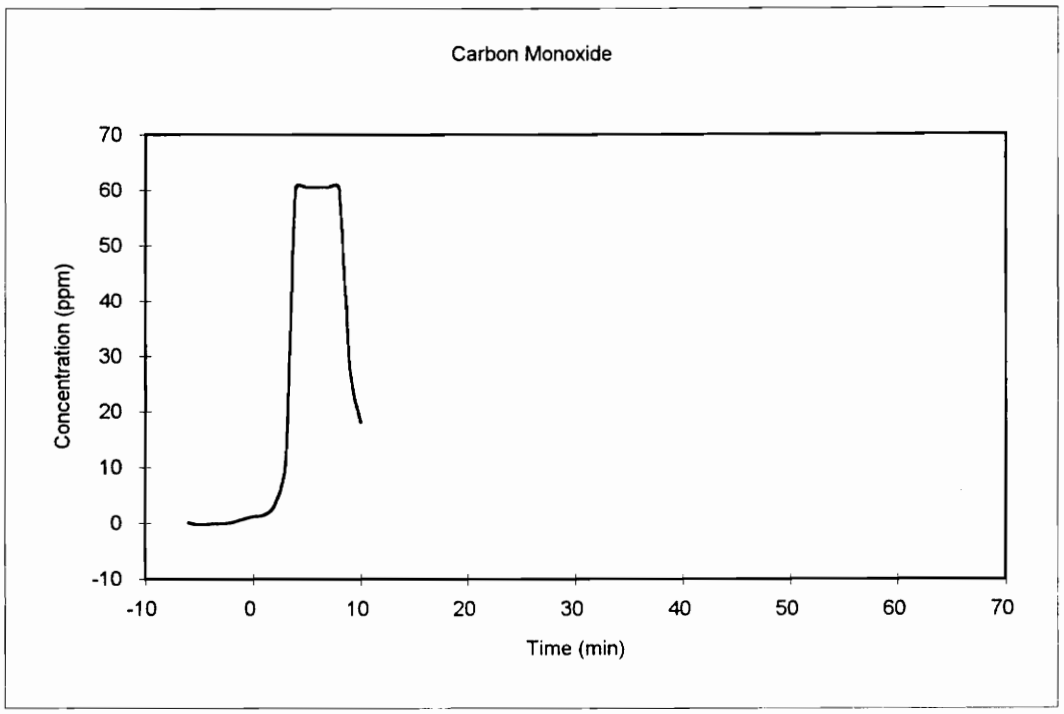

(c)

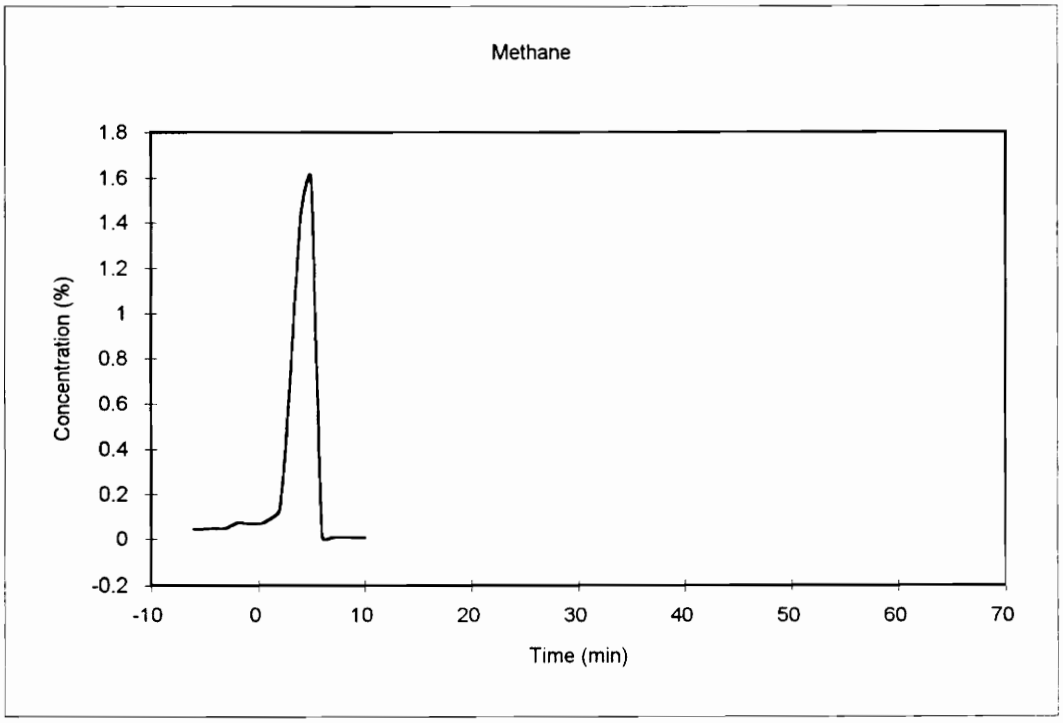

(d)

Figure 5-9 (c, d) Carbon Monoxide and Methane Gas Traces for Test 2.

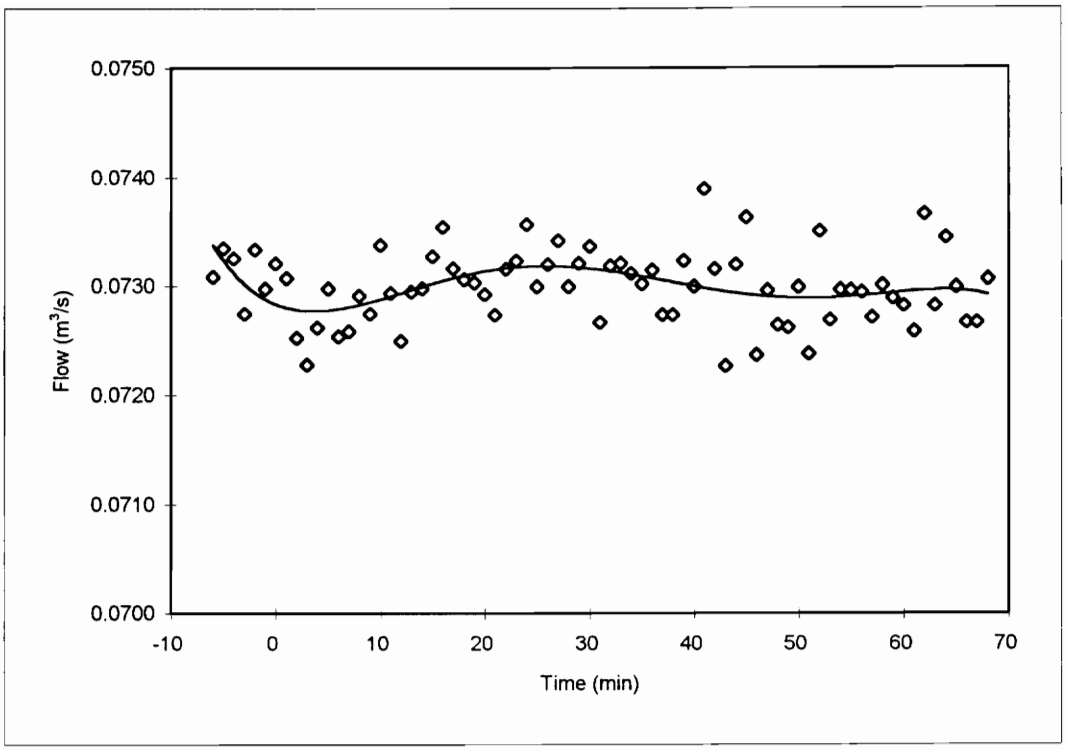

Airflow	Frequency
0.072	0
0.07225	0
0.0725	5
0.07275	17
0.073	19
0.07325	20
0.0735	8
0.07375	5
0.074	1
More	0

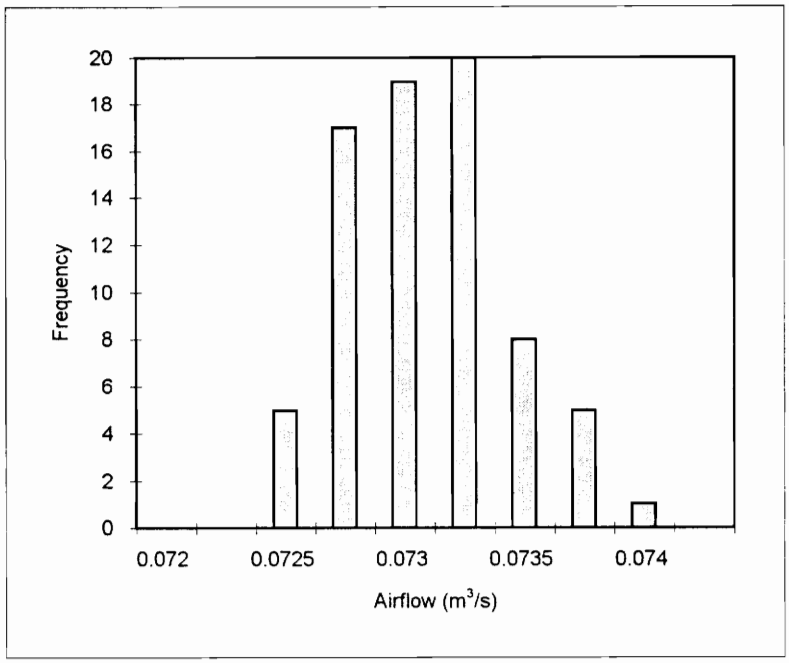

Figure 5-10: Airflow Trend and Histogram for Test 2.

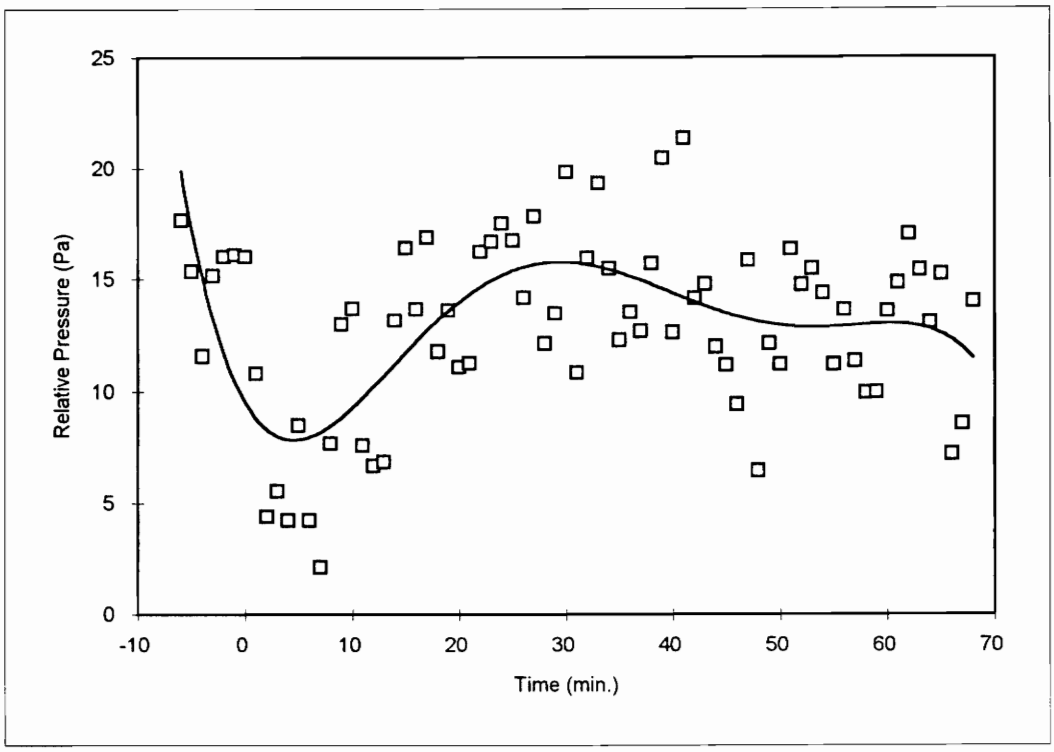

Pressure	Frequency
0	0
2	0
4	1
6	4
8	6
10	5
12	11
14	15
16	16
18	13
20	2
22	2
24	0
More	0

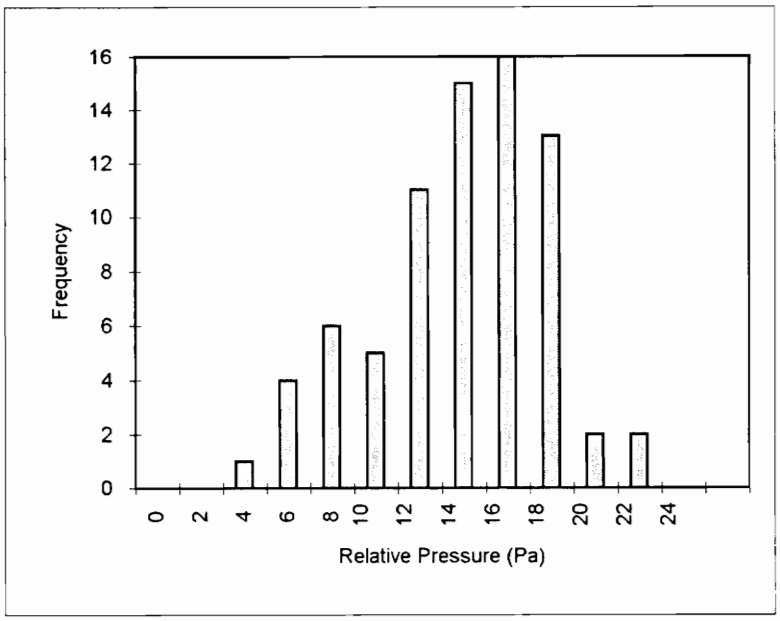

Figure 5-11: Duct Relative Pressure Profile and Histogram for Test 2.

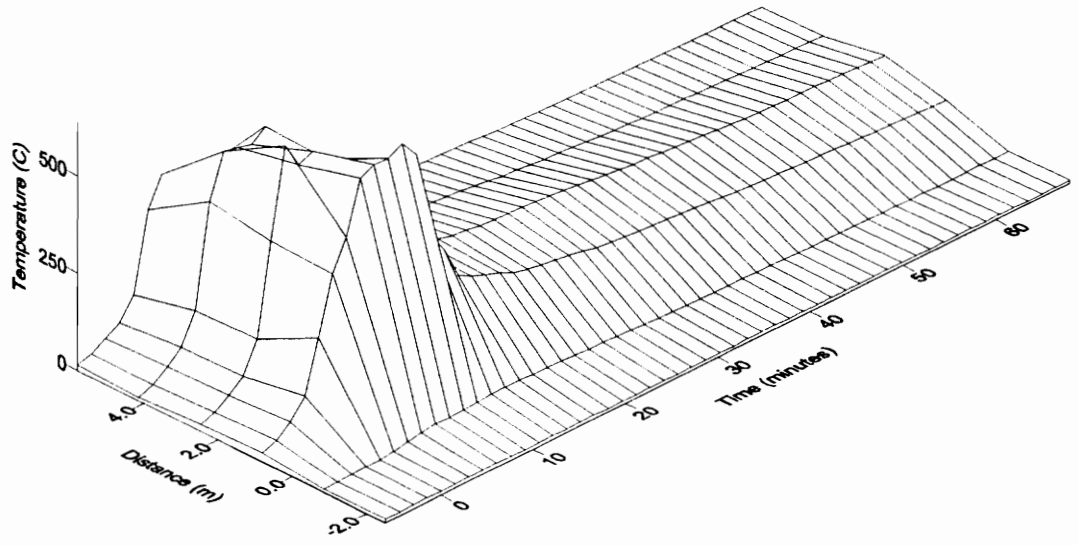

(a)

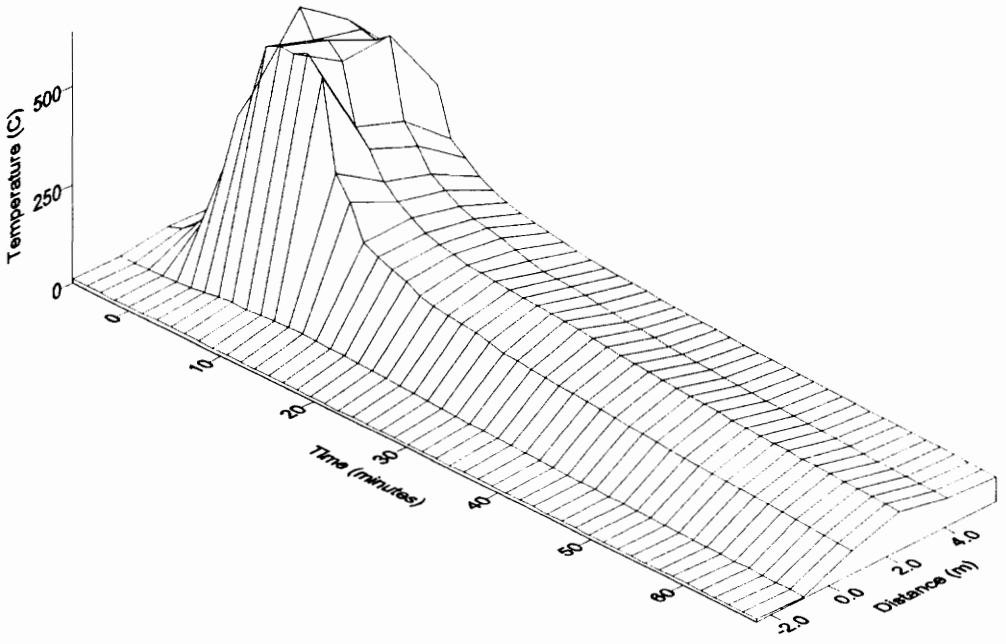

(b)

Figure 5-12: Forward and Reverse Views of the Temperature Surface for Test 2.

5.2.4. Test 3

This test was to observe the effects of adding a water mist to the air upstream of the plywood fire burning in a fuel-rich state. The fire was observed to grow until reaching a fuel-rich state, at which time the spinning disk fogging system was initiated. A video tape was made of this fire, a brief synopsis of which is provided in table 5-5.

5.2.4.1. Gas Trace Profile

The attempts to initiate this fire revealed that there is some relationship governing the likelihood that the fire will accelerate to a fuel-rich state. In the previous two fires the fuel-rich state was achieved with little effort, whereas this fire required the addition of diesel fuel about 9 minutes after the initial attempt to ignite the fire was made. Following the addition of the extra fuel the fire rapidly accelerated to a fuel-rich state. The gas traces for this test are shown in figure 5-13.

After the oxygen concentration had dropped to nearly zero percent and had stabilized, reference time 2.5 minutes, the disk humidifier fogging system was initiated. A brief increase in the oxygen concentration followed, figure 5-13a, mirrored by a drop in the carbon dioxide level, figure 5-13b. This change lasted about 2 minutes, at which time the oxygen and carbon dioxide traces returned to their levels before the fog was started. Shortly after the return to initial levels the oxygen and carbon dioxide traces indicate the decay of the fire as they return to there natural levels.

During this test the carbon monoxide sample was diluted approximately 100 times, even at this level the dilution appeared to be insufficient. The carbon monoxide trace, figure 5-13c, shows the initial increase to begin at about -1 minute. Between times 1 and 3, and 5 and 7 minutes the trace indicates a drop in the CO levels, these are most likely due to an overload of the monitor, similar to that experienced in test 1. The portion of this data that appears to be of significance is the downward spike that occurs at time 4 minutes. This anomaly can be correlated to the similar conditions seen in the oxygen and carbon dioxide traces. It appears that at the time of the fog system operation there was a reduction in the CO concentration that permitted measurement by the monitor.

The methane trace, figure 5-13d, shows a relatively steady growth in the CH_4 levels up to time 4 minutes. At this time the trace shows a fall to a 0% indication from time 6 to 8 minutes, followed by an increase. The final decreasing methane concentration appears to follow a decay pattern seen in the other gas traces. The initial drop in the methane level, at time 4 minutes, occurs at the same time that the momentary spikes were seen in the other gases. Since the methane does not return to its initial pattern in the same manner it is unclear whether the drop is due to changes in the fire or an overload of the monitor.

5.2.4.2. Pressure Profile

The pressure across the orifice indicated the airflow profile shown in figure 5-14. The airflow profile appears to be relatively constant through to the reference time of 25 minutes. After this time the profile exhibits a marked drop in the airflow that lasts for about five minutes, at which time the airflow increases appearing to oscillate about the mean of the initial airflow level. The histogram of this data appears to show two normal

sets of data, one with a mean of about 0.072 m^3/s and the other with a mean of about 0.062 m^3/s.

Looking solely at the histogram, it could be possible to suggest that there was some change in the airflow that could be associated with the throttling effect. However, a comparison to the trend illustrates that the occurrence of the lower airflow can be associated with the period when the fire had decayed to the point of extinction.

The relative pressure in the duct, figure 5-15, illustrates that this index exhibited a great deal of scatter throughout the duration of the test. A trend can be fitted to this data that shows a decrease in the absolute value of this index as the fire began to develop. Once the fire began to accelerate the relative pressure leveled off and began to rise. The histogram related to this data shows a nearly normal distribution with mean of about 12 Pa, that is slightly skewed to the upper end.

5.2.4.3. Temperature Profile

The temperature profile for this test, figure 5-16, illustrates that there was little or no reverse stratified flow of gases from the fire. The delay in the acceleration of the fire is visible in figure 5-16a by the slight rise in the temperature during the -10 to -2 minute interval, this correlates to the steady oxygen-rich period that preceded the acceleration to a fuel-rich state. The rapid increase in the temperature, as the fire accelerated is also visible in this figure. The temperature surface appears to have a decrease in the temperature that occurs at a time of four minutes. This correlates to the application of the

water mist. A return of the temperature to its initial peak levels occurs, following this depression, before the temperature decays as the fire dies.

Table 5-5: Test 3 Video Tape Synopsis

Ref. Time	Description
-0:09:23	Diesel fuel and wood chips lit.
-0:09:21	Daylight from viewport obscured by smoke, some flame visible
-0:09:00	Viewport not visible - camera zoomed back - so significant smoke visible although flame cannot be seen (may be due to light metering).
-0:08:50	Some dense black smoke is visible exiting the tunnel.
-0:08:33	Camera zooms in, some flame visible.
-0:08:27	Smoke appears to be grayish.
-0:08:04	Momentary absence of smoke, small flaming material visible.
-0:08:00	Dense smoke thickening.
-0:05:34	Small flicker of flame visible through thick, dark gray smoke, flame on floor.
-0:04:55	Smoke clearing, flame visible on floor and up right side (viewed from exhaust).
-0:04:30	Light is visible in viewport, flame on floor and about half way up right side. Comment: added wood shaving to assist with ignition.
-0:03:59	Flames licking top on right side only.
-0:03:11	Flames now in lower right corner only (flames diminishing). Some flames reaching about half way up right side.
0:00:58	Diesel oil added.
0:00:48	Thick black smoke, only flames on floor visible.
0:00:45	No flame visible.
0:00:25	Camera zooms back, thick black smoke visible out of tunnel. Quantity of smoke is increasing.
0:01:10	Color of smoke appears to be lightening.
0:02:38	Rapid increase in quantity of smoke (medium gray in color).
0:02:25	Camera zooms back to tunnel, smoke obscures entire view.
0:03:55	Camera zooms away, smoke is dark gray to black
0:03:35	Large quantities of smoke blowing directly to camera, appears light gray in color.
0:03:23	Comment: here comes the fog.
0:03:06	Comment: go for fog.

Table 5-5: Test 3 Video Tape Synopsis - Continued

Ref. Time	Description
0:03:00	Comment: it is on.
0:03:19	Flames visible through smoke, orange on floor.
0:03:42	Comment: Smoke is going down.
0:04:25	Flame obscured by white/gray smoke.
0:06:07	Flames visible on left side, lower corner
0:06:14	Flame visible on left side.
0:06:18	Most of flame on floor, not much appearing on top.
0:06:23	Some flame visible on top, does not appear as intense as that on floor and left side.
0:06:25	Appears as though there has been a collapse, resulting in a pile of burning debris on floor, about lower half of tunnel affected.
0:06:43	Right side does not appear to be burning.
0:07:05	Fairly intense flame visible on roof, but that from debris on floor is still more intense.
0:07:12	Material seems to have "delaminated" and extends into tunnel from the left side, about 1 third of the way across.
0:07:39	Large piece from left side collapses onto floor.
0:07:56	Much of the flaming (yellow) on the floor has subsided. Yellow flaming is on top only.
0:08:03	Flaming appears to be from floor and top only, nothing from side.
0:08:58	Most of flame on floor is gone. Still flame from top, bright yellow in color.
0:09:05	Smoke appears to thicken.
0:09:51	Smoke obscuring floor, some flame visible on top, smoke appears bluish in color.
0:10:12	Only flame/color visible is on top through the blue gray smoke.
0:10:32	Smoke clearing, no flaming visible on floor, but some on top.
0:10:39	Slight glow visible from floor, but no apparent flame.
0:10:58	Slight lick of flame visible up left side.
0:11:00	Slight lick of flame visible up right side.

Table 5-5: Test 3 Video Tape Synopsis - Continued

Ref. Time	Description
0:11:09	Material back appears to droop about 1/3 of height downwards.
0:11:13	Acceleration and formation of twin vortex of flame on top.
0:11:25	Vortex of flame on left appears to disappear, vortex on right is weakening.
0:11:34	Increase in flames on left side.
0:12:20	Strongest flaming occurring on right side, bounded by debris on floor and material on top. Vortex is rotating in counter-clockwise direction.
0:12:40	No clear flames remaining on top.
0:12:49	Thick smoke/haze appears about the flaming section.
0:13:15	Flaming is now just on floor, with slight lick on right side, vortex structure has disappeared.
0:13:28	Smoke appears to thicken.
0:13:55	Flame intermittently visible through smoke.
0:14:23	Only a small flicker of flame is visible in centerline of debris on floor.
0:14:31	Some licks of flame up right side.
0:14:37	Smoke clears. Some flames on floor, partially obscured by debris.
0:15:05	Smoke begins to thicken.
0:15:31	Very little flame visible through smoke.
0:17:20	Only evidence of fire is slight glow of embers through smoke.
0:17:59	Smoke clears momentarily, glowing embers can be seen, but no flames.
0:19:25	Camera zooms away from tunnel, smoke appears to have thinned, but no flame or embers visible in tunnel.
0:20:46	End of tape.

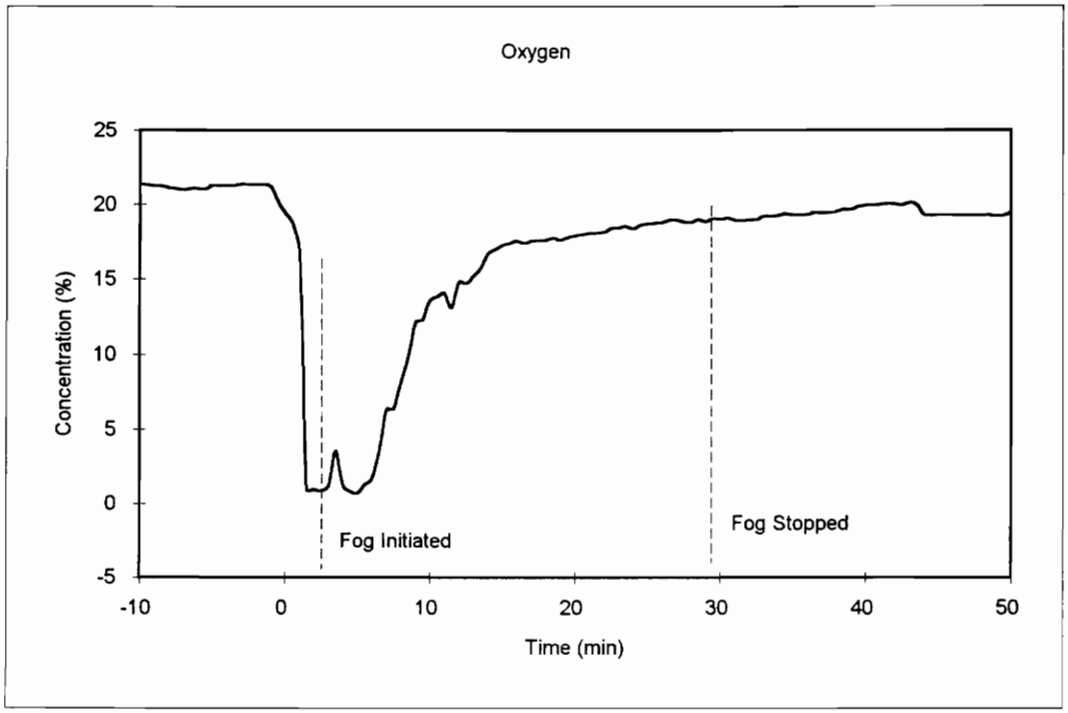

(a)

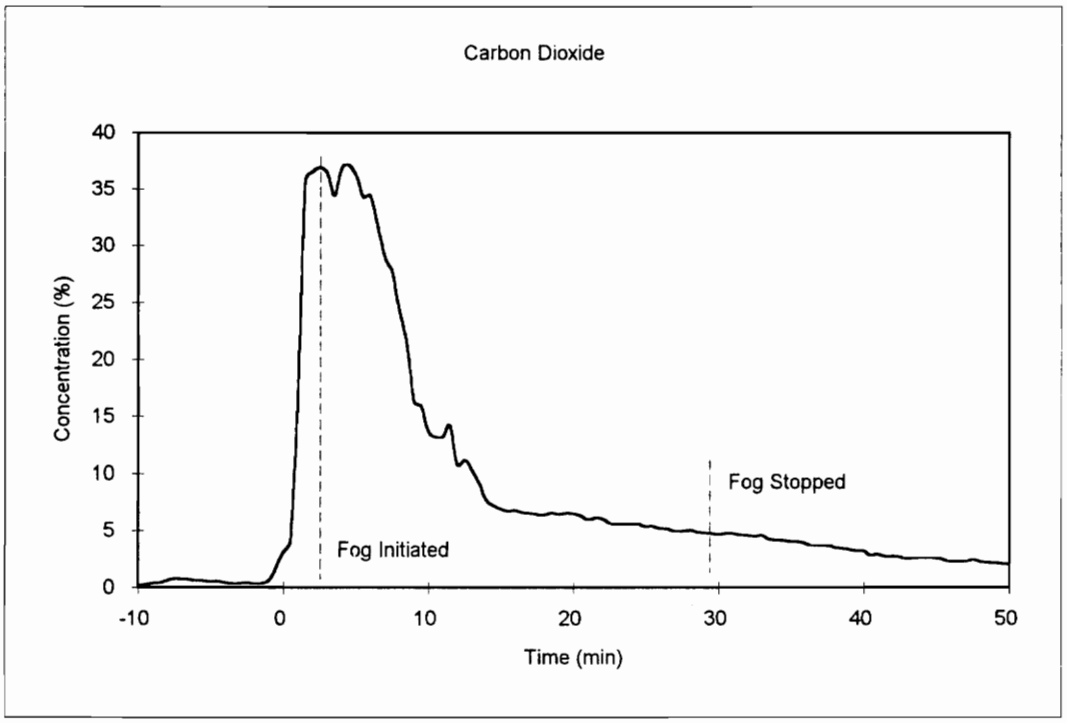

(b)

Figure 5-13 (a, b): Oxygen and Carbon Dioxide Gas Traces for Test 3.

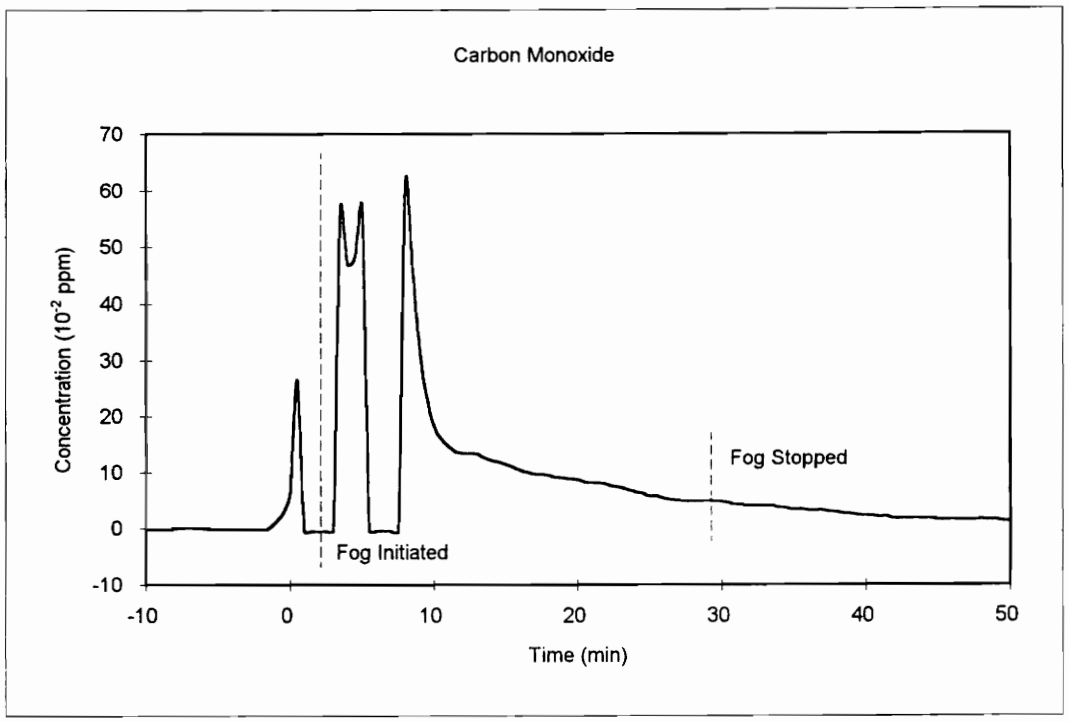

(c)

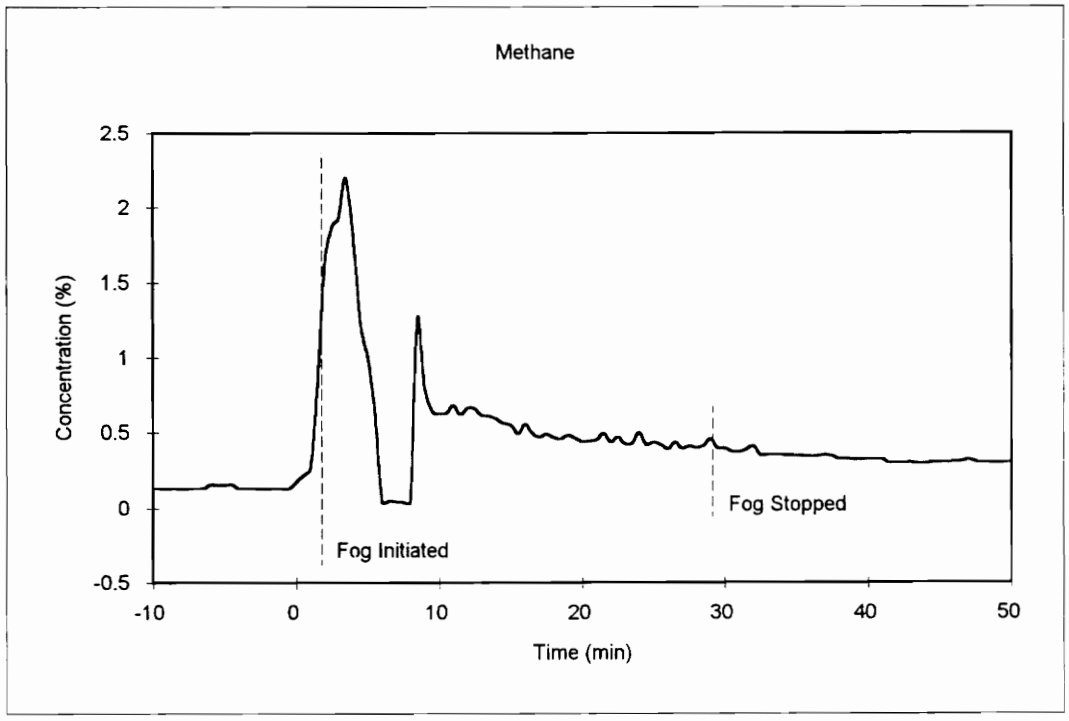

(d)

Figure 5-13 (c, d): Carbon Monoxide and Methane Gas Traces for Test 3.

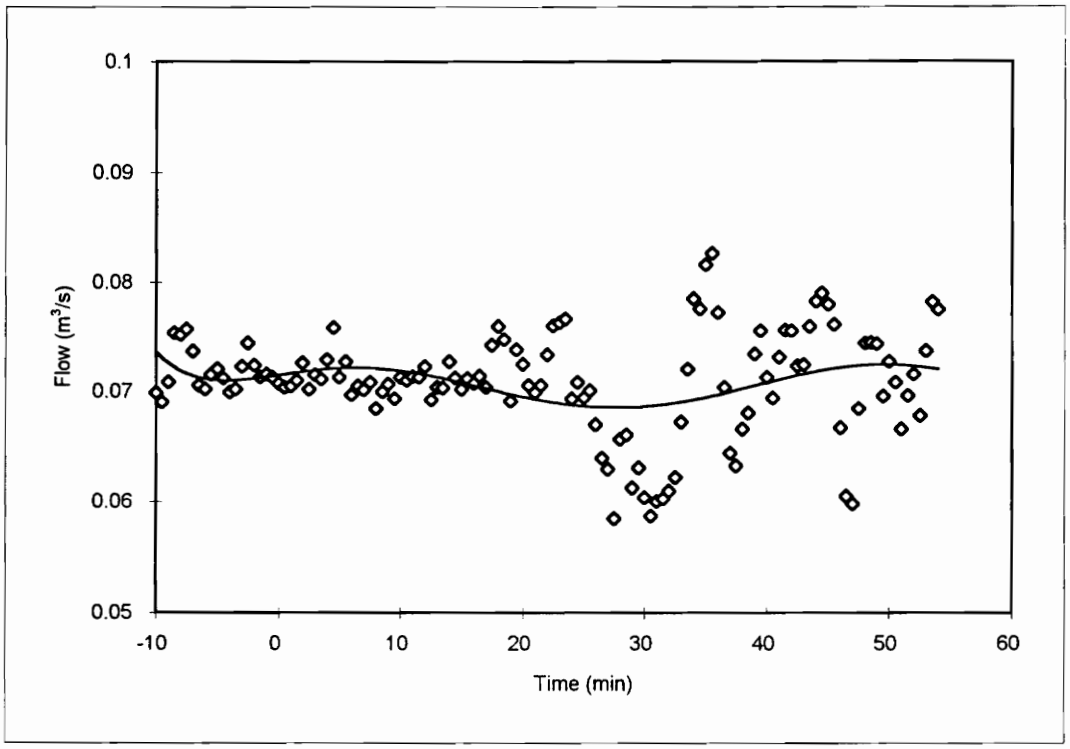

Bin	Frequency
0.06	3
0.062	6
0.064	5
0.066	2
0.068	7
0.07	17
0.072	41
0.074	19
0.076	14
0.078	8
0.08	5
0.082	1
0.084	1
0.086	0
0.088	0
0.09	0
More	0

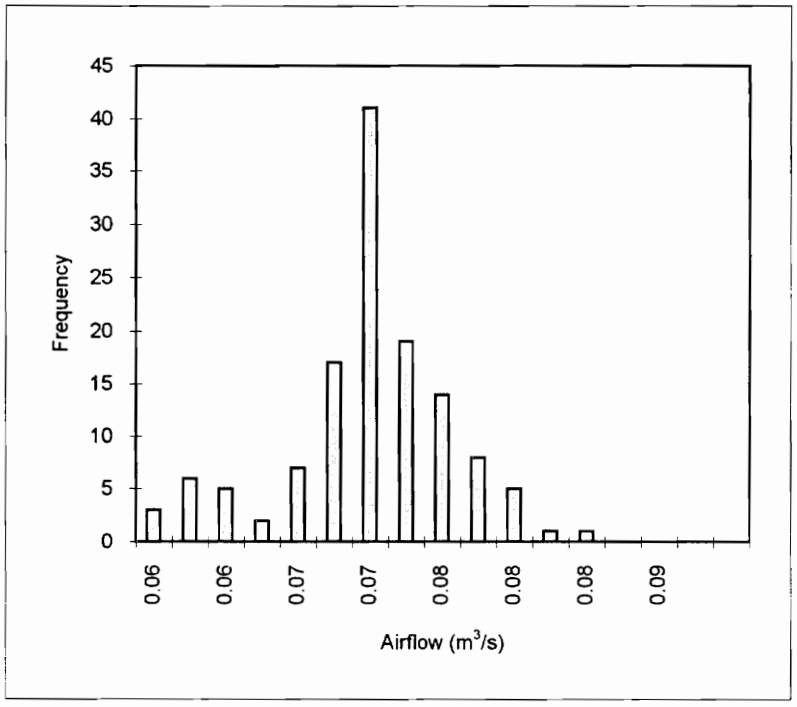

Figure 5-14: Airflow Trend and Histogram for Test 3.

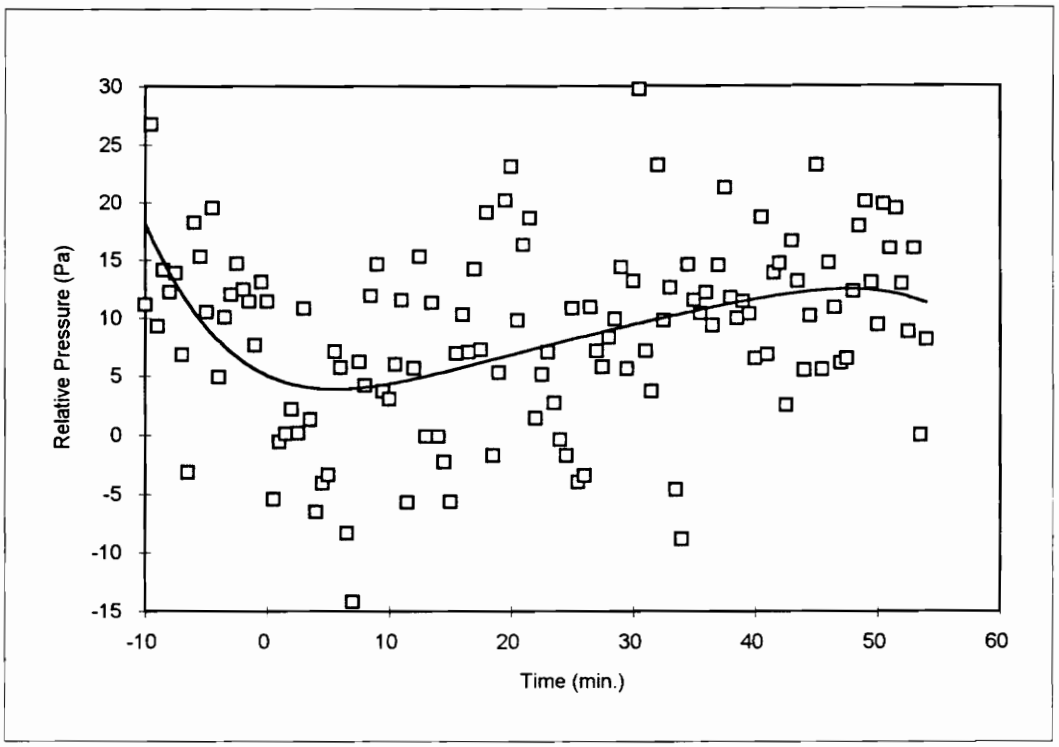

Pressure	Frequency
-20	0
-15	0
-10	1
-5	6
0	13
5	13
10	33
15	41
20	14
25	6
30	2
More	0

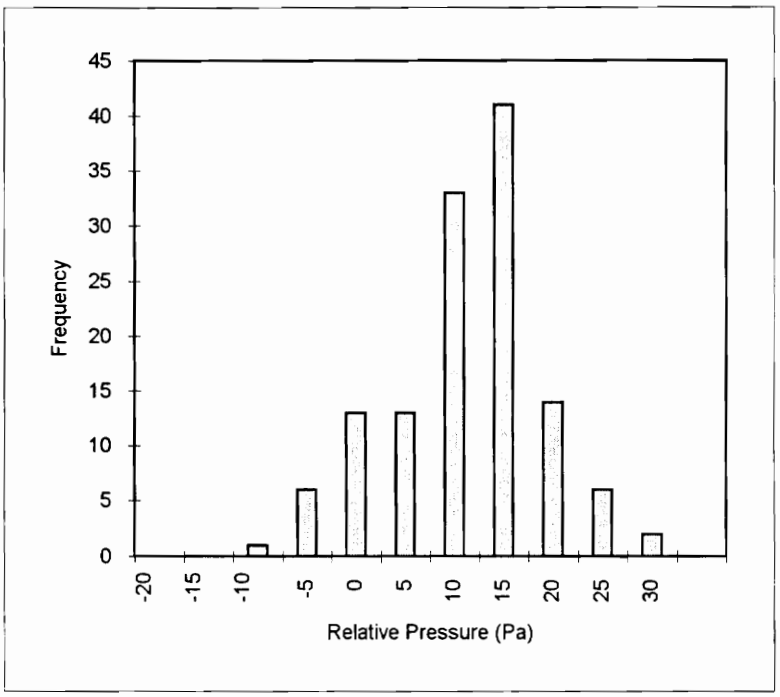

Figure 5-15: Duct Relative Pressure Profile and Histogram for Test 3.

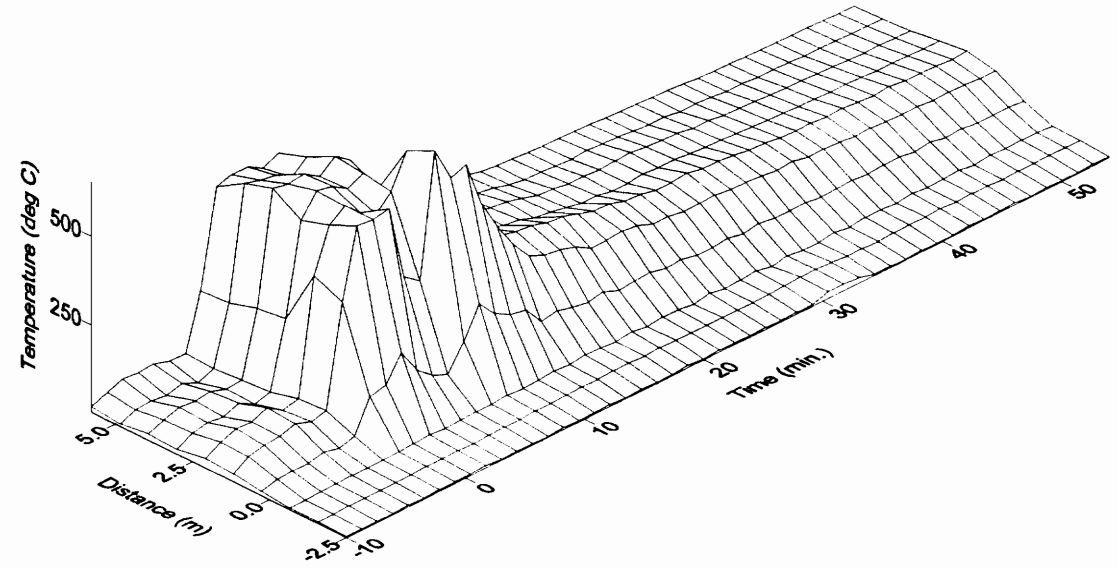

(a)

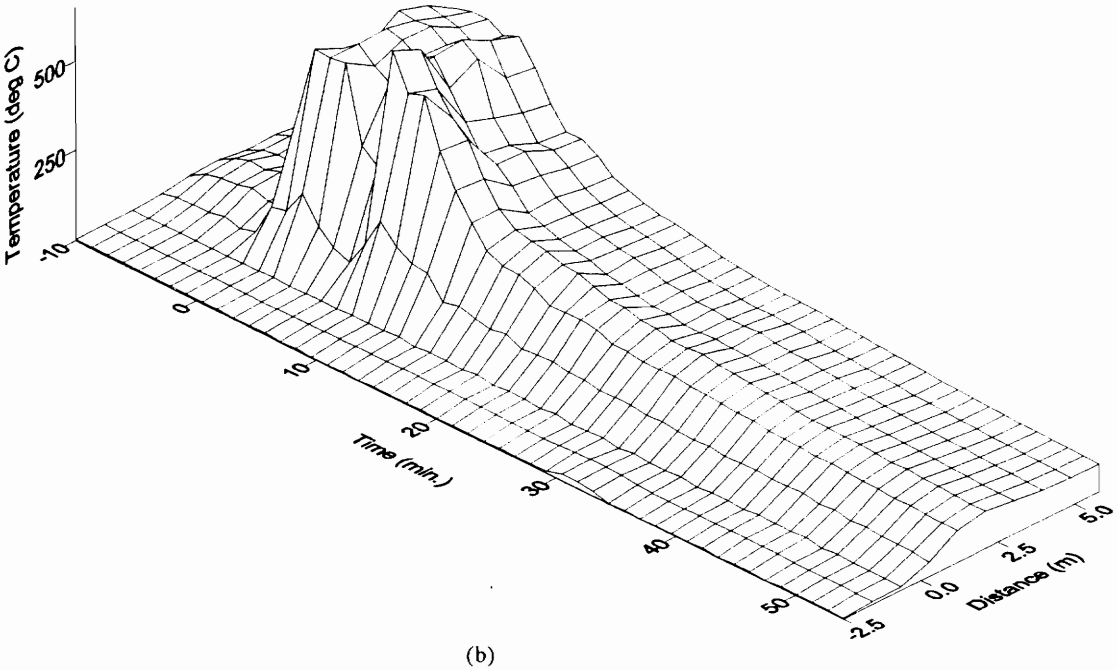

(b)

Figure 5-16: Temperature Surfaces Views, Forward and Reverse, for Test 3.

5.2.5. Test 6

This test was to observe the effects of the propane combustor/water vapor fire suppression system on a plywood fire. This fire was not recorded on video tape.

5.2.5.1. Gas Trace Profile

The reference time for the initiation of this fire shows a brief step in the oxygen and carbon dioxide levels, this was again due to some brief difficulties associated with the ignition of the fire. See the gas traces shown in figure 5-17. This is, however, followed by the very rapid transition towards the fuel-rich state. Once the fire was obviously fuel-rich, oxygen levels less than 2% on the data recorder monitor, the combination fire extinguisher was ignited.

During this test the propane burner in the extinguisher was ignited before the water mist sprayers were initiated. The most immediate result was the extinction of flames in the fire section of the tunnel upon the ignition of the gaseous propane fuel. The exhausts of the tunnel, which had been mostly translucent became an opaque white. The opaque white smoke was lingering, maintaining a plume about 50 feet into the air.

Following the ignition and water sprays of the combination extinguisher the oxygen concentration showed an increase, figure 5-17a, mirrored by a decrease in the carbon dioxide concentration, figure 5-17b. Both of these gas traces show a spike, momentarily reversing the trend toward fire extinguishment, at a time of 5 minutes. The traces return

to their normal pattern following this digression. Based upon the burning characteristics of the combination extinguisher, and the available fuel supply, it appears that this irregularity is due to the drop in the propane supply rate.

The carbon monoxide trace, figure 5-17c, shows a consistent growth to a level of about 29000 ppm. The peak in this trace lies about halfway between the ignition of the propane burner and its extinguishment. The peak also appears to correlate the anomalous spikes in the other two gas traces, occurring at about 5 minutes. The total width of the increased level of CO, about 12 minutes, correlates well to the width of the oxygen and carbon dioxide traces during the period of fire involvement.

The rate at which the propane was supplied to the burner rapidly dropped off after ignition. The evaporation rate of the propane was such that the liquefied gas was cooled to the point of inhibiting further evaporation at the desired rate. To combat this tendency the propane bottle was placed in a bucket of hot water, an act that proved to be of some assistance, delaying the flow rate drop by about two minutes.

This fire was extinguished completely before all of the fuel could be consumed. Upon opening the tunnel the fuel charge was found to be intact, with only minor indications of the fire on the outside surfaces. The inside surfaces of the fuel charge showed that charring of the wood had occurred to about half the depth of the wood panels, on all four surfaces, and over the entire length of the charge. The indication of the degree of charring is that all of the interior surface area was involved in the fire within 2-1/2 minutes of the initial acceleration. Furthermore, considering that the vast majority of the consumption of

the wood occurred during the five minute period in which the fire was fuel-rich leads to the estimate that the peak fuel pyrolysis rate exceeded 27 kg/hr m^2 (5.5 lb/hr ft^2).

5.2.5.2. Pressure Profile

The level of airflow shows an increasing trend over the duration of this test, see figure 5-18. A slight drop in the airflow rate occurs at about 10 minutes, the trend is reversed at 20 minutes. There appeared to be nothing noteworthy occurring during this period time that could account for the change in the trend. The histogram of this data does not appear to indicate anything of note. It does, however, appear to be reasonably normal in its distribution. But, looking at the trend graph, it is clear that the data is not random.

The relative pressure graph, figure 5-19, shows a different tale of the events. This data appears to break into three clumps; the first, up to 5 minutes, shows a decease in the absolute value of the relative pressure. From 5 to 12 minutes the data is clumped at the highest absolute value of the pressure. Following 12 minutes the data appears to be randomly distributed about the mean of all of the data. Possible correlations can be predicted. The change from the first to second clumps occurs at the time when the propane flow to the combustor is affected by the cooling of the liquefied gas. The change from the second to third clumps occurs near the time when the combustor went out due to the total consumption of the propane. At this time, 12 minutes, the fire was essentially out, oxygen concentration about 20 percent and the carbon dioxide about 1 percent.

5.2.5.3. Temperature Profile

The temperature profile for this test is shown in figure 5-20. One noticeable feature of this profile is the presence of elevated temperatures upstream of the ignition point, this is associated with the combustor, and does not indicated any reverse stratified flow. No reverse stratified flow was observed in the duct during the course of this test.

A smooth, although steep, rise in the temperature is indicated in figure 5-20a. The decay in the temperatures of this fire, figure 5-20b, appear to be a near mirror image of the growth. This would, further, indicate that the fire was rapidly extinguished. The small saddle in the profile that occurs at a depth of about 4 meters may be due to the relevant thermocouple being shielded between lids or the fiberglass insulation.

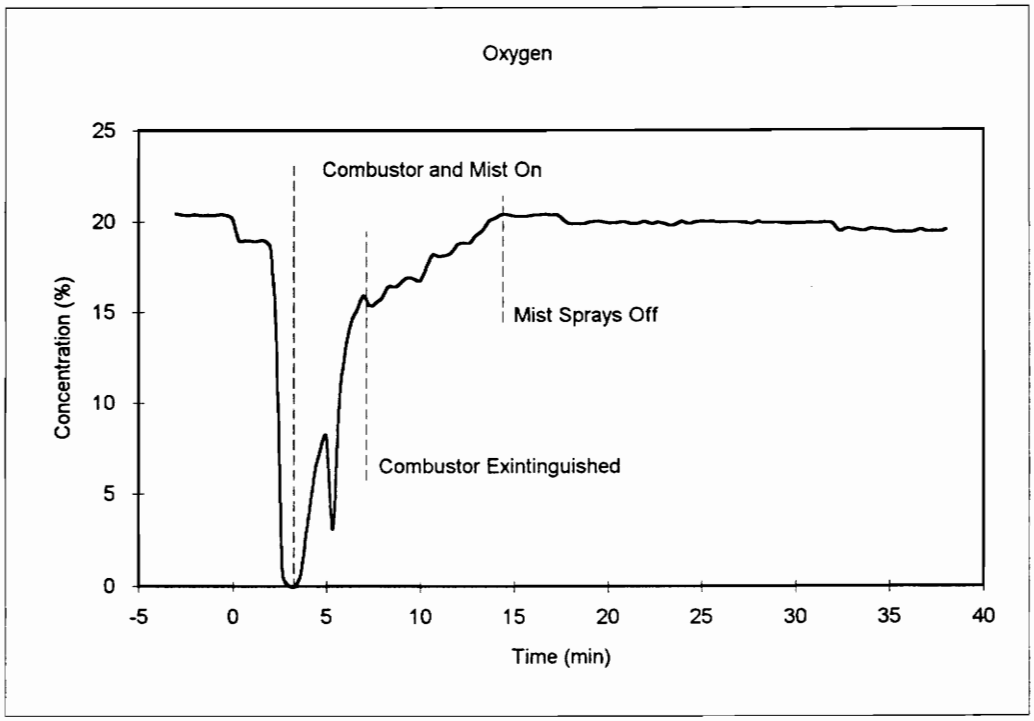

(a)

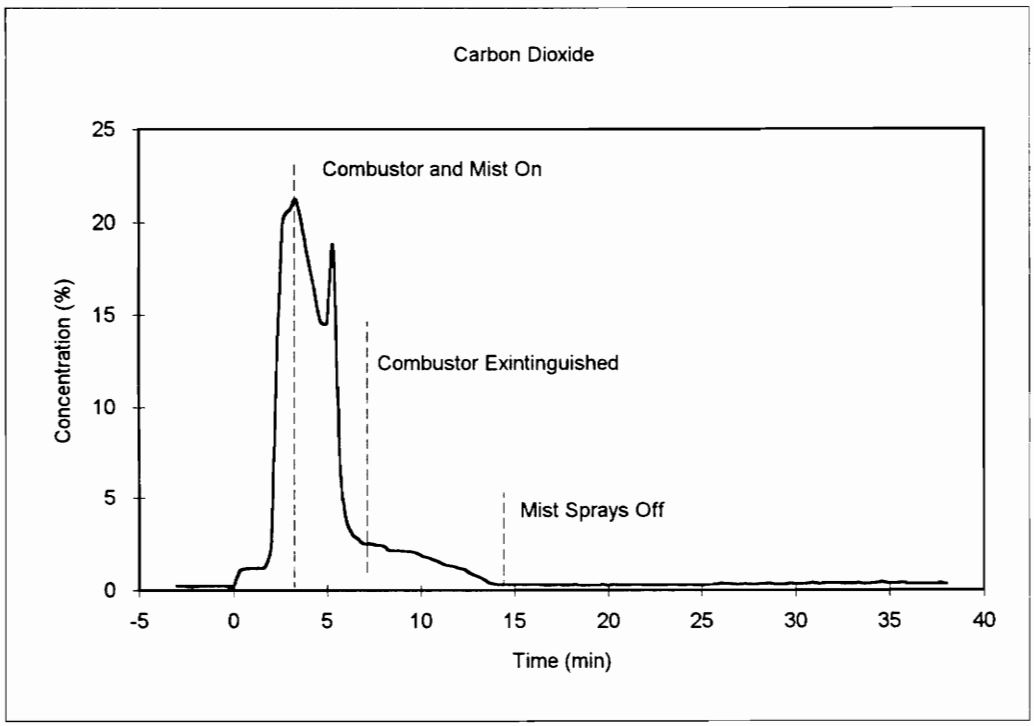

(b)

Figure 5-17 (a, b): Oxygen and Carbon Dioxide Gas Traces for Test 6.

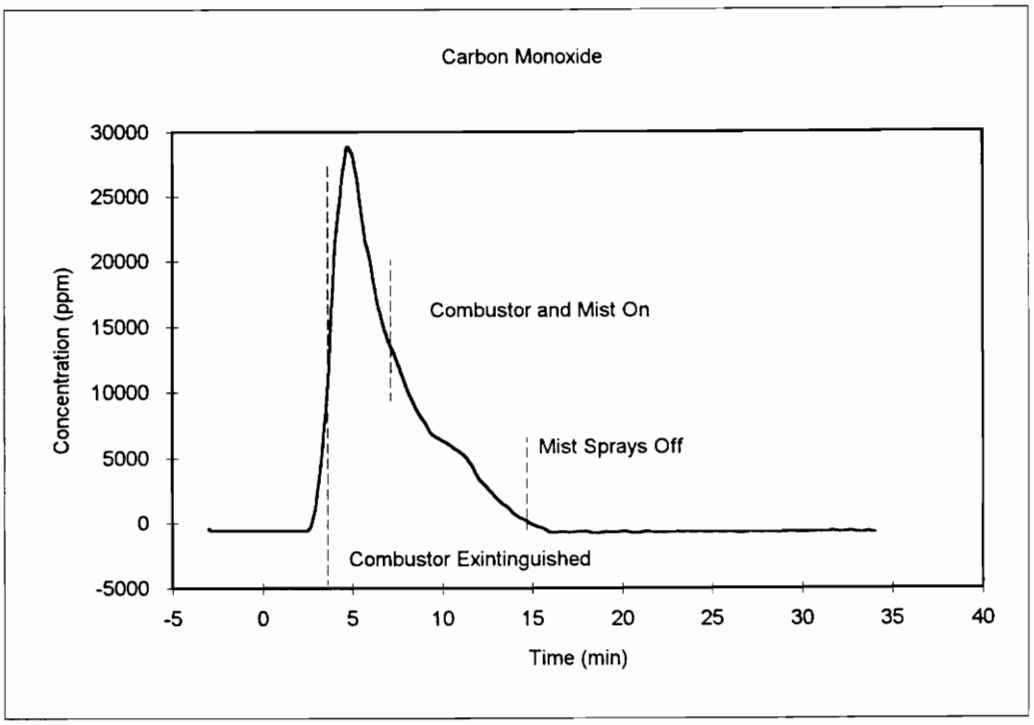

(c)

Figure 5-17 (c): Carbon Monoxide Gas Trace for Test 6.

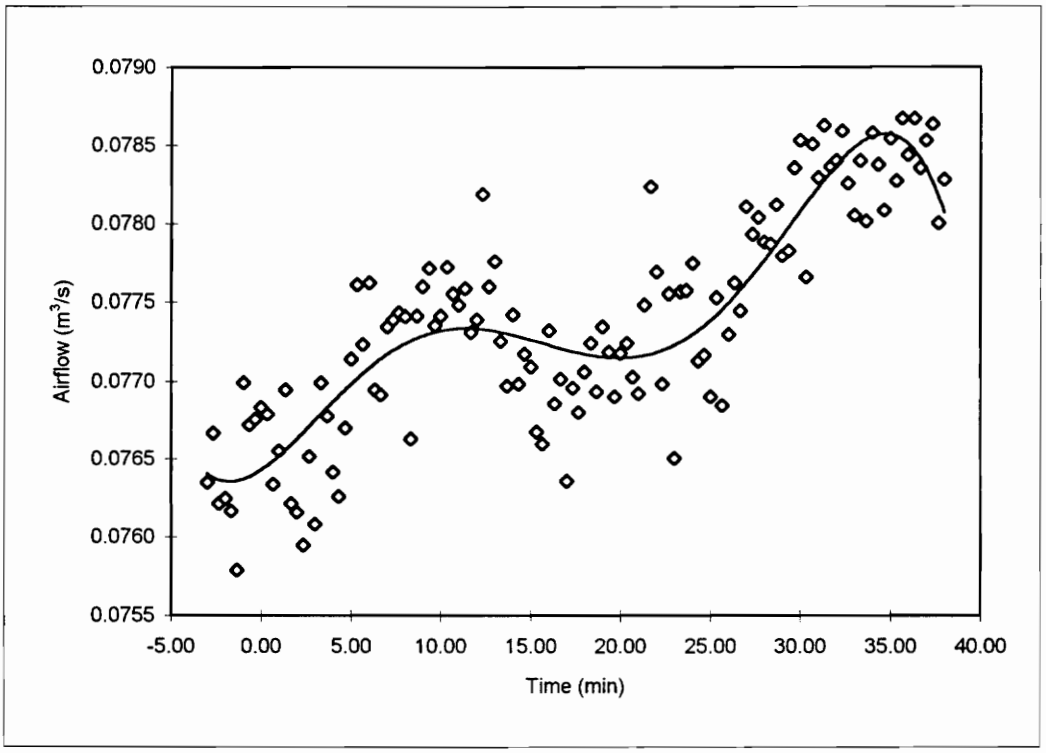

Airflow	Frequency
0.0760	2
0.0763	6
0.0765	5
0.0768	9
0.0770	20
0.0773	13
0.0775	17
0.0778	16
0.0780	6
0.0783	9
0.0785	11
0.0788	10
0.0790	0
More	0

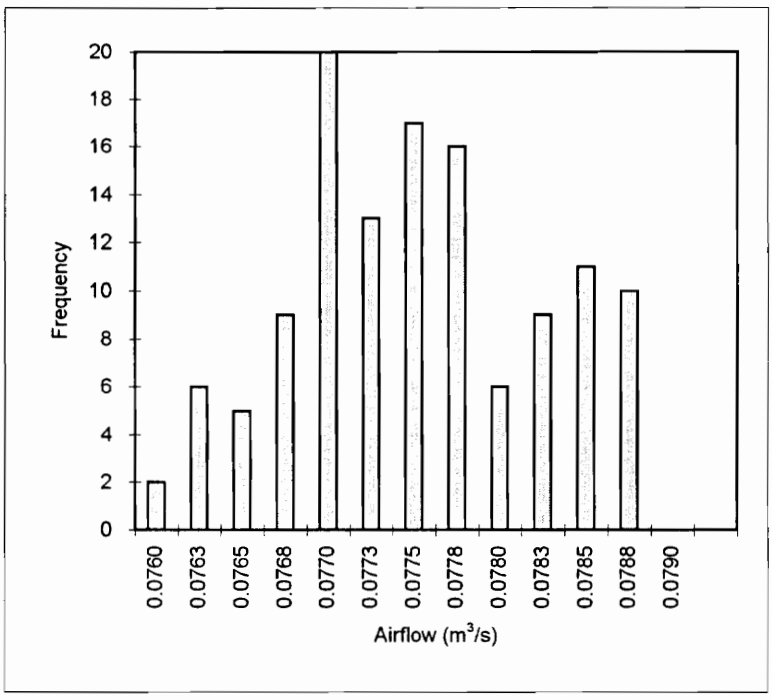

Figure 5-18: Airflow Trend and Histogram for Test 6.

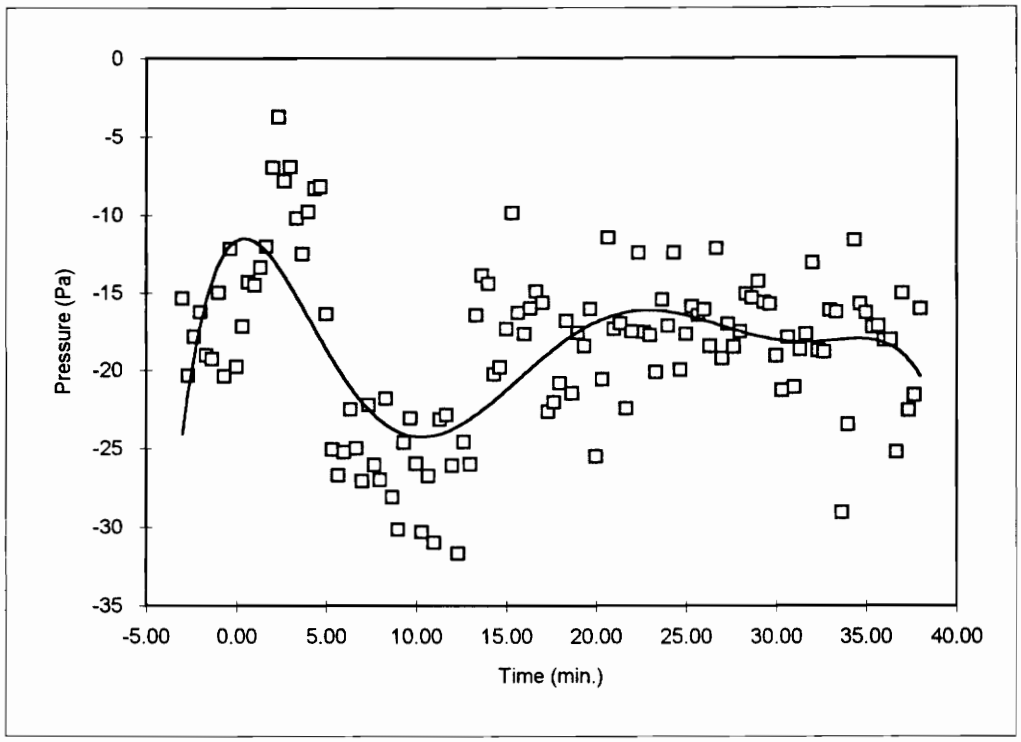

Pressure	Frequency
-35	0
-30	4
-25	15
-20	23
-15	57
-10	17
-5	7
0	1
More	0

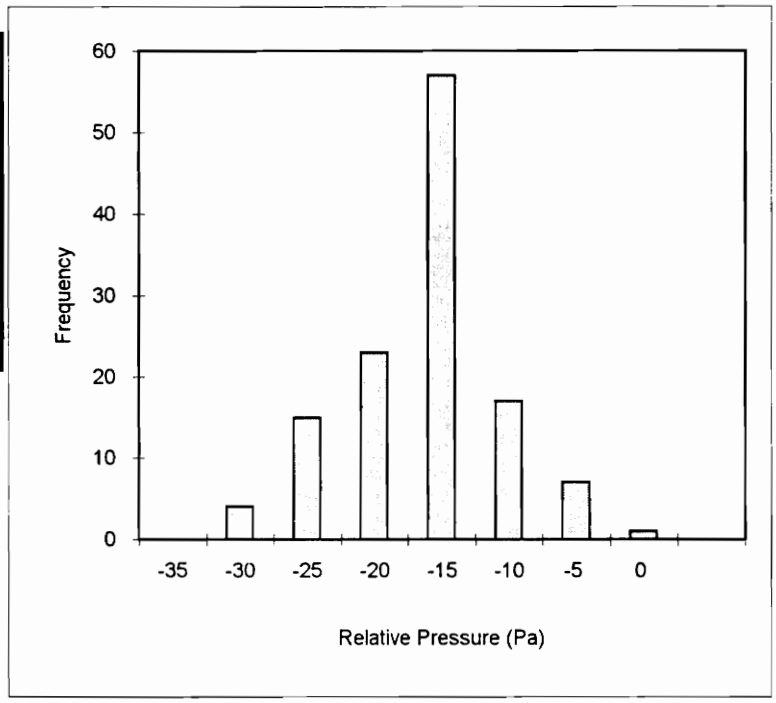

Figure 5-19: Duct Relative Pressure Profile and Histogram for Test 6.

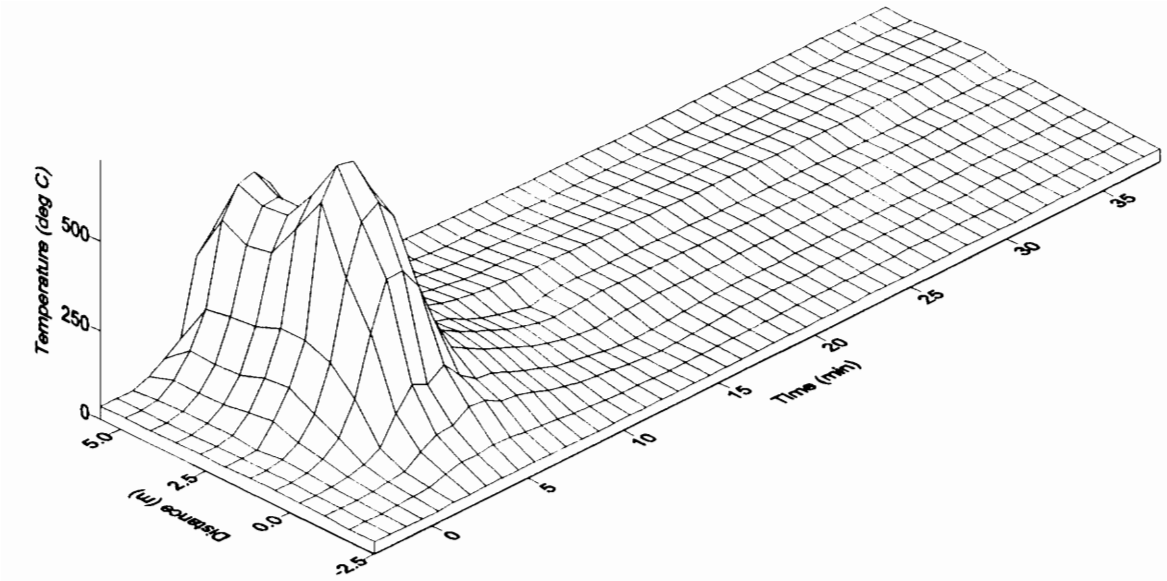

(a)

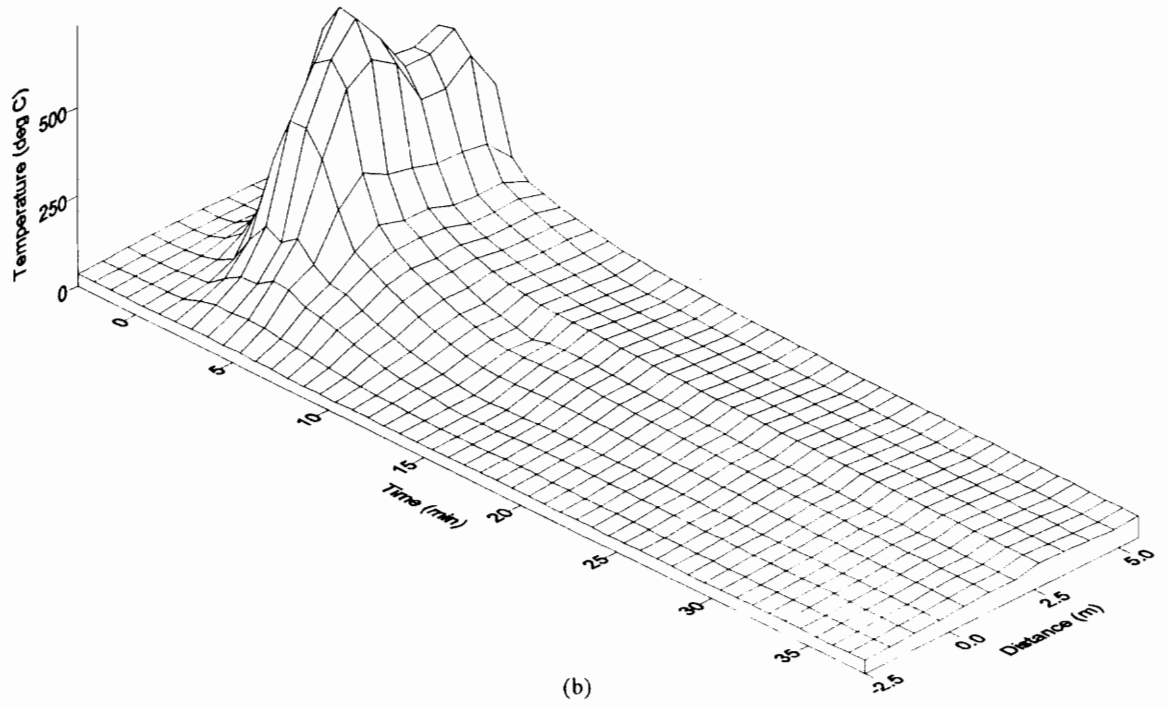

(b)

Figure 5-20: Temperature Surface Views, Forward and Reverse, for Test 6.

5.3. Coal Fire Tests

This research was intended to investigate the effect of water mist on fuel-rich coal fires. The tests covered in this section form the brunt of this work and will be the basis of the conclusions reached. A typical fire of a coal fueled test is illustrated in the photographs of plate 5-3.

5.3.1. Procedures

The procedures for the coal fueled tests were essentially the same as those for the wood fuel tests. The major difference being the configuration of the fuel. For these tests the coal fuel, in lump form, was supported against the interior surfaces of the tunnel by steel grating. Expanded steel grate was formed into an open ended box approximately 24 cm (9.5 inches) square and 2.5 m (8 ft) long.

Lumps of coal were placed on the floor of the tunnel to form a continuous bed along the length of the fuel section of the tunnel. The grate was inserted on the floor coal and centered in the tunnel cross-section. Coal was then placed between the grate and the walls of the tunnel until continuous beds of coal were formed along both sides. Coal was placed on the top of the grate to form a continuous bed, as the lids were being set in place.

As with the wood fueled tests, the thermocouples were put in place at appropriate intervals as the lids were being set.

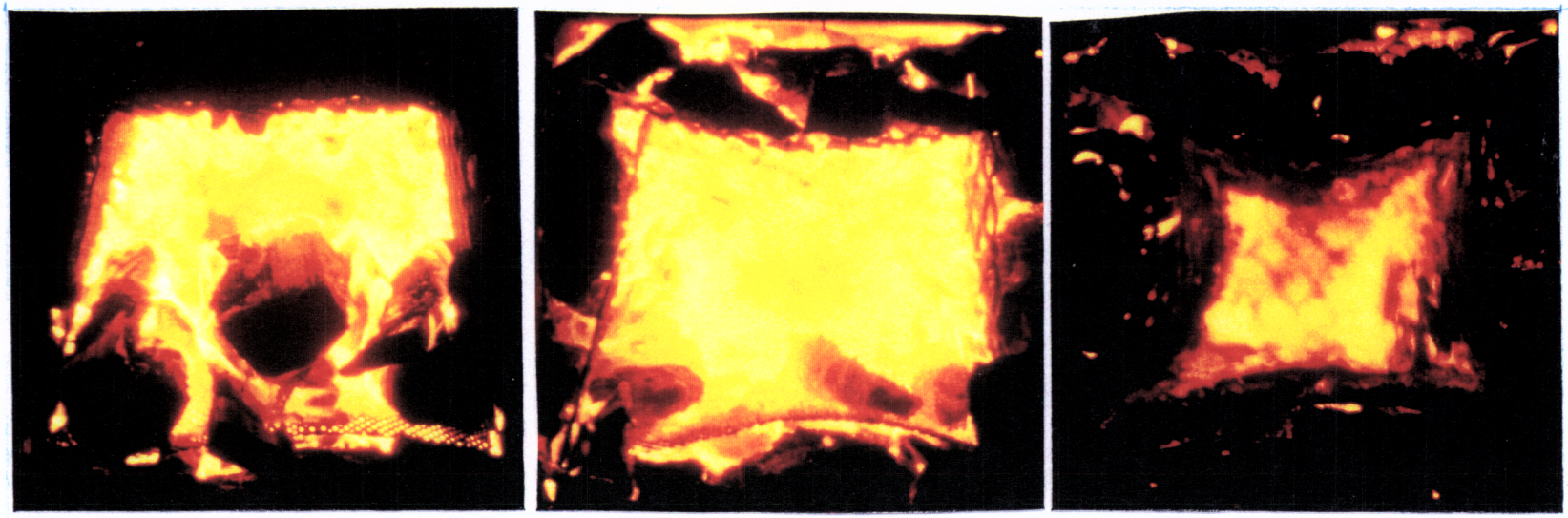

Plate 5-3: Views of Coal Fire

5.3.2. Test 4

In this test coal was used as the fuel in the fire tunnel, the fire was allowed to burn without attempts to bring it under control. In this manner, a baseline for coal fires was obtained. A video tape of this test was made, with a brief synopsis given in table 5-6.

The initial fuel load for this test consisted of 60 kg of bituminous coal from the southwest Virginia coal region. When the tunnel was opened, following the test, 20 kg of coke was removed. The size of the coke was approximately that of the initial coal lumps, about 1/3 of this weight was what one might call ash. It should be mentioned that this test was terminated at a reference time of 100 minutes, by which time the gas traces indicated oxygen-rich conditions. Termination of the test was performed by turning off the ventilating fan, closing in the wastegate, and leaving the orifice plate in place. The test was ceased due to impending darkness. During the clean-up process of the tunnel the view window showed a band of condensation that appeared to indicate that some stratification of the air in the tunnel had occurred. This was most likely due to closing off the in flowing air, allowing the heated gases to flow back towards the inlet of the tunnel.

5.3.2.1. Gas Trace Profile

Ignition of this fire required some secondary assistance, beyond the initial attempt. The initial source of ignition was a small fire of newspaper, diesel oil, and split wood intended for fireplace use. The action of this source is evident in the oxygen and carbon dioxide traces, figure 5-21. Notice that there is a decrease of about 5 percent in the oxygen and

an increase in the carbon dioxide of about 4 percent, followed by a return to near normal levels. Once additional wood was supplied to the ignition source the fire begins to accelerate in a two-stage mode. The first four minutes of this growth shows a drop in the oxygen from 19 to 13 percent, with a corresponding increase in the carbon dioxide concentration from 1 to 7 percent. Once the fire reached the 13 percent oxygen concentration its rate accelerated to drop the oxygen to 0 percent in the subsequent two minutes. This growth is mirrored in the carbon dioxide profile.

During the course of the fire the oxygen remains at a constant level, figure 5-21a; indicated as slightly negative value most likely due to the calibration levels. At the time when the oxygen level reaches 0 percent, the carbon dioxide level, figure 5-21b, shows a relative maximum. Through the time that the oxygen content is 0, the carbon dioxide level drops from 19 percent to a relative minimum of 17 percent returning to another relative maximum of 19 percent before decaying off. The relative maxima of the carbon dioxide correlate in time to the period that the oxygen is below the limits of the sensor. It is during this period of time that the marked increase in the carbon monoxide, figure 5-21c, level is seen. The peak in the CO level, 35000 ppm correlates to the relative minimum of the carbon dioxide. The carbon monoxide level is near 4 percent, which can account for the corresponding 2 percent drop in the CO_2 level. It is apparent that the carbon monoxide level rises very quickly as the fire becomes fuel-rich and falls off as rapidly as the fire begins to decay.

5.3.2.2. Airflow and Relative Pressure Profile

The airflow profile, figure 5-22, from this test shows a marked drop in the flow quantity that correlates well to the acceleration of the fire to the fuel-rich regime. The airflow slowly increases as the fire decays. The data appears to be randomly distributed about the trend line that is shown. The histogram shows what can be visualized as a bimodal distribution. That is two normally distributed data sets, the first with a mean of about 0.0715 m^3/s and the second with a mean of about 0.0730 m^3/s. If this split in the data is real then this is some evidence of the throttling process. The airflow does decrease as the fire gains intensity, and increases as the fire begins to decay.

The relative pressure profile, figure 5-23, shows a similar pattern in the pressure changes. The pressure drops rapidly as the fire gains intensity and begins to return to the normal level as the fire decays. The histogram of this data shows a similar bimodal pattern as the airflow. The use of an absolute change in the pressure here is, possibly, more appropriate than the direction, since if throttling was occurring the expected result would be an increase in the static pressure upstream of the fire. The data here shows the static pressure decreasing. This may be associated with the location of the probe, as discussed in section 6.3.3 of this thesis.

5.3.2.3. Temperature Profile

The temperature profile for this test is shown in figure 5-24. This figure shows the small bump in the temperature near the -10 minute point that associates with the initial attempt

to ignite the fire. This bump is followed by a temperature drop as the ignition fire began to die out. The temperature profile shows an increase in the temperature at time 0, as the fire accelerates to the fuel-rich regime. The overall face of the temperature profile, at a depth of zero meters indicates that no reverse stratified flow developed, and none was seen in the video tape. In the time period between 0 and 20 minutes, there is a valley associated with the depth of about 2 meters, this is believed to be due to the thermocouple being shielded from the fire, either behind a block of coal or between the lids. A drop in the temperature is shown between 22 minutes and 40 minutes, this is an artificial drop due to data in this region being rejected. The extreme range of this data as recorded (around 20000°C for some readings) indicates that the data is erroneous. This may also account for the spiked appearance of several points on the surface.

The duration of the temperature profile, greater than an hour and a half, indicates that the fire was continuing to burn, in a glowing phase for a time that continued beyond that recorded. The level of these temperatures may also be buffered by the heat retained by the brick walls of the tunnel.

Table 5-6: Synopsis of Video Tape Documenting Fire Test 4

Ref. Time	Description
-9:30	Fire lit
-9:12	Smoke obscures daylight at end of tunnel
-9:07	Flames contact top
-8:05	Daylight visible at end of tunnel
-7:28	Settling if ignition source
-6:57	Further settling of ignition source
-6:40	Only small flames left if initial ignition source
-6:10	Smoke visible from top coal
-5:04	What appeared to be smoke may be shimmer
-4:45	What appears to be smoke from to begins to disappear
-3:09	Only flame from ignition source is a small flicker on the left side and some flaming below (but above coal).
-2:20	Flames from ignition source do not appear to contact coal
-1:46	Settling occurs in ignition source
-1:27	Access lid opened to add more fuel to ignition source
-1:19 to -0:31	10 additional sticks are added to the ignition source pile
-0:23	Access lid closed
-0:10	Last stick added begins to catch fire
0:20	Smoke from wood begins to obscure daylight from the end of the tunnel
0:39	Flame visible below bottom grate
0:44	Flames begin to contact top
1:23	Flames from floor begin to intensify
1:55	Smoke from to begins
2:06	Smoke at top begins to exhibit an orange glow
2:20	Visible flaming at top erupts
2:38	Visible flaming on left side
3:09	Flaming at top extends fully across opening
3:10	Flaming visible on right side
3:39	Ignition source settling, about half consumed
4:15	Yellow flame swirl visible down centerline, behind ignition source

Table 5-6: Synopsis of Video Tape Documenting Fire Test 4

Ref. Time	Description
4:36	Settling in ignition source
5:00	Distinct bowing of floor grating visible
5:35	Settling of ignition source material, piece rolls up on end, left side
6:22	Ignition source distinctly glowing
7:35	Ignition source about two-thirds consumed
15:00	Sag visible in top grate
16:24	Top grate appears to have collapsed at far end of fuel charge
17:30	Sag in top definite, with flames between the top coal and the lids
17:45	Collapse in top grate clearly visible at far extreme of the fuel load
18:55	Most of ignition source is gone, except for pieces in lower left and right corners
19:09 to 19:36	Interruption in tape
19:44	Most of flaming appears to have subsided. Buckling of side grates is beginning
26:25	Daylight appears to be visible at the far end of the tunnel
28:02	Only major flaming appears at the far end of the fuel load
30:28	Daylight definitely visible at the far end of the tunnel, strong glowing phase is evident at upstream end
30:32	Camera relocated at exhaust end
30:36	Large swirl in flames is carrying flame away from fuel, rotating clockwise to view in exhaust end of tunnel
31:02	Flames seem to be blowing straight down side of tunnel
33:57	Daylight visible in view port
42:21	Strong glowing combustion apparent, flames still on side of opening only
47:14	Brick on top surface appears to be glowing (distinguishable from coal)

Table 5-6: Synopsis of Video Tape Documenting Fire Test 4

Ref. Time	Description
50:35	View port boarded off
51:00	All of coal is brightly glowing, some flames still exist on sides
53:51	Glow in coals has gone from red to yellowish, glow from fire bricks still apparent, some bricks on lids have separated from backing
59:51	Most of flaming has subsided.
1:07:22	Some flame is visible between the bricks of the lids, this appears to be from the backing material burning
1:15:00	Settling of the coal mass towards the floor is becoming apparent, gaps of about one-quarter inch appear between the coal and the lids, bricks in the vicinity of the fire are definitely glowing (incandescent)
1:20:45	Very little flaming left (on right side viewed from exhaust end)
1:23:40	View of fire terminates

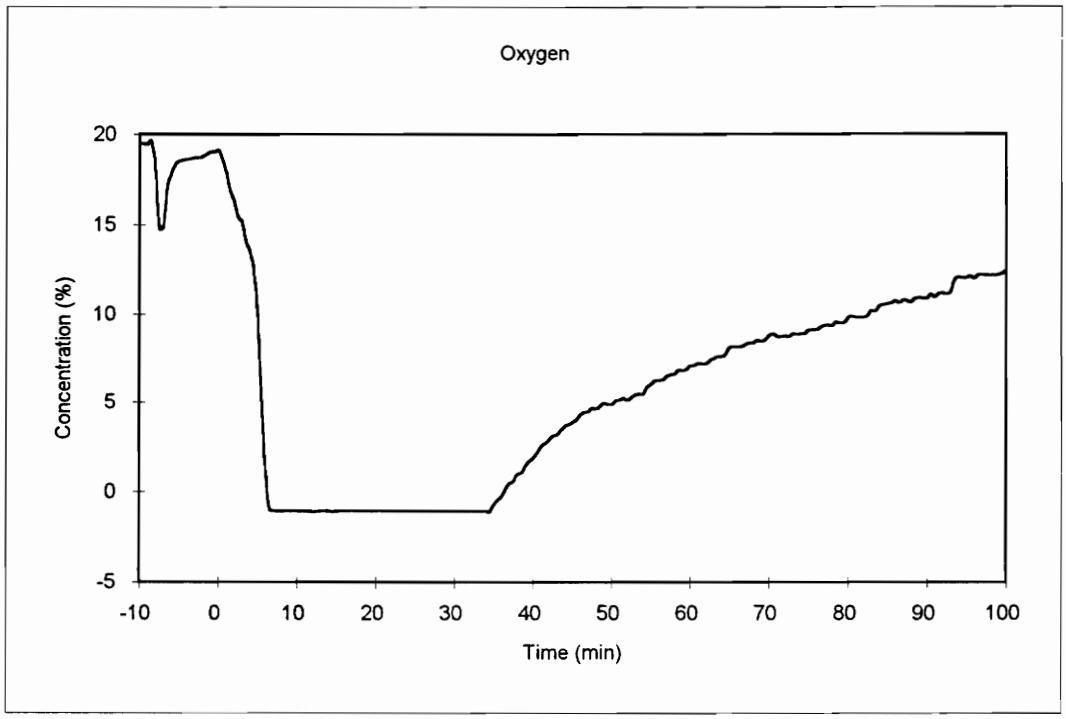

(a)

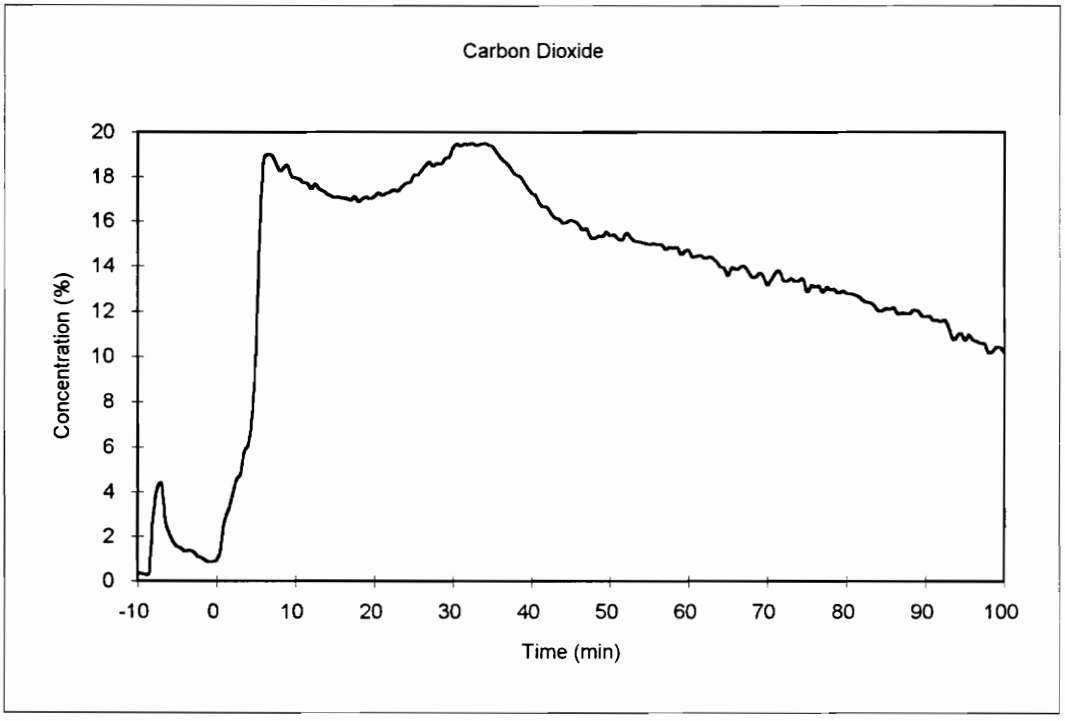

(b)

Figure 5-21 (a, b): Oxygen and Carbon Dioxide Gas Traces for Test 4.

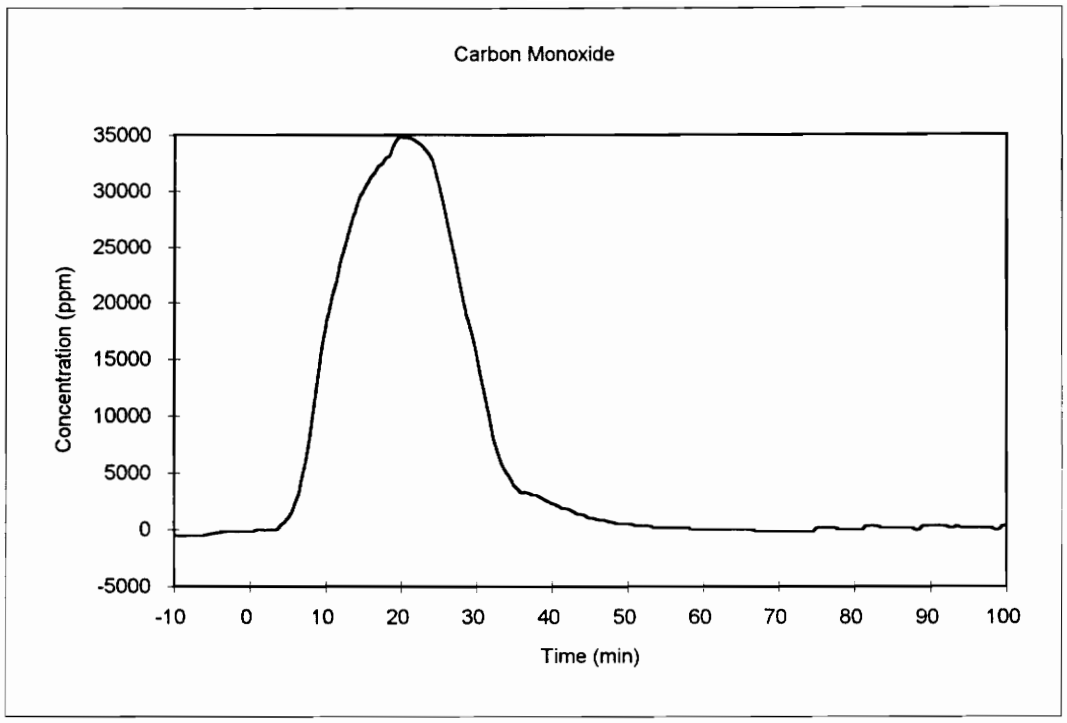

(c)

Figure 5-21 (c): Carbon Monoxide Gas Trace for Test 4.

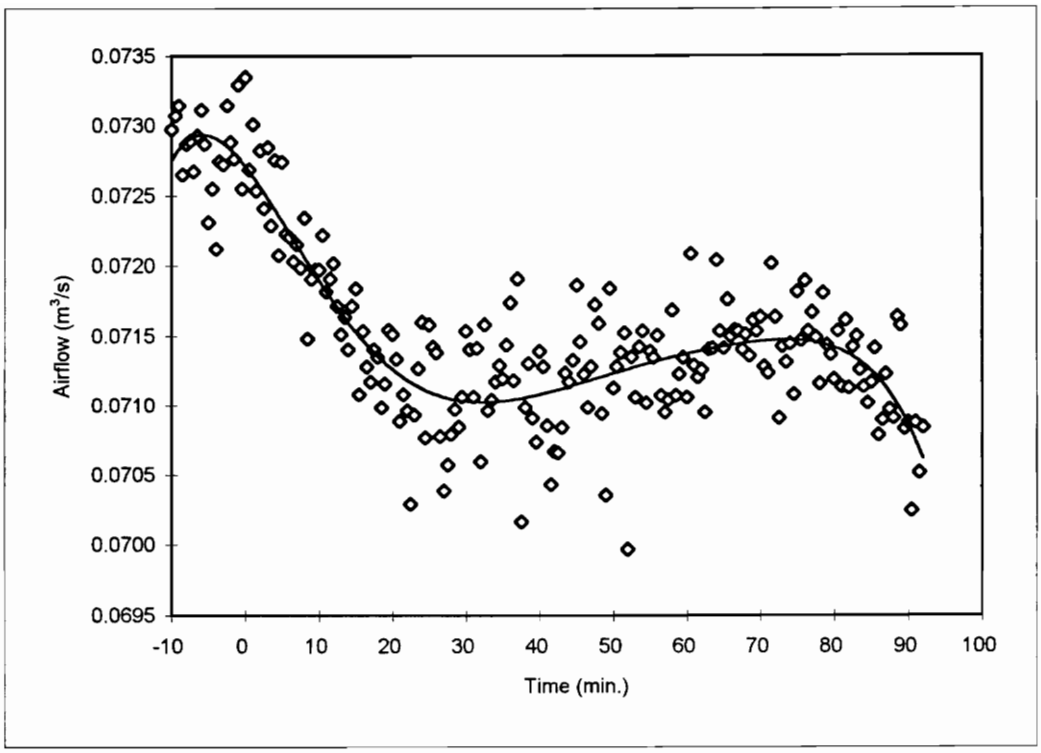

Bin	Frequency
0.0695	0
0.0698	0
0.0700	1
0.0703	2
0.0705	4
0.0708	6
0.0710	27
0.0713	32
0.0715	44
0.0718	34
0.0720	14
0.0723	11
0.0725	4
0.0728	9
0.0730	10
0.0733	5
0.0735	2
More	0

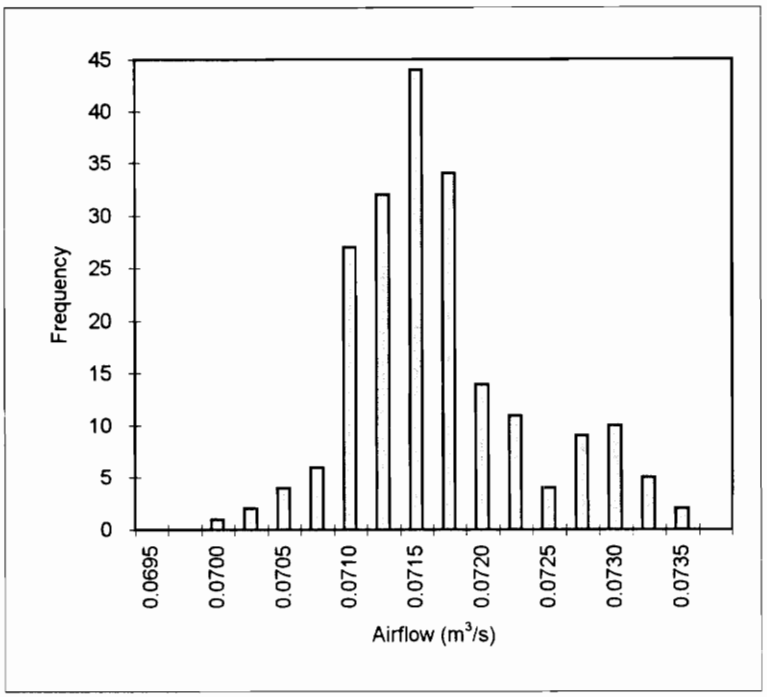

Figure 5-22: Airflow Trend and Histogram for Test 4.

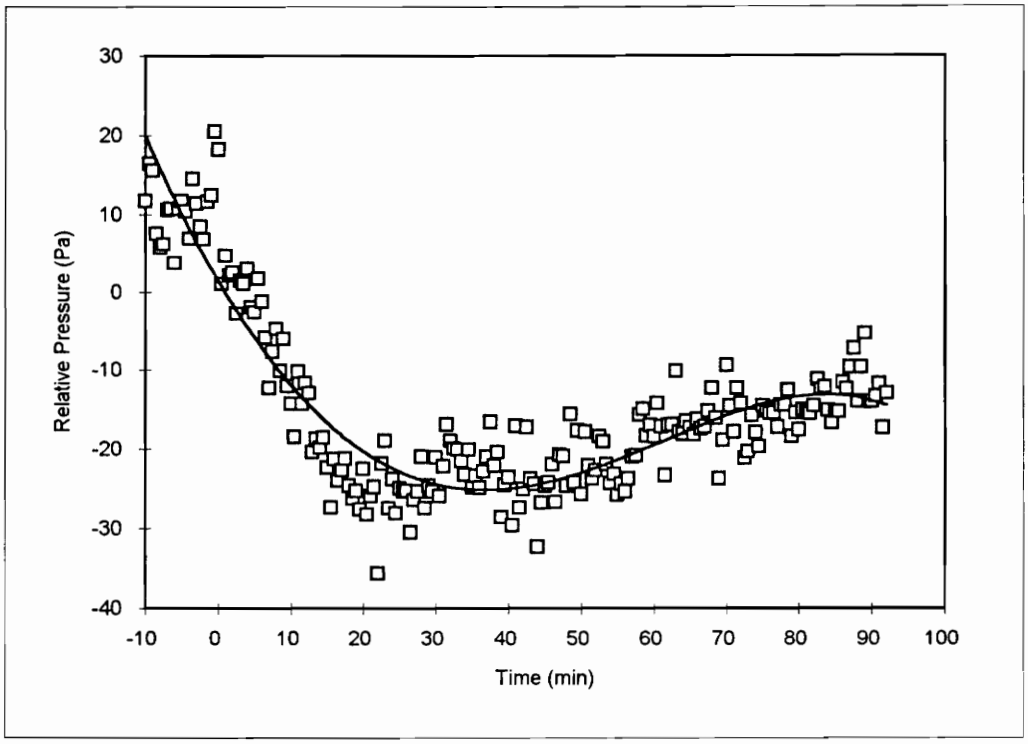

Pressure	Frequency
-40	0
-35	1
-30	2
-25	23
-20	53
-15	53
-10	31
-5	8
0	5
5	9
10	6
15	10
20	3
25	1
More	0

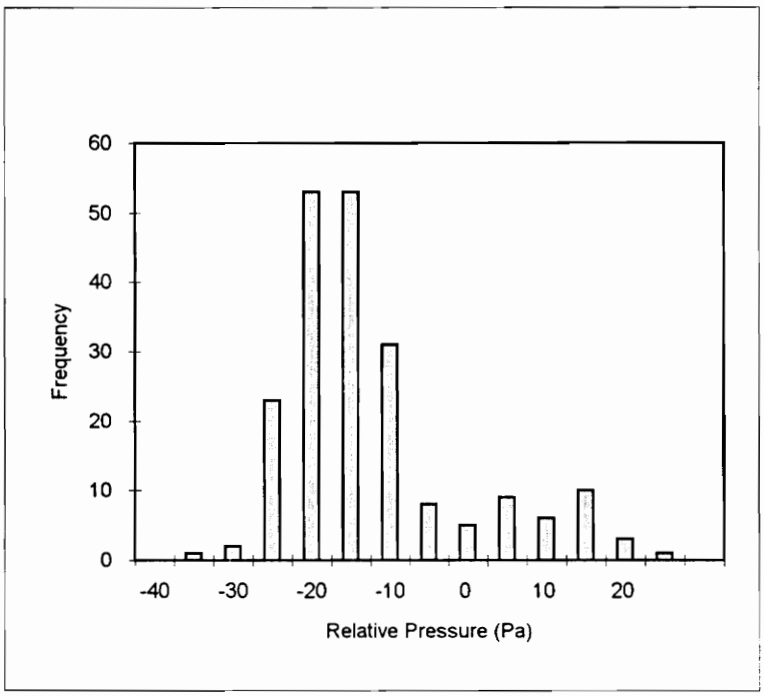

Figure 5-23: Duct Relative Pressure Profile and Histogram for Test 4.

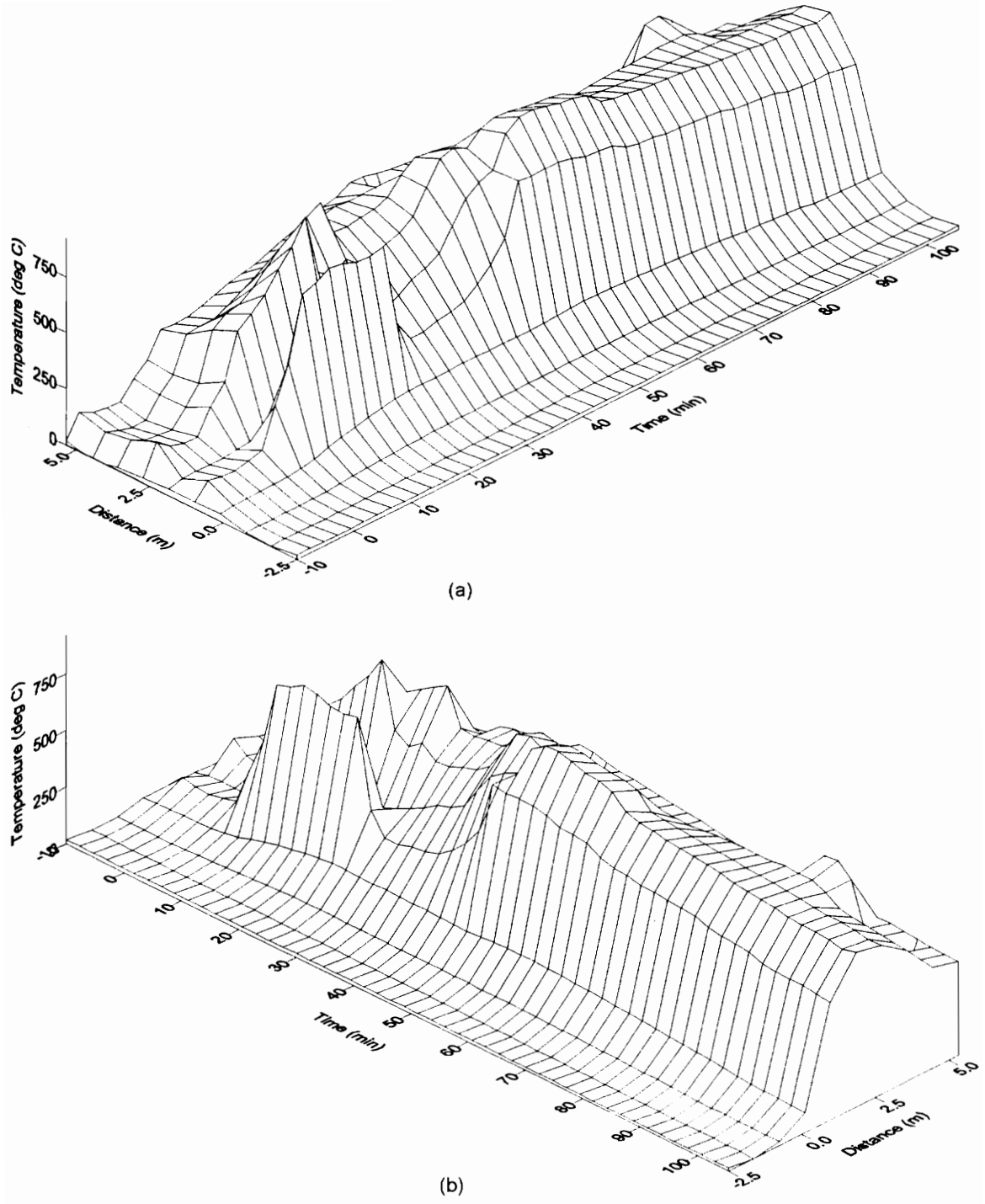

Figure 5-24: Temperature Surface Views, Forward and Reverse, for Test 4.

5.3.3. Test 5

This test was to observe the impacts of adding water mist to the air upstream of the coal fire burning in the wind tunnel. The fire was observed to grow to a fuel-rich state, at which time the mist generation system was initiated. The fog system employed during this test was the pneumatic assisted atomizing nozzles placed about four diameters upstream of the fire.

The initial fuel load for this test was 50 kg of bituminous coal from the southwest Virginia coal mining district. Approximately 36 kg of products were removed from the tunnel following the test. The products consisted of unburned coal, coke, and some ash. A vast majority of the remaining material was coal that showed signs of pyrolysis on the surface exposed towards the interior, but unburned elsewhere. The effect of the fire on the coal located at the top of the fire is shown in the photographs of plate 5-4.

5.3.3.1. Gas Trace Profile

The growth of this fire shows a slightly different pattern to that of the previous coal fueled test. The oxygen concentration slowly drops from about 20 percent to 17 percent in the first 10 minutes after the ignition fire was lit, see figure 5-25a. The fire accelerates dropping the oxygen concentration to 10 percent in the next two minutes and to 0 percent in the subsequent 2-1/2 minutes. The carbon dioxide profile, figure 5-25b mirrors this activity.

Plate 5-4: Coal Fuel After Water Spray.

The carbon dioxide shows a relative maximum of about 17 percent and of about 18 percent corresponding the period that the oxygen concentration is at a constant minimum. The profile of the initial maximum leading to a relative minimum is similar to that experienced during the previous coal fueled test. A rapid increase in the carbon monoxide, figure 5-25c, concentration is associated with the first relative maximum in the carbon dioxide concentration.

The fogging system was initiated at about reference time 10 minutes. At which time the carbon dioxide shows a relative minimum of about 15 percent. The carbon dioxide concentration increases to the second maximum about 5 minutes after the fogging is begun. The decay of the carbon dioxide concentration from this maximum correlates to the increasing oxygen concentration. The span of the carbon monoxide growth also correlates well to the span of the carbon dioxide relative minimum, as was seen in test 4.

The carbon monoxide profile shows the expected growth and decay to the reference time of 15 minutes. Following this time the trace exhibits two definite spikes (17 and 37 minutes) and a slight hump (23-30 minutes), these are considered to be anomalous. They can be associated with the clogging of the disk filter element through which the gas sample was drawn, with subsequent metering errors to the CO monitor.

5.3.3.2. Pressure Profile

The airflow trend for this test shows two characteristics. The first is a relatively wide distribution of points about the trend line shown in figure 5-26. The trend line shows a

slight drop in the airflow as the fire accelerates. This is followed by an increase in the airflow at ten minutes, this correlates to the initiation of the fogging system. As the fire begins to decay the airflow shows a decrease at about 45 minutes. The second characteristic of this data is the periodicity of the data that is about 5 minutes. That is, the data does not appear to be randomly scattered about the trend line, but cycles back and forth with a five minute period. The only guess for this would be fluctuations in the frequency of the electric power delivered to the fan. (This guess being made on the consideration that the speed of the fan, and hence airflow delivered, is proportional to the frequency of the current.)

The histogram of this data appears to be relatively normal in the distribution, with perhaps a skewness of the data toward the lower end.

The duct relative pressure chart, figure 5-27, shows the data in what appear to be two segments. The first segment shows the relative pressure increasing as the fire accelerates, a break in this data correlates to the initiation of the fogging system. With the initiation of the fogging system the relative pressure drops and levels off as the fire decays. The histogram shows the data skewed toward the lower end, which is easily explained as the fire spent much of the time in the decaying condition. This data does not have the readily apparent periodicity of the airflow data.

5.3.3.3. Temperature Profile

The temperature data associated with this test, figure 5-28, illustrates the relatively slow growth of the coal fire, compared to the wood fires. The change in the growth rate is

visible near time zero as the slope of the temperature surface increases. Due to the time that the fire took to reach this point only the first 10 minutes preceding the acceleration to the fuel-rich state are shown. These graphs also show that there was no reverse stratification of airflow, nor was any visible in the video tape prior to the initiation of the fogging system. In both views a distinct valley is visible at a depth of about 1.5 meters, this is believed to be due to the thermocouple being shielded from the fire. This may be due to the thermocouple element being caught between the bricks, or between a piece of the coal and the lid.

The temperature ridge shows a brief decrease in the peak temperature between 10 and 21 minutes. The beginning of this drop correlates with the initiation of the fogging system. The return to the normal level may be associated the fire re-stabilizing to the presence of the water vapor and the thermocouples close contact to the top coal. The fire intensity dropped off rapidly after the introduction of the water mist, however, some close flames and glowing combustion remained after the fire had been returned to an oxygen-rich regime.

The reverse view, figure 5-28b, illustrates the effect of opening the tunnel and exposing the thermocouples to the open environment. The surface shows rapid cooling that occurred as a result of opening the tunnel.

Of a noticeable occurrence in the temperature surface is the periodic nature visible at the 0 meter line. This line shows a period of about 10 minutes, which is marginally correlatable to every other period in the airflow profile (figure 5-26).

Table 5-7: Test 5 Video Tape Synopsis

Ref. Time	Description
-0:08:42	Fire lit, view outside of vent port.
-0:08:35	View into vent port of ignited fire.
-0:07:36	Camera being moved to exhaust end.
-0:07:31	View into exhaust end of tunnel, no flame visible.
-0:07:26	Camera lower, flame visible.
-0:07:15	Some flame and daylight visible in tunnel.
-0:06:40	Only flame appears to be the ignition source.
-0:05:32	Smoke begins to thicken.
-0:05:25	Camera backs off, fire not visible
-0:04:45	Camera zooms out, smoke appears to disappear.
-0:04:35	Camera zooms in, smoke (blue-gray) visible at outlet of tunnel, still no indication that coal has begun to burn.
-0:04:30	Flames from ignition source appear to contact top.
-0:04:03	Smoke appears to be thickening and intensity of the ignition source flames appear to be decreasing.
-0:02:55	Gray-black smoke begins to obscure view to flames. Still only flaming appears in the ignition source wood.
-0:02:42	Clockwise vortex of flame visible in upper right hand side. (This is the opposite direction from what would be expected.)
-0:02:20	Only flame visible is in lower left side. Very slight on upper right side.
-0:02:12	Flash of smoke or flame in upper left side.
-0:02:10	Slight flicker of flame on coal in upper left corner.
-0:02:02	Smoke obscures much of the view, light from fire is only evidence of burning. Can see only left half of tunnel.
-0:01:55	All of burning is obscured by smoke.
-0:01:47	Some of flame visible, again only on left side of the tunnel.
-0:01:35	Comment: Appears that smoke is turning black.
-0:01:20	Stronger burning on left side, visible through smoke.
-0:00:12	Intensity of flames appears to be dropping, daylight visible near top of fuel support frame, above ignition source.

Table 5-7: Test 5 Video Tape Synopsis - Continued

Ref. Time	Description
0:00:03	Most of burning appears to be ignition source, although some flames appear in side and bottom coal, (may be diesel fuel).
0:01:09	Smoke begins to obscure view, some daylight still apparent in to half of the picture.
0:01:20	Most of view obscured by smoke, some flames visible in central region and in lower right corner.
0:02:03	Comment: Oxygen about 18%.
0:02:30	Fire not visible through smoke.
0:04:10	Camera zooms back - thick dark gray to black smoke visible.
0:05:40	Smoke color changing to darker black and thickening.
0:06:40	Smoke plume definitely thicker and darker.
0:06:44	White smoke clearly visible blowing away from upstream side of tunnel (on out side), leakage.
0:07:18	Smoke plume now quite thick.
0:09:36	Smoke cloud thick and black.
0:09:40	Camera zooms in, cloud appears to lighten a bit at the edges.
0:11:15	Thick smoke appears to have a slight brownish tinge, but still dark gray.
0:11:55	Comment: smoke getting lighter.
0:12:08	Comment: something seems to be wrong with the CO cell.
0:12:41	Comment: Smoke definitely getting thinner.
0:13:37	Some flame barely visible in bottom of frame.
0:13:51	Color of flame is becoming apparent in lower portion of picture.
0:14:14	Flames clearly visible in lower half of tunnel.
0:15:05	Flame that is visible on floor appears to be being pushed downwards.
0:17:17	Flame burning on floor, "black out" area appears to exist in central region.
0:17:25	Flame about half way up left side, one third up right side and across floor.
0:17:30	Thick smoke may be obscuring burning on top.
0:17:43	Comment: Don't think that is burning on top.

Table 5-7: Test 5 Video Tape Synopsis - Continued

Ref. Time	Description
0:16:52	Puff of smoke obscures entire picture.
0:16:57	Burning of floor and sides appears to intensify, still no flames apparent on top.
0:17:05	Comment: Can see flame jets running along back. (These are not visible in the tape.)
0:17:10	Some luminescence appears in the central region, possible flaming.
0:17:39	Intensity of flames appears to be increasing, any flaming on top is still not visible in the smoke.
0:17:53	Flames appear to be dropping out of the smoke that is moving along the top.
0:18:02	Halo of flame appears to exist at lower interface of thick smoke layer at top of tunnel.
0:20:15	Smoke layer appears to be thinning, flames becoming visible on top region.
0:20:35	Comment: Gas burning towards the camera, not lighting the coal as just previously. Appearance is some yellow flames on coal surface, but most of the smoke appears to be luminescent.
0:21:00	Puff of smoke obscuring view.
0:21:06	Intensity on top appears to be increasing, floor decreasing.
0:21:46	Most of flaming appears to be occurring at upstream end, with luminescent smoke flowing to downstream
0:23:50	Illumination of fog apparent in central region. Largest flames in upper right corner.
0:24:23	Flames that are being produced on sides appear to be being pushed to the sides.
0:24:40	Some vortex action present, but not distinct, strongest effect appears to be that of having the flames pushed out of the way, towards the sides.
0:25:51	Sag in the top portion of the coal support frame clearly visible.
0:26:06	Some flames from floor, light flickers, but downstream of glowing portion of floor.

Table 5-7: Test 5 Video Tape Synopsis - Continued

Ref. Time	Description
0:31:13	Flames subsided it light flickers on side, still strong region in upper right side. Distinct glow in smoke has gone.
0:38:29	Smoke appears to be thickening, flames light in upper left, medium in upper right.
0:38:36	Comment: 45 Minutes
0:46:10	Flame in upper left out, flame in upper right is weakening.
0:46:25	Flame in upper right exhibits weak and intermittent counter-clockwise vortex.
0:49:03	Camera focused away from fire.
0:54:05	View of end of the fuel section. Comment: it's not burned it.
0:57:31	View of coal near ignition source. Vee pattern of flame spread is visible.

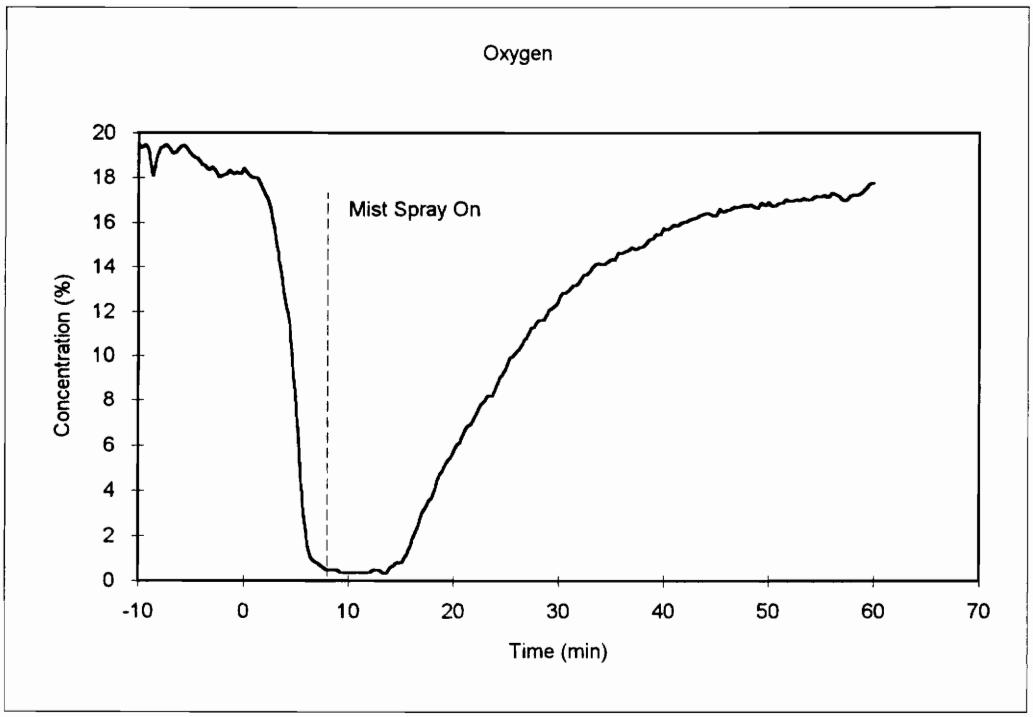

(a)

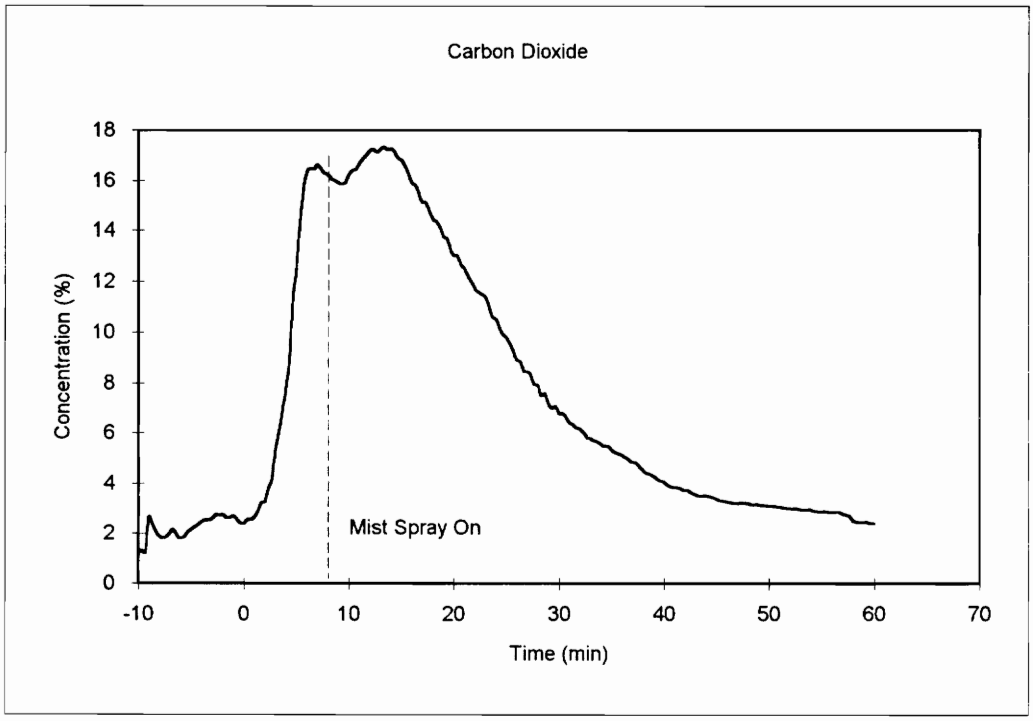

(b)

Figure 5-25 (a, b): Oxygen and Carbon Dioxide Gas Traces for Test 5.

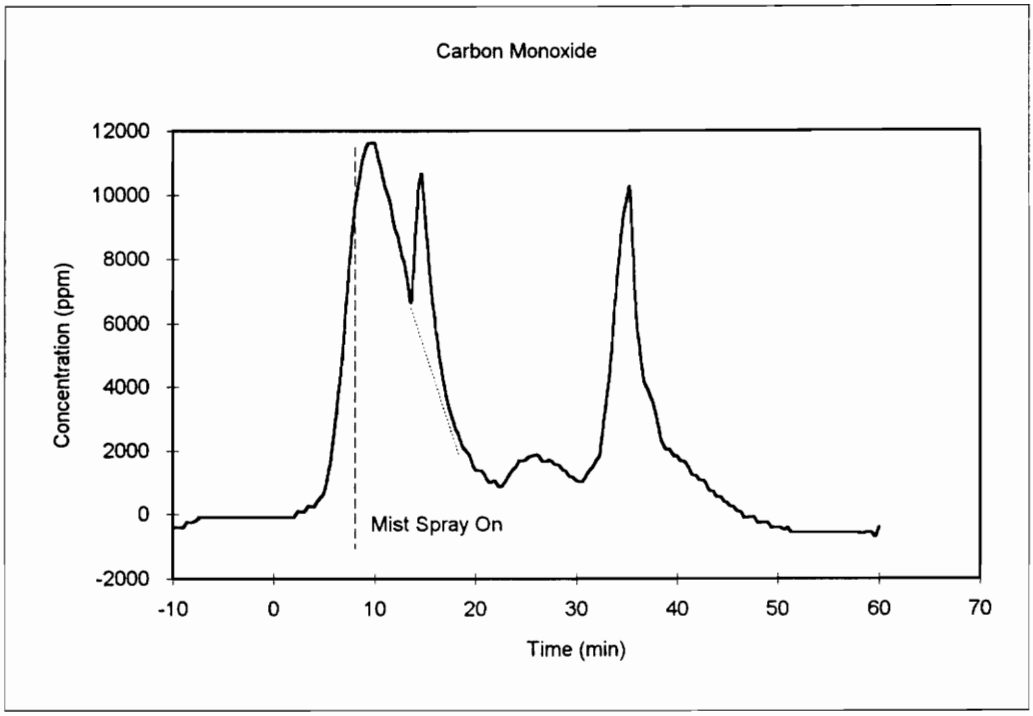

(c)

Figure 5-25 (c): Carbon Monoxide Gas Trace Profile for Test 5.

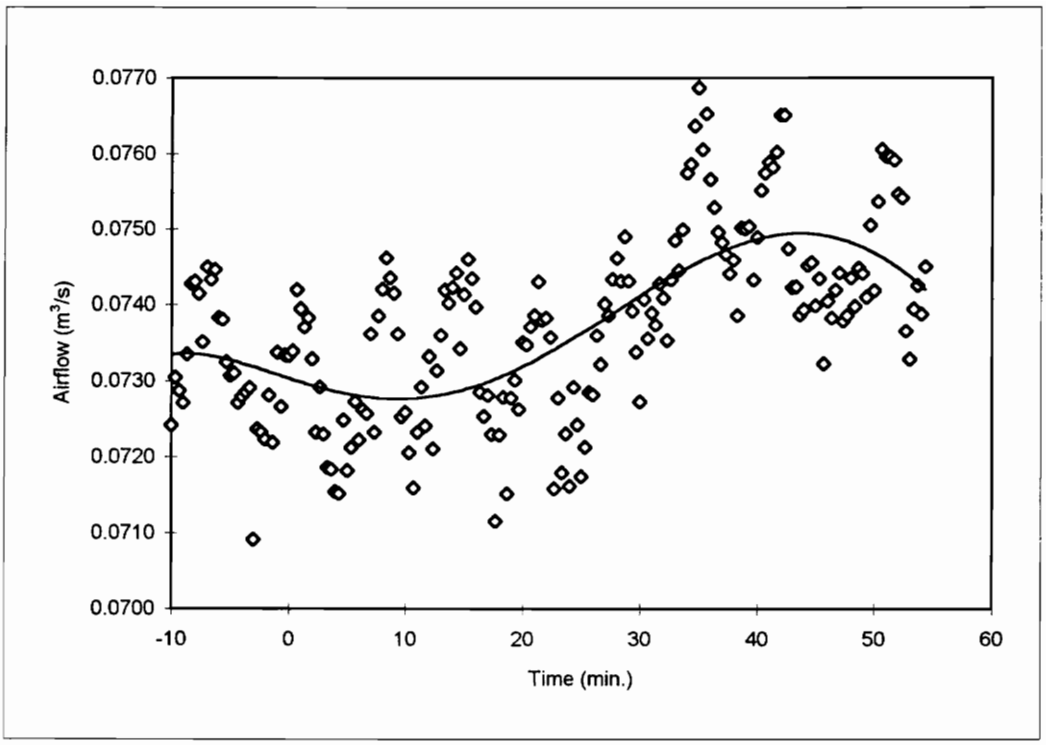

Airflow	Frequency
0.0700	0
0.0705	0
0.0710	1
0.0715	1
0.0720	11
0.0725	20
0.0730	26
0.0735	19
0.0740	36
0.0745	41
0.0750	15
0.0755	8
0.0760	10
0.0765	4
0.0770	4
More	0

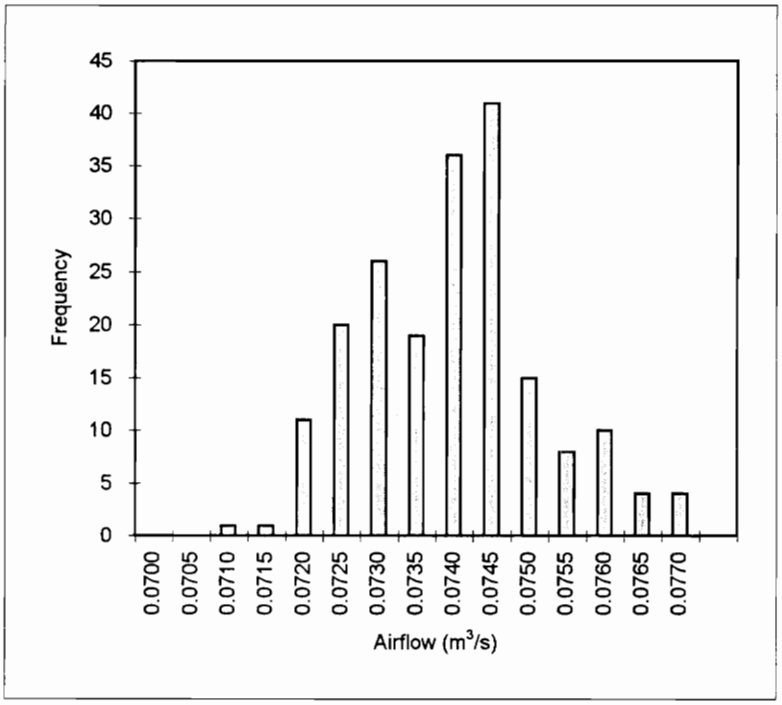

Figure 5-26: Airflow Trend and Histogram for Test 5.

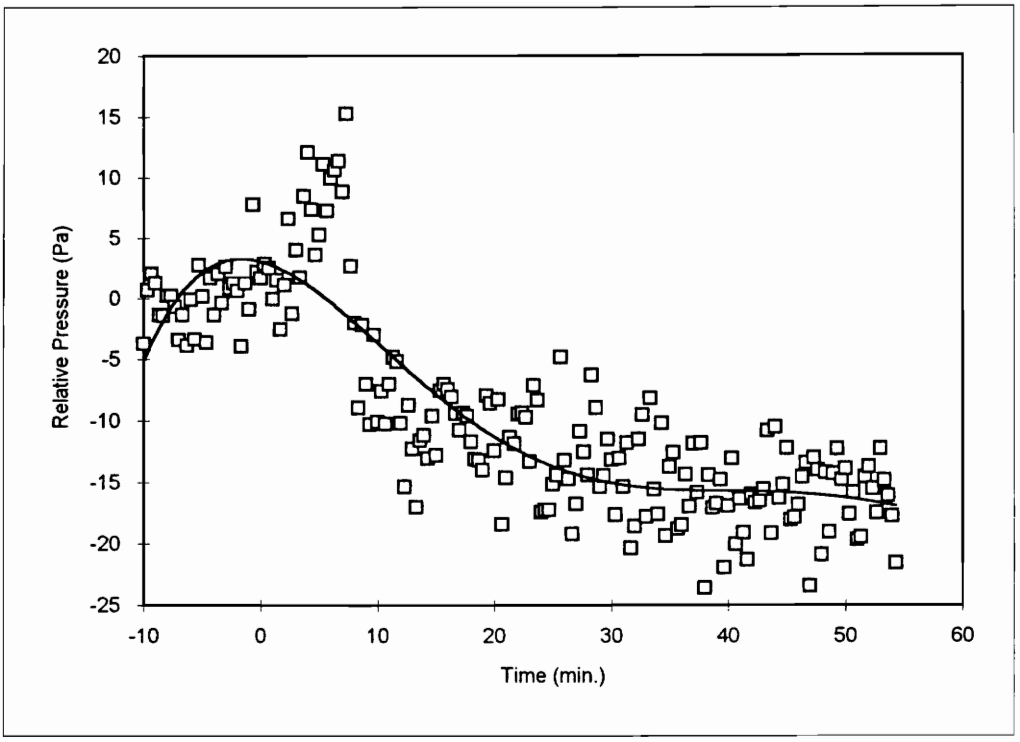

Pressure	Frequency
-25	0
-20	8
-15	45
-10	56
-5	26
0	22
5	24
10	8
15	4
20	1
25	0
More	0

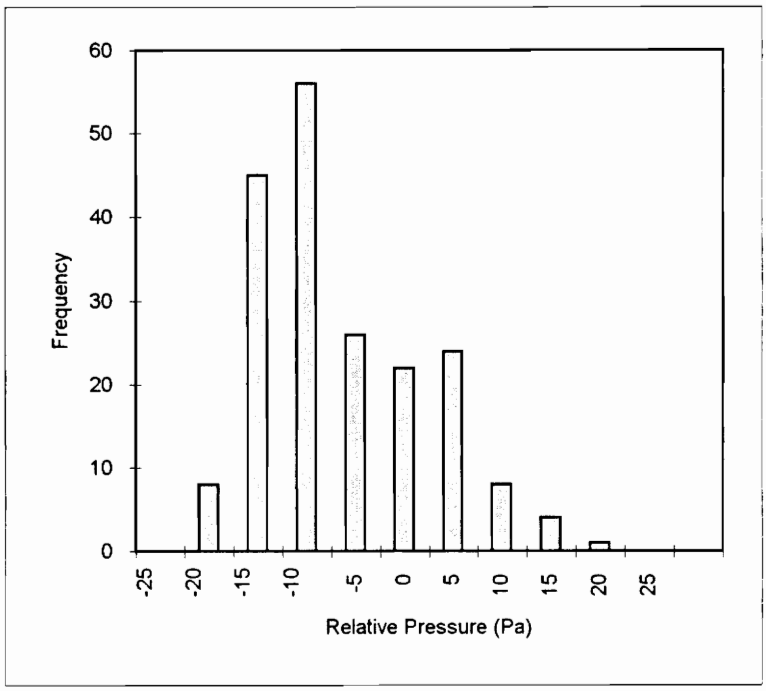

Figure 5-27: Duct Relative Pressure Profile and Histogram for Test 5.

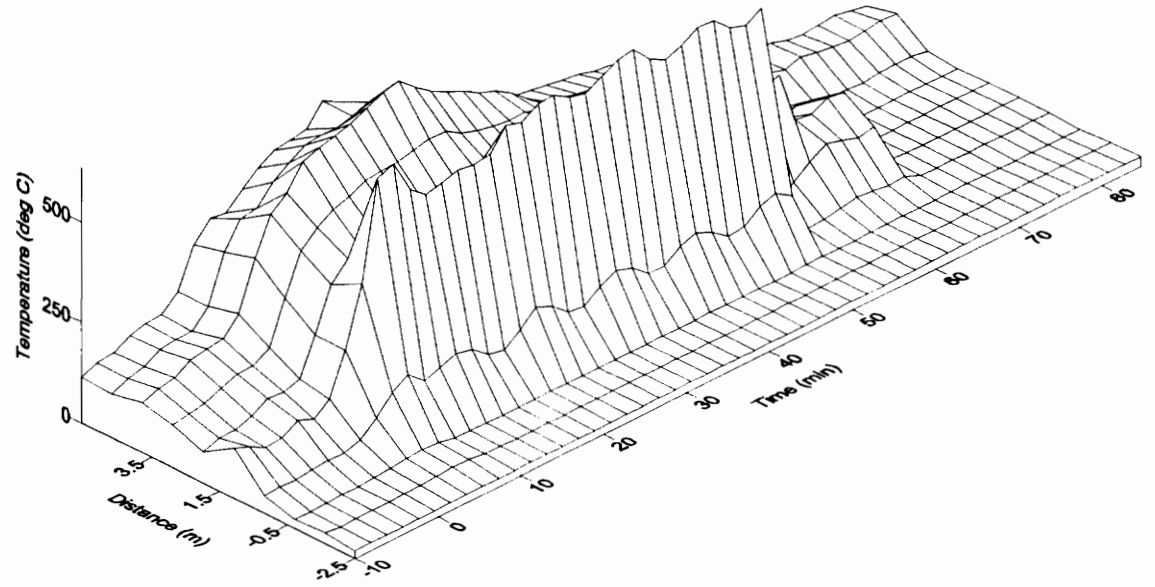

(a)

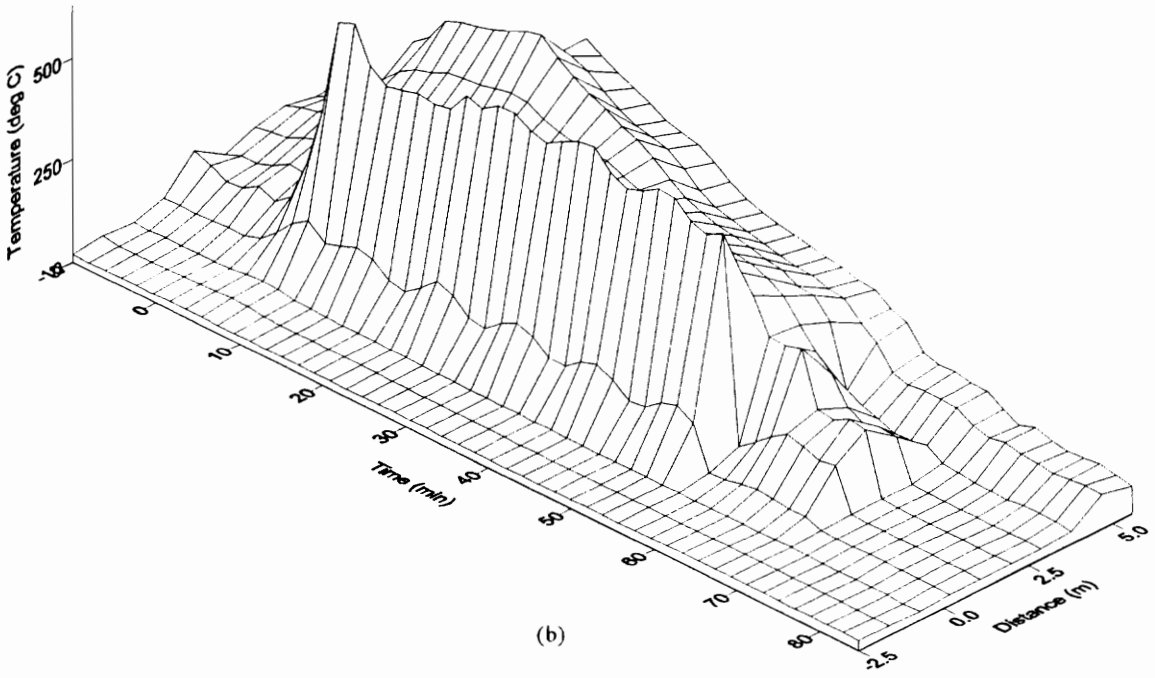

(b)

Figure 5-28: Temperature Surface Views, Forward and Reverse, for Test 5.

5.3.4. Test 7

This test was to observe the effects of the propane combustor/water vapor fire suppression system on a fuel-rich coal fire. A synopsis of the video tape made during this test is given in table 5-8. An event of specific note in the video tape is the mild propane explosion that occurred during the time when propane bottles were being exchanged at time 14-15 minutes.

This test is also noted in that several techniques were applied, in succession to attempt to suppress the fire. The first was the propane combustor combination extinguisher that was the original intent of this experiment. This device proved to rapidly suppress the fire for the period that it was active. This is based on the observations made in the video rather than gas analysis. The propane supply provided for about 10 minutes of combustor burning. The combustor flame went out at 19 minutes, the water sprays on the combustor were turned off at 23 minutes. The spinning disk humidifier was activated at about 26 minutes. At about 38 minutes water was sprayed directly into the fan inlet. All attempts to extinguish the fire were stopped at 53 minutes.

5.3.4.1. Gas Trace Profile

The gas trace profiles for this test are shown in figure 5-29. The oxygen and carbon dioxide traces show the common mirror image profile. The initial ignition of the fire is visible in the brief spike in the traces that occur at minus 6 minutes. Beginning at time zero the fire shows the two stage acceleration that has been visible in other two coal

fueled tests. The fire accelerates, dropping the oxygen concentration from 20 percent to 12 percent in the first 5 minutes, then dropping to about 2.5 percent in the next 3 minutes. The break in the slope is visible in both the oxygen and carbon dioxide curves.

The oxygen trace, figure 5-29a, shows a relatively stable concentration of about 2 percent during the period that the combustor portion of the extinguisher was active, 9 to 19 minutes. Following the extinction of the combustor the oxygen concentration increases to about 6 percent, at a time of about 23 minutes. At this time water flow to the misters in the extinguisher was turned off. The oxygen concentration shows a decrease lasting about 2 minutes, until the spinning disk system was activated. Following activation of the spinning disk system the oxygen concentration continues to increase as the fire decays.

The carbon dioxide trace, figure 5-29b, indicates a relative maximum occurring about two minutes before the extinguisher system was initiated. The drop in the CO_2 level, following the relative maxima was used to determine the fully-fuel-rich state of the fire. The concentration of carbon dioxide increases shortly after the extinguishing system was started. After the combustor portion of the extinguisher is turned off the CO_2 level drops and remains fairly stable until the misting system is initiated and the fire begins its final decay.

Concentrations of carbon monoxide, figure 5-29c, follow a pattern very similar to that observed in test 4. The profile in this test, however, does not show the extreme peak that was observed in the initial coal fueled tests. The initial growth of the CO level in this test is also similar to that observed in test 5.

5.3.4.2. Pressure Profile

The airflow trend and histogram for this test are shown in figure 5-30. The airflow trend shows a steady decrease in the overall airflow through the 40 minute time mark. A slight increase in the airflow is shown in the trendline that does correspond to the time period in which the combination extinguisher was active. This figure illustrates only the time until the water was sprayed directly into the fan. Following this action the trend indicated a marked decrease in the airflow. This was most likely an artificial condition caused by water collecting on the static pressure taps.

The airflow histogram illustrates a relatively normal distribution of the data about a mean of 0.0725 m^3/s. This data appears to be slightly skewed towards the lower flow end. In the absence of reliable data for the later portion of the fire life it is difficult to determine if the data indicates any throttling effects.

The duct relative pressure profile, figure 5-31, shows a sharp increase in the pressure during the acceleration phase of the fire. A slight drop in the relative pressure occurs that corresponds with the time that the combination extinguisher was in operation. Following the cessation of the water mist in the extinguisher the trend shows a return to the increasing relative pressure. The histogram must be interpreted based on the relationship between the range distribution and the trend data. Without additional information, the histogram appears to represent a bimodal distribution that could be indicative of throttling effects. However, the first peak in the data, about 5 Pa, occurs about an inflection in the trend and at the relative minimum at 21 minutes; the second peak, about 25 Pa is the combination of the first and second relative maxima. For these reasons the data cannot be

construed to be indicative of throttling, although the trendline shows a definite pressure trend that can be associated with changes in the fire status.

5.3.4.3. Temperature Profile

The temperature surface views for this test are shown in figure 5-32. An initial spike in the temperature, near the upstream end of the fire, indicates the first burning of the ignition source. That this source experience some decay prior to the coal igniting is evident in the saddle that is visible between -6 and 0 minutes. The action period of the combination extinguisher is visible in the hump in the temperature at a distance of -2.5 to 0 meters from the time of 9 to 21 minutes. The presence of this hump and the sharp break in the surface at the 0 meter distance is indicative of the absence of reversed stratified flow. No evidence of this condition was seen in the visual record of this test or in the field observations. This test was terminated at a time when the oxygen concentration returned to a value greater than 15 percent. That the fire was still active at this point is shown by the continued high temperatures at the end of the data set.

There is a "hollow" in the data during the time period 15 to 41 minutes that extends back to a depth of about 3.5 meters. This is due to the rejection of temperature data that was obviously erroneous, evidenced by the ridiculously high values. The duration of the elevated temperature state may be due in part to heat stored within the bricks.

Table 5-8: Test 7 Video Tape Synopsis

Ref. Time.	Description
-0:07:53	Fire has been lit.
-0:07:29	Flame from ignition source appear to be contacting top.
-0:05:20	There still appears to be some daylight in the upper right corner (viewed from upstream end).
0:08:28	Comment: 2.97% oxygen.
0:08:43	Bubble is visible in water delivery tube, indicating start-up of combination extinguisher system.
0:08:50	Mist visible through combustor.
0:08:58	Propane flame ignites.
0:09:47	Water visible pooling on floor of the fire entrance section.
0:10:57	Focus on flame in upper-left of coal section, still appears to be burning fairly vigorously.
0:11:25	Comment: Color of smoke has changed.
0:11:43	Camera being moved to exhaust end of tunnel.
0:12:09	Camera at exhaust end of tunnel, coal flames are red-orange on the lower right and left sides. Propane combustor flame clearly visible.
0:12:23	Products down stream of coal appear to have a red-orange glow.
0:13:02	Fire not visible, camera off line to fire.
0:13:33	Fire again visible as camera is re-centered.
0:13:47	Intensity of flames on sides of tunnel appears to be increasing. Combustor flames are still visible.
0:14:30	Combustor flame goes out.
0:14:31	Large puff of smoke blocks all visibility.
0:14:33	Bright orange flash down stream of the coal section.
0:14:35	Fire has rapidly accelerated with extinction of the combustor (even though the nozzles are still delivering water).
0:14:42	Large puff of smoke.
0:14:45	Some flaming visible through smoke, appears to be subdued.
0:14:48	Flame visible in combustor. Slight flame visible in coal fuel section.
0:14:50	Smoke obscures all flames.

Table 5-8: Test 7 Video Tape Synopsis - Continued

Ref. Time	Description
0:14:52	Clearing smoke reveals combustor flames and what appears to be flames accelerating along fuel length.
0:16:41	Flames appear to be increasing, but look like glowing gases rather than flames neat the fuel source.
0:17:08	Flame in combustor still clearly distinct from burning coal.
0:19:05	Most notable is the flames holding to the floor with little or no flaming on top, some flame in upper right corner, appears near the upstream end of the fuel load.
0:20:01	Flame in combustor disappears.
0:20:03	Flaming in the coal fuel section appears to have accelerated.
0:20:42	Flame appears to be moving towards the back, has expanded to cover floor and sides.
0:22:24	Appearance of dark center "hole" with bright yellow/white flames. Surrounded by reddish pink halo.
0:22:30	Comment: Water mist from combustor stopped.
0:23:09	Full circle of flames around dark central region.
0:27:34	Spinning disk spray on, intensity of flame appears to be subsiding in upper right hand side.
0:36:37	Vigorous section of flame is in lower left corner and on sides. Primarily left side.
0:40:42	No flame apparent in top coal.
0:41:12	Comment: spray water directly into the fan.
0:45:32	Fire tunnel no longer taped.

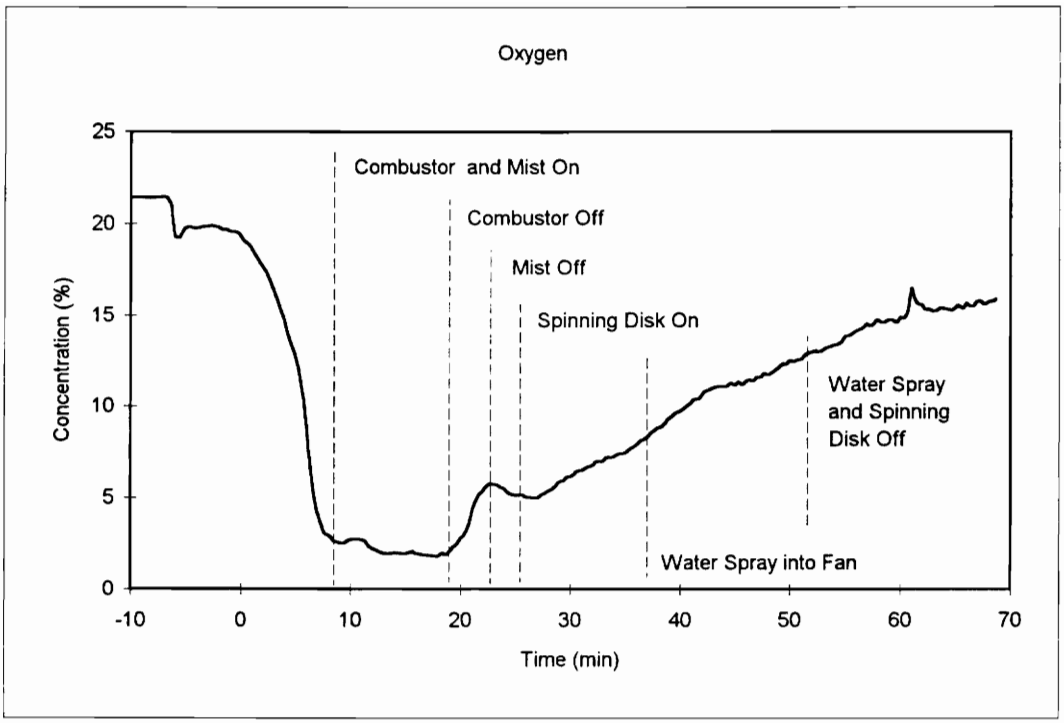

(a)

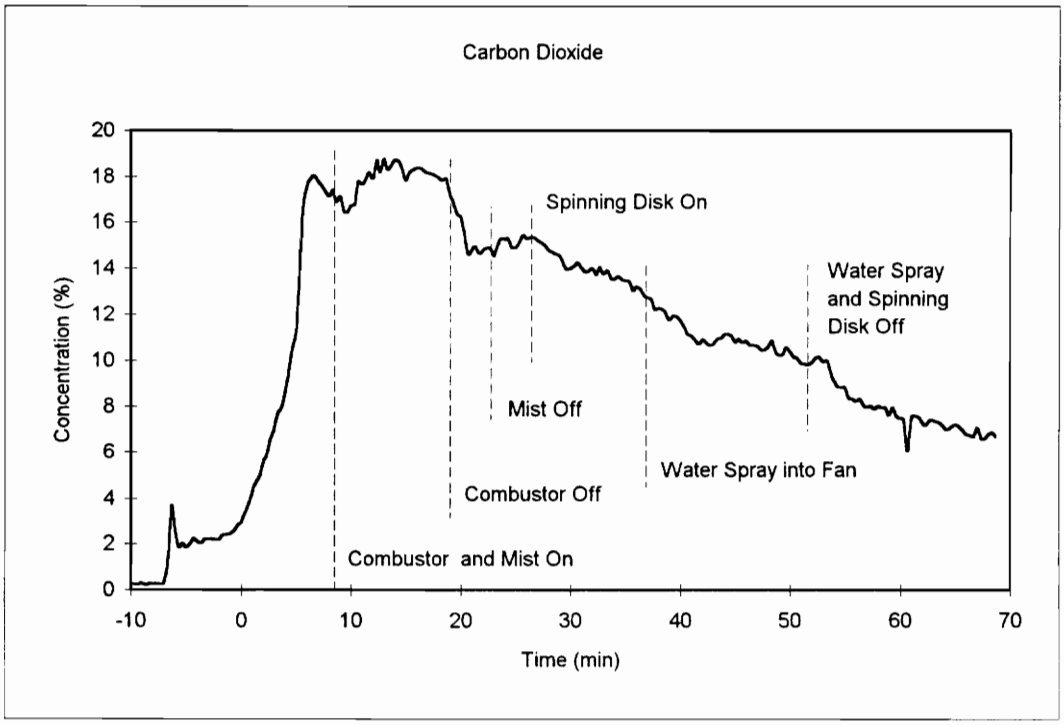

(b)

Figure 5-29 (a, b): Oxygen and Carbon Dioxide Gas Traces for Test 7.

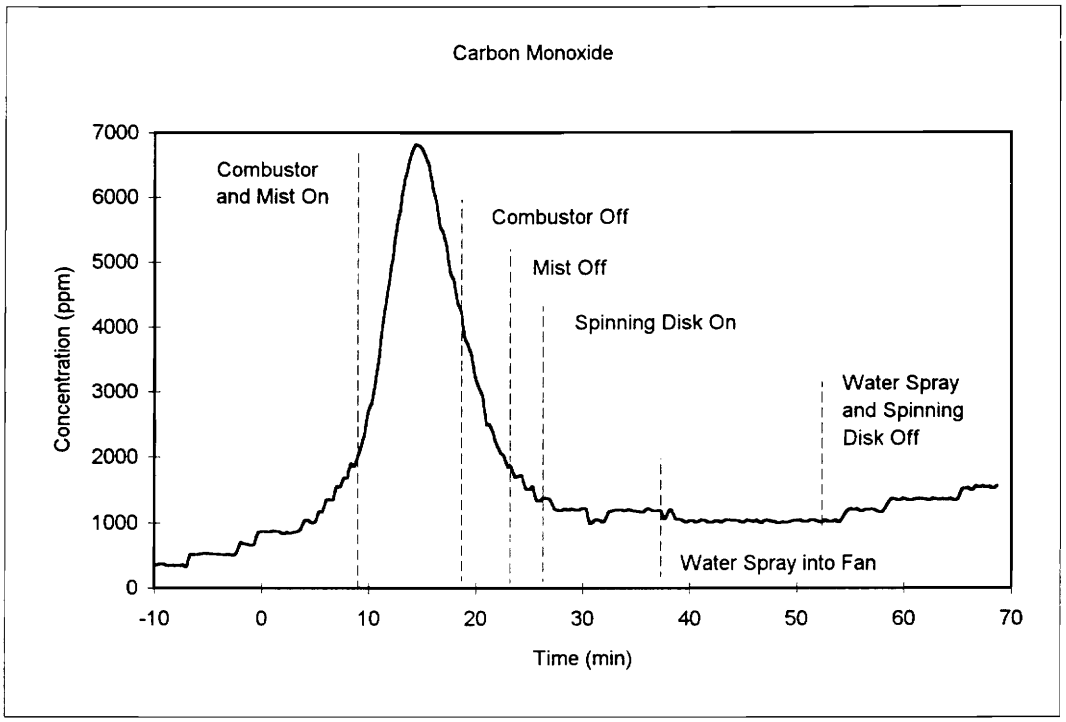

(c)

Figure 5-29 (c): Carbon Monoxide Gas Trace Profile for Test 7.

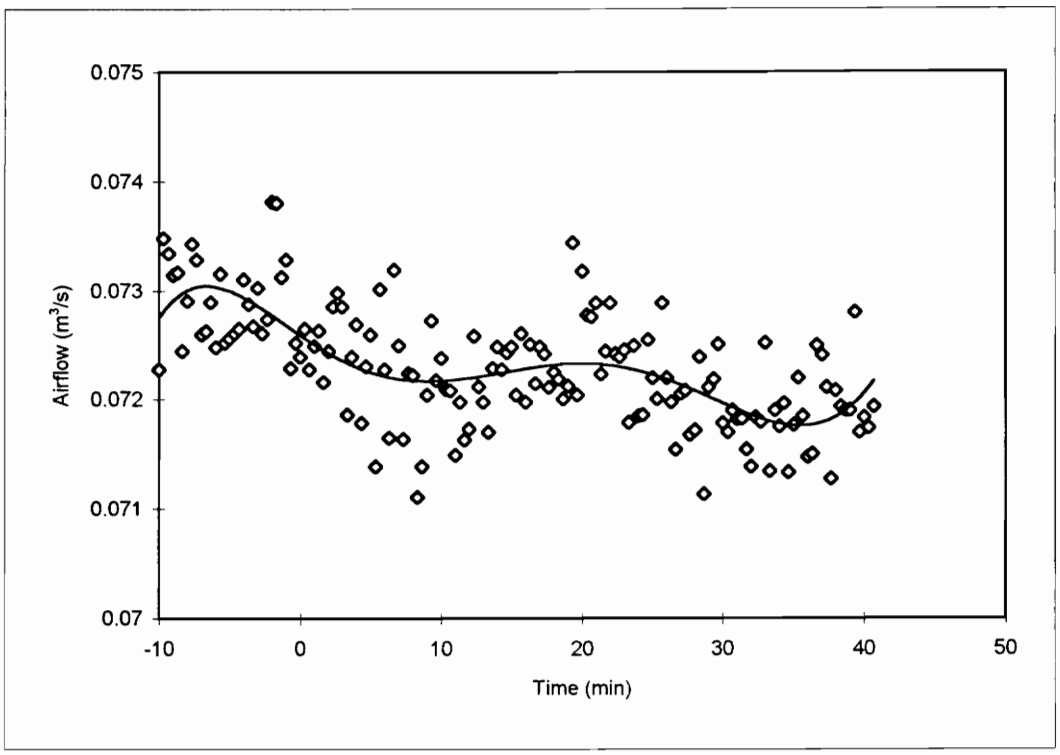

Airflow	Frequency
0.0715	10
0.072	38
0.0725	56
0.073	34
0.0735	15
0.074	2
More	0

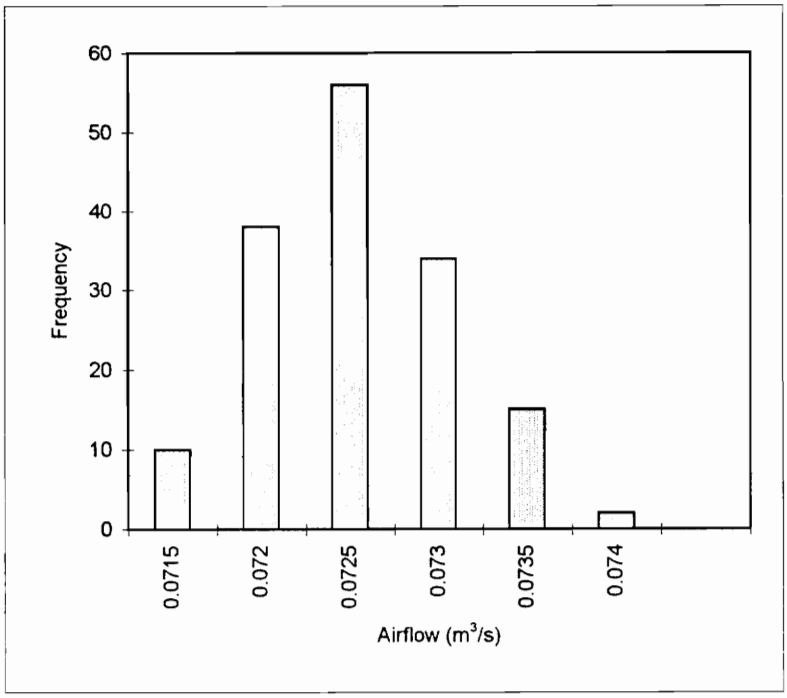

Figure 5-30: Airflow Trend and Histogram for Test 7.

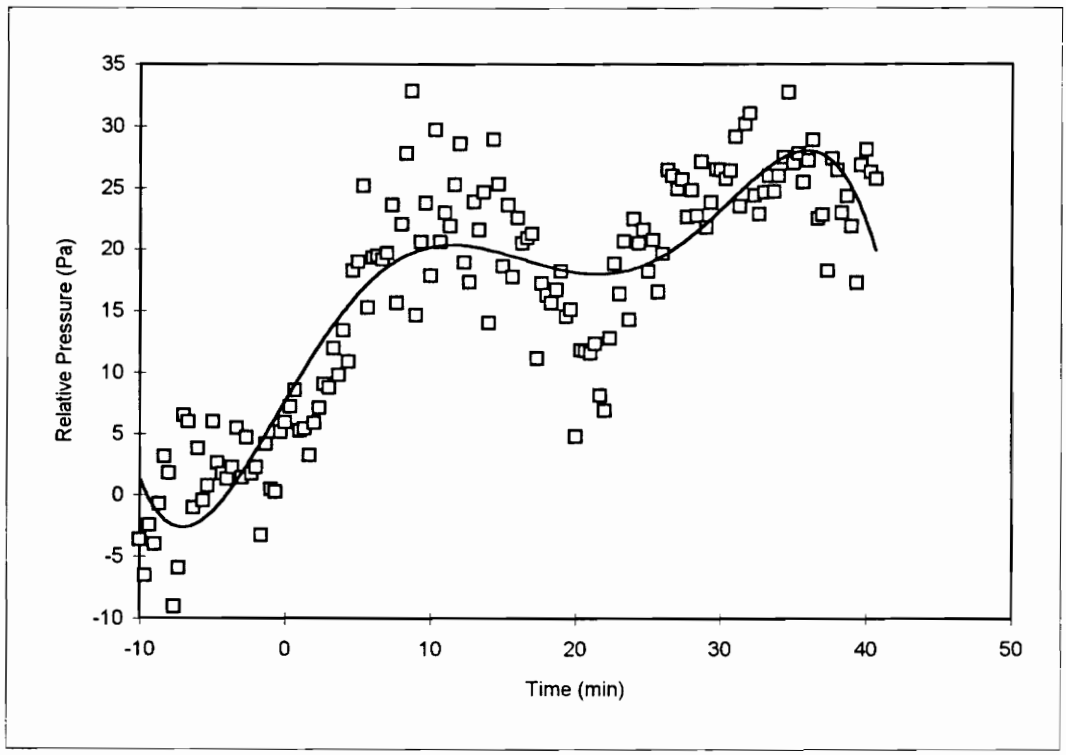

Pressure	Frequency
-5	3
0	8
5	18
10	17
15	13
20	26
25	36
30	30
35	4
More	0

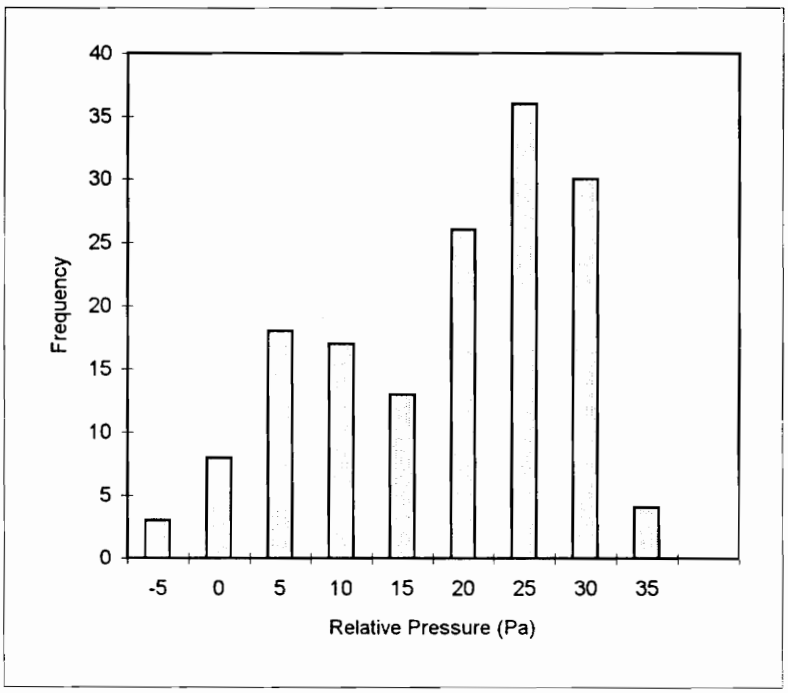

Figure 5-31: Duct Relative Pressure Profile and Histogram for Test 7.

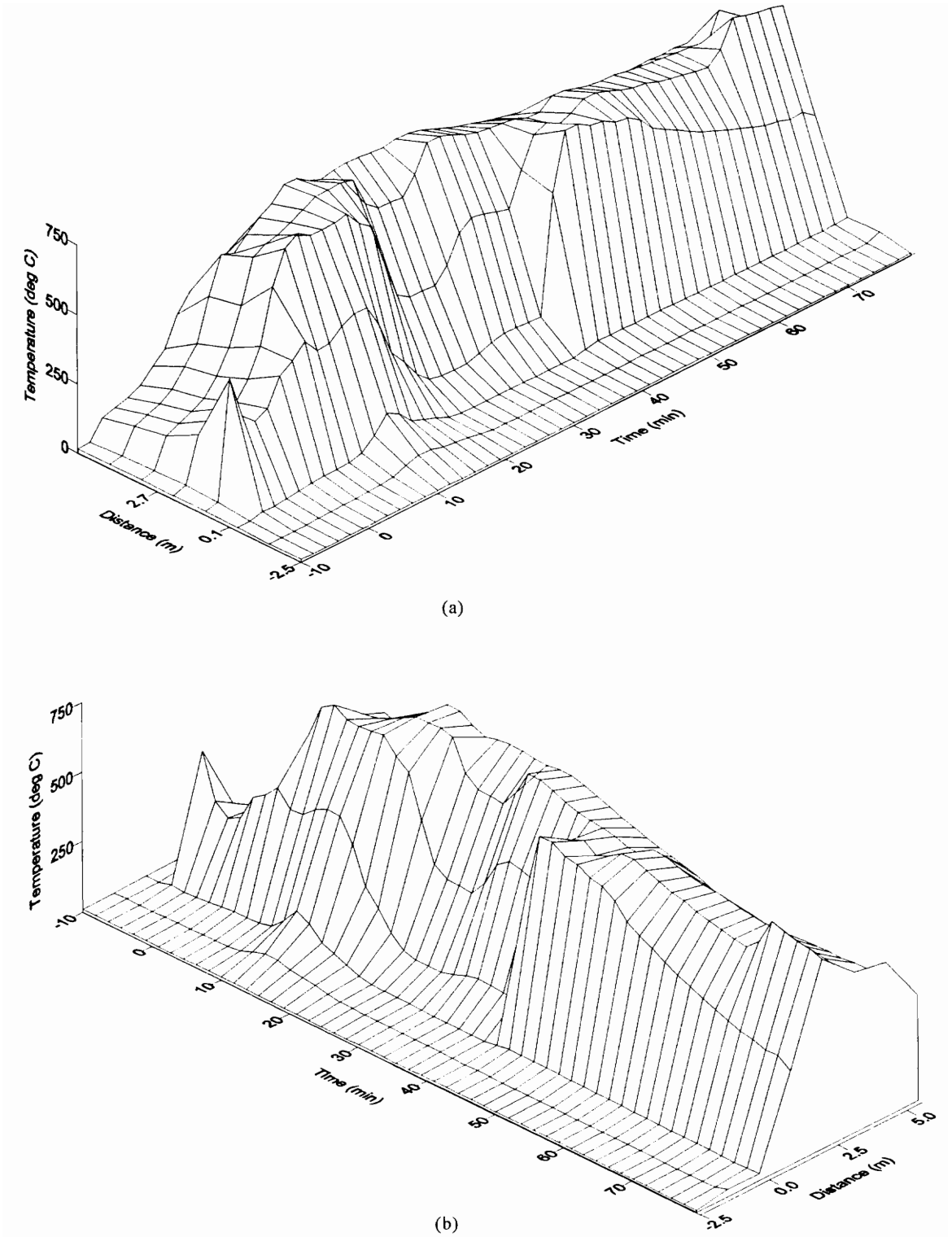

Figure 5-32: Temperature Surface Views, Forward and Reverse, for Test 7.

6. Discussion

This chapter, *Discussion*, will lead to the following chapter in which the conclusions of this research are to be drawn. Thus this chapter will be somewhat subjective in its approach to the evaluation of the results presented in the previous chapter. Based upon the general observations that have been made during the course of the documented research it seems prudent to cover aspects ranging from the development of the wind tunnel through to the fire tests. This will include the design of the tunnel, the procedures used, the data collection system, data analysis, and observations of the experiments.

6.1. Tunnel Design

The design of the tunnel was an important factor in the test program and is worthy of some discussion. Again, this will be based on the functional units of the tunnel structure.

6.1.1. Fire Section

The design of the fire section of the wind tunnel proved to be very convenient for the conduct of the tests. By having a fully opened top the fuel could be easily loaded into the

tunnel and the ash could be easily removed. The fiberglass insulation that was used as gasket material appeared to function well in restricting the leakage of fumes from the fire. An area that appeared to be a source of greater leakage was the mortar joints between the bricks.

When the lids were removed from the tunnel following the first of the coal fuel tests the gasket material was observed to have melted and fused to the fire brick. This condition shows just how hot the fire actually was. The internal temperature of the tunnel could also be seen during the tests in the glowing of the brick in the vicinity of the fires.

A mild explosion of propane gas, during the last test, proved the use of the vent immediately upstream of the fire. The vent was observed to leap about 4 inches as a result of the explosion. The vent settled back into position after the explosion had passed. No damage to the tunnel structure or facilities was observed immediately after the explosion nor at the conclusion of the test.

6.1.2. Airflow Control

The airflow control system, based on the orifice and waste gate, proved to be capable of providing a consistent and repeatable supply of air to the fire. Although a full suite of flow control orifices were designed and tested only one was used during the fire tests.

Differences in the design and field performance of the airflow control system were experienced. This condition is illustrated in figure 6-1. The case shown is based on the performance of orifice number 6, in the series. The remaining orifices exhibited similar

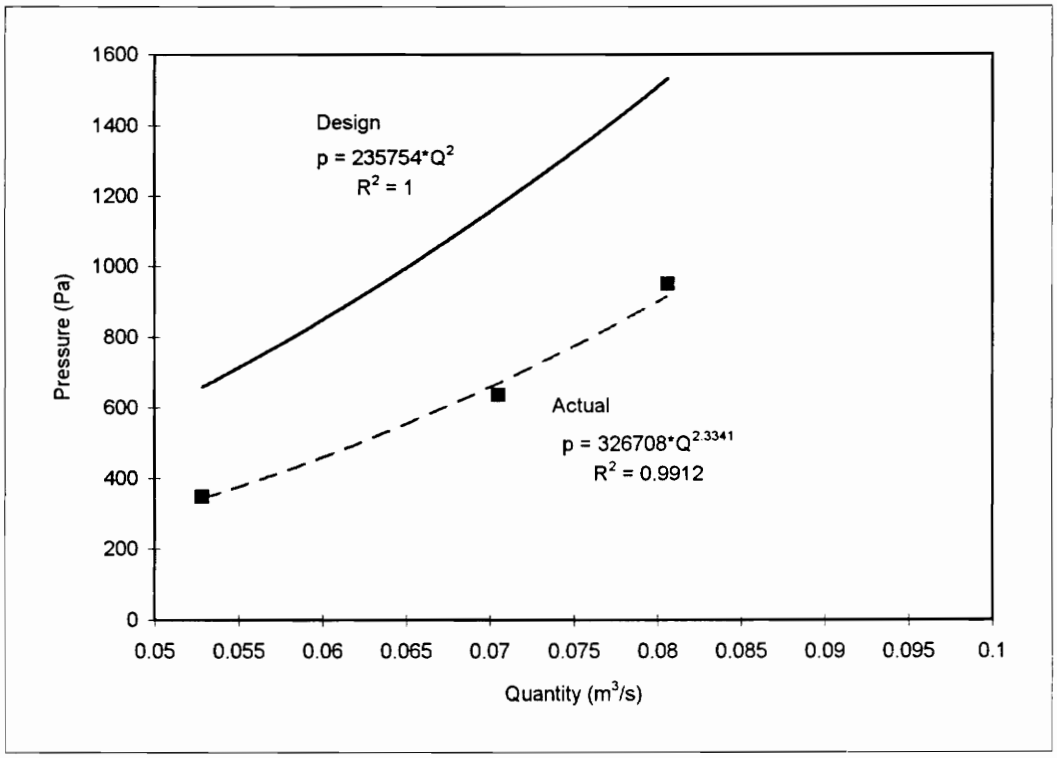

Figure 6-1: Actual and Design Pressure-Quantity Diagrams for Orifice 6.

deviations in their performance. The indication being that the characteristics of the tunnel can be predicted based upon the test data.

The airflow profiles developed during the flow quantity tests show that a relatively flat profile is developed across the duct immediately in front of the fire. A typical profile is shown in figure 6-2. All of the measurements taken show a similar pattern, including a slightly higher velocity on the right hand side of the duct. This is most likely due to acceleration of the air at the bend upstream. The peak velocity in the skewed region is about 34% higher than the mean velocity in the duct, thus v_{mean} is about 0.75 v_{max}. The impact of this condition is most likely negligible to the overall system.

6.1.3. Fogging Systems

Three separate fogging systems were used to generate the large quantities of water mist required in controlling the fuel-rich fires. Problems that were found with these systems can be associated with either the scale of the experiments or with the design of the fogging system itself. One key problem with the fog is the interaction of the mist particles with the walls of the tunnel, and the interaction of the mist with itself. During the lower levels of airflow experienced during the tests these two actions (impingement and coalescence) appeared to be significant in the reduction of the fog that could reach the fire.

The spinning disk system was initially chosen for its ability to produce a fog that is well dispersed in the desired size range. The ability to produce a relatively large quantity of fog without the introduction of additional air was also a chief consideration. In order to make

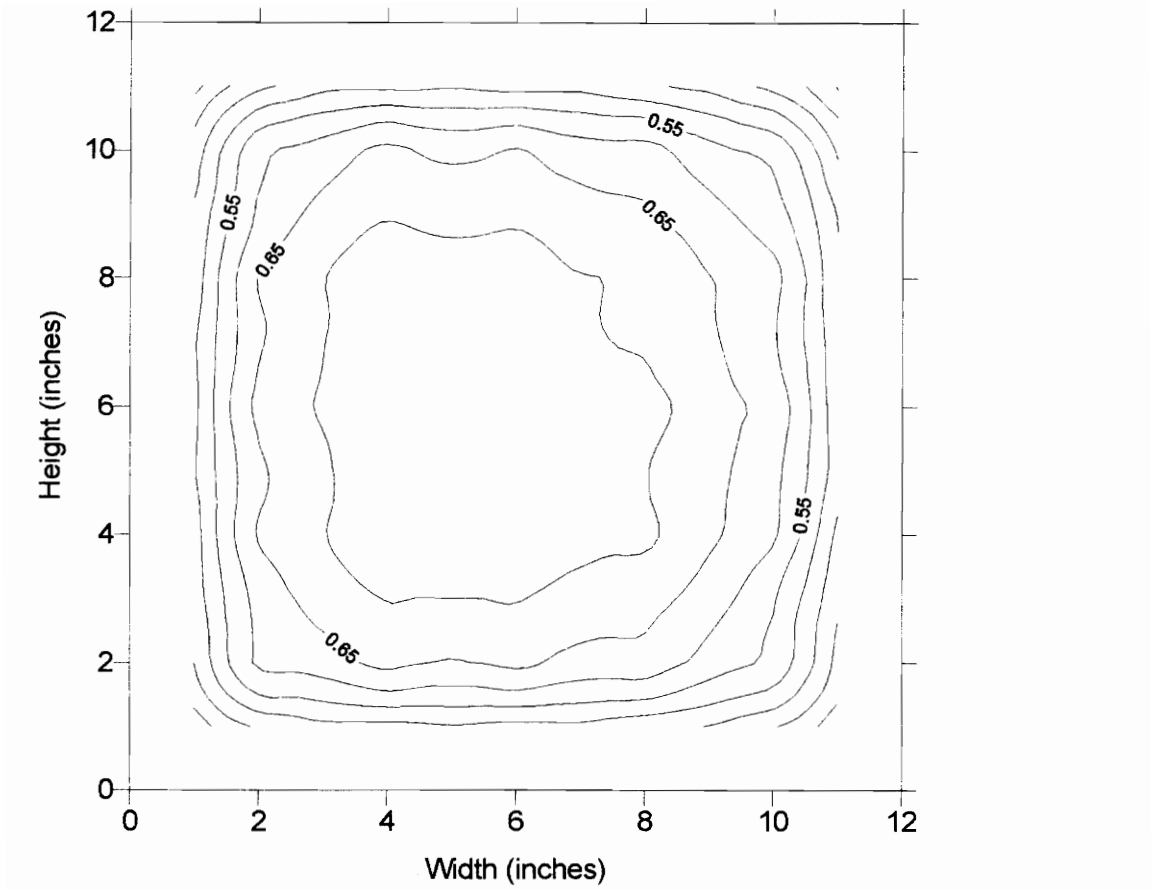

Figure 6-2: Typical Velocity Profile (m/s) - Orifice 6, Waste Gate Half Open

visual observations of the fire, the spinning disk was placed upstream of the ninety degree bend and window. As mentioned previously, in section 5.1.2, the ability of the air to carry fog decreased as the airflow quantity decreased.

Observations made during the full sized wood fire (test 3) indicated that a very large quantity of the water was being lost from the air. This reduction in the amount of water available in the fog may have attributed to the apparent lack of effect by the fog on the fire. The results from the fog system tests, for the spinning disk, indicate that under the test airflow conditions only 45 percent of the water is effectively converted to a fog. Thus, for the 0.035 kg/s (33 gph) rated capacity of the fogging system, 0.016 kg/s (15 gph) was converted to fog, while 0.019 kg/s (18 gph) ran along the floor of the tunnel to leak points.

The overall lack of efficiency in the system for carrying the fog in the tunnel entry, or mine entry for that matter, needs to be a consideration in the application of fog systems for controlling fuel-rich mine fires. This will be of particular interest if the fog must be carried over a long distance, of perhaps many hundreds of meters, under high Reynolds number conditions. The bulk turbulent flow will increase the likelihood of collisions and interaction between the water droplets. As the droplets agglomerate they will reach a point where they can no longer be carried in the air stream and will begin to "rain" out. The action of the turbulent air will increase the likelihood that the water particles will come in contact with the drift surfaces causing the water to be removed from the air by impingement.

An alternative fogging system was used for the first of the fogged coal tests. This system used an array of twelve pneumatically assisted impingement spray nozzles. The nozzles used for the test were about the smallest made their manufacturer. The bench test of the array seemed to indicate that the nozzles were effectively producing a fine mist with little loss in the jet region of the nozzle output. When the array was installed in the wind-tunnel the results seemed quite different, most probably due to the impingement of the sprays against the interior surface rather than the interaction of the individual sprays.

During the tests in the tunnel, compressed air was supplied to the nozzles with a portable compressor rather than off of the compressed air system in a near by building. The key weakness in this scheme may have been inadequate filtration of the air prior to being used by the nozzles. The air carried oil and other contaminants that could have affected the performance of the nozzles. Such an effect may have been intermittent since the systems appeared to work nominally after removal from the tunnel, when connected to the building services.

One comment regarding the application of the pneumatically assisted nozzles used in the above array, and in the combustor, which follows, is that the quantity of air required for the desired atomization represents about 0.13 % of the entire tunnel airflow per nozzle. In the case of the nozzle array the increase in airflow due to the nozzles was about 1.6 %, and in the case of the combustor about 0.52 %.

Based upon the observation that in an enclosed environment, such as the mine entry or ship's compartment, much of the effect of the water can be attributed to the displacement of oxygen, the combination extinguisher was developed. The net effect desired of the

combustor was to reduce the oxygen concentration to a level below that at which flaming combustion could be sustained. To accomplish this a propane flame was used to convert some of the oxygen to carbon dioxide and water vapor, and to produce heat for the vaporization of liquid water into water vapor. The liquid water was injected into the combustor with the same type of nozzle that was used in the above array, to be converted to a vapor.

With the combustor in operation, the combination extinguisher appeared to effectively convert much of the injected water into a vapor, at least until the bulk temperature fell below the boiling point of the water. When the combination extinguisher was tried against the wood fueled fire the flaming combustion of the wood was extinguished at the time that the propane fuel was ignited. During this test (number 6), injection of the water began after the propane flame was ignited. The fire was quickly brought back to a point where it could not rekindle, leaving much of the initial fuel load un-burnt.

Given the very positive results indicated by the rapid extinction of the plywood fire a very optimistic approach was made in the attempt to control a fuel-rich fire of coal fuel. During this test (number 7), the water spray system was initiated prior to the ignition of the propane burner. This was done in the hopes that the water spray might provide a barrier between the fire and the propane fuel prior to the ignition. Since this extinguisher consumes and displaces oxygen little evidence for the control of the fire can be gained from the gas trace data. Some of the most compelling evidence of the control that was gained over the fire is visible in the video tape. A point of considerable importance is the rapid regrowth of the fire at time 0:21:35, where 5 seconds after the combustor flame was

extinguished (to change fuel bottles) the fire has rapidly accelerated despite the continued application of water mist.

This transformation in the state of the fire was rapidly reversed when the second fuel bottle was attached and the burner re-ignited. (Following the mild explosion in the tunnel.) The effect of the combination extinguisher is visible in the gas data when one considers that the period of the fire lasts for only about 10 minutes. This is compared to 30 minutes for the baseline fire (test 4) and about 8 minutes for the purely fogged fire (test 5).

6.2. Procedures

The general procedures used during the tests are covered briefly in chapter 5 of this thesis. The discussion of the procedures here is intended to review the possible relationships between the procedures and the data that was collected.

6.2.1. Start-up Tests

The start-up tests were used to verify the design of the tunnel prior to the initiation of the actual fire tests. These tests included verification of the flow control system and the airflow profile entering the fire section.

6.2.2. Wood Fuel Tests

The wood fueled tests used slabs of pine plywood formed into an open ended box with interior dimensions of about 26 centimeters (10.25 inches) square. A piece of the

fiberglass insulation was used as a gasket between the fuel box and the brick tunnel, at the upstream end to limit the flow of air on the outside of the fuel load. During the growth phase of the fires, there appears to be tongues of flames flowing through the gap where the top piece of wood is screwed onto the side pieces. While it can be considered that the flame did in fact pass through this gap it is also likely that the flame could have been quenched by the gap. In either case the outcome of the flame is relatively insignificant compared to the growth of the fire in the confines of the interior duct.

Insertion of the thermocouples through the fuel was made with holes drilled in the wood for the placement of the couples.

6.2.3. Coal Fuel Tests

The coal fueled tests were made with lump coal of about 2.5 centimeter size (1 inch), where possible large flat pieces where used to provide a flat surface for the fire to spread upon. The lumps were held around the interior surface of the tunnel with a metal grate, folded from expanded metal grating. The inside dimension of the grate was about 24 centimeters (9.5 inches) square.

One aspect of concern with the use of lump coal versus full size slabs of coal is the increased surface area. The additional surface area would allow the fire to spread more quickly and have a greater fuel vaporization area for a given length of duct. The result of this appears to be that the fire would be more fuel-rich for a given length compared to a slab fueled fire and that the fire would burn more quickly for a given fuel load.

Efforts to ignite the coal required that a wood fueled fire be lit at the upstream end of the coal fuel. The ignition fire nearly filled the entry causing increased local air velocity for the fixed flow quantity. The higher velocity appears to have effectively fanned the flames assisting in the growth of the fire and lighting of the coal. The affect of the initial wood fire is probably of little consequence in the efforts to extinguish the coal fire as most of the wood had been consumed by the time that the extinguishing efforts were made. This fact is visible in the video tape records of each of the tests.

6.3. Data Collection Systems

The data collection system used during the testing proved to be fairly reliable in its function and ease of use. The specific strengths and weakness of the system that were encountered will be covered in more detail below.

A point of some concern with the data collection system is the rate at which sampling is performed. To evaluate a wave form it is typical to sample at a rate ten times the event period, this allows for the development of a representative wave form. During the tests performed the sample recording rate varied between 3 samples per minute and 1 sample per minute. This resulted in data sets with between 50 and over 200 valid data records. Due to the long duration of these tests relative to the growth of the fire and its transition for oxygen-rich to fuel-rich the most critical data collection period is during the growth phase. The transition from an oxygen-rich to a fuel-rich state takes about 10 percent or less of the total time of the fire life.

6.3.1. Gas Monitoring

Many of the conclusions that are drawn in this thesis are based on the gas content of the exhausts. This is due to the fact the gas concentration records, particularly for oxygen and carbon dioxide, are the most complete through the life cycle of the fire. The instruments used were basic off-the-shelf types that might be used as part of a mine monitoring system. The characteristics of these instruments have been discussed in chapter 4.2.3.1 of this thesis.

The measurement of the carbon dioxide and oxygen proved to be the most reliable of the measurements taken of the gas concentrations. The carbon monoxide measurements are affected by the fact that an extreme dilution of the sample was required to obtain a range that was acceptable to the sensor. The dilution factor that was finally used for the coal fires was 500 times. This extreme dilution magnified one problem that was found concerning the low end calibration of this sensing unit. The unit zero was calibrated against ambient air in a machine shop, when the unit was taken to the outside the zero seemed to drift downwards so that ambient conditions were indicated as a minus concentration. With the diluent added the resulting indicated carbon monoxide concentration varied between -500 and -1000 ppm. This fact is relatively insignificant compared to the peak values of carbon monoxide that approached 35000 ppm during test 4. The trend in the concentration of carbon monoxide during the test is clearly visible, despite the off-set induced by the shift in calibrated zero.

Measurement of methane concentration was inhibited by the type of cell that was used. The pellistor cell requires oxygen to be available for the catalytic oxidation of the methane and combustible gases that are being measured. Clearly when the fire was in a fuel-rich

regime measurements of the combustible gases could not be made with the pellistor cell. In test 4, prior to the demise of the methane cell, a peak is shown in the methane concentration that correlates with the peak carbon monoxide concentration. It is unclear what may have affected the readings indicated by the sensor. The calibration of the methane sensor could not be checked following this test, nor could it be calibrated in later attempts after giving the sensor time to relax. Clearly the sensor had been excessively poisoned during test 4, and perhaps was affected by the previous tests.

Should further testing be desired, with the application of methane measurements, the gas sample should be diluted with fresh air prior to introduction to the sensor. This could be done with a mixing system similar to that used for the carbon monoxide measurements. One consideration is that a separate vacuum pump would be required to facilitate this. The actual sample could be mixed with the fresh air and measured prior to passing through the pump, or the pump could be used to move the fresh air into the system mixing with the sample that has been drawn through the carbon dioxide cell (as is currently configured). Another alternative is the use of compressed air, this would be restrictive based on the pressure capacity of the metering system and would require in line filters to remove water and oils from the air.

The development and decay stages of each of the fires are clearly evident in these data. The carbon dioxide traces, in the coal fires, also provide the indication that the fire has become truly fuel-rich, evidenced by the drop in carbon dioxide (in favor of carbon monoxide).

6.3.2. Temperature Measurements

The measurements of the temperature were taken with J-type thermocouples, that is Iron-Constantan type. Thermocouples of this type are usually rated to a maximum temperature of 1200°C. The couples were located on the centerline of the tunnel about 2 centimeters below the top inside surface.

One problem that was found with the thermocouples was that they did not seem to provide an accurate temperature reading as the fire was directly in contact with the couple. Based on the assumption that the adiabatic flame temperature for most hydrocarbons is about 2500°C, the couples may be affected by the direct contact with the flame. Since the measurements did provide data that was obviously in error much of the data over 1000°C was rejected from the each data set. When the remaining temperature data was plotted as a surface across depth and time a fair representation of the growth of the fire remained.

These surfaces do seem to provide fair and reasonable indication of the location and intensity of the fire.

Some of the thermocouples appeared to have been affected by the positioning during the tests. During one of the tests a thermocouple exhibited a highly delayed reaction to warming. Since this particular couple was downstream of the fire it is likely that it had slipped up between the bricks on the lids, thus it was indicating the heating of the bricks rather than of the air. During the second coal test one of the couples appears to have been in contact with a piece of the coal fuel. Indications for this condition are a delayed reaction in the elevation of the temperature, and the later readings of temperatures well

above the valid range. The later being an implication that the couple was in direct contact with the flame, meaning that is was not caught between two of the bricks.

6.3.3. Pressure Measurements

The pressure measurements were made across the metering orifices with static pressure tubes set at the centerline of the duct. The pressure drop across the orifice proved to be a consistent measure of the airflow, based on the results of the start-up tests of this part of the system.

A weakness of the pressure measurement system is clear in the records of the duct static pressure. This measurement can be used as a relative measurement to observe changes in the system status even if the true magnitude of the change is not evident. Had the measurements of the duct static pressure been an accurate representation of the true physical state then all of the data would have a positive value; a simple fact of having a forced ventilation wind tunnel.

6.3.4. Video Tape and Photographs

The use of video tape and photographs of the fire tests provides a record of the experiments that can allow for a degree of subjective analysis after the fact. The general application of a video record provides a continuous record of the visual observations, to the degree that the fire is visible. Photographs, on the other hand, provide a sequential record of moments during the test. Both of these systems allow for the repeated observation of the growth and decline of the fire.

Unfortunately the nature of the experiments precluded having the cameras immediately adjacent to the area of interest. Downstream viewing of the fire was hampered by the thick smoke; observation of the upstream conditions during fogging was prevented by the total opacity of the fog. Despite the obvious limitations of trying to film the fires the visual records of the fires appear invaluable in the permanent records of the tests conducted.

During most of the experiments, photographs of the fires were taken through a number 12 filter. This filter blocks much of the green through violet spectrum and is typically used in visible light aerial photography to cut through haze. During the experiments the filter was used to reduce the blue and green contamination in the pictures so that the reds and yellows from the fire would stand-out against any background. Photographs obtained by this method are illustrated in plates 5-1 and 5-3.

6.4. Data Analysis

Perhaps one of the most difficult aspects of the thesis is the data analysis. It is entirely arguable that the conduct of only seven tests can hardly be used to prove or disprove the concept of the effect of water mist on a fuel-rich fire. Furthermore, the fact that four of the seven tests were applied to wood fuel hardly qualifies them as applicable to coal fires.

These arguments can be seen as the justification for the discussion section of this thesis.

A very compelling argument of the acceptance of the conclusions that can be drawn from the data pool is the consistency in the development stages of the fires. All of the fires in the tunnel exhibit very similar growth patterns, including the noticeable acceleration as the oxygen concentration falls below 12 percent. The existence of this point is consistent with the findings of Roberts and Clough (1967a).

6.4.1. Gas Analysis

An interesting analytical procedure is to observe the slope of the gas traces. Ideally this is the first derivative of the trace profile, however, for simplicity the slope between two successive data points was used. The resulting line was further smoothed by using a five period moving average. The results from test 4, the baseline coal fire, are shown in figure 6-3. The oxygen trace profiles, figure 6-3a, show the rapid growth of the fire and the transition between the oxygen-rich and the fuel-rich regimes, occurring at a time of 6 minutes, as the concentration drops below 12 percent. At this point the change in concentration moves from about -2 % per minute to -6 percent per minute.

Once the fire has reached a fully fuel-rich stage, the oxygen comes to a steady state value. As observed during this test it is somewhat below 0 %, a physical impossibility. The recording of this condition may be due to one of two factors, either a calibration error or the interaction of an unknown species on the oxygen sensor. The post-test calibration check revealed no significant drift in the set points for the instrument, however, this does not rule out the role of the calibration set points.

At a time of about 35 minutes the oxygen concentration begins a steady rise as the fire begins to decay. The exponential character of this portion of the curve seems to indicate that the fire makes a relatively quick transition away from the fully fuel-rich stage to allowing some unreacted oxygen through the fire zone. However, the final demise of the combustion process is slow as the fire ultimately burns through the glowing phase.

The carbon dioxide traces, figure 6-3b, show a similar growth profile as the oxygen traces. Of particular interest in the carbon dioxide trace is the relative minimum that occurs in conjunction with the total depression of oxygen (see figure 6-3a). This characteristic in the carbon dioxide concentration can be expected when one considers that this gas is the result of oxidation of carbon monoxide. While the fire is fully fuel-rich there is insufficient oxygen available to fully oxidize the carbon monoxide that is produced, thus the concentration of carbon dioxide should have a relative minimum that corresponds to the peak levels of carbon monoxide.

When the carbon monoxide traces, figure 6-3c, are reviewed the expected peak value is found to correlate to the relative minimum in the carbon dioxide trace. The fact that the concentration trace exhibits a spiked peak, rather than a steady state value, may indicate that the fire did not reach a steady state of carbon monoxide production. If this was the case, it is possible to surmise that the fire section did not provide an adequate fuel supply due to two possible factors. First, there was an insufficient mass of fuel available.

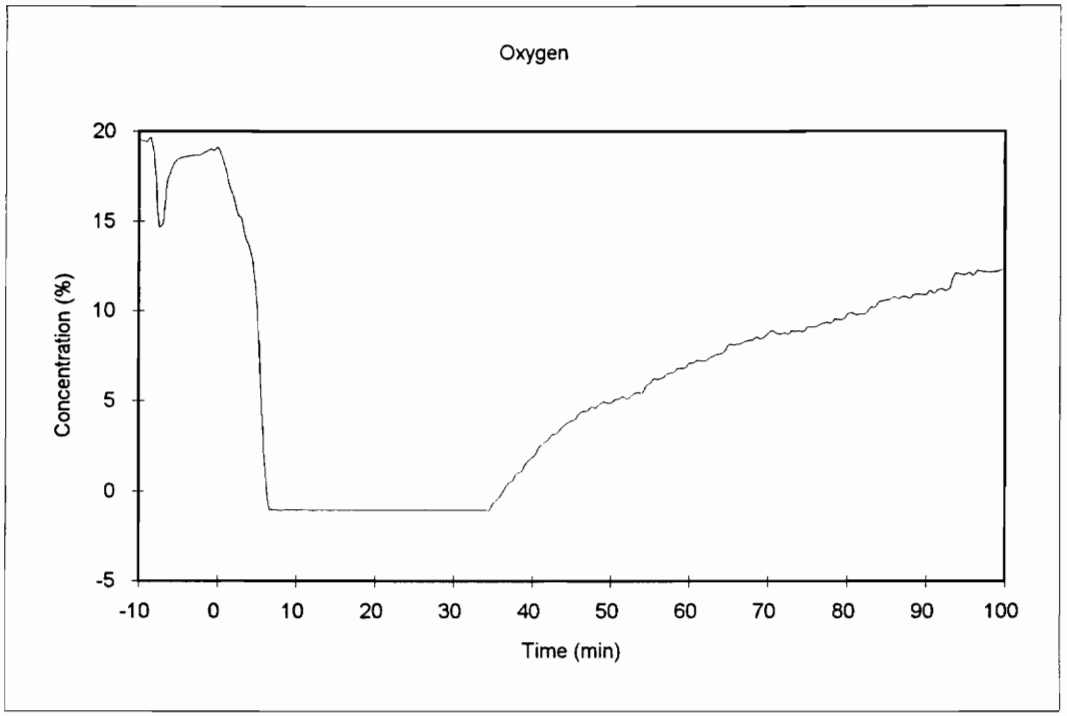

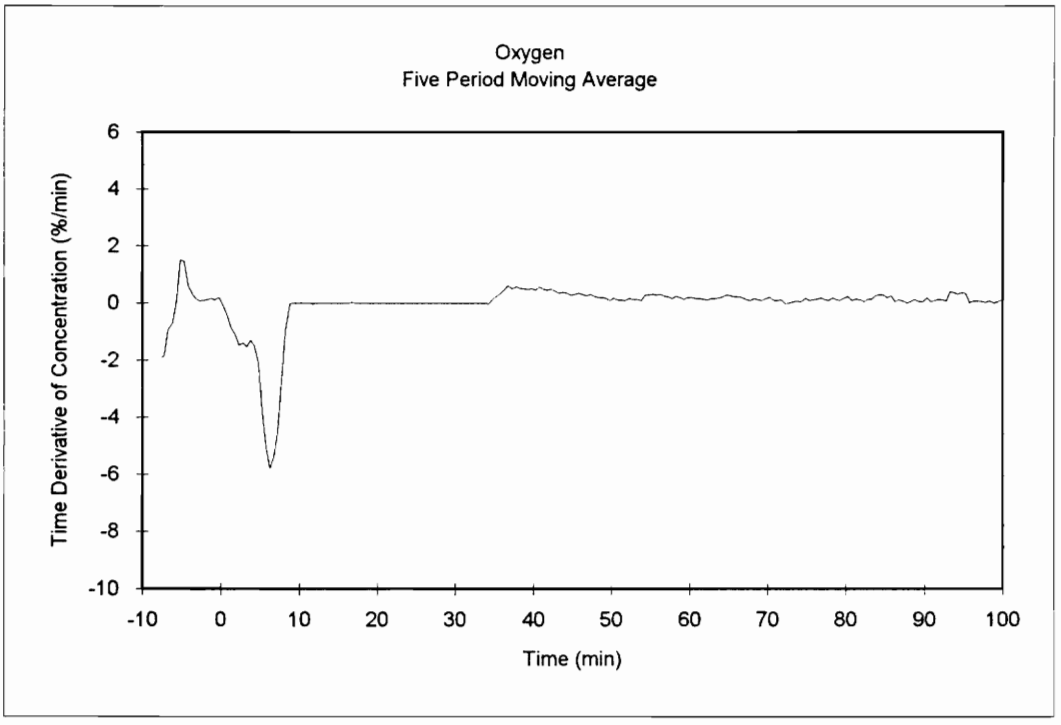

Figure 6-3a: Oxygen Trace and First Time Derivative for Test 4.

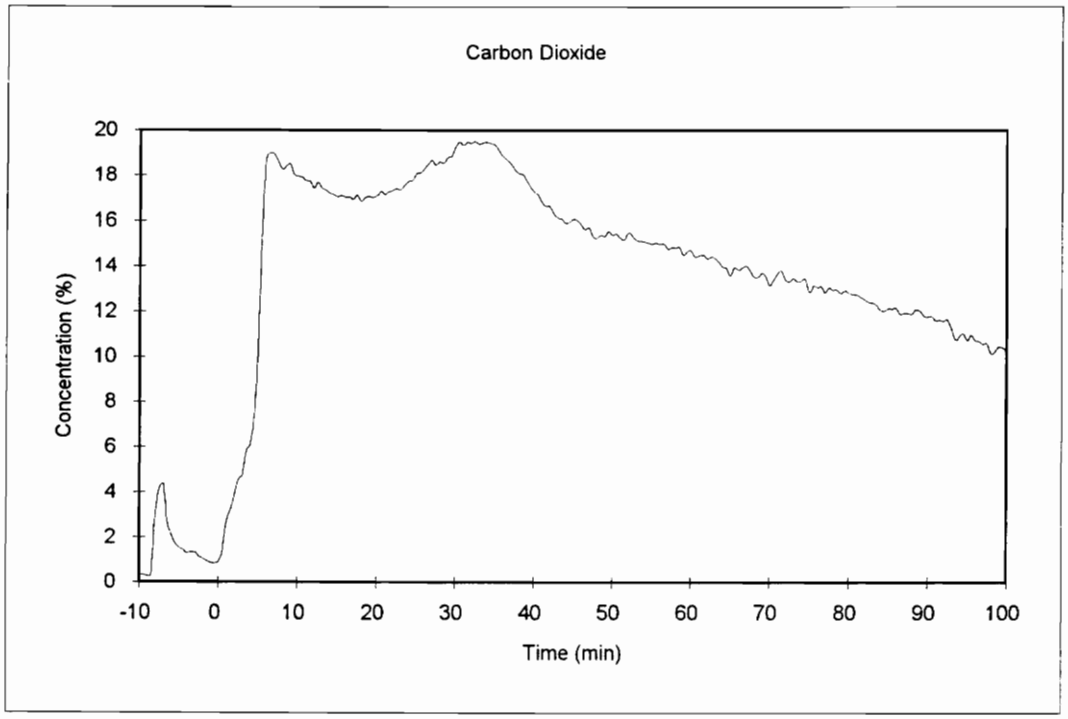

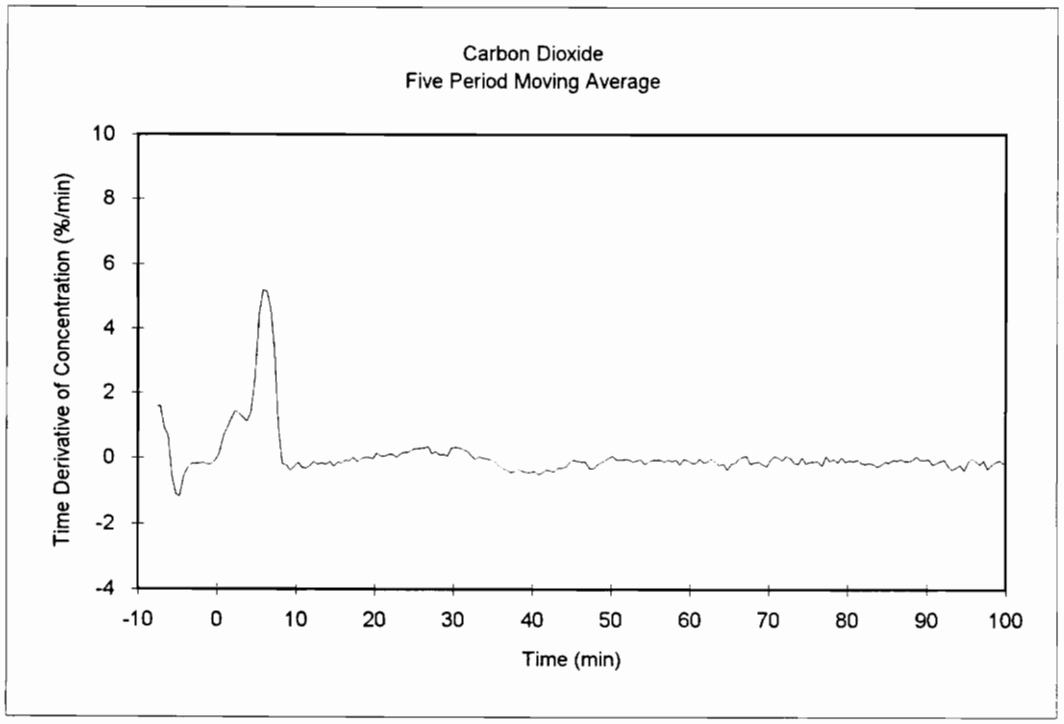

Figure 6-3b: Carbon Dioxide Trace and First Time Derivative for Test 4.

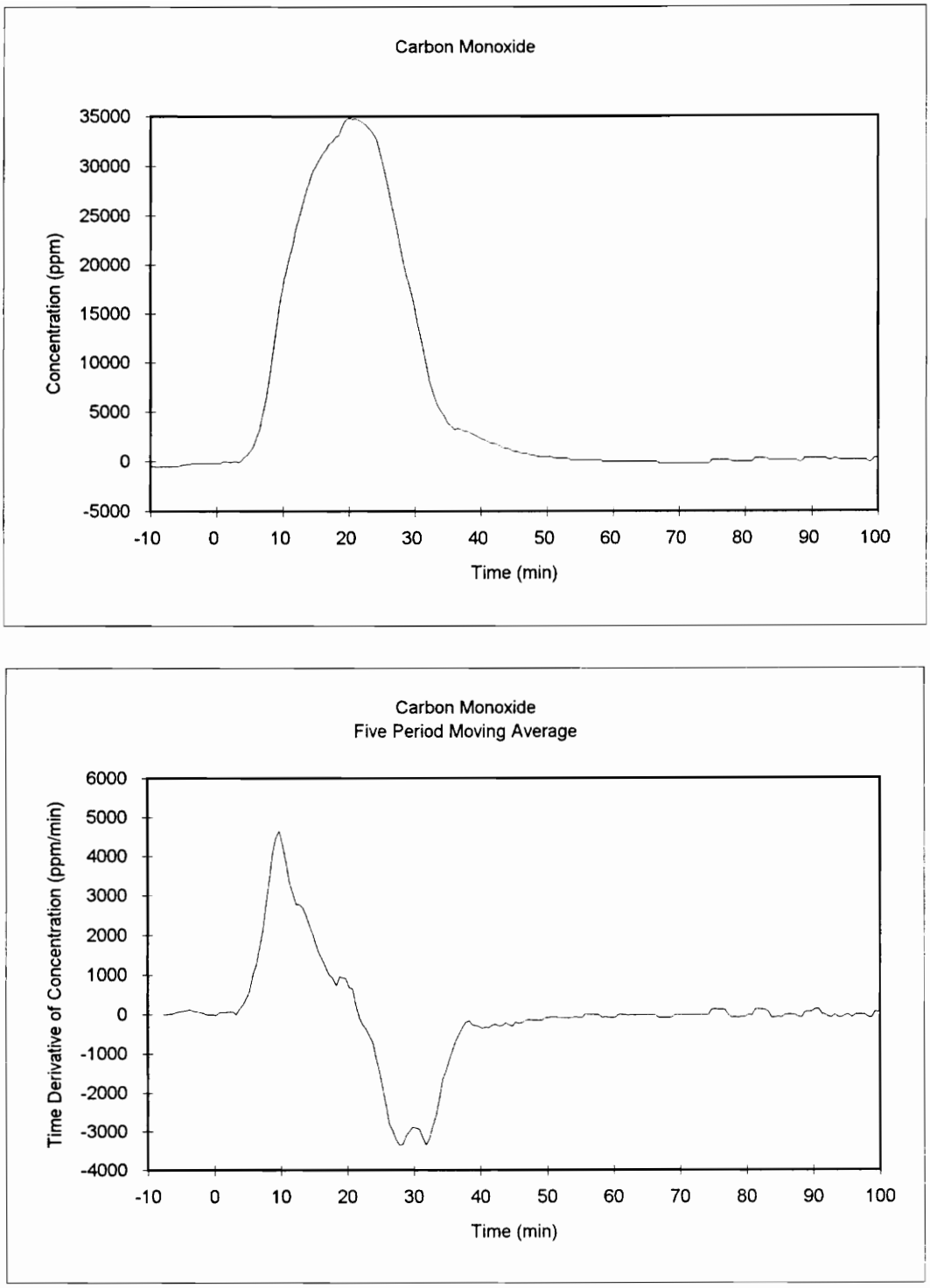

Figure 6-3c: Carbon Monoxide Trace and First Time Derivative for Test 4.

Second, there was insufficient surface exposure of the available fuel. The second case is unlikely since lump coal fuel was used, rather than slabs of coal. If there was an insufficient amount of fuel available this would indicate that more of the tunnel would need to be fuel lined, beyond the 8-1/2 diameters used during testing. It is unlikely that an addition 1-1/2 diameters, to a total of 10 as originally designed, would be sufficient. In order to obtain the steady state carbon monoxide production, further testing should consider a fuel load of as much as 20 diameters of the tunnel. (Perhaps even as much as 30 diameters, as suggested by Roberts (1971) as the length of the pyrolysis zone of a fully developed fuel-rich fire.)

The results of the first time derivatives during test 5, the fogged coal fueled fire, are shown in figure 6-4. The oxygen traces, figure 6-4a, shows the rapid growth of the fire. Although the transition from an oxygen-rich to a fuel-rich regime occurs at about 12 percent, it is not as pronounced as that observed in tests 4 and 7. The oxygen concentration reaches a steady-state value just above 0 %. This condition lasts about 8 minutes, at which time the oxygen concentration rapidly increases, in an exponential profile as the fire decays. The initial increase in the oxygen concentration, at a time of 16 minutes, occurs about 7 minutes after the water sprays have been turned on. The duration of the total oxygen depression in this test, 8 minutes, is less than one-third of that observed in the baseline test, 30 minutes. Furthermore, the oxygen concentration in this test reaches 15 percent at least 80 minutes sooner than the baseline test, following the initial increase in oxygen concentration.

The carbon dioxide traces, figure 6-4b, show the decreasing concentration as the fire becomes fully fuel-rich. This point was used as the indication that the conditions desired

had been achieved, and the water sprays could be initiated. There is a brief lapse between the water sprays being started and a reaction by the fire. The reaction observed in these traces is an increase in the concentration of carbon dioxide. The final decay of the carbon dioxide concentration occurs in conjunction with the increasing oxygen concentration, indicating the decay in the fire intensity.

Two possible explanations for the increase in carbon dioxide following the initiation of the water sprays can be presented. First, that the amount of fuel available is being decreased, that is the water sprays are effectively working against the fire. Second, that water is undergoing dissociation, with a net increase in the available oxygen to support oxidation of carbon monoxide. Although this case may be a factor, the dissociation of water is endothermic (about 27214 kJ/kg) and would be occurring very close to, or in the flame structure, therefore have a quenching effect. It can be noted that the dissociation of water becomes appreciable at temperatures exceeding 1300 °C (Keenan, et al. 1969).

The carbon monoxide trace, figure 6-4c, indicates a pattern that is very similar to that experienced in the baseline test. The peak level of carbon monoxide is about 1/3 of that seen in the baseline test, however, the levels are very similar based on the fire growth. The concentration when the water sprays were started was about 10000 parts per million, at a time of 9 minutes, in the baseline test the concentration at 9 minutes was about 9000 parts per million. The trace of this tests shows a decreasing slope following the initiation of the water sprays. The beginning of the drop in carbon monoxide concentration correlates to the increasing carbon dioxide at a time of 10 minutes.

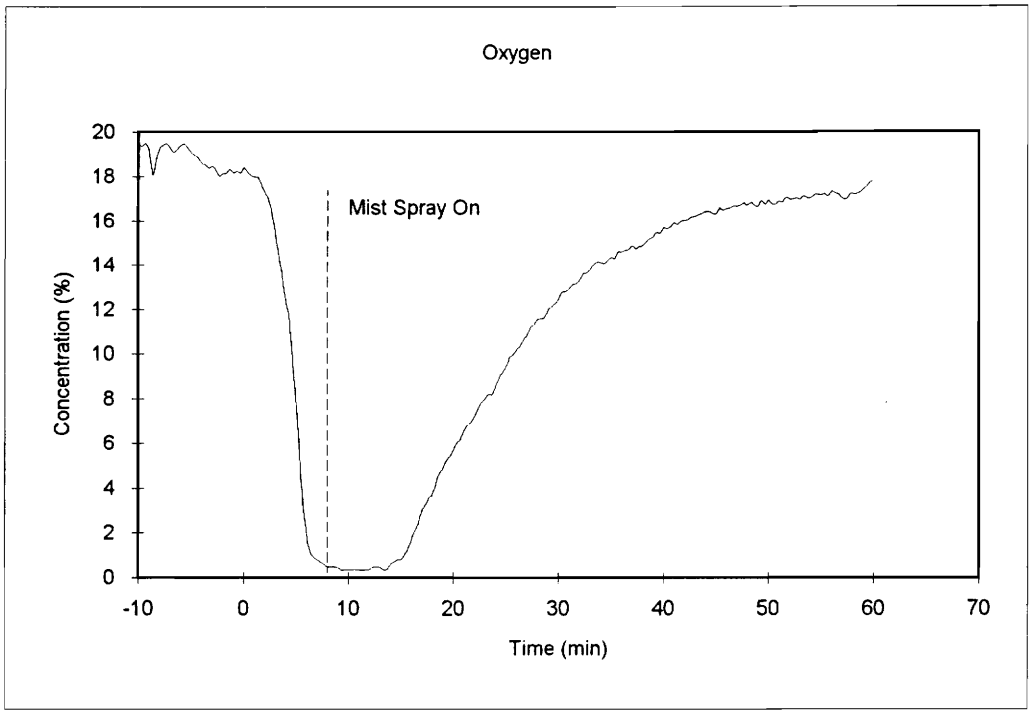

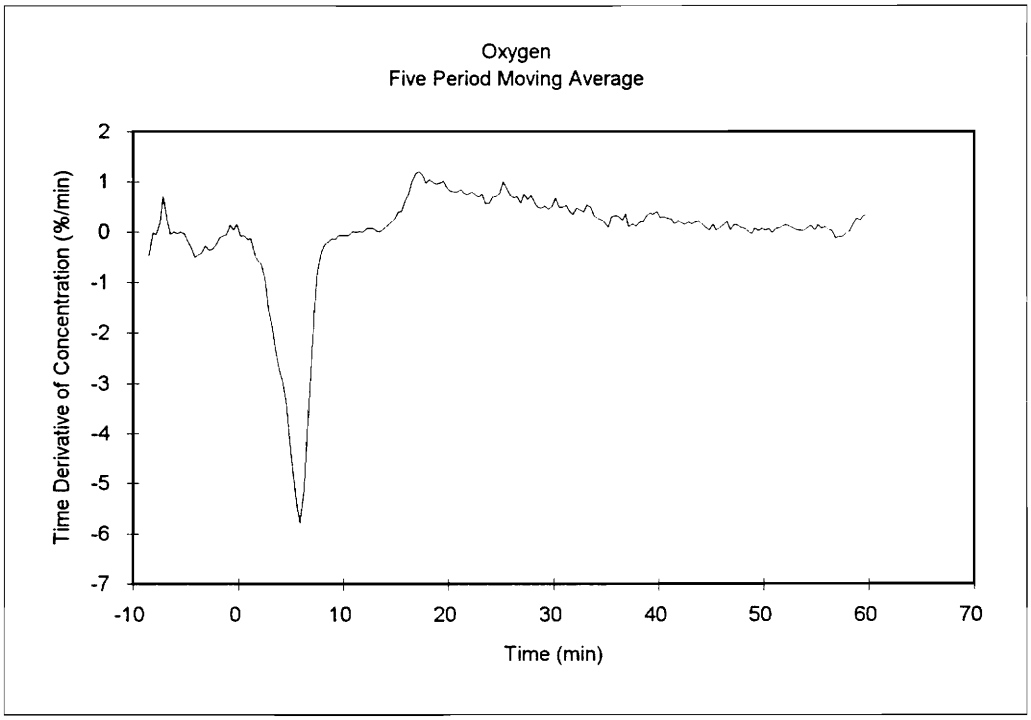

Figure 6-4a: Oxygen Trace and First Time Derivative for Test 5.

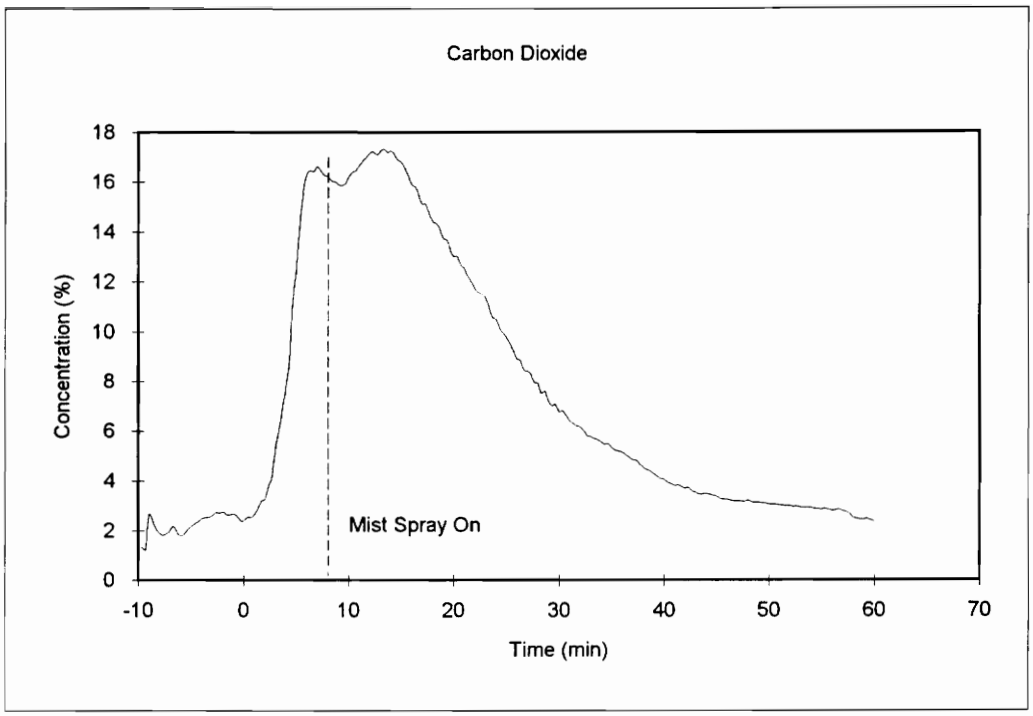

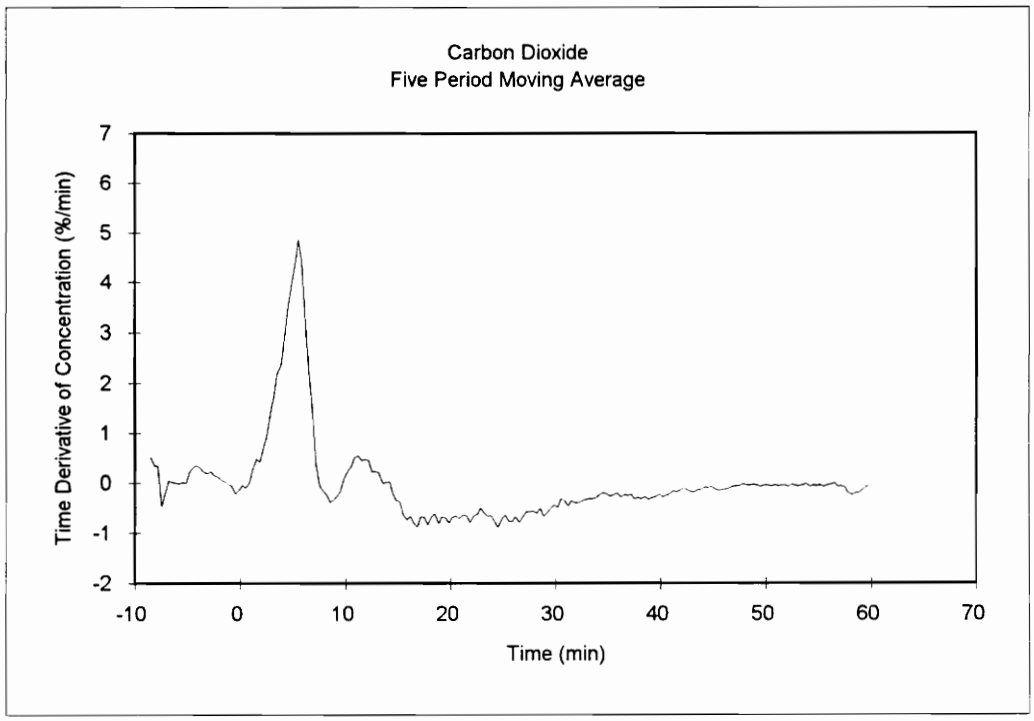

Figure 6-4b: Carbon Dioxide Trace and First Time Derivative for Test 5.

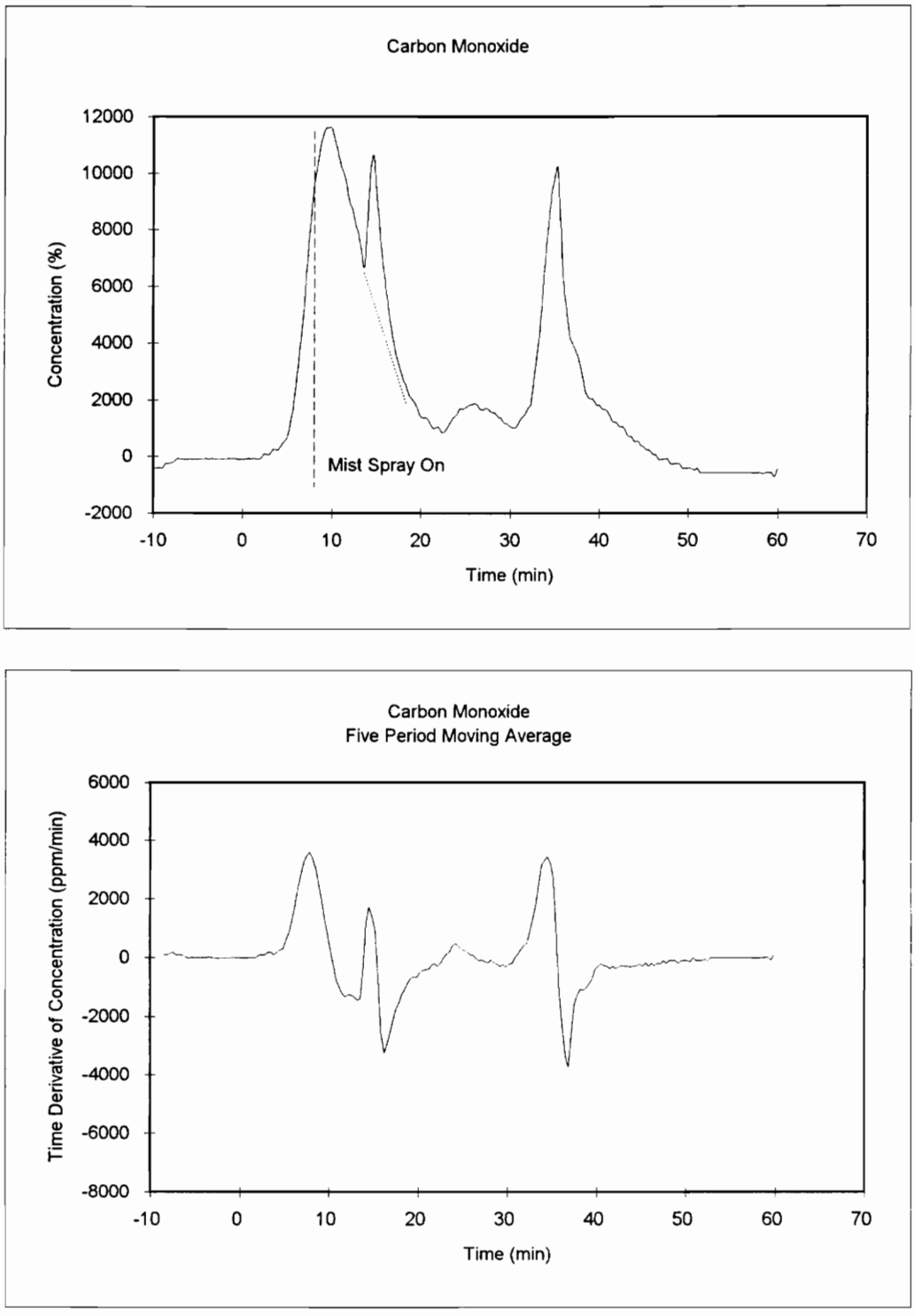

Figure 6-4c: Carbon Monoxide Trace and First Time Derivative for Test 5.

The spikes on the carbon monoxide traces that occur at times 15, 25, and 36 minutes should be neglected since they can be correlated to problems experience with the sample metering system for this gas. Neglecting the first of these spikes, and projecting the initial decay slope, as shown in figure 6-4c, the width of the period where the gas is greater that 1500 parts per million is about 15 minutes, compared to about 35 minutes in the baseline test.

The results of the first time derivatives during test 7, the combination extinguisher on coal fueled fire, are shown in figure 6-5. In the oxygen traces (figure 6-5a), the transition between the oxygen-rich and fuel-rich regimes is clear as the slope of the changes from -2 %/min to -5 %/min at a time of 5 minutes. Once the fire has reached full growth the slope of the trace line settles, very quickly to nearly zero. At this point the combination extinguisher is ignited with the misters on. When the combustor is turned off, with the misters left on, the concentration of oxygen rises, until the misters are turned off.

The elevation of the oxygen concentration during this time period is most likely due to unreacted oxygen that was previously being consumed by the combustor. Obviously, some of this newly available oxygen will be consumed in the fire; however, the fact that some passes through the fire zone is indicative that the fire was being suppressed by the action of the combination extinguisher. The suppressing effect of the mist alone can be seen in the reaction of the fire in reducing the oxygen concentration of the exhaust during the time period between mist being turned off and the spinning disk being started. The reaction of the newly available oxygen is visible in the acceleration of the fire following the flame out of the combustor. The effect of the mist provided by the spinning disk is evident

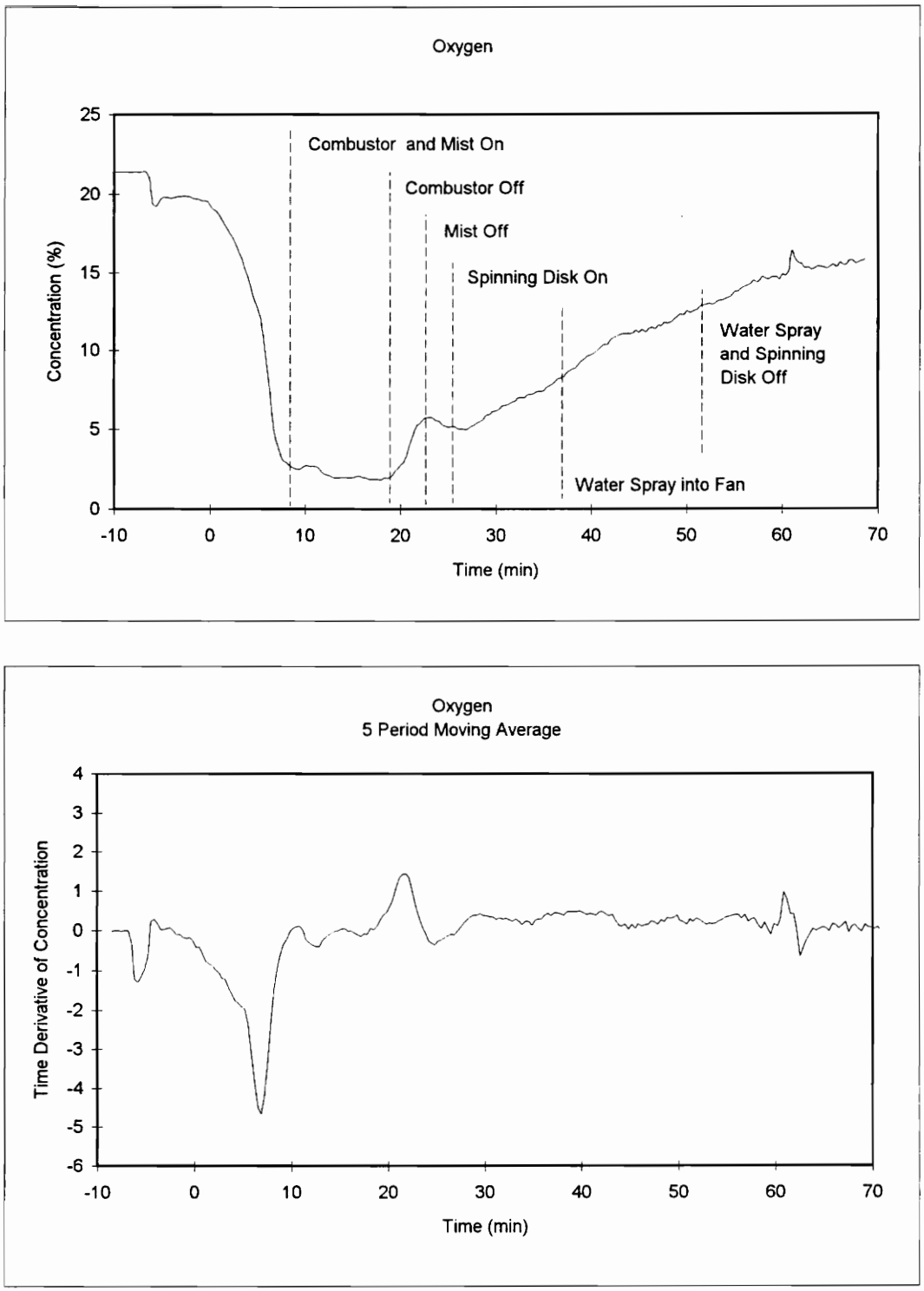

Figure 6-5a: Oxygen Trace and First Time Derivative for Test 7.

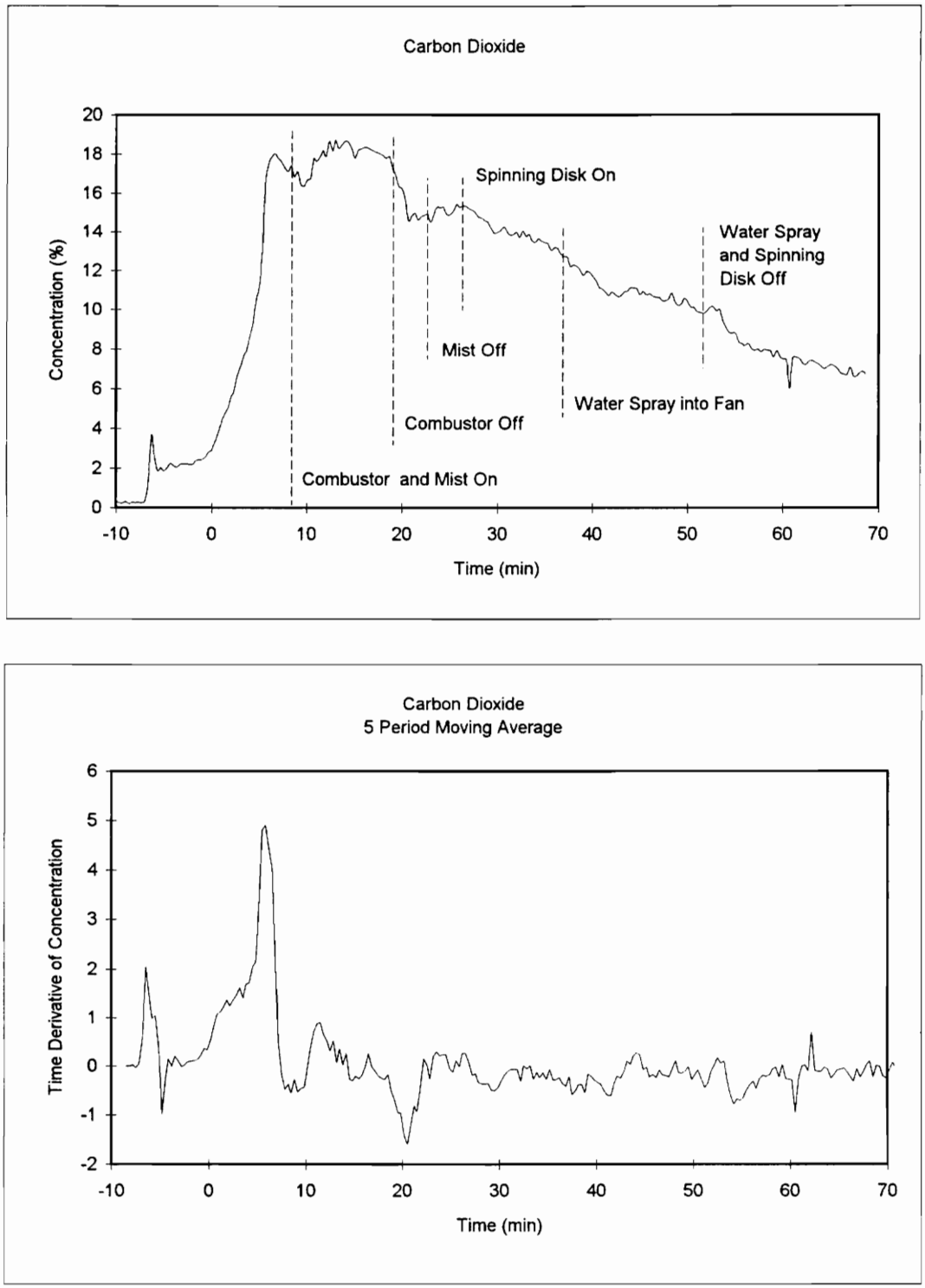

Figure 6-5b: Carbon Dioxide Trace and First Time Derivative for Test 7.

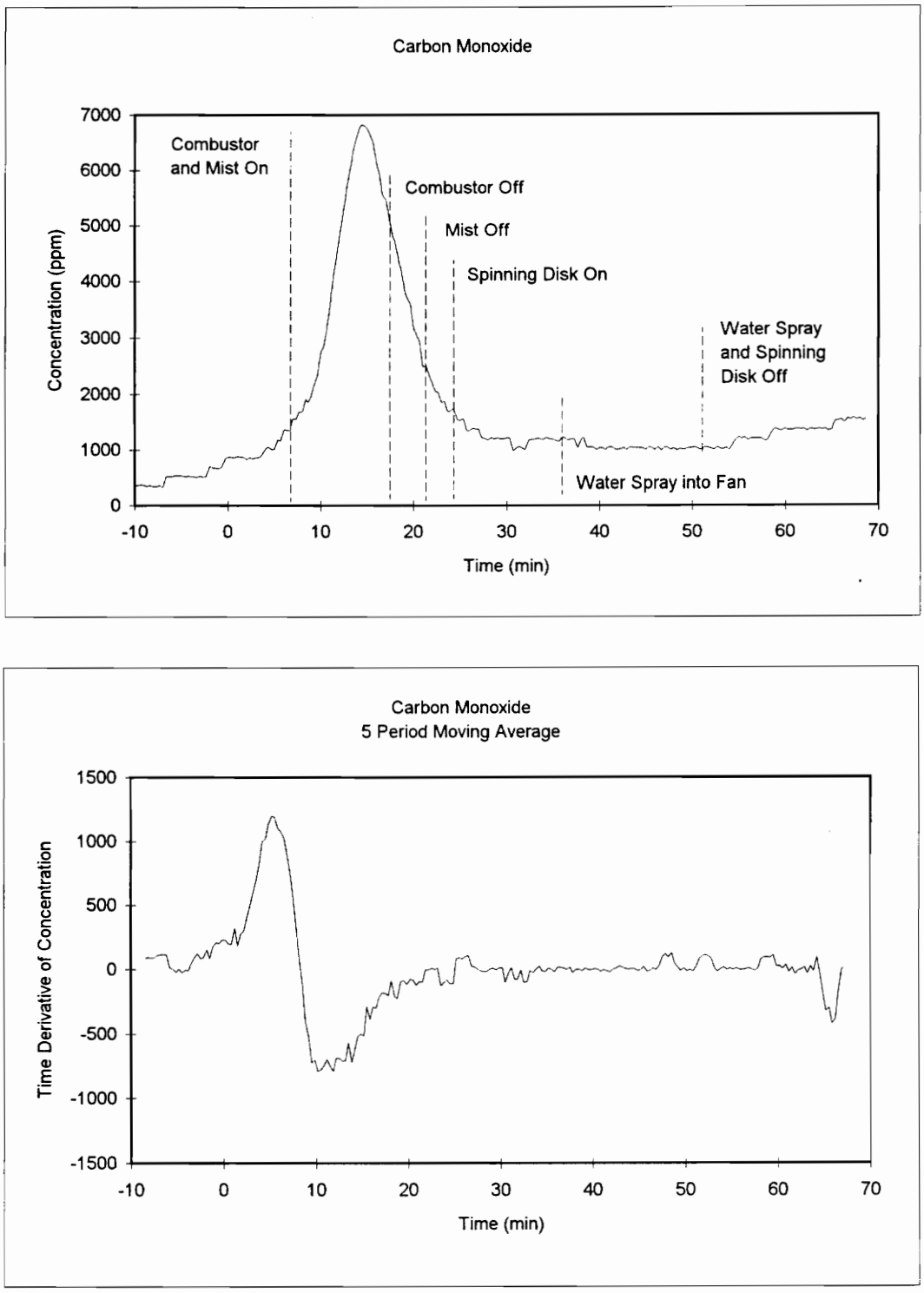

Figure 6-5c: Carbon Monoxide Trace and First Time Derivative for Test 7.

in the rise in the oxygen concentration following its start-up. Spraying water directly into the fan, to supplement the spinning disk appears to have had little or no effect.

A more provocative effect of the combination extinguisher can be seen in the carbon dioxide traces (figure 6-5b). The expected response of carbon dioxide during the fully fuel-rich phase of the fire is shown in the traces from test 4 (figure 6-3). In the baseline test the carbon dioxide concentration has a relative minimum during the period of fuel-rich combustion. In test 7 the concentration of carbon dioxide begins a decrease as the fire enters the fuel-rich phase, at time 7 minutes; approximately 1 minute after the combination extinguisher is lit this concentration rises again to a level of about 19 percent. The return to that level occurs much more quickly than would be expected relative to the baseline test. A sharp decline in the carbon dioxide concentration correlates to extinction of the combustor, as the associated increase in oxygen. The remainder of the carbon dioxide trace neatly mirrors the oxygen trace. The time derivative line for carbon dioxide seems to show much more erratic behavior than the same line for oxygen. This may be due to the dynamic interactions in the CO/CO_2 chemistry.

The carbon monoxide trace, figure 6-5c, shows a single spike that is similar in form to that experienced in the baseline test. The growth of the carbon monoxide concentration appears to be retarded compared to the baseline and fog only tests. This spike appears to be relatively symmetric above 1500 part per million concentration. The width of the spike in this range is about 18 minutes, compared to about 35 minutes during the baseline test.

6.4.2. Pressure Profiles and Airflow Rates

One of the factors used as a constant between the tests was the airflow rate. Since the airflow was metered off of the differential pressure across an orifice calibrated to standard pressure the airflow measurements are in standard volumetric units. Figure 6-6 shows the mean airflow rates and ± 1 standard deviation for the seven tests. This chart illustrates that all of the tests, except number 6, exhibit an airflow between 0.070 and 0.072 m^3/s. Test number three appears to have a very wide standard deviation, fully encompassing the first standard deviation of the remaining tests, except 6. Test 3 also shows the lowest mean airflow.

In the presentation of the results, in chapter 5, some mention of the pressure and airflow data was made. In that chapter the range and distribution of the airflow and a relative pressure data was made. The descriptive statistics of this data are shown tables 6-1 and 6-2.

Based on the assumption that the data is normally distributed, the skewness represents a measure of how well the samples are centered on the mean. Unfortunately the skewness tends to be a weak indicator of the data and should be used with caution when its value is less than $\sqrt{15/N}$ for the respective data set (Press W. H., et al. 1992). This indicator value is given in the descriptive statistics tables. Based on this limit of application only test 4 shows evidence of skewness in the airflow data. Tests 2 and 4 show evidence of skewness in the relative pressure data.

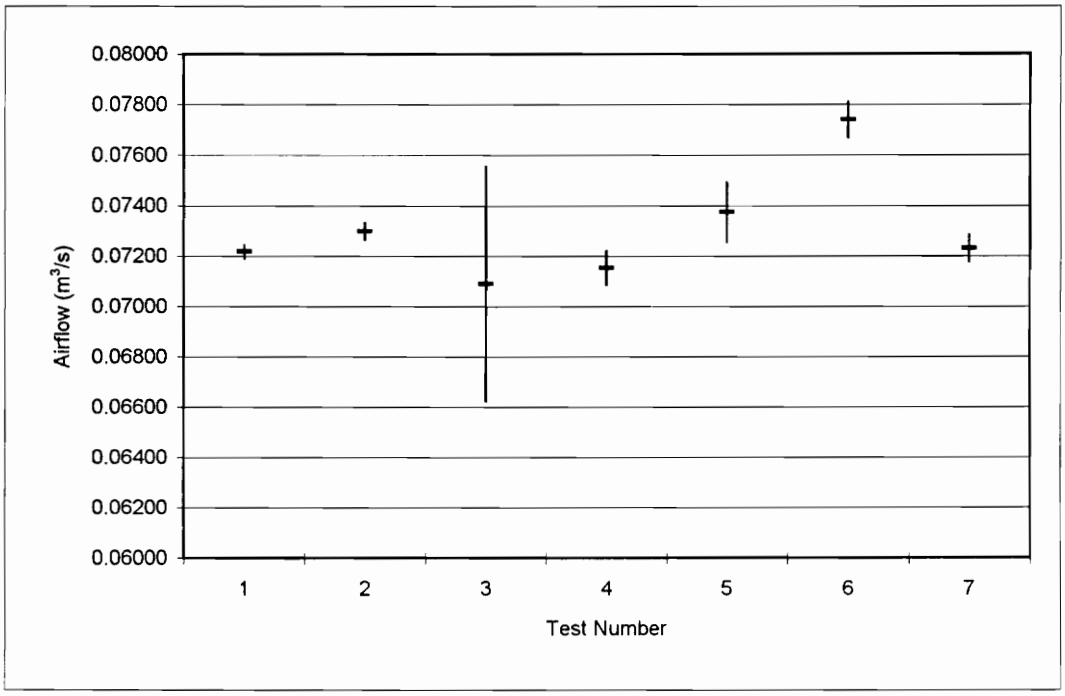

Figure 6-6: Mean Airflow Rates with ±1 Standard Deviation.

Table 6-1: Descriptive Statistics of Reported Airflow Data.

Flow Statistics	1	2	3	4	5	6	7
Mean	0.0722	0.0730	0.0709	0.0715	0.0737	0.0774	0.0723
Standard Error	3.7E-05	3.9E-05	4.1E-04	4.6E-05	8.4E-05	6.4E-05	4.3E-05
Median	0.0721	0.0730	0.0710	0.0714	0.0738	0.0774	0.0723
Mode	#N/A	#N/A	#N/A	0.07197	0.07384	0.07735	0.07204
Standard Deviation	0.0003	0.0003	0.0046	0.0007	0.0012	0.0007	0.0005
Sample Variance	7.3E-08	1.1E-07	2.2E-05	4.4E-07	1.4E-06	5.0E-07	2.9E-07
Kurtosis	-0.4861	-0.0195	0.7534	0.3318	-0.1896	-0.7530	-0.0678
Skewness	0.2841	0.0935	-0.5524	0.7328	0.1965	0.0245	0.2992
Range	0.0011	0.0016	0.0242	0.0034	0.0060	0.0029	0.0027
Minimum	0.0716	0.0723	0.0585	0.0700	0.0709	0.0758	0.0711
Maximum	0.0727	0.0739	0.0827	0.0733	0.0769	0.0787	0.0738
Sum	3.897	5.474	9.145	14.664	14.673	9.596	11.207
Count	54	75	129	205	199	124	155
Confidence Level (95.00%)	7.2E-05	7.6E-05	8.0E-04	9.1E-05	1.7E-04	1.2E-04	8.5E-05
(SQRT 15 / Count)	0.5270	0.4472	0.3410	0.2705	0.2745	0.3478	0.3111
(SQRT 96 / Count)	1.333	1.131	0.863	0.684	0.695	0.880	0.787

Table 6-2: Descriptive Statistics of Reported Duct Pressure Data.

Duct Pressure Statistics		2	3	4	5	6	7
Mean		12.9203	8.7187	-14.8876	-9.4186	-18.4413	16.0740
Standard Error		0.4638	0.6905	0.7900	0.6067	0.4833	0.8110
Median		13.5882	9.87242	-17.3083	-11.7368	-17.7133	18.7669
Mode		#N/A	#N/A	-24.6013	2.04939	-17.3955	18.1874
Standard Deviation		4.0167	7.8427	11.3117	8.5592	5.3815	10.0963
Sample Variance		16.134	61.507	127.954	73.260	28.960	101.936
Kurtosis		0.1216	0.1494	0.9415	-0.2981	0.1286	-0.8064
Skewness		-0.5487	-0.2376	1.2396	0.6701	-0.1260	-0.5495
Range		19.224	43.871	56.125	40.289	27.942	41.917
Minimum		2.1136	-14.1551	-35.6567	-25.0247	-31.6880	-9.0920
Maximum		21.338	29.716	20.469	15.265	-3.746	32.825
Sum		969.0	1124.7	-3052.0	-1874.3	-2286.7	2491.5
Count		75	129	205	199	124	155
Confidence Level(95.00%)		0.9090	1.3534	1.5484	1.1892	0.9472	1.5894
(SQRT 15 / Count)		0.4472	0.3410	0.2705	0.2745	0.3478	0.31109
(SQRT 96 / Count)		1.131	0.863	0.684	0.695	0.880	0.7870

The apparent skewness in the test 4 airflow data is supported in the airflow histogram shown in figure 5-22. This histogram illustrates, however, that the data may be bimodal. The significance being that the data set may contain two differing conditions, unthrottled and throttled flow, rather than being a single data set that is skewed to the upper end of a single normal distribution. The indicated skewness in the test 4 relative pressure data is also apparent in the respective histogram, figure 5-23. The skewness in this data set is likely of the same cause as that in the test 4 airflow.

There is some evidence for skewness in the relative pressure data from test 2, as indicated in table 6-2. The significance of this figure is marginal, however, since the magnitude of the skewness value is less than 1.25 times the minimum criteria value of $\sqrt{15/N}$. The histogram of the data set, see figure 5-11, seems to show a data set that has a mean around 15 Pascals, and does appear to have a longer tail on the left side than the right. It is difficult, however, to say that the data set is definitely skewed from the mean.

The kurtosis is a measure of the data spread compared to an ideal normal curve for the data. A positive kurtosis indicates that the data is more clumped at the mean, whereas a negative value indicates that the data exhibits a wider spread than would be expected. Application of this tool should be made with caution when its value is less than $\sqrt{96/N}$ for the respective data set (Press et al. 1992). None of the airflow data shows a kurtosis that is sufficiently strong to consider that the data is not normally distributed. In the relative pressure data, test 4 shows a positive kurtosis that may be of significance and test 7 shows a negative kurtosis that may be of significance.

A review of the relative pressure histogram from test 4, figure 5-23, shows a data set that exhibits a relatively high number of the samples clumped near the mean. This data set also shows a longer tail on the right side than on the left. If, as has been mention concerning the skewness of this data, the distribution is taken as being indicative of throttling, much of the data on the right side (greater than 0 Pascals) can be eliminated. With this done the graph could be taken as a normal distribution with a small standard deviation. In this case the kurtosis would be relatively insignificant. It is therefore possible to consider the kurtosis indicated for this test 4 data is insignificant.

Concerning the test 7 data, the kurtosis figure would tend to indicate that the data is wide spread about the mean, tending to flatten the normal curve. Based on the histogram of this data, figure 5-31, there is again evidence of a possible bimodal distribution. If this were the case the kurtosis figure could be caused by melding of the two normal distribution near the respective means. This case could be supported by the consideration that the histogram appears to show skewness of the data to the right, with a long tail to the left. The data set does indicate that skewness maybe a factor, table 6-2. However, the data trend shows that the data series does not follow a random pattern, but is time dependent.

The statistical evaluations made here have been to aid in the determination of any significant features in the airflow and relative pressure data. Other than the anomalies mentioned above, there is no compelling evidence that the data collected is not random in the respective distributions. This statement provides that the airflow during each test was effectively constant about a determinable mean. While the time dependent nature of the data, illustrated in chapter 5, appears to show that there may have been airflow throttling

in some of the tests, a definite conclusion cannot be made from this data. The presence and nature of throttling associated with airway heating could be determined from tests specifically designed to obtain that data. Testing of this nature could be performed in a wind tunnel fitted with an electrically heated section. This type of test would provide a stable heat source, and could be quickly repeated or cycled.

6.5. Observations

Throughout the course of the experimental program that has been documented here, a number of observations occurred from time to time that are worthy of some mention. In particular, the include the absence of reverse stratified flow, the definition of the fuel-rich state, and the capacity of the airstream to carry the fog.

6.5.1. Reverse Stratified Flow

One of the most surprising observations during all of the tests was the lack of reversed stratified flow, or "roll-back." The presence of roll-back was predicted in the design process by working with a Froude number greater than 1.0. In the absence of a backing layer the development of a Richardson number is not possible. One possible explanation for the lack of visible roll-back is the sudden contraction effect that occurs at the entrance to the fuel load. The sudden contraction would cause a local acceleration of the air, with the net effect of reducing the local Froude number. Such an explanation is unlikely based on the physical observations.

Had a sudden contraction been a significant factor some degree of recirculation would have existed at the contraction. Such recirculation is not evident as the leading edge fuel, at the top of the load, was unburned. If recirculation was occurring the fuel should have been affected by hot gases carried forward. The conditions found after the tests are consistent with the observations made in the video tape and photographic records. That the fuel burning on the top was, in fact, displaced away from the leading edge of combustion on the floor in the direction of bulk airflow. From this observation it is possible to deduce that there was no significant movement of air, heated or otherwise, in an upstream direction from the seat of the fire.

6.5.2. Limits of the Fuel-Rich State

While the tests were being conducted, one question that was raised concerned the definition of the fuel-rich state. The most basic definition is that the fire is truly fuel-rich when there is no oxygen remaining in the products of combustion. The broader definition by Roberts and Clough (1967a) is that fuel-rich behavior begins when the oxygen concentration downstream of the fire falls below 15 percent. The experimental basis for this observation was a series of wood fires in a duct.

In the experiments conducted for this thesis the transition to fuel-rich behavior appears to occur at a point when the downstream oxygen levels are closer to 12 percent. This is evident in the gas concentration traces for tests 4, 5, and 7, see figures 6-3a, 6-4a, and 6-5a. As mentioned in section 6.4, it is near the 12 percent concentration that a distinct acceleration in the fire's growth rate is visible. The appearance here is that the fire is

physically fuel-rich for the coal fuel when the oxygen concentration in the products of combustion is less than 12 percent.

Based upon the chemical definition of the fuel-rich state the fire does not reach this point until the level of carbon dioxide begins to decrease, in favor of carbon monoxide. The fire begins returns to an oxygen-rich state as the carbon dioxide levels fall, with a coinciding increase in the oxygen concentration. Based on the observed fire decay curves, there does not appear to be distinct rate change in the fire decay as the oxygen concentration returns above 12 to 15 percent.

For field application the definition of Roberts and Clough (1967a) can be used by fire-fighters during the initial attempts to gain control over the fire. When the oxygen concentration, downstream of an open fire, falls below 15 percent the indication should be that the tactics being employed are ineffective. When approaching a fire that is already fully fuel-rich the presence of any oxygen in downstream products can indicate that the intensity of the fire is decreasing. This could be used to determine the degree to which the fire is being controlled, and the relative effectiveness of the new tactics. The danger, to the fire-fighters, possible survivors, and the mine is not over until the fire is entirely extinguished.

6.5.3. Fog Capacity

The capacity of the air to carry a fog appears to be related to several factors. These include the relative velocity of the fog droplets to the main air mass, the size distribution of the particles, and the

The upper, practical, limit of air to carry liquid water is in the neighborhood of 1 kg water per 1 kg of air (McPherson 1993b). This is based on an airflow velocity of 4 m/s and a water rate of 5 l/s-m^2, which for standard conditions give the water/air ratio of 1, as indicated above. Assuming a mass mean particle diameter of 25 μm there would be about 110 billion droplets per cubic meter. A very dense natural fog, with a visibility of 25 meters, has a density of about 0.0045 kg per cubic meter (George 1951). A fog of this magnitude would have about 550 million droplets, 25 μm diameter, per cubic meter.

The water:air ratio of 1 kg/kg that was determined from McPherson (1994b), is intended for used in water spray coolers, and is clearly inappropriate for determining a maximum fog density. Assuming quiescent conditions and a mean water particle velocity of 5 cm/sec (0.01 % of the gas value of about 46000 cm/sec), the mean time between collisions of the water particles is estimated to be 20 per sec per cm^3. A fog of this density would quickly turn into a rain.

Based on the results of test number 4, the purely fogged case, the fog rate was 0.018 kg per second, providing a fog density of about 0.26 kg/m^3. Considering that the fire was fully engulfing the available fuel, this fog provided a water flux of 0.065 kg/m^2-s^1, which about one-quarter the 27 g/m^2-s^1 stated as being necessary by Scheffy and Williams (1991a and 1991b). The density found in this test was also significantly less than the maximum practical value of 0.45 kg/m^3 reported by McPherson (1993b), with respect to water spray dust collectors.

It seems clear that the maximum capacity of the mine airstream to carry a fog will be less than that of the spray scrubbers, since the fog must be carried much further. The maximum capacity may even be less than that found in this wind tunnel. The capacity of the air to carry a very dense fog over long distances, and the optimum initial particle size distribution leaves significant room for further study on these phenomena.

7. Conclusions

The purpose of this thesis was to determine the effect that the application of water mist has on a fuel-rich fire in a model coal mine entry. Namely, can the fire be brought under control with water supplied as a fine mist or vapor. To ascertain the effects of the water mist a series of experiments were conducted in a wind tunnel model coal mine entry. The tests included baseline tests, in which no extinguishing effort was made, the use of a purely fog system, and a system where fog was supplemented with a propane gas combustor.

As has been discussed in this thesis, the application of water mist has an effect of reducing the intensity of the fuel-rich fires, and may be effective in total extinguishing them. This chapter covers the observations that lead to the conclusions that the water mist exhibits the desired effects, the ramifications for large scale testing, and some general recommendations regarding the use of water mist.

A note of particular importance is the limited range of effect due to the mist that was observed during the testing. Based upon the observations made, the water mist is most effective while the fire is most intense. While the water mist is effective against the fire, its strongest impact is seen in the immediate time frame of its application. This is in

agreement with the results presented by Mawhinney (1994) for compartment fires in ships and buildings.

7.1. Efficacy of Water Mist

Regarding the effectiveness of water mist on the fuel-rich fires, mixed results were obtained. During the wood fueled tests the application of water fog seemed to have an initial positive effect, but the continued application of mist did not appear to significantly shorten the life of the fire. During the coal fueled test the application of water mist appears to have had an effect of shortening the life of the fire to about one-third that of the baseline test.

7.1.1. Wood Fires

The use of the spinning disk humidifier, as the misting device, did not appear to be particularly successful in controlling the fuel-rich plywood fire. There may be several explanations for this observation. First, the application of water mist may have had no effect at all.

Second, the amount of water mist reaching the fire was insufficient to affect the fire to a significant degree. As was observed in the testing of this fog system a large percentage of the water did not get ejected as a fog. Some of this water was lost due to impingement in the tunnel, while some droplets simply "rain-out" being too large to be carried effectively in the air. The system testing also revealed that the total flow rate through spinning disk did not meet the ratings provided by the manufacturer at any of the airflow rates tested.

A third possibility is that the natural decay point of the fire coincided with any effect of the water mist. This is the most likely explanation for test 1, where the decay of the fire is consistent with the application of the fog stream. It appears a less likely explanation in test 3, where a momentary increase in the oxygen, and decrease in carbon dioxide, coincide with the initiation of the fogging system. Following the blips in the gas traces the fire appeared to return to its natural coarse, despite the continuing supply of fog.

The apparent initial positive reaction in the wood fire of test 3 seems to indicate that the fog had a desirable effect, but the water supply was insufficient. To this end, the use of pneumatically assisted water spray nozzles where chosen for the coal fueled tests.

7.1.2. Coal Fires

The application of a water mist to a fuel-rich coal fire was efficacious in leading to the extinction of the fire. There are two principle supporting facts to this statement. First, the fire to which the water mist was applied showed a fuel-rich life of about one-third of the baseline fire. Second, the initial rate of oxygen increase, as the fire began to decay was nearly twice that of the baseline fire. This is shown in figures 7-1 and 7-2. Notice the oxygen traces and the carbon dioxide traces are virtual mirror images for each respective test.

The continued application of the water mist resulted in a fire that was virtually extinguished one hour after its acceleration to the fuel-rich state. The baseline fire continued to produce an exhaust with less than 15 percent oxygen over an hour and a half

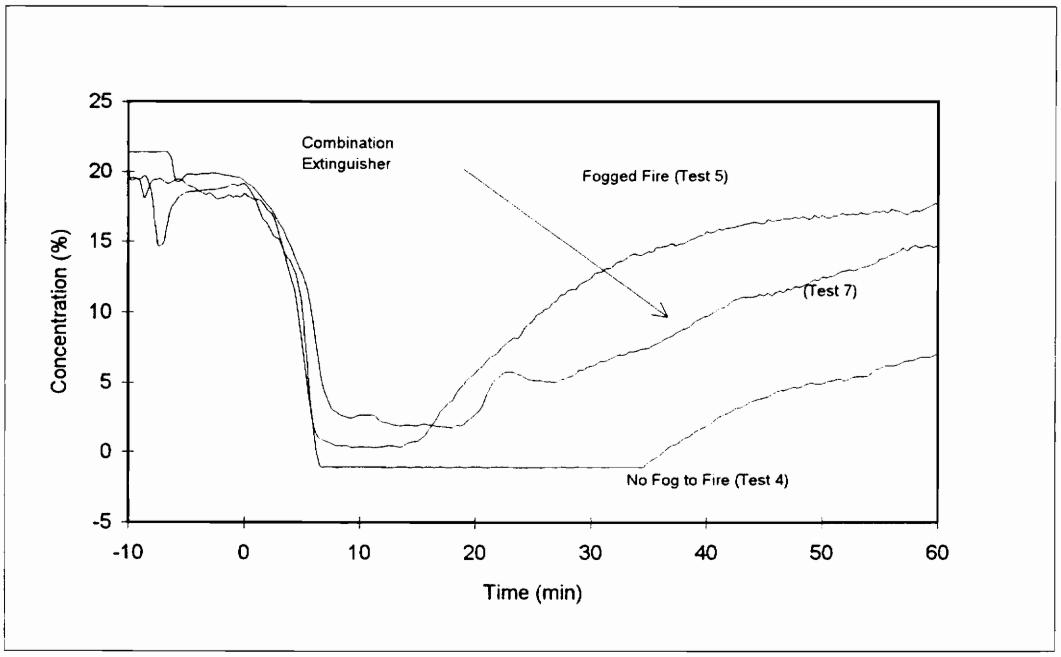

Figure 7-1: Comparison of Oxygen Traces for Coal Fueled Test Fires (Loomis and McPherson 1995).

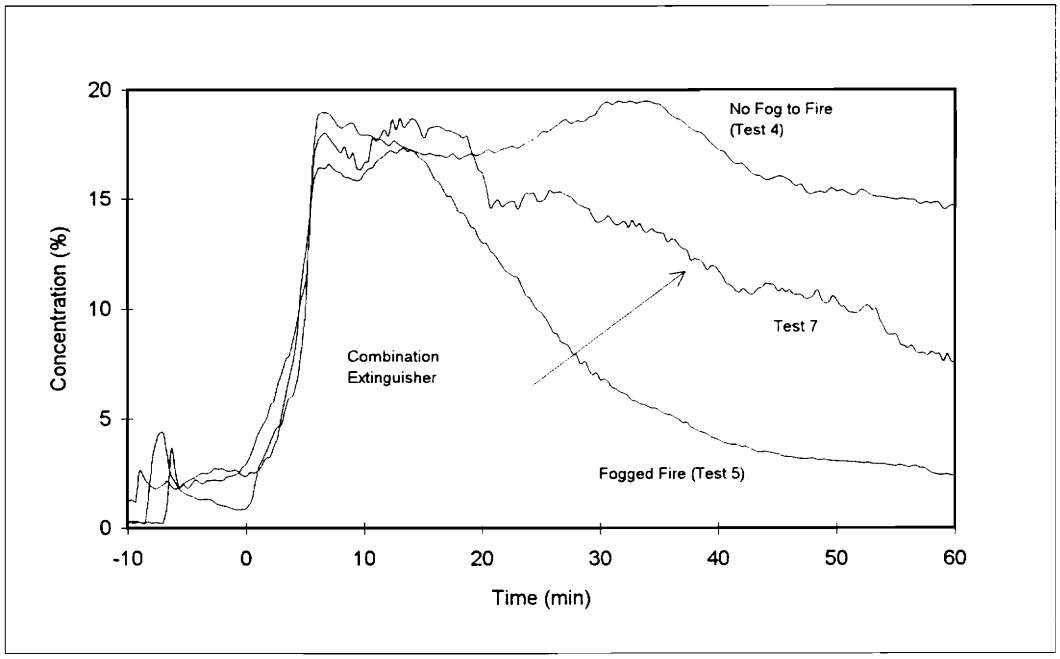

Figure 7-2: Comparison of Carbon Dioxide Traces for Coal Fueled Test Fires (Loomis and McPherson 1995).

after its acceleration to the fuel-rich regime. Furthermore, the remaining mass in the tunnel after the extinguished fire was nearly twice that of the baseline test. Much of the remaining material from test 5 was basically unburned, whereas the remains from the baseline test consisted mostly of coke and ash.

7.2. Efficacy of Combination Extinguisher

The device that has been referred to, throughout this thesis, as the Combination Extinguisher used both the oxygen depleting effect of a controlled fire and the vaporization of water as a combating agent against the fires. In this extinguisher water was vaporized by the heat from the propane flame. The overall oxygen gas concentration downstream of this device was computed to be just less than 13 %, low enough to inhibit the action of flaming combustion.

The development, and testing, of this combination extinguisher was conducted in an effort to evaluated its possible performance, despite the fact that it is clearly not "permissible" in the sense of current coal mine practice and regulation. The general intent of the design was to reduce the oxygen concentration of the air entering the fire area. This was done, first, by a flame combustor, then by the vaporization of a water fog. Much of the heat generated in the combustor was utilized in heating the water mist, thus cooling the total mixture to a point that it would not prove an ignition hazard to the surrounding coal.

7.2.1. Wood Fire

The results show that the combination extinguisher very quickly suppressed the fire, and kept it out. The was shown rather dramatically in the total extinction of flame in the fire zone following the ignition of the propane combustor. Compared to the coal fueled test, the wood fueled test was subdued instantly. However spectacular this may seem, no distinct conclusion can be gained. It is likely that the fire was "blown-out" during the rapid ignition of propane. Although this does not explain the reason that the fire showed no regrowth, it seems the most probable explanation. Regrowth of the fire may have been hindered by the presence of the water mist that was being injected into extinguisher.

7.2.2. Coal Fire

The effectiveness of the combination extinguisher against the coal fueled fire was most clearly demonstrated by the abatement of smoke during the period of its action. The gas measurements also indicate that the fire was being brought under control even after the combustor was put-out, and the misting sprays were left on. The evidence for this lies in the elevating oxygen levels followed by declining levels after the water sprays were turned off. The falling oxygen concentration is indicative of the fire returning to its fully fuel-rich state. For a comparison of the action of this device, to the purely fogged and baseline fires, see figures 7-1 and 7-2. The overall effect of the Combination Extinguisher system lies between the purely fogged and baseline cases.

7.3. Recommendations for Full Scale Tests

The experiments conducted during the course of the work documented in this thesis were conducted on a relatively limited budget. It is imagined that should full scale tests be performed that the budget would be larger relative to the scale, and that the monitoring systems portion of the budget would represent a smaller percentage than that of the small scale tests. In general three possibilities exist for locating full scale tests. First, the tests could be conducted in an existing coal mine entry. Second, the tests could be performed in a surface facility specially constructed for the purpose of the tests. Third, the tests could be conducted in an underground test tunnel, in a rock mass other than coal.

It is unlikely that a mine operator would be interested in allowing tests of this nature to be conducted in an active mine, therefore the first location is probably out of the question. The second location presents the problem of a significant expense in these days of reducing budgets, and although it would be a fine solution it is most likely not fiscally feasible. The third solution, to use an underground test facility is probably the most likely case. This would, however, involve subjecting part of an existing facility to conditions that would result in permanent damage to the facility. An alternative would be to conduct the tests in an abandoned civil structure, such as a road or railway tunnel.

It is fairly easy to identify some of the technical problems that would be associated with the conduct of full-scale tests. One of the first would be supporting the fuel during the tests. This could be accomplished with closely spaced trays of coal along the sides and top, while coal fuel could be spilt on the floor of the tunnel.

Another, very significant, technical problem would be protecting the structure, be it a mine entry, road tunnel, or surface model. One possible means would be the application a thick cement layer to the opening surfaces. The cement would likely spall away during each test, necessitating rework between tests. It should, however, be capable of preventing significant damage to the airway. An advantage to the use of a cement coating is also that it would allow instruments and data transmission lines to be set and insulated from direct contact with the fire.

Data collection for a large scale test would also need to be more in depth than that used for the tests documented here. In addition to the continuous gas monitoring system, and temperature and pressure measurements, several other technical measurements should be considered. The collection of discrete gas samples for chromatographic analysis would allow for detailed gas species distribution to be made. The use a particle counter to determine the density and particle size distribution of the fog in the airway upstream of the fire. The use of infra-red imagers could also provide data on the effective thermal attenuation provided by the fog. Within the fire zone, consideration should also be made for the employment of flame detectors to monitor the speed of advancement of the fire at different portions of the tunnel cross-section; both vertically and horizontally.

Despite the obvious technical problems that would be associated with full scale testing, perhaps the highest hurdle would be funding. However, a facility designed for the conduct of fuel-rich fire research would be invaluable for the study of fires in a mining environment, in coal and metal/non-metal mines, and in the United States and elsewhere.

7.4. Other Recommendations

In this section some additional general recommendations are addressed. These are based on the experience that was gained during the conduct of the initial experiments. The subject here is the means by which the tools used during the course of this research could be applied for use in the field.

7.4.1. Water Mist Suppression System

The increasing interest in water mist fire suppression systems as a replacement for Halon system has sparked development of commercially available systems. These systems, for use in building and ship compartments use a dedicated tank of water and compressed air or nitrogen (anon. 1994b). It is conceivable that a commercial system could be fitted on a trailer, or self-propelled vehicle, that could be transported throughout an operating coal mine.

The use of nitrogen as the pneumatic assisting agent will serve a double duty in the mine entry. It will perform the task of producing the fine mist droplets, and will serve as a diluent for the existing oxygen. The diluting effect is small compared to the production of the water vapor, however, since water to nitrogen ratio will be about 2.9 kg (H_2O)/kg (N_2).

In a conceptual configuration this system should meet the following basic requirements:

1) Carry sufficient water on-board for 15 to 30 minutes of continuous operation.

2) Carry sufficient bottled gaseous nitrogen on-board for 15 to 30 minutes of continuous operation.

3) Be equipped with an on-board water pump that can be connected to any water range in the mine.

4) Be equipped with an on-board air compressor, and by pass system to connect to compressed air ranges in the mine.

The size and number of spray heads used should be capable of supporting the production of 1.05 kg/s (17 gpm) of water fog at 25 - 200 micron diameter. This flow rate is about 1/3 of the statutory minimum of 50 gpm that must be available.

The density of the fog that would be generated is sufficient to reduce visibility to nearly zero, in normal day light conditions. With this basic consideration it would seem that personnel could not make a safe approach to the fire will the fogging system is active. However, with active monitoring of the downstream exhausts it would be possible to determine a point at which the fogging rate could be reduced. Under the conditions of a reduced fog rate personnel could, perhaps, approach the fire using the lower density fog as a radiative shield, in addition the water that it is carrying.

7.4.2. Combination Extinguisher

Concerning the design of a full-sized combination extinguisher some generic suggestions can be offered regarding design. First, the use of pilot light appears to be a better alternative than the spark igniter that was used in the working prototype. Second, the fan should be coupled with the fuel flow controller to ensure that the desired combustion chemistry is maintained. When coupled together, these two would help to assure that no un-burned fuel exits the combustor.

When designing a full-sized unit the fuel type used should be balanced with minimizing the overall size of the unit. The use of propane is nice since it is injected into the combustor in a gaseous phase, however, in a large scale unit a heater/evaporator may be required to provide a constant flow of fuel. The use of diesel oil could be advantageous from the point of view of availability. However, it may be hampered by a larger/longer combustor section; and the requirement for very small injection nozzles necessitating careful fuel handling to avoid contamination.

In any case, the provision of a quenching screen should be made to prevent any flame from leaving the unit. The water injection section portion should also be of sufficient length to assure that vaporization of the water occurs prior to re-entering the mine airway.

The use of such a system in the field presents one significant technical problem. Due to the heated nature of the vapor mixture entering the fire zone placing fire-fighting personnel would have no access to the fire. In a manner similar to that of the pure fog

based system, gas monitoring could be used determine the point where the combustor could be extinguished. (This gas monitoring would need to be more detailed to determine the effects of the combustor versus the effects of the coal.) The misting system alone could be used to provide the fire-fighters a radiative shield as they make an approach to the fire.

7.4.3. Throttling

A bit of discussion was made on the theory and effects of ventilation throttling as a result of the ensuing fire, including addition in the results and discussion chapters. In general, the presence of throttling during the test fires cannot be ruled out, although strong evidence is not clearly present. One key issue here is that the tunnel was not adequately configured to study and quantify the throttling effect. The dynamic nature of the fire itself being a limiting factor. Verification of the throttling effect could, however, be performed in a relatively small scale tunnel, perhaps on the order of 120 centimeters square. Such a tunnel could be equipped with an electric heated that would not impact the true resistance of the airway, but would allow for the carefully controlled addition of heat to the air stream.

7.5. Closing Comments

The work that has been documented in this thesis shows that the use of water fog against fuel-rich fires in coal mine entries has promise for application. The very dense fogs that were generated during these experiments proved to be effective in bringing the fuel-rich

fires back to an oxygen-rich state. Although the fires were subdued in these experiments the fog was most effective during the period in which the fire was most intense.

Any designed application of water mist / vapor systems need to consider that they are not discrete in their attack on a seated fire. That is they flood the entire area under consideration and are therefore limited as the fire is reduced in scale. A mine equipped with a fog generation system of the scale described herein could find a duel use under a fire scenario. First, in the event of a major fire that has become fuel-rich, or is approaching that condition the high fog rate should be used. Under condition of smaller fires, or a subdued fuel-rich fire, the continued application of a lower density fog could be useful in providing some thermal shielding to the fire-fighters.

With the increasing interest in fog based systems that is evident in the industrial and marine sector the hardware is becoming available and relatively inexpensive to construct fogging systems. The major limitation the application of these commercial systems in the mining environment appears to be developing a system the produces droplets small enough to survive an arduous journey through the mine entry to a fire that may be several hundred meters away.

8. SUMMARY

8.1. Introduction

Most often a fire that erupts in a mine is small and brought under control relatively quickly. There are a few, however, that get out of control and result in extraordinary effort in trying to save lives of miners and the mine, while placing rescue personnel at a high risk. One of the most frightening possibilities is that the fire becomes fuel-rich. A fuel-rich fire is one in which the available fuel exceeds the available oxygen required for complete combustion. The fuel and air mixture differences can be illustrated with the fuel/air ratio.

Oxygen Rich

$$\left(\frac{Fuel}{Air}\right)_{Mixture} < \left(\frac{Fuel}{Air}\right)_{Stoichiometric}$$

Fuel Rich

$$\left(\frac{Fuel}{Air}\right)_{Stoichiometric} < \left(\frac{Fuel}{Air}\right)_{Mixture}$$

When a fire is burning in the oxygen-rich regime the fire is spreading through local heating of the fuel supply by radiation and convection from the existing flames. This is the same manner that a fire spreads when it is burning in the open. The resulting changes to the

bulk airstream temperature and composition are relatively insignificant (Roberts and Clough 1967a), while the fuel/air ratio is well below the stoichiometric mixture.

When the fire enters fuel-rich propagation its size and temperature of the products are such that sufficient heat is transferred from the gas stream to the fuel lining to begin pyrolysis of the fuel. This results in a fire that is self accelerating to the limiting condition that all of the available oxygen is reacted (Roberts and Clough 1967a). The excess fuel is carried in the high temperature products. This highly volatile mixture can react with fresh air resulting in a re-eruption of the fire at some subsequent cross-cut. Once the fire has entered the fuel-rich mode of propagation its rate of growth can accelerate by such means to 10 times that of the oxygen-rich mode (Roberts and Blackwell 1969). Estimations of the heat transfer characteristics show that up to 65% of the heat generated by the fuel-rich fire is available for the further liberation of fuel from the surrounding surfaces (de Ris 1970).

Stepping back from the physical/chemical distinction between an oxygen and fuel-rich fire, as described above, it is important to get a feel for where this transition will occur in a burning fire. Roberts and Clough (1967a) describe the change of propagation mode to occur at about 15% oxygen in the products of combustion. Their experiments were conducted in a wood lined duct. When the oxygen concentration is greater than or equal to 15 percent the fire is moving in an oxygen-rich mode. As the oxygen concentration drops below 15 percent the fire tends towards the fuel-rich propagation. Distinction in this case has been made by observation of the fire spread.

Further correlation to the fuel-rich mode exists at the same concentration of 15-16 percent oxygen in the products of combustion. At this level flaming combustion is inhibited and the pyrolysis reactions are not occurring in the structure of the diffusion flame (Burrell and Seibert 1912); the implication being that a further increase in the airflow, and hence quantity of oxygen, will result in increasing the amount of flaming combustion. The outcome is an increase in the heat released and an acceleration in the rate of the fire spread. A reaction documented by Roberts (1970) indicated that a 4 fold increase in the airflow to a fuel-rich fire had the reaction of causing the fire to burn more vigorously.

Many various techniques have been employed to try and fight large fires burning in coal mines. These include direct attack with rock dust or water, application of foams, inertization with nitrogen, carbon dioxide, or exhaust gases from turbine engines, and sealing of the affected area. Despite the wide range of fire fighting techniques that is available it seems that in most cases of large fires the result is the ultimate use of sealing the fire area or the entire mine. It is desirable, then, to take a step back and see if there is some means to fight large, and in particular fuel-rich, fires that will minimize the likelihood that sealing will be resorted to. One possible method that has been suggested is the application of water mist to the fuel-rich fire (McPherson 1993a).

The application of a water mist to the fire appears to have several advantages. These include: ability for the water to remain suspended in the air stream for an extended period of time; and hence to be carried further into the fire zone; and using the water mist as a shield from the thermal radiation emitted by the fire (Reischl 1979). The presence of water vapor is the air will also reduce the overall radiant heat transfer from the fire to the surrounding drift walls (McPherson 1993b). Furthermore, the evaporation and

superheating of 1 kilogram of water from 20 to 750 °C requires some 4000 kilojoules of energy, heat that is then no longer available for fuel pyrolysis. A heat rate that is equal to 4 megawatts per kilogram of water per second. This water will also coat fuel in the downstream workings as the product gases cool to below the prevailing dew point.

To determine the possible efficacy of water mist as a fire-fighting agent for fuel-rich fires a series of experiments has been conducted at the Department of Mining and Minerals Engineering, Virginia Polytechnic Institute and State University. These experiments have shown that water mist has a positive effect in reducing the intensity of fuel-rich fires in a 30 cm square wind tunnel.

8.2. Experiments

A wind tunnel was designed and constructed for the purpose of conducting fire tests, see figure 8-1. The tunnel is of forced ventilation configuration utilizing a centrifugal fan. Airflow to the fire test section is metered from the fan with an orifice and waste gate system. Adjustments to the position of the waste gate change the airflow through the orifice, while the fan operates at a constant speed. The tunnel makes a ninety degree bend from the fan and airflow metering section to the fire section. This bend is fitted with a Plexiglas window, through which development of the fire can be observed.

The fire section of the tunnel is 30 cm square with a total length of 9 meters. The first three meters, after the bend, is constructed of welded steel plate and ensures that the airflow entering the fire section is in a flat profile across the entire cross-section. The remaining length is constructed of mortared fire brick, erected on a welded steel bridge

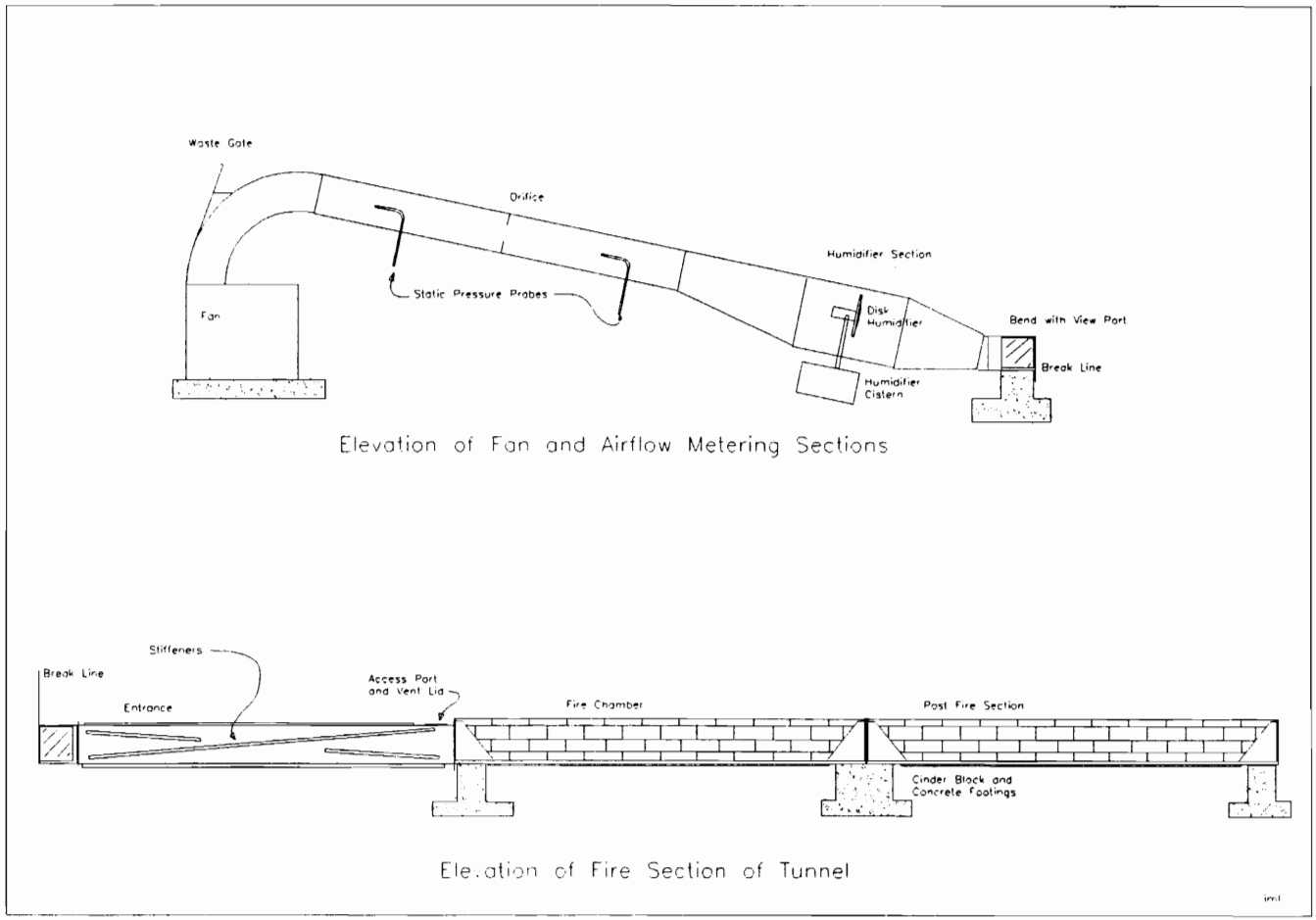

Figure 8-1: Elevation Drawing of Fire Tunnel.

structure. Test fires are placed in the first half of the fire brick section of the tunnel. The second half of the fire brick section is intended to ensure that the products of combustion are fully mixed and without stratification before exiting to the atmosphere.

Monitoring of the system is conducted with the use of a computer based data collection system. This system monitors carbon dioxide, oxygen, carbon monoxide, and (for a time) methane, differential pressure across the orifice, and temperatures at 9 locations in the tunnel.

Seven experiments were conducted in the fire tunnel. Four of these tests have involved the use of plywood fuel, while the other three used coal as the fuel. All of these tests involved ignition by a relatively small fire that progressed from oxygen-rich to fuel-rich burning. In some cases the small ignition fires required additional coaxing in order to push the mode of propagation to the fuel-rich regime. The airflow velocity into the fire section of the tunnel was held constant for all of the tests at approximately 0.76 m/s (150 ft/min).

8.3. Results

The first three and the sixth tests used plywood as the fuel source, which provided for a test of the tunnel and its systems and the collection of useful data without subjecting the tunnel to the extreme conditions that were expected (and found) during the coal fueled tests. It is worth noting that the response of the plywood fires was very similar to those conducted by previous researchers (Roberts and Clough 1967; Hwang and Chaiken 1978; Chaiken et al. 1979; and Lee et al. 1980). Further, as expected, the wood fires reacted

much more quickly than the coal fires. In all, these tests proved useful in verifying that the type of fire being developed in the wind tunnel was similar to that described as a fuel-rich duct fire by the previous researchers. Because the fuel source provided a smooth surface on which the fire could spread; the buoyancy effects in the spreading of the duct fires were very apparent, as were the oxygen-rich and fuel-rich propagation modes, as described above.

Test number 4 was conducted with coal as the fuel. The test was the baseline for this fuel type and no attempt was made to extinguish the fire. The oxygen, carbon dioxide, and carbon monoxide concentrations are shown in figure 8-2. Notice that the oxygen and carbon dioxide are near mirror images of each other during both the oxygen-rich and fuel-rich states of burning and that the increasing levels of carbon monoxide in the products appears to be somewhat delayed. One can observe that the carbon dioxide concentration has two distinct peaks that bound the major increase in the carbon monoxide. This situation is expected and can easily be explained when one considers that carbon monoxide is an intermediate in the formation of carbon dioxide. Clearly, in the absence of sufficient oxygen less of the carbon monoxide is being further oxidized to carbon dioxide. As the amount of fuel available for consumption begins to drop off more of the carbon monoxide can be converted to carbon dioxide, hence the reversal of the trend. This is followed by the ultimate return to an oxygen-rich state as the fire begins to burn only in the coal embers, ultimately consuming all of the available fuel.

This test was terminated nearly two hours after the initial ignition source was lit. At this point the fan was shut off and the remaining fuel allowed to burn-out in unventilated

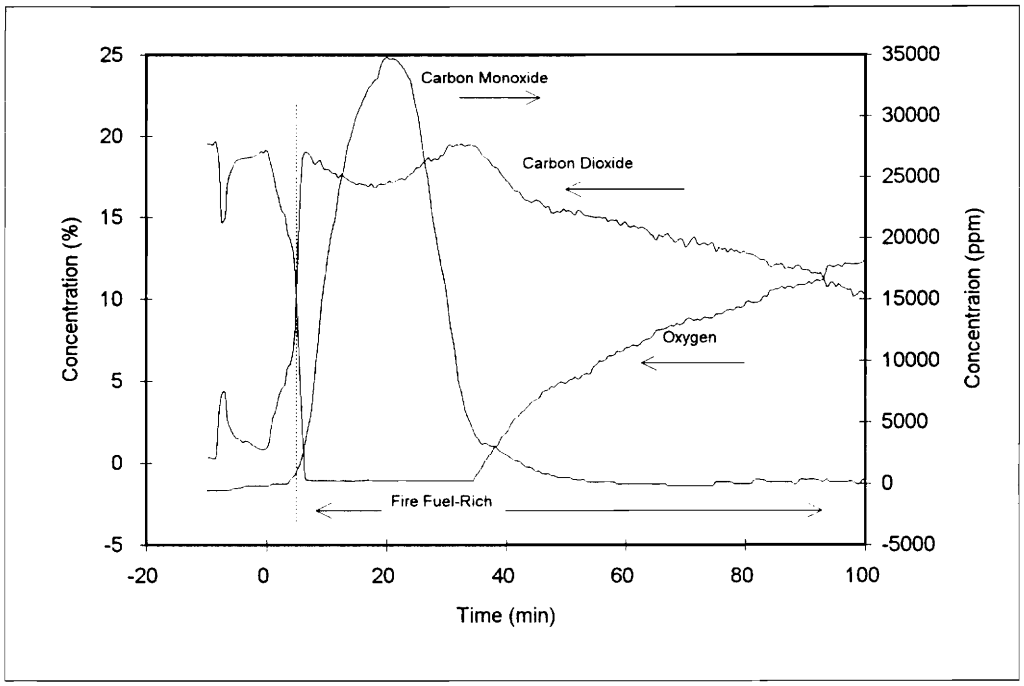

Figure 8-2: Combined Gas Traces for Test 4 (Loomis and McPherson 1995).

conditions. Inspection of the fire tunnel the following day revealed that almost the entire fuel charge had been "coked" leaving some 33 % of the initial mass as coke and bottom ash. A small portion of what remained, at the entrance to the fuel charge, was unburned coal indicating that any burning in the upstream direction was insignificant compared with the fire spread in the downstream direction.

Application of a fogging system to control a fuel-rich coal fire was made during test 5. The concentration traces for oxygen, carbon dioxide, and carbon monoxide are shown in figure 8-3. This fire shows a very similar pattern of growth to that of test 4. The fogging system was initiated, with a water flow rate of 0.037 l/sec (35 gal/hr), following the noticeable decrease in the concentration of carbon dioxide, indicating the fire was fully fuel-rich. Based upon flow tests of the fogging system it is estimated that approximately 50 % of the water injected reached the fire as fog, 25 % reached the fire running along the floor, and the remainder not reaching the fire at all. After the fogging system was initiated field observation and monitored data indicated the fire was being extinguished. The color of the smoke appeared to lighten from nearly black to grayish, while the carbon dioxide concentration made a momentary rise followed by continuous decrease. The oxygen concentration began to rise (from 0 %) approximately 8 minutes after the fogging was initiated. The result was a return to an oxygen-rich (>15 % O_2) fire some 80 minutes sooner than the fire in test 4.

This test was terminated approximately 60 minutes after the rapid growth leading to the fuel-rich state. At termination the fan and fogging system were left on, however the fire section of the tunnel was opened to reveal the most downstream fuel. Inspection of the fuel indicated that pyrolysis had been occurring on the surfaces facing into the tunnel. As

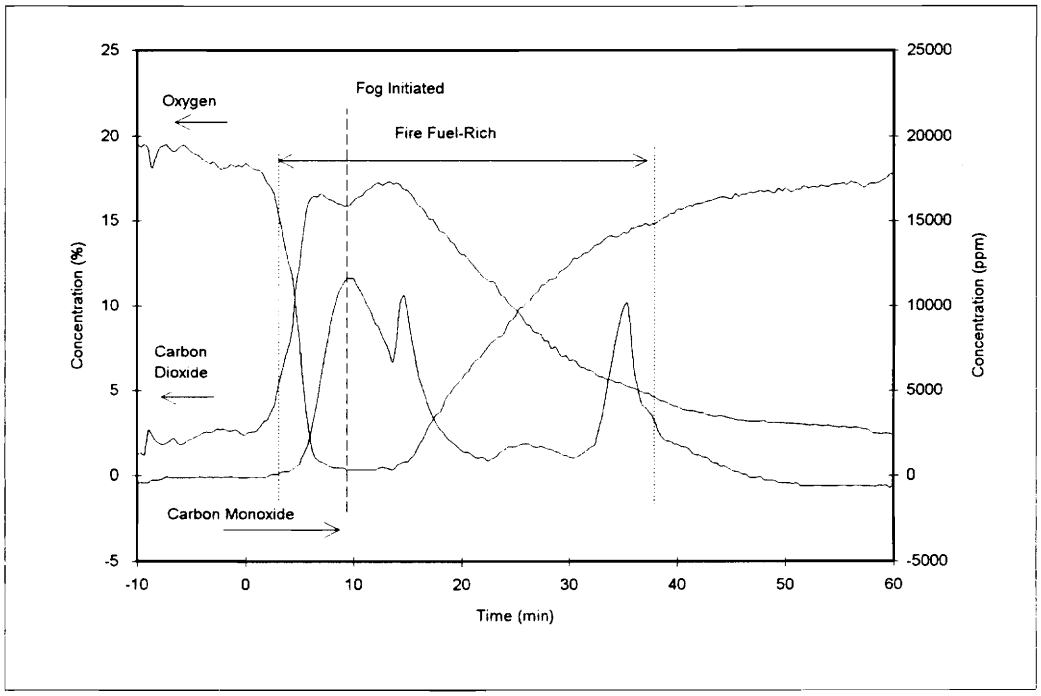

Figure 8-3: Combined Gas Traces for Test 5 (Loomis and McPherson 1995).

the remainder of the fuel was exposed it was visually apparent that all of the fuel had been exposed to some degree of pyrolysis, and that the fire was still in a state of growth when the fogging was initiated. This was indicated by a vee shaped pattern of deeper pyrolysis, facing back towards the ignition source. What was most apparent was the fact that the application of the fog had rapidly reduced the size of the fire and the state of burning back to oxygen-rich much faster than if the fire had been allowed to continue to burn on its own. Later removal of the remaining fuel indicated that some 65 percent of the initial fuel mass remained as unburned fuel (partially pyrolysed), coke, or ash. There was no indication that the fuel had continued to burn after the wind tunnel was opened.

The carbon monoxide trace exhibits a shape that is similar to that in test 4, without the very high peak value. The rate of increase in the carbon monoxide concentration is similar to that in test 4. In test 4 the CO level attains a peak concentration of 35000 ppm. The peak level of CO in test 5 is held to just over 11000 ppm at a time corresponding to the initiation of the water sprays. The two peaks, at 16 minutes and at 35 minutes can be associated to problems with the CO sample metering system and should be ignored.

Test number 7 investigated the effect of a combination extinguishing system. This system used a propane flame to consume some of the available oxygen and the heat of combustion to vaporize water to displace the remaining oxygen. The oxygen concentration downstream of the combustor was about 13 percent. The gas traces from this experiment are shown in figure 8-4. The pattern of growth exhibited by this fire is similar to that of tests 4 and 5. When the fire was observed to reach a fully fuel-rich state, exhibited by the decreasing carbon dioxide concentrations, the combination extinguisher was ignited. This included initiation of both the water sprays and the propane burner.

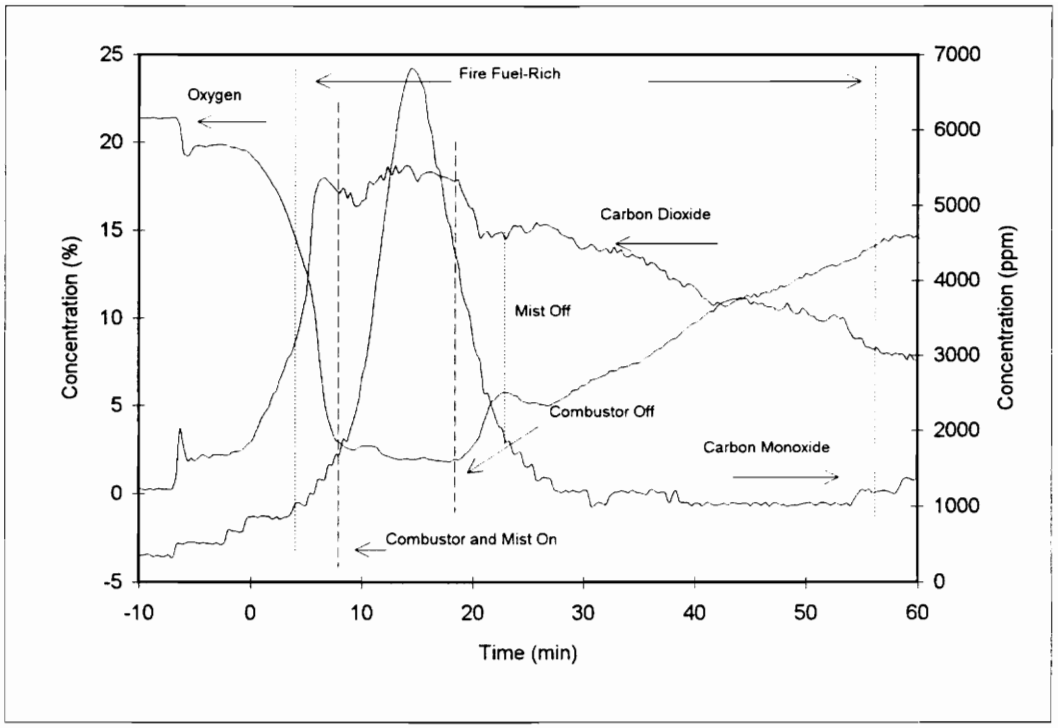

Figure 8-4: Combined Gas Traces for Test 7 (Loomis and McPherson 1995).

The initial effect of the extinguisher is visible in the carbon dioxide trace, as the concentration of this gas begins to rise again at about 10 minutes. The action of the combustion process in the extinguisher is evident in the depressed oxygen concentrations during the period between 9 and 19 minutes. Notice that the oxygen concentration begins to rise after the combustor portion of the extinguisher is put out. This effect is mirrored in the carbon dioxide concentration. Once the mist was turned off the oxygen concentration, again, began to drop. This appears to indicate the fire was trying to revert back to a fully fuel-rich state, the implication being that the fire was under some degree of control by the combustor and mist but had not been extinguished. At a time of about 28 minutes water mist was supplied to the fire using the spinning disk humidifier. This point shows the oxygen concentration again increasing as the fire begins its ultimate decay.

During the period that the combustor was in operation it was possible to view the fire and the extinguisher from the exhaust end of the tunnel. From this point of view the fire was observed to be significantly inhibited, compared to the baseline fire (test 4) at the same period. Once the propane flame in the extinguisher was put out the coal fire appeared to accelerate. This period of time is illustrated in figure 4 as the time between the Combustor Off and the Mist Off.

The carbon monoxide concentration shows a similar pattern as that in test 4, but without the extreme value seen in that test. The carbon monoxide trace is also similar to that seen, initially, in test 5.

The tunnel was opened at a time of about 75 minutes so that the state of fuel consumption could be observed. There appeared to be a fair amount of fuel remaining in tunnel. This fuel continued to burn for several hours following the cessation of data collection.

At no time during the experiments was a water gas explosion experienced. The possibility of the reaction of water on the incandescent coal producing carbon monoxide and hydrogen gas has been an objection the application of mist in practice (McPherson 1993a).

8.4. Conclusions

The tests that have been conducted show that there is a positive impact related to the application of water mist to a fuel-rich duct fire. The fact that the test fire was brought under control can be seen in figures 8-5 and 8-6 that compare the carbon dioxide and the oxygen traces from tests 4, 5, and 7. It is clear that both the control fire and the test fire experienced similar growth profiles, but have radically different decay profiles. Since the fires sustained similar and expected growth profiles it is reasonable to assume that had nothing been done the decay of tests 5 and 7 would have been similar to that of test 4. However, by the application of the fogging suppression system the fire in test 5 was extinguished in such a manner as to leave nearly twice the amount of unpyrolyzed fuel as was left from test 4.

One question that was raised during the course of these investigations concerned the point at which the fire should be considered fuel-rich. The definition of Roberts and Clough (1967) that the fire behaves in a fuel-rich manner when the oxygen concentration falls to below 15 % in products of combustion appears to be valid. Although, in the experiments

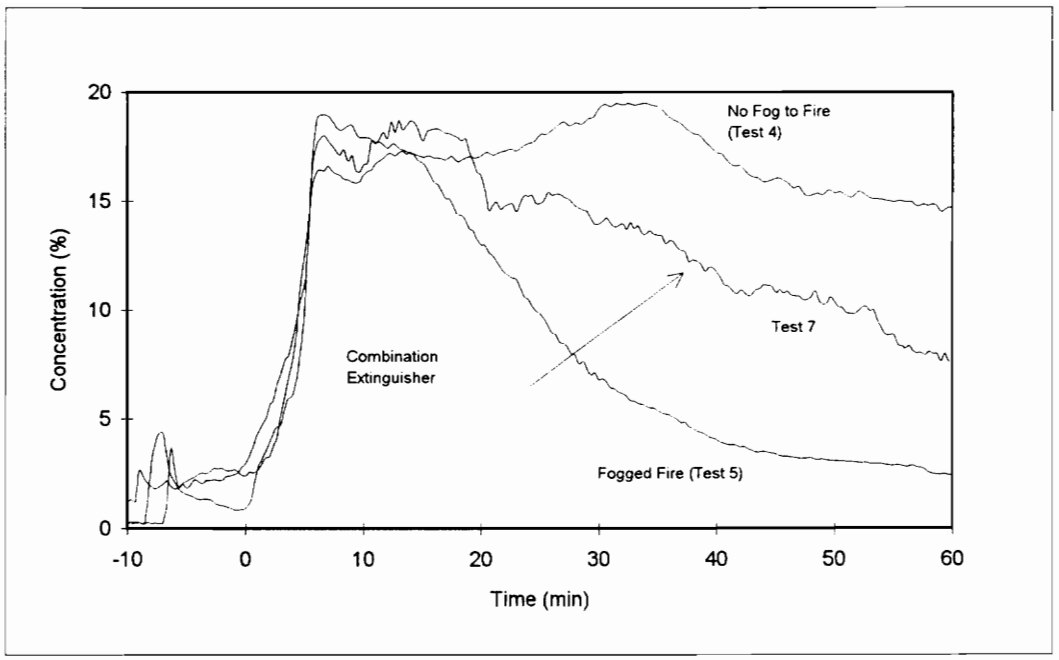

Figure 8-5: Oxygen Traces for Tests 4, 5, and 7 (Loomis and McPherson 1995).

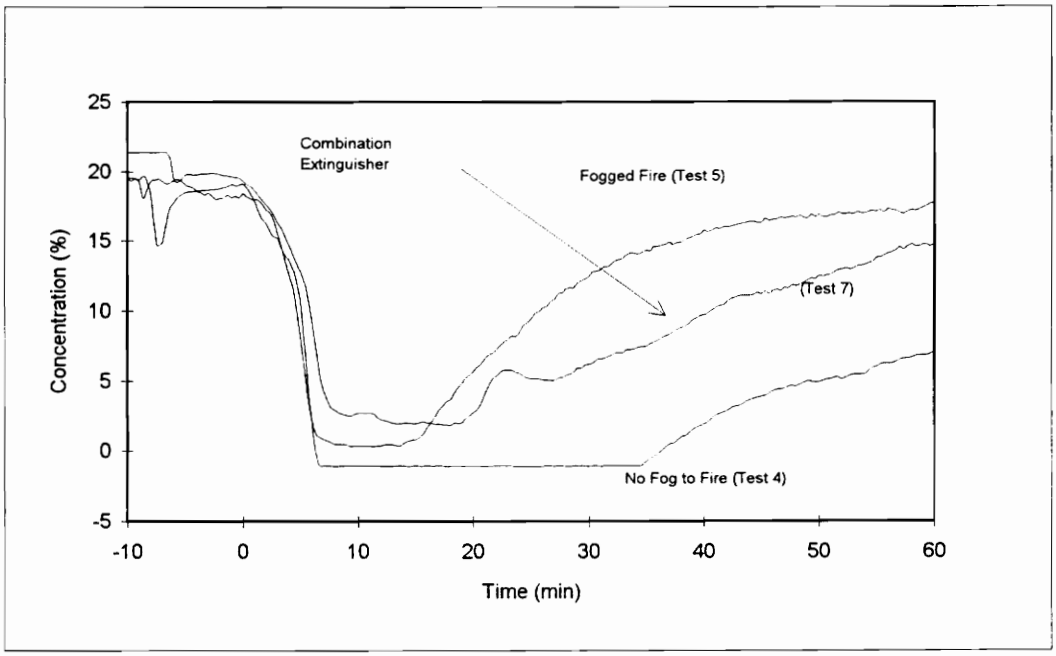

Figure 8-6: Carbon Dioxide Traces from Tests 4, 5, and 7 (Loomis and McPherson 1995).

conducted here the transition from oxygen-rich to fuel-rich behavior appears to occur nearer to 12 % oxygen. This point was visible in all of the tests, but shows up quite clearly in the oxygen trace of test 7, figure 4. Notice the change of slope in the oxygen line at a time of about 5 minutes. The chemical definition of the fuel-rich state is also clear in the tests covered here, indicated by the increasing carbon monoxide and decreasing carbon dioxide. The range over which the fires are shown as fuel-rich in figures 2, 3, and 4 are based on the less than 15 percent oxygen criterion

The first definition, by Roberts and Clough (1967), can by used by fire-fighters during the initial attempts to gain control over a fire. If the oxygen concentration begins to fall close to 15 % downstream of the open fire, the indication should be that tactics being used are ineffective. On the other hand, once the fire has become fuel-rich the chemical definition will be important to determining the degree to which the fire is being controlled. The presence of in the oxygen downstream of the fire indicates that intensity of combustion is decreasing, and that fire-fighting efforts are being effective. The danger, of course, has not been overcome until the fire is entirely extinguished.

The effect of the combination extinguisher appears to have been to inhibit the fire during the period of time that the extinguisher was operational. With the fire in a subdued state the reduced quantity of mist seems to have been more able to control the fire, as evidenced by the increasing oxygen concentration following the flame out in the extinguisher.

What has been shown here to be effective is the application of water mist to a fuel-rich fire burning in a laboratory scale model of a coal mine entry. This still leaves the question concerning the application of this technique in a full scale mine entry. The general theory

can certainly be expanded to the full scale in such a manner as to account for heat removal, fuel coating, and oxygen displacement. But, this still leaves the questions concerning the flame structure and turbulent flow patterns that may be more prevalent in the full scale model. Experimentation at the full scale level is also subject to other problems, the first being that no reasonable mine operator can be expected to allow this type of experiment to be conducted in his operation. Equally impractical is the construction of a full-scale model capable of sustaining the intense heat loads generated by a large coal fire. The most practical solution to conducting full-scale tests seems to be the use of an existing underground test tunnel. In any case, the major inhibiting factor appears to be research funding.

Even before such a full scale test can be performed estimates must be made of the extrapolated parameters. Principally the quantity of fog required for a similar fire burning in a full scale entry. Based on the scaling factors used in the design of the fire tunnel, a fogging system capable of producing approximately 1.05 l/sec (17 gal/min.) of a water mist in the size range of, perhaps 25 to 200 μm. This flow rate is approximately one-third of the statutory minimum, 50 gal/min. Such technology is currently available for the protection of building and ship compartments. With some ingenuity it seems possible that such a system could be made mobile for rapid deployment within a coal mine.

9. REFERENCES

Anonymous (1966) Confusion Worse Confounded - Report on West Virginian Colliery Disaster. *Colliery Guardian*, Vol. 212, No. 5468, February 4, p.146.

Anonymous (1989) "WB-AAI-B High Resolution and WB-FAI-B High Speed Interface Cards, Operator's Manual," Omega Engineering, Inc., Stamford Connecticut.

Anonymous (1992a) Industrial Ventilation, Inc., "Centrifugal Humidifier, Series-30," Publications 3/92 3M and 20290, Boise, Idaho

Anonymous (1992b) City Technology CiTiceL List, Document Ref., a:\CiTiceL.LST Issue 12, City Technology Centre, Portsmouth, England.

Anonymous (1994a) 30CFR50, "Notification, Investigation, Reports and Records of Accidents, Injuries, Illnesses, Employment, and Coal Production in Mines," *Code of Federal Regulations, Mineral Resources*, CFR Title 30, Part 50, Washington D. C.

Anonymous (1994b) "Fine Water Spray System" Securiplex Technologies Inc., Dorval, Quebec, Canada

Bacharach, J. P. L., A. L. Craven, and D. P. Stewart (1986), "Underground Mine Fire Control with Inerting Systems," *The Canadian Institute of Mining Bulletin*, Vol. 79, No. 885, January, pp. 67-72.

Banerjee, S. P. (1987) "Experience of Inert Gas Injection in Combating Fires in Indian Coal Mines" Chapter 62, Proceedings of the Third U.S. Mine Ventilation Symposium, University of Pennsylvania, University Park, PA, pp. 438-443.

Bolstad, J. W., R. D. Foster, and W. S. Gregory (1983) "A Numerical Model Describing the Heat Transfer Between Combustion Products and Ventilation System Duct Walls," Fire Dynamics and Heat Transfer, the 21st National Heat Transfer Conference, July 24-28, pp.133-8.

Burrell, G. A. and F. R. Seibert (1912) Gas Analysis as an Aid in Fighting Mine Fires, BuMines, Technical Paper 13, 16 pp.

Chaiken, R. F., J. M. Singer, and C. K. Lee (1979) Model Coal Tunnel Fires in Ventilation Flow, BuMines, RI 8355, 32 pp.

Chaiken, R. F., and J. W. Martin (1992), "In-situ Gasification and Combustion of Coal" *SME Mining Engineering Handbook,* 2d Edition, H. L. Hartman Editor, pp. 1954-1970. Society for Mining, Metallurgy, and Exploration, Inc. Port City Press, Inc., Baltimore.

Charters, D. A., W. A. Gray, and A. C. McIntosh (1994), "A Computer Model to Assess Fires Hazards in Tunnels (FASIT)," *Fire Technology*, Vol. 30, No. 1, pp. 134-154.

Comitis, S. C., D. Glasser, and B. D. Young, (1994), "An Experimental and Modeling Study of Fires in Ventilated Ducts. Part I: Liquid Fuels," *Combustion and Flame*, Vol. 96, No. 4 (March), pp. 428-442.

Cooper, L. Y., (1982), "Heat Transfer From a Buoyant Plume to an Unconfined Ceiling," Journal of Heat Transfer, Vol. 104, No. 3 (August), pp. 446-451.

Derick, R. L. (1993) "Mine Emergency Response Before, During, and Following a Large Underground Coal Mine Fire," Society for Mining, Metallurgy, and Exploration, Inc. Preprint Number 93-68, for presentation February 15-18, 1993, Reno, Nevada, 7 pages

de Ris, J. (1970) "Duct Fires," *Combustion and Science Technology*, 2, pp. 239-258.

Drysdale, D. (1985), *An Introduction to Fire Dynamics*, John Wiley and Sons, Inc.

Egan, M. R. (1993) Impact of Air Velocity on the Development and Detection of Small Coal Fires, BuMines, RI 9480, 16 pp.

Eschenburg, H. M. W. (1982) Underground Fires, Environmental Engineering in South African Mines, Chapter 30, The Mine Ventilation Society of South Africa, Cape and Transvaal Printers, Cape Town, pp. 791-799.

Evans D., and D. Pfenning, (1985), "Water Sprays Suppress Gas-well Blowout Fires," Oil and Gas Journal, Vol. 83, No. 17 (Apr. 29), pp.80-86.

Foust, A. S., L. A. Wenzel, C. W. Clump, L. Maus, and L. B. Anderson, (1980) *Principles of Unit Operations*, 2nd edition, John Wiley and Sons, Inc.

Froger, C. E. (1986) "Nitrogen Fights French Underground Fires," *World Mining Equipment*, Vol. 10, No. 5, May, pp. 34-37.

Gallick, J. M. (1991) "Mine Emergency Preparedness -- Firefighting, What Else Can You Do?" Coal Mining, Technology, Economics and Policy 1991, Session Papers from the American Mining Congress Coal Convention, Pittsburgh, June 2-5, 1991, pp. 427-433.

Gaydon, A. G. and H. G. Wolfhard (1970) *Flames; Their Structure, Radiation, and Temperature*, Chapman and Hall Ltd, London

George, J. J. (1951), "Fog," *Compendium of Meteorology*, American Meteorological Society, Committee on the Compendium of Meteorology, Waverly Press, Inc., pp. 1179 - 1189.

Glassman, I. (1977) *Combustion*, Academic Press.

Haessler, W. M. (1989), *Fire: Fundamentals and Control*, M. Dekker, New York, 250 pages

Hottel, H. C. (1954) "Radiant Heat Transmission," *Heat Transmission*, E. H. McAdams, ed., McGraw-Hill Book Co., New York. (Ref. by Bolstad, Foster, and Gregory 1983)

Huntley, D. W., R. J. Painter, J. K. Oakes, D. R. Cavanaugh, and W. G. Denning (1984) *Underground Coal Mine Fire, Wilberg Mine, Emery Mining Corporation,* Report of Investigation, MSHA.

Hwang, C. C., R. F. Chaiken, J. M. Singer, and D. N. H. Chi (1976) "Reverse Stratified Flow in Duct Fires: A Two Dimensional Approach," 16th Symposium (International) on Combustion, pp. 1385-95.

Hwang, C. C. and R. F. Chaiken (1978) Effect of Duct Fire on the Ventilation Air Velocity, BuMines, RI 8311, 19 pp.

Hwang, C. C. and C. D. Litton (1984) "A Study of Critical Conditions in Mine Fires," 20th Symposium (International) on Combustion, pp 1673-79.

Keenan, J. H., F. G. Keyes, P. G. Hill, and J. G. Moore (1969), *Steam Tables*, John Wiley and Sons, Inc., New York

Kennedy M. and G. Taylor (1967) "Temperature distributions downwind of stationary mine fires," *British Journal of Applied Physics*, 18, pp 349-56.

Kuo, K. K. (1986), *Principles of Combustion*, John Wiley and Sons, Inc.

Lefebvre, A. H., (1989) *Atomization and Sprays*, Hemispher Publishing Corp., New York

Lee, C. K., R. F. Chaiken, J. M. Singer, and M. E. Harris (1980) Behavior of Wood Fires in Model Tunnels Under Forced Ventilation Flow, Tests with Untreated Wood, BuMines, RI 8450, 58 pp.

Loomis, I. M. (1994) Virginia Polytechnic Institute and State University, Proposal to Virginia Polytechnic Institute and State University, Graduate Student Assembly, "Application of the Cooled Products of Combustion in the Fighting of Fuel-Rich Coal Mine Fires," 21 January, 5 pages plus forms.

Loomis, I. M., and M. J. McPherson (1995) "Application of Water Mist for the Control of Fuel-Rich Fires in Model Coal Mine Entries," Prodeeding of the 7th U. S. Mine Ventilation Symposium, Lexington, KY, Society for Mining, Metallurgy, and Exploration, Inc.

Moon, M. R. (1993) "Remote Seal Construction at the Wilberg Mine, *Mining Engineering*, Vol. 45, No. 12 (Dec.), pp 1487-1490.

Mawhinney, J. R. (1993) "Engineering Criteria for Water Mist Fire Suppression Systems." Proceedings, Water Mist Fire Suppression Workshop, March 1-2, 1993, National Institute of Standards and Technology, NISTIR 5207, pp. 37-73.

Mawhinney, J. R. (1994) "Water Mist Suppression Systems May Solve an Array of Fire Protection Problems," *NFPA Journal*, Vol. 88, No. 3 (May/June), pp. 46 - 57.

McPherson, M. J. (1991) University of California, Berkeley, letter to Dr. E. Topuz, Virginia Polytechnic Institute and State University, December 5, 13 pages with enclosures.

McPherson, M. J. (1993a) "The Development and Control of Open Fires in Coal Mine Entries." Proceedings, 6th U.S. Mine Ventilation Symposium, June 21-23, 1993, Chapter 30, SME, Inc., pp. 197-202.

McPherson, M. J. (1993b) *Subsurface Ventilation and Environmental Engineering,* Chapman and Hall, London.

Mitchell, D. W. (1990) *Mine Fires, Prevention, Detection, Fighting*, McClean Hunter, Chicago

Moon, M. R. (1993), "Remote Seal Construction at the Wilberg Mine," *Mining Engineering,* Vol. 45, No. 12, December, pp 1487-1490.

Nagy, J., E. M. Murphy, and D. W. Mitchell (1960), Controlling Mine Fires with High-expansion Foam. USBM RI5632, 28 pp.

Nagy, J. (1987) "Wilberg Mine Fire: Cause, Location, and Initial Development" Appendix H to *Underground Coal Mine Fire, Wilberg Mine, Emery Mining Corporation,* Huntly, *et al.* 1984

Naquet, J. (1990), "A Mine Fire Isolated from a Distance," *Mining Magazine*, March, pp 206 - 209.

Notarianni, K. A., and N. H. Jason (1993), Editors, Water Mist Fire Suppression Workshop, March 1-2, 1993: Proceedings, United States Department of Commerce, National Institute of Standards and Technology, NISTIR 5207, 147 pp.

O'Connor, J. A., J. S. Malesky, and T. C. Higgins (1950), Fighting a Fire in No. 59 Mine Peabody Coal Co., Springfield Sangamon County, Ill., U.S. BuMines IC 7564, 19 pp.

Olsson, S., and Ryderman, A. (1990), *Extinguishment of Oil Spray Fires with Water - Experimental Procedures and Test Data.* (SP RAPPORT 1990:32), Swedish National Testing and Research Institute, Borås, Sweden.

Pope, A., and J. J. Harper (1966) *Low-Speed Wind Tunnel Testing*, John Wiley and Sons, Inc.

Press, W. H., S. A. Teukolsky, W. T. Vettering, and B. P. Flannery (1992), *Numerical Recipes in C*, Second Edition, Cambridge University Press, pp. 610 - 615.

Ramlu, M. A. (1991) *Mine Disasters and Mine Rescue,* A. A. Balkema, Rotterdam.

Reischl, U. (1979) "Water Fog Stream Heat Radiation Attenuation" *Fire Technology*, 15 (November), pp 262-70

Roberts, A. F. (1950) Fires in Timber Lining of Mine Roadways: A Comparison of Data from Reduced-Scale and Large-Scale Experiments. Safety in Mine Research Establishment, Res. Rept. H.M Sta. Off., London.

Roberts, A. F., and G. Clough (1967a) "The Propagation of Fires in Passages Lined with Flammable Materials," *Combustion and Flame*, Vol 11, pp. 365

Roberts, A. F., and G. Clough (1967b) Model Studies of Heat Transfer in Mine Fires, Research Report No. 247, Safety in Mines Research Establishment, Buxton, England. (Ref. by de Ris, 1970).

Roberts, A. F., and J. R. Blackwell (1969) The Possibility of the Occurrence of Fuel-Rich Mine Fires," *The Mining Engineer*, September, pp. 699-708.

Roberts, A. F. (1970) "Fires in Ducts under Forced Ventilation Conditions," *Fire Technology*, 6 (February), pp. 13-21.

Roberts, A. F. (1971) "Comments on 'Duct Fires' by J. de Ris," *Combustion Science and Technology*, 3, pp. 263-6

Scheffy, J. L., and F. W. Williams (1991a) "The Extinguishment of Fires using Low Flow Water Hose Streams - Part I," *Fire Technology*, Vol. 27, No. 2, May, pp. 128 - 144.

Scheffy, J. L., and F. W. Williams (1991b) "The Extinguishment of Fires using Low Flow Water Hose Streams - Part II," *Fire Technology*, Vol. 27, No. 4, Nov., pp. 291 - 320.

Sengupta, M. (1990), *Mine Environmental Engineering*, Vol. II, CRC Press, Boca Raton, pp. 145 - 168.

Solomon, R. E. (1994) "NFPA is Developing a Standard on Water Mist Systems," *NFPA Journal*, Vol. 88, No. 3 (May/June), p. 53.

Strehlow, R. A. (1984) *Combustion Fundamentals*, McGraw-Hill

Thomas, P. H., (1958), The Movement of Buoyant Fluid Against a Stream and the Venting of Underground Fires, Fire Research Note 351/1958, Fire Research Station, Borehamwood, Herts, England. (Ref. in Hwang, et al., 1977)

Thomas, P. H., (1968), The Movement of Smoke in Horizontal Passages Against an Airflow, Fire Research Note 723/1968, Fire Research Station, Borehamwood, Herts, England. (Ref in Hwang, et al., 1977)

Timko, R. J., R. L. Derick, and E. D. Thimons (1987) "Analysis of a Fire in a Colorado Coal Mine - a Case Study," Proceedings of the Third U.S. Mine Ventilation Symposium. University of Pennsylvania, University Park, PA, pp. 444-452.

Timko, R. J., and F. N. Kissel (1993), Hazards of Underground Coal Mine Fires, Society for Mining Metallurgy, and Exploration, Inc. Preprint Number 93-121, for Presentation February 15-18, 1993, Reno, Nevada. 7 pages.

Vafai K., and A. J. Lacalle (1989) "Transient Ceiling Jet Development in Large Scale Fires," *International Communications in Heat and Mass Transfer,* Vol 16, No. 4, pp. 513-523.

Vandsburger, U. (1994), Course Notes; ME5214 - Combustion, Spring Semester 1994, Virginia Polytechnic Institute and State University.

Vanpée, M., and H. G. Wolfhard, (1960) Ignition by Hot Gases, BuMines RI5627, 12 pages.

Van Wylen, G. J., and R. E. Sonntag (1986), *Fundementals of Classical Thermodynamics*, 3d edition English/SI Version, John Wiley and Sons, New York, New York.

Vaughan-Thomas, T. (1964), "The Use of Nitrogen in Controlling and Underground Fire at Fernhill Colliery," *The Mining Engineer*, Vol 123, No. 42, pp. 311-336.

Vennard, J. K., and R. L. Street (1976), *Elementary Fluid Mechanics*, 5th Edition, SI Version, John Wiley and Sons, Inc., pp. 342-353.

Westfield, J., H. C. Brumbaugh, and R. W. Whittaker (1950), Extinguishing Fire with Carbon Dioxide in the Valier Mine, Valier Coal Co. Valier, Franklin County, Ill., U.S. BuMines IC7563, 10 pp.

Wighus, R. (1991) Extinguishment of Enclosed Gas Fires with Water Spray. The University of Edinburgh, *Third International Symposium on Fire Safety Science, IAFSS*, Abstracts 30 pages. Edinburgh, Scotland.

Wilde, D. G. (1967) "Fires in Mines; Recent Experiences," *Colliery Guardian,* December 1, pp. 629-632.

Ian Morton Loomis

Ian attended Bartlett High School, in Anchorage Alaska, and graduated there in the spring of 1983. He attended the New Mexico Institute of Mining and Technology, in Socorro, New Mexico, where he graduated, with Honors, in the spring of 1987, with a bachelor of science degree in Mining Engineering. While there, he received numerous scholarships and the coal industry's "Old Timers Award." Ian was also elected to the Tau Beta Pi association, New Mexico Gamma chapter.

Following this graduation, Ian went to work for Dravo Engineering Companies, Inc., and later Westinghouse Electric Corporation, at the Waste Isolation Pilot Plant, in Carlsbad, New Mexico. His first assignment was as a shift engineer in a materials handling shaft refit. Subsequent assignments included engineering responsibility for the underground facilities and structures, leading to cognizant responsibility for the entire underground ventilation system at this nuclear waste disposal site. While with Westinghouse, Ian received a George Westinghouse Signature Award for work involving the continuous monitoring of the natural ventilation pressure in the underground facility.

Ian is a registered Professional Engineer in the state of New Mexico, an Associate Member of the Society for Mining, Metallurgy, and Exploration, Inc., and a Fellow of the Mine Ventilation Society of South Africa.